Stony Brook University

Holographic QCD

A Dissertation Presented

by

Keun young Kim

to

The Graduate School

in Partial Fulfillment of the Requirements

for the Degree of

Doctor of Philosophy

in

Physics

Stony Brook University

August 2009

Stony Brook University

The Graduate School

Keun young Kim

We, the dissertation committee for the above candidate for the Doctor of Philosophy degree, hereby recommend acceptance of this dissertation.

Ismail Zahed - Dissertation Advisor
Professor, Department of Physics and Astronomy

Edward Shuryak - Chairperson of Defense
Professor, Department of Physics and Astronomy

Peter Stephens
Professor, Department of Physics and Astronomy

Dmitri Kharzeev
Senior Scientist, Brookhaven National Laboratory

This dissertation is accepted by the Graduate School

Lawrence Martin
Dean of the Graduate School

Abstract of the Dissertation

Holographic QCD

by

Keun young Kim

Doctor of Philosophy

in

Physics

Stony Brook University

2009

The gauge/gravity duality conjecture provides a novel and useful tool for studying strongly coupled systems. This duality maps difficult strong coupling problems to tractable weak coupling gravity problems. Furthermore, complicated non-perturbative phenomena can be described by simple geometrical pictures.

The gauge/gravity duality was first applied to explain the strong coupling regime of QCD (sQCD) such as strongly coupled quark gluon plasma (sQGP) produced at the Relativistic Heavy Ion Collider (RHIC) and hadronic physics. Recently it has been exploited to study properties of condensed matter systems such as superfluidity, superconductivity, and the Hall effect. The various dual theories of non-relativistic conformal field theory (CFT) also have been considered.

In this thesis I review my work on sQCD using the gravity dual model also called holographic QCD (hQCD).

1) The baryon form factor and nuclear force,

2) Phase and properties of baryonic dense matter,

3) The effect of finite baryon density or chemical potential on meson properties,

4) Non-equilibrium properties of sQGP.

These are important applications of the gauge/gravity duality since hQCD gives us a tractable theoretical tool for studying the finite baryon density problem and time-dependent dynamics of sQGP.

Contents

List of Figures

List of Tables

Acknowledgements

I would like to express sincere gratitude towards my extraordinary advisor Prof. Ismail Zahed whose supervision and encouragement helped me all the time during my research. Without his patience and guidance this thesis would not have been possible. I would like to thank Prof. Sang-jin Sin for the fruitful collaboration, support, and encouragement. I would also like to thank my former advisers Prof. Bum-hoon Lee, Prof. Martin Rocek and Prof. Jin Wang for their guidance and help. I am fortunate to have learned from Prof. Edward Shuryak and Prof. Peter van Nieuwenhuizen. I would like to thank my committee members, Prof. Peter Stephens and Prof. Dmitri Kharzeev.

I thank the members of Nuclear Theory Group and my fellow graduate classmates, I will always remember every one of them, they have all made graduate school research a more enjoyable time in my life, and I appreciate and value their friendship. Special thanks go to Clint Young and Tan Ahn for correcting my poor English many times.

Finally I dedicate this thesis to my grandmother, my father, my mother, my sisters Young Kim, Kang-Jin Kim, Eun-young Kim and my wife Eun-young Lee. This work would not have been possible without their love, support and sacrifices.

Chapter 1

Introduction

1.1 Overview

The gauge/gravity duality conjecture [1] provides a novel and useful tool for studying strongly coupled systems. For a general review see [2] and references therein. This duality maps difficult strong coupling problems to tractable weak coupling gravity problems. Furthermore, complicated non-perturbative phenomena can be described by simple geometrical pictures.

The gauge/gravity duality was first applied to explain the strong coupling regime of QCD (sQCD) such as strongly coupled quark gluon plasma (sQGP) produced at the Relativistic Heavy Ion Collider (RHIC) and hadronic physics. There are many review articles on this application [3–11]. Recently it has been exploited to study properties of condensed matter systems such as superfluidity, superconductivity, and the Hall effect [12]. The various dual theories of non-relativistic conformal field theory (CFT) also have been considered [13].

In this thesis I review my work[1] [14–21] on sQCD using the gravity dual model called holographic QCD (hQCD).

We start with a brief review on some of general holographic methods and holographic "QCD" models.[2] At the end of this chapter we describe the outline of this thesis.

[1] With Prof. Ismail Zahed and Prof. Sang-jin Sin.

[2] There is no exact holographic QCD model yet, so the "QCD" model means that the model mimics some aspects of QCD.

1.2 Holographic methods

In this section we will review some of the holographic methods widely used in the strongly correlated systems including QCD and some condensed matter system. We will explain a "big picture" and "recipes" of the holographic technique as non-technically as possible. We will not try to be general or rigorous. We also avoid discussing many subtleties. For more complete discussion we refer to [3–10]. The aim of this section is to provide the conceptual background and heuristic arguments before discussing the technical details in the main text. To make this introduction as simple as possible some subtle points which are important in practice but not important for a big picture are relegated to the footnotes.

1.2.1 Green's functions

We start with the 5 (or more) dimensional gravity theory. 3+1 dimension will be identified with the spacetime where our field theory is defined and the extra one dimension is identified with the energy scale of the field theory. If there are more dimensions then they are compactified, for example as a small sphere, not to be observed. In this section we will ignore this compactified dimension for simplicity.

The object we are interested in is the partition function of the field theory, which gives us various correlators (Green's functions). The basic idea is to get the field theory partition function by computing the gravity partition function. There are two issues. One is the fact that getting the gravity partition function is also (possibly more) nontrivial in general. Thus the problem does not become easier by going to gravity. The other one is the mismatch of spacetime dimension. Both problems are resolved by considering the on-shell gravity action with non-normalizable classical solutions. In brief the sum over all paths in the gravity partition function is reduced to the single contribution due to the classical solution, which amounts to the saddle point approximation. [3] In this procedure the 5 dimensional action is reduced to the 4 dimensional boundary

[3]The validity of this saddle point approximation needs to be justified. For a detail we refer to [3]. Specifically it is valid at the large number of color (N_C) and large t'Hooft coupling ($\lambda := g^2_{YM} N_c$), which correspond to the weak gravity and the strongly coupled field theory regime.

term, which we will describe in more detail below.

Let ϕ be some gravity field living in 5 dimension and ϕ_{cl} be a classical solution of the equations of motion. By plugging ϕ_{cl} in the action we can get the on-shell action which may be decomposed as two parts after integrating by part. One is the part giving the equation of motion and the other is the part giving the boundary value since it's a total derivative term. We are left with the boundary term since the equation of motion part vanishes. The value of this boundary term depends on the nature of ϕ_{cl}. If ϕ_{cl} approaches to zero sufficiently fast, which is a usual assumption in the field theory, there will be no contribution. Here, in AdS/CFT setup, we assume a non-normalizable solution with $\phi_{cl} \to \phi^0_{cl}$ at the boundary, so that there is a nontrivial contribution in the boundary term. Consequently the 5 dimensional "bulk" action is reduced to 4 dimensional "boundary" action after taking care of the integration over the extra dimension. Since it is the integration of a total derivative the resulting action only depends on the boundary value (ϕ^0_{cl}) of the bulk field. It is the boundary value of the classical field that is identified with the source of the field theory.

With the above consideration of the "on-shell" gravity action which is denoted by $S_{gravity}\left[\phi_{cl} \to \phi^0_{cl}\right]$, the AdS/CFT correspondence is the statement that

$$Z[\phi^0_{cl}] := \left\langle e^{i\int d^4x\, \hat{O}\phi^0_{cl}} \right\rangle_{gauge} = e^{iS_{gravity}\left[\phi_{cl}\to\phi^0_{cl}\right]} \ , \tag{1.1}$$

where $\hat{O}$ is a operator whose source is ϕ^0_{cl}. Since the classical path will dominate the gravity path integral, the RHS represents a saddle-point approximation to the gravity path integral.

In summary, to compute a correlator for an operator $\hat{O}$ in the field theory we follow the steps: First determine which field ϕ is dual to $\hat{O}$ [4] and solve the gravity equations of motion for ϕ with the boundary condition ϕ^0_{cl}.[5] Then plug this solution (ϕ_{cl}) into the gravity action, which yields the "on-shell" action

[4] Which operator is correspond to which field is not trivial. We usually deduce this by the dimension and symmetry. For example, metric fields ($g_{\mu\nu}$) correspond to the energy momentum tensor ($T^{\mu\nu}$) of the field theory.

[5] Usually the differential equation is the second order and we need two boundary conditions. One is fixed by ϕ^0_{cl} and the other condition comes from the regularity or by the incoming requirement of the positive energy mode at the black hole horizon.

and gives the RHS of (1.1). It is identified with the generating functional of the field theory so by varying with respect to ϕ^0_{cl} we can get the correlator of the corresponding operator of the field theory. Note that $S_{gravity}$ can be identified the generating functional for the connected Green's functions.

1.2.2 Thermodynamics

By Euclideanizing the action we can study the thermodynamics via thermal field theory. The temperature is introduced with periodic imaginary time.

Let us consider the Wick rotation to Euclidean time and compactify the time direction with a period $\beta := 1/T$. Then (1.1) reads

$$e^{-\beta F} \equiv Z[\phi^0_{cl}] = \left\langle e^{-\beta \int d^3x \hat{O}\phi^0_{cl}} \right\rangle_{gauge} = e^{-S^E_{gravity}\left[\phi_{cl}\to\phi^0_{cl}\right]} , \tag{1.2}$$

$$F = TS_{gravity}\left[\phi_{cl} \to \phi^0_{cl}\right] , \tag{1.3}$$

where $Z[\phi^0_{cl}]$ is interpreted as the thermodynamic partition function in the presence of the source ϕ^0_{cl} and F is a thermodynamic potential such as Helmholtz free energy or Grand potential.

The temperature is not arbitrary and is related to the black hole geometry. The vacuum of the field theory corresponds to the vacuum solution of the Einstein equation. The relevant solution called AdS metric is the solution with the negative cosmological constant. In general this solution contains black hole (or black brane) solution analogous to Schwarzschild black hole which shows singular behavior near the horizon. Roughly speaking the temperature is determined by the horizon position to avoid the conical singularity of the geometry. The entropy of the system is related to the area of the horizon. In this case F is identified with Helmholtz free energy.

We also can consider the chemical potential or the related conserved charge. A conserved charge is equivalent to the existence of a global symmetry in the field theory. In general, from gauge/gravity point of view, the global symmetry of the field theory is related to the local (gauge) symmetry of the bulk theory. Thus we need to consider the gauge theory in the bulk. For example let us consider the global $U(1)$ symmetry of the boundary field theory. It may amount to introducing the $U(1)$ Maxwell field in the bulk. Thus the minimal bulk action is Einstein-Maxwell theory with one nonvanishing component A_0.

In the boundary field theory the conserved charge is conjugate to the chemical potential (μ), which is nothing but a boundary value of a bulk field, $A_0(\infty)$. [6] The corresponding operator $\hat{O}$ is the number operator $\hat{N}$. In this case the F is identified with the grand potential. By choosing a suitable gauge field we also can study the system with some background electric field or magnetic field.

Once we know the thermodynamic potential we can compute all thermodynamic quantities using the standard thermodynamics relations. If there are more than one possible classical solution then we should compare thermodynamic potentials to determine the stable gravity configuration. It is the holographic realization of the phase transition.

1.2.3 Linear response and transport properties

In the previous section we discussed the properties of the equilibrium state. Now we want study non-equilibrium properties. One approach is linear response theory, the response of the system to a small perturbation. It is characterized by some transport coefficients, which are related to the retarded Green's function by Kubo's formula. For example the conductivity can be calculated as

$$\sigma^{xx} = \lim_{\omega \to 0} \frac{1}{\omega} \mathrm{Im} G_R^{xx}(\omega, \vec{0}) \tag{1.4}$$

where $G_R^{xx}(\omega, \vec{0})$ is the retarded Green's function defined as

$$G_R^{xx}(\omega, \vec{0}) = \int dt d\vec{x} e^{i\omega t} \theta(t) \langle [J_x(t, \vec{x}), J_x(0, \vec{0})] \rangle \tag{1.5}$$

where J_x is the current.

The point is that we can calculate $G_R^{xx}(\omega, \vec{0})$ from the gravity [23–25]. The method is a generalization of (1.1): (1) By Wick rotation we work with the Euclideanized action. (2) Compute the two point correlator, which is identified with the Green's function. The Green's functions are defined up to the

[6] A_0 is not gauge invariant. However the gauge is fixed by the regularity condition at the black hole horizon in the presence of the black hole or by the consistency with the thermodynamics [22]. *i.e.* $A_0(0) = 0$. Thus the boundary value is well defined and the equivalent gauge invariant identification is $\int_0^\infty F_{z0}$, which also has a direct meaning of the chemical potential, the amount of work to put a particle into a system. As a result $A_0(\infty) = \mu$ is always valid in the axial gauge $A_z = 0$.

boundary condition. (3) To get the retarded Green's function (not advanced or Feynman Green's function) we use the incoming boundary condition at the horizon.[7]

We will finish this section with a heuristic derivation of Kubo formula. First consider the small perturbation by weak external fields $\{\phi_i(x)\}$ coupled to a set of operators $\{\hat{O}^i(x)\}$ at the thermal equilibrium. Then the Hamiltonian is modified by

$$\delta\hat{H} = -\int d^d x \phi_i(t,\vec{x})\hat{O}^i(t,\vec{x}). \tag{1.6}$$

The standard time-dependent perturbation will give us the expectation value of the operators

$$\delta\langle\hat{O}^i(x)\rangle = \int d^{d+1}x' G_R^{ij}(x,x')\phi_j(x') + \mathcal{O}(\phi^2) \tag{1.7}$$

where $G_R^{ij}(x,x')$ is the retarded Green's function. In the translational invariant system the result reads in the Fourier space

$$\delta\hat{O}^i(k) = G_R^{ij}(k)\phi_j(k) + \mathcal{O}(\phi^2) \tag{1.8}$$

Let us consider the Ohm's law for an time-varing electric field. The spacial part of the current is given by

$$J^i = \sigma^{ij}E_j \ , \tag{1.9}$$

In the language of the linear response theory, $\phi_i \to A_i$ and $\hat{O}^i \to J^i$, and $E_x(k) = i\omega A_x(k)$ in the gauge $A_t = 0$. By comparing (1.8) and (1.9) we get

$$G_R^{xx} = i\omega\sigma^{xx} \tag{1.10}$$

Thus Kubo formula, which relates transport coefficient to the retarded Green's function, yields

$$\sigma^{xx} = \lim_{\omega\to 0}\frac{1}{\omega}\mathrm{Im}G_R^{xx}(\omega,\vec{0}) \tag{1.11}$$

[7]This has been justified using Schwinger-Keldysh formalism [26].

Another studied example in gauge/gravity is the shear viscosity (η):

$$\eta = -\lim_{\omega\to 0}\frac{1}{\omega}\mathrm{Im}G_R^{xy,xy}(\omega,\vec{0}) \tag{1.12}$$

where

$$G_R^{xy,xy}(\omega,0) = \int dtd\vec{x}e^{i\omega t}\theta(t)\langle[T_{xy}(t,\vec{x}),T_{xy}(0,\vec{0})]\rangle \tag{1.13}$$

1.2.4 Holographic models

The gauge/gravity duality is originated from AdS/CFT duality, which says that some large N_c and large λ *CFT*, Conformal Field Theory (for example $\mathcal{N}$=4 super Yang-Mills in 4D), is dual to some weak classical gravity theory in the *AdS* background metric (for example Type IIB supergravity in AdS_5 metric).[8] This duality is related to the dual role of the D-brane or Dp branes, p+1 dimensional gravitating objects which couple to the specific type of charge called Ramond-Ramond charge (RR charge).[9]

First the large number (N_c) of Dp-branes on top of each other can be interpreted as a source generating a background metric which is usually the AdS metric or its variants. It is analogous to the Schwarzschild black hole metric sourced by a large number of (very massive) point particles, "D0 branes".[10] The gravity theory is defined in this background metric. The dual field theory is $U(N_c)$ gauge theory and the gauge fields are related to the small fluctuations of N_c D-branes. *i.e.* the dual role of the D-branes are the source for the background (where closed strings or gravity degrees of freedom live) and their own small fluctuations (which amount to the excitations of open strings or gauge field degrees of freedom).

[8]This is a weak form of AdS/CFT. In a stronger form there is no restriction on the parameters and two theories are completely equivalent. In this thesis we will use a weak form.

[9]It would be more logical to start with this D-brane argument at the beginning when we discuss gauge/gravity duality. However I decided not to do so since I wanted to present how to apply gauge/gravity duality to the real physical problems at first by avoiding any formal argument. In the previous sections D-branes do not play any role in a practical sense. Now D-branes becomes essential to discuss the flavor degrees of freedom and I introduce the concept here. However the techniques presented in the previous section are still valid with the D-brane's action instead of the Einstein action for the gravity part.

[10]A usual point particle is not a D-brane. Only from the dimensional perspective it is a "D0 brane".

In this setup N_c D-branes give us the *pure* $U(N_c)$ gauge theory description. To consider the quark degrees of freedom, additional structure is needed. It has been shown that adding quarks in the gauge theory amounts to embedding N_f *probe* branes in the spacetime generated by N_c branes, where N_f is the number of flavor. In order not to disturb the original geometry (or original gauge theory) we assume $N_f \ll N_c$, which corresponds to the quenched approximation in the field theory.

To study the pure gauge theory we study the background metric itself. To study the dynamics of the flavor degrees of freedom we study the dynamics of the flavor branes in the background metric. It has been shown that the D-brane dynamics is determined by two actions: the Dirac-Born-Infeld (DBI) action and the Chern-Simons (CS) action. Schematically they are written as

$$S^{DBI} \sim \int d^{p+1}x \; e^{-\phi} \; \mathrm{tr} \sqrt{-\det(g_{MN} + 2\pi\alpha' F_{MN})} \; , \tag{1.14}$$

$$S^{CS} \sim \int C_3 \wedge \mathrm{tr}\, F \wedge F \wedge F \; . \tag{1.15}$$

The DBI action describes the interaction of the flavor field (F_{MN}) with the background gravity (g_{MN})[11] and dilaton field (ϕ), while the CS action[12] describes the interaction with the RR field (C_3).

To study the thermodynamics and linear response we can use the same formalism presented in the previous section with the D-brane action as the gravity action.

There are two models which have been most studied. One is D3/D7 model [27] and the other is D4/D8 model called also Sakai-Sugimoto model (SS model) [28]. The former uses N_f D7 flavor branes in the geometry of N_c D3 branes and the latter uses N_f D8 branes in the geometry of N_c D4 branes. They will be explained in chapter 2 in more detail. In this thesis the SS model is the main model we study.

Here we simply describe what has been done with the SS model in studying QCD. The SS model yields a first principle effective theory of mesons. Many meson properties such as mass spectra, hidden local symmetry, vector meson

[11] The metric is the induced metric on the flavor brane from the background metric.

[12] While the DBI action is the general form, the CS action in (1.15) is not a general form. It depends on the dimension and the form of the RR field.

dominance, and the KSRF relations are successfully derived. [29] The baryon is realized as a soliton and its properties such as its spectrum and form factor are in good agreement with experiment [19, 30–43]. The nuclear force from these holographic baryons is computed by both the soliton picture [21, 44] and effective point particle action [45, 46]. The SS model at finite temperature has been discussed in [47–49] and at finite baryon(or isospin) density in [15, 17, 50–56]. Isospin chemical potential [57–59] and glueball decay [60] have been discussed. The similar topics have been discussed also for D3/D7 model [27, 61–74].

1.3 Outline

In chapter 2 we define the SS model and collect the relevant formulas to appear in the subsequent chapters. We also present the D3/D7 model for comparison with SS model. The D3/D7 model will be discussed and compared with SS model in chapter 4 and chapter 5.

In chapter 3 we study the thermodynamics of baryonic dense matter using the SS model. For homogeneous matter we introduce the baryon number density through the Chern-Simons term. For inhomogeneous matter we deform the space to consider the Wigner-Seitz cell *approximated* by S^3. By identifying the Euclidean DBI action with the grand potential we can study the thermodynamics.

In chapter 4 we study the conductivity of dense holographic QCD by introducing a static external electric field on the probe branes. In chapter 5 the response function of a homogeneous and dense hadronic system to a time-dependent (baryon) vector potential is discussed for the SS model and the D3/D7 model. In chapter 6 we discuss the density's effect on the meson's properties.

In chapter 7 the baryon form factor is worked out using the holographic baryon realized as an instanton in the 5D Yang-Mills and Chern-Simons system. In chapter 8 by considering two instantons in the same model we study the nuclear force.

Chapter 2

Sakai-Sugimoto model

2.1 Introduction

In this section we summarize the Sakai-Sugimoto model (SS model) which is D4/D8-$\overline{\text{D8}}$ set up. We will be very brief only for notation and completeness. For a thorough presentation we refer to [28, 75] and references therein.

As presented in the section 1.2.4 the physic of flavor branes are determined by two actions: DBI action and CS action. Let us consider N_f probe D8-branes in the N_c D4-branes background. With $U(N_f)$ gauge field A_M on the D8-branes, the effective action consists of the DBI action and the Chern-Simons action:

$$\begin{aligned} S_{\text{D8}} &= S_{\text{D8}}^{DBI} + S_{\text{D8}}^{CS} \ , \\ S_{\text{D8}}^{DBI} &= -T_8 \int d^9x \ e^{-\phi} \ \text{tr} \sqrt{-\det(g_{MN} + 2\pi\alpha' F_{MN})} \ , \qquad (2.1) \\ S_{\text{D8}}^{CS} &= \frac{1}{48\pi^3} \int_{D8} C_3 \text{tr} \, F^3 \ , \qquad (2.2) \end{aligned}$$

where $T_8 = 1/((2\pi)^8 l_s^9)$, the tension of the D8-brane, $F_{MN} = \partial_M A_N - \partial_N A_M - i\,[A_M, A_N]$ $(M, N = 0, 1, \cdots, 8)$, and g_{MN} is the induced metric on D8-branes. To make explicit expressions we need to know the background metric, delaton, and RR fields produced by N_c D4 branes and the form of the gauge fields A_M, which will be reviewed in the following sections. The formulas in this subsection will be presented again when they are needed. However collecting the formulas here will make every pieces as a whole picture.

2.2 N_c Dp branes background

In this subsection we review the D4 brane backgrounds and D3 brane backgrounds. For more details we refer to [75].

2.2.1 N_c D4 branes

There are two background solutions for D4 branes: Soliton background and black hole background. The former corresponds to the zero temperature or low temperature and the latter corresponds to the high temperature.

Soliton Background: zero tempearture

The metric, dilaton ϕ, and the 3-form RR field C_3 in N_c D4-branes background are given by

$$\begin{aligned} ds^2 &= \left(\frac{U}{R}\right)^{3/2}\left(-dt^2+\delta_{ij}dx^i dx^j+f(U)d\tau^2\right)+\left(\frac{R}{U}\right)^{3/2}\left(\frac{dU^2}{f(U)}+U^2 d\Omega_4^2\right)\ , \\ e^{\phi} &= g_s\left(\frac{U}{R}\right)^{3/4}\ ,\ F_4\equiv dC_3=\frac{2\pi N_c}{V_4}\epsilon_4\ ,\ f(U)\equiv 1-\frac{U_{\rm KK}^3}{U^3}\ , \end{aligned} \tag{2.3}$$

where $x^\mu = x^{0,1,2,3}$, $\tau(\equiv x^4)$ is the compact variable on S^1. U and Ω_4 are the radial coordinate and four angle variables in the $x^{5,6,7,8,9}$ direction. $V_4 = 8\pi^2/3$ is the volume of unit S^4 and ϵ_4 is the corresponding volume form. To avoid a conical singularity at $U = U_{\rm KK}$ the period of $\delta\tau$ of the compactified τ direction is set to

$$\delta\tau = \frac{4\pi}{3}\frac{R^{3/2}}{U_{\rm KK}^{1/2}} =: 2\pi R_{KK} =: \frac{2\pi}{M_{\rm KK}}\ . \tag{2.4}$$

This supergravity solution above is regular everywhere and is completely specified by the string coupling constant, g_s, the Ramond-Ramond flux quantum(*i.e.*the number of D4 branes), N_c, and the constant $U_{\rm KK}$. The remaining parameter R is given by

$$R^3 \equiv \pi g_s N_c l_s^3\ , \tag{2.5}$$

where l_s are the string length.

The field theory defined by Kaluza-Klein mass($M_{\rm KK}$) and the four-dimensional coupling constant at the compactification scale, g_{YM}

$$M_{\rm KK} \equiv \frac{2\pi}{\delta\tau} = \frac{3}{2}\frac{U_{\rm KK}^{1/2}}{R^{3/2}} \ , \quad g_{YM}^2 = 3\sqrt{\pi}\left(\frac{g_s U_{KK}}{N_c l_s}\right)^{1/2} \tag{2.6}$$

The parameters R, $U_{\rm KK}$, and g_s may be expressed in terms of $M_{\rm KK}$, $\lambda(= g_{YM}N_c)$, and l_s as

$$R^3 = \frac{1}{2}\frac{\lambda l_s^2}{M_{\rm KK}} \ , \quad U_{\rm KK} = \frac{2}{9}\lambda M_{\rm KK} l_s^2 \ , \quad g_s = \frac{1}{2\pi}\frac{\lambda}{M_{\rm KK}N_c l_s} \tag{2.7}$$

Black hole background: finite tempearture

For a finite temperature we have two possible geometries.

One is to follow the standard prescription: analytically continue the time coordinate $t \to t_E = it$, periodically identify t_E with period $\delta t_E = \frac{1}{T}$, and impose anti-periodic boundary condition on the fermions around the t_E-circle. That is simply the Euclideanized version of (2.3),

$$ds^2 = \left(\frac{U}{R}\right)^{3/2}\left(dt_E^2 + \delta_{ij}dx^i dx^j + f(U)d\tau^2\right) + \left(\frac{R}{U}\right)^{3/2}\left(\frac{dU^2}{f(U)} + U^2 d\Omega_4^2\right) \ ,$$

which dominates at low temperature.

The other is to consider the black hole geometry, which is another saddle point of the Euclidean path integral over supergravity (or rather, string) configuration.

$$\begin{aligned} ds^2 &= \left(\frac{U}{R}\right)^{3/2}\left(f(U)dt_E^2 + \delta_{ij}dx^i dx^j + d\tau^2\right) + \left(\frac{R}{U}\right)^{3/2}\left(\frac{dU^2}{f(U)} + U^2 d\Omega_4^2\right) \ , \\ e^{\phi} &= g_s\left(\frac{U}{R}\right)^{3/4} \ , \ F_4 \equiv dC_3 = \frac{2\pi N_c}{V_4}\epsilon_4 \ , \ f(U) \equiv 1 - \frac{U_T^3}{U^3} \ , \end{aligned} \tag{2.8}$$

which dominates at high temperature. To avoid a conical singularity at $U = U_T$ the period of dt_E of the compactified τ direction is set to

$$\delta t_E = \frac{4\pi}{3}\frac{R^{3/2}}{U_T^{1/2}} =: \frac{1}{T} \ . \tag{2.9}$$

The relation between parameters are as follows

$$g_{YM}^2 = 4\pi g_s \quad \Rightarrow \quad \lambda = 4\pi g_s N_c \ . \tag{2.10}$$

The phase transition between soliton background and black hole background occurs when $\delta\tau = \delta t_E$ *i.e.* at the critical temperature T_c

$$T_c = \frac{M_{\rm KK}}{2\pi} \ . \tag{2.11}$$

It corresponds to confinement/deconfinement transition.

2.2.2 N_c D3 Background

D3 brane background are as follows.

$$\begin{aligned} ds^2 &= \left(\frac{U}{R}\right)^2 \left(f(U)dt_E^2 + \delta_{ij}dx^i dx^j\right) + \left(\frac{R}{U}\right)^2 \left(\frac{dU^2}{f(U)} + U^2 d\Omega_5^2\right) \ , \\ e^\phi &= 1, \ F_5 \equiv dC_4 = \frac{2\pi N_c}{V_4}\epsilon_4 \ , \ f(U) \equiv 1 - \frac{U_T^4}{U^4} \ , \end{aligned} \tag{2.12}$$

where to avoid the conical singularity the temperature is determined as

$$\delta t_E = \frac{\pi R^2}{U_T} =: \frac{1}{T} \ , \tag{2.13}$$

and R is

$$R^4 = 4\pi g_s N \alpha'^2 \ , \quad g_{YM}^2 = 4\pi g_s \ , \tag{2.14}$$

In the literature there are a few widely used different conventions in expressing the metric components. We list some of them here for future use.

Relation to other conventions:
For $z := \frac{R^2}{U}$ and $z_H := \frac{R^2}{U_T}$,

$$\begin{aligned} ds^2 &= \frac{R^2}{z^2}\left(-f dt^2 + d\vec{x}^2 + \frac{dz^2}{f}\right) + R^2 d\Omega_5^2 \, , \\ f &= 1 - \frac{z^4}{z_H^4} \ , \quad T = \frac{1}{\pi z_H} \, . \end{aligned} \tag{2.15}$$

For $y = \frac{z}{z_H}$,

$$ds^2 = \frac{R^2}{z_H^2 y^2}\left(-f dt^2 + d\vec{x}^2 + z_H^2 \frac{dz^2}{f}\right) + R^2 d\Omega_5^2\,, \tag{2.16}$$
$$f = 1 - y^4\,, \qquad T = \frac{1}{\pi z_H}\,.$$

For $u = \frac{z^2}{z_H^2}$,

$$ds^2 = \frac{\pi^2 T^2 R^2}{u}\left(-f(u)dt^2 + d\vec{x}^2\right) + \frac{R^2}{4f(u)u^2}du^2 + R^2 d\Omega_5^2\,, \tag{2.17}$$
$$f = 1 - u^2\,, \qquad T = \frac{1}{\pi z_H}\,,$$

2.3 DBI action

Since we know the background fields we can compute DBI action. We first calculate the induced metric (the pull back of the metric from the background metric). Then make the gauge field specific. In the last subsection we show the general DBI action formula and specific form corresponding to the specified gauge field or approximation scheme.

2.3.1 Induced metric

D8 brane in D4 brane background

The induced metric on the D8 branes from the gravity background (2.3) and (2.8) may be written as

$$ds^2_{\rm D8} \equiv g_{tt}dt^2 + g_{xx}\delta_{ij}dx^i dx^j + g_{UU}\,dU^2 + g_{SS}d\Omega_4^2 \tag{2.18}$$
$$\equiv \alpha\left(\frac{U}{R}\right)^{3/2} dt^2 + \left(\frac{U}{R}\right)^{3/2}\delta_{ij}dx^i dx^j + \left(\frac{R}{U}\right)^{3/2}\gamma\, dU^2 + \left(\frac{R}{U}\right)^{3/2} U^2 d\Omega_4^2\,, \tag{2.19}$$

where for the KK background

$$\alpha \;\to\; 1\;, \quad \gamma \;\to\; \frac{1}{f(U)} + \left(\frac{\partial x^4}{\partial U}\right)^2 \left(\frac{U}{R}\right)^3 f(U)\;,$$
$$f(U) \;\to\; 1 - \left(\frac{U_{\rm KK}}{U}\right)^3\;, \tag{2.20}$$

and for the BH background

$$\alpha \to f(U)\;, \quad \gamma \to \frac{1}{f(U)} + \left(\frac{\partial x^4}{\partial U}\right)^2 \left(\frac{U}{R}\right)^3\;,$$
$$f(U) \;\to\; 1 - \left(\frac{U_T}{U}\right)^3\;. \tag{2.21}$$

The embedding information is encoded only in γ and thereby g_{UU}.

D7 brane in D3 background

Instead of considering a general case let us consider the massless quark embedding as an illustration and for a future use. In this case analytic solutions are available [98]. The induced metric on D7 brane from (2.15) becomes simply $AdS_5 \times S^3$ independent of the gauge field.

$$ds^2 = \frac{z^2}{R^2}(-f dt^2 + d\vec{x}^2) + f^{-1}\frac{R^2}{z^2}dz^2 + R^2 d\Omega_3^2\;, \quad f \equiv 1 - \frac{z_H^4}{z^4}\;, \tag{2.22}$$

If we work in units of $R = 1$ SUGRA and SYM quantities will be tied by $\alpha' = 1/\sqrt{\lambda}$ with $\lambda = 4\pi g_s N_c$.

2.3.2 Gauge Fields

Since $\mathcal{A}$ is $U(N_f)$ valued, it may be decomposed into an $SU(N_f)$ part(A) and a $U(1)$ part($\widehat{A}$),

$$\mathcal{A} = A + \frac{1}{\sqrt{2N_f}}\widehat{A}\;, \qquad \mathcal{F} = F + \frac{1}{\sqrt{2N_f}}\widehat{F}\;, \tag{2.23}$$

where $A \equiv A^a T^a, F \equiv F^a T^a$ and the $SU(N_f)$ generators T^a are normalized as

$$\mathrm{tr}\,(T^a T^b) = \frac{1}{2}\delta^{ab}\;. \tag{2.24}$$

Without index the gauge field and the field strength should be understood as a 1 form and 2 form respectively.

2.3.3 DBI action

General expression

D8 brane action

With the induced metric (2.18) and the pertinent guage fields, the general DBI action follows as

$$\begin{aligned} S_{\rm DBI} = -\mathcal{N}\ {\rm tr} \int d^4x dU\ e^{-\phi} g_{SS}^2 \Big[& -g_{00} g_{xx}^3 g_{UU} - g_{xx}^3 F_{0U} F_{0U} \\ & -g_{xx}^2 g_{UU} \sum_i F_{0i} F_{0i} - g_{00} g_{xx}^2 \sum_i F_{iU} F_{iU} \\ & -g_{00} g_{xx} g_{UU} \sum_{i>j} F_{ij} F_{ij} - g_{xx} \sum_{i>j} F_{ij} F_{ij} F_{U0} F_{U0} + \cdots \Big]^{1/2} \end{aligned} \tag{2.25}$$

where $e^{-\phi} = g_s (U/R)^{3/4}$ and $\mathcal{N} \equiv T_8 \Omega_4$. The D_8 brane tension is T_8 and Ω_4 is the volume of a unit S^4. [1] The F^3 and F^5 terms cancel by symmetry. Among the F^4 terms we only retained the relevant term for our discussion below.

D7 brane action

Similiary

$$\begin{aligned} S_{\rm DBI} = -\mathcal{N}\ {\rm tr} \int d^4x dZ\ g_{SS}^{3/2} \big[& -g_{00} g_{xx}^3 g_{ZZ} - g_{xx}^3 F_{0Z} F_{0Z} \\ & -g_{xx}^2 g_{ZZ} \sum_i F_{0i} F_{0i} - g_{00} g_{xx}^2 \sum_i F_{iZ} F_{iZ} \\ & -g_{00} g_{xx} g_{ZZ} \sum_{i>j} F_{ij} F_{ij} - g_{xx} \sum_{i>j} F_{ij} F_{ij} F_{Z0} F_{Z0} + \cdots \Big]^{1/2} \end{aligned} \tag{2.26}$$

The result is analogous to the D4/D8 case (2.25) with three differences: 1) $\mathcal{N} = T_7 \Omega_3$; 2) there is no contribution from the dilaton; 3) $g_{SS}^{3/2}$ appears instead of $g_{SS}^{4/2}$, since the compact space is S^3 not S^4.

[1] We absorb $2\pi\alpha'$ into the gauge field for notational convenience. It will be recalled in the final physical quantities.

Baryonic background gauge field

The $U(1)$ charge at the boundary is related to $U(1)$ gauge field in the bulk.

$$A_t = A_t(U) \ , \tag{2.27}$$

and the chemical potential is related to the $A_t(\infty)$. To accommodate a static baryonic electric field on D8 branes both in vacuum and matter, we follow [90] to define

$$A_t = A_t(U) \ , \quad A_x = -Et + h_x(U) \ . \tag{2.28}$$

The magnetic field is

For example the DBI action (2.25) is written as

$$S_{\rm DBI} = -\mathcal{N} \int dU \ e^{-\phi} g_{SS}^2 g_{xx} \times \sqrt{|g_{tt}| g_{xx} g_{UU} - (2\pi\alpha')^2 \left(g_{xx} (A_t')^2 + g_{UU} (\dot{A}_x)^2 - |g_{tt}| (A_x')^2 \right)} \tag{2.29}$$

With the induced metric (2.18) and the guage fields (2.28). $\mathcal{N} \equiv (2N_f) T_8 V_4$. $2N_f$ comes from the fact that we consider N_f branes and anti-branes and $V_4 (= 8/3\pi^2)$ is the volume of the unit S^4 which is due to the trivial integral over S^4. $'$ is the derivative with respect to U and $\dot{}$ is the derivative with respect to t

$1/\lambda$ expansion

In the soliton background the 5D Yang-Mills action yields as the leading terms in the $1/\lambda$ expansion of the DBI action,

$$S_{YM} = -\kappa \int d^4x dZ \ {\rm tr} \left[\frac{1}{2} K^{-1/3} \mathcal{F}_{\mu\nu}^2 + M_{\rm KK}^2 K \mathcal{F}_{\mu Z}^2 \right] \ , \tag{2.30}$$

where we change the variables as

$$K \equiv 1 + Z^2 \ , \quad U = U_0 K^{1/3} \ , \quad dU = \frac{2U_0}{3} \frac{Z}{K^{2/3}} dZ \ , \quad f = 1 - \frac{1}{K} \ ,$$

$\mu, \nu = 0, 1, 2, 3$ are 4D indices and the fifth(internal) coordinate Z is dimensionless. There are three things which are inherited by the holographic dual gravity theory: $M_{\rm KK}, \kappa$, and K. $M_{\rm KK}$ is the Kaluza-Klein scale and we will set $M_{\rm KK} = 1$ as our unit. κ is defined as

$$\kappa = \lambda N_c \frac{1}{216\pi^3} \equiv \lambda N_c a \ , \ . \tag{2.31}$$

$\mathcal{A}$ is the 5D $U(N_f)$ 1-form gauge field and $\mathcal{F}_{\mu\nu}$ and $\mathcal{F}_{\mu Z}$ are the components of the 2-form field strength $\mathcal{F} = \mathrm{d}\mathcal{A} - i\mathcal{A} \wedge \mathcal{A}$.

For $N_f = 2$ the action (2.30) is reduced to

$$\begin{aligned} S_{YM} &= -\kappa \int d^4x dZ \ \mathrm{tr} \left[\frac{1}{2} K^{-1/3} F_{\mu\nu}^2 + K F_{\mu Z}^2 \right] \\ &\quad -\frac{\kappa}{2} \int d^4x dZ \ \left[\frac{1}{2} K^{-1/3} \widehat{F}_{\mu\nu}^2 + K \widehat{F}_{\mu Z}^2 \right] \ , \end{aligned} \tag{2.32}$$

where the $SU(2)$ and $U(1)$ parts are completely desentangled in the Yang-Mills action.

Mesonic fluctuation around the background field

If we consider the fluctuation $(A_\alpha(x^\alpha))$ around the classical configuration $\mathbb{A}_0$ (3.10), which is due to homogeneous matter at $Z = 0$, the action can be expanded as

$$\begin{aligned} &\frac{R^{2/3}\mathcal{N}}{2g_s}(2\pi\alpha')^2 \mathrm{tr} \int dU U^{5/2} \frac{1}{\sqrt{-\alpha\gamma}} \left[\frac{2\alpha\gamma\Delta^{-1}}{(2\pi\alpha')^2} + 2\Delta(\partial_U \mathbb{A}_0) F_{U0} + \Delta^3 F_{U0} F_{U0} \right. \\ &\left. \quad + \Delta\alpha \sum_i F_{iU} F_{iU} + \Delta\gamma \left(\frac{R}{U}\right)^3 \sum_i F_{0i} F_{0i} + \Delta^{-1}\alpha\gamma \left(\frac{R}{U}\right)^3 \sum_{i>j} F_{ij} F_{ij} \right] \ , \end{aligned}$$

up to quadratic terms. $F_{\alpha\beta} \equiv \partial_\alpha A_\beta - \partial_\beta A_\alpha - i[A_\alpha, A_\beta]$ and

$$\Delta \equiv \frac{1}{\sqrt{1 + \frac{(2\pi\alpha')^2}{\alpha\gamma}(\mathbb{A}_0')^2}} \ . \tag{2.33}$$

Similarly for D3/D7 model,

$$S = N\mathrm{tr}\int d^4xdZk_1\left[\Delta^3 F_{Z0}F_{Z0} + \Delta k_2\sum_i F_{0i}F_{0i}\right.$$
$$\left. +\Delta k_3\sum_i F_{iZ}F_{iZ} + \Delta^{-1}k_2k_3\sum_{i>j}F_{ij}F_{ij}\right] ,$$

where the information of the background field $\mathbb{A}_0$ is encoded in Δ and

$$N = \frac{\lambda N_f N_c}{2(2\pi)^4} , \qquad \Delta = \sqrt{1+d^2Z^{-6}} ,$$
$$k_1 = Z^3 , \qquad k^2 = Z^{-4}f^{-1} , \qquad k^3 = f^{-1} . \tag{2.34}$$

2.4 CS action

The 5D Chern-Simons action is obtained from the Chern-Simons action of the D8 branes by integrating F_4 RR flux over the S^4, which is nothing but N_C.

$$S_{CS} = \frac{N_c}{24\pi^2}\int_{M^4\times R}\omega_5^{U(N_f)}(\mathcal{A}) , \tag{2.35}$$

$\omega_5^{U(N_f)}(\mathcal{A})$ is the Chern-Simons 5-form for the $U(N_f)$ gauge field:

$$\omega_5^{U(N_f)}(\mathcal{A}) = \mathrm{tr}\left(\mathcal{A}\mathcal{F}^2 + \frac{i}{2}\mathcal{A}^3\mathcal{F} - \frac{1}{10}\mathcal{A}^5\right) , \tag{2.36}$$

For $N_f = 2$ it reads more explicitly

$$S_{CS} = \frac{N_c}{24\pi^2}\int\left[\frac{3}{2}\widehat{A}\mathrm{tr}\,F^2 + \frac{1}{4}\widehat{A}\widehat{F}^2 + \frac{1}{2}\,\mathrm{d}\left\{\widehat{A}\ \mathrm{tr}\ \left(2FA + \frac{i}{2}A^3\right)\right\}\right] \tag{2.37}$$

$$= \frac{N_c}{24\pi^2}\epsilon_{MNPQ}\int d^4xdZ\left[\frac{3}{8}\widehat{A}_0\mathrm{tr}\,(F_{MN}F_{PQ}) - \frac{3}{2}\widehat{A}_M\mathrm{tr}\,(\partial_0 A_N F_{PQ})\right.$$
$$+\frac{3}{4}\widehat{F}_M N\mathrm{tr}\,(A_0F_{PQ}) + \frac{1}{16}\widehat{A}_0\widehat{F}_{MN}\widehat{F}_{PQ} - \frac{1}{4}\widehat{A}_M\widehat{F}_{0N}\widehat{F}_{PQ}$$
$$\left.+\frac{3}{2}\partial_N(\widehat{A}_M\mathrm{tr}\,A_0F_{PQ})\right] + \frac{N_c}{48\pi^2}\int\mathrm{d}\left\{\widehat{A}\ \mathrm{tr}\ \left(2FA + \frac{i}{2}A^3\right)\right\} , \tag{2.38}$$

Chapter 3

Thermodynamics of Dense Matter

3.1 Homogeneous matter

3.1.1 Introduction

Dense hadronic matter is of interest to a number of fundamental problems that range from nuclear physics to astrophysics. QCD at finite baryon density is notoriously difficult: (1) the introduction of a chemical potential causes most lattice simulations to be numerically noisy owing to the sign problem; (2) the baryon-baryon interaction is strong making most effective approaches limited to subnuclear matter densities.

In the limit of a large number of colors N_c, QCD is an effective theory of solely mesons where baryons appear as chiral skyrmions. Dense matter in large N_c is a skyrmion crystal with spontaneous breaking of chiral symmetry at low density, and restored or stripped (Overhauser) chiral symmetry at high density. While some of these aspects can be studied qualitatively using large N_c motivated chiral models [77], they still lack a first principle understanding.

In this chapter we study the property of dense matter using SS model. In section 2, we introduce the $U(1)_V$ field $\mathcal{A}_0$ in bulk and show how the baryon charge density n_B affects its minimal profile. In section 2 and 3, we construct the bulk hamiltonian and derive the energy density as a function of the identified baryon density. The energy density is found to grow about quadratically

with the baryon density. We conclude in section 4. Throughout, the canonical formalism will be used.

3.1.2 Thermodynamics from branes

Let $\mathcal{A}_0(U)$ be a $U(1)_V$ valued background gauge field in bulk. Its boundary value is related to the baryon chemical potential [14, 50, 73, 74]. In the absence of the source, the effective action of the D8-branes (3.24) becomes

$$S_{\rm D8} = -\frac{N_f T_8 V_4}{g_s}\int d^4x\, dU U^4 \left[f\left(\tau'\right)^2 + \left(\frac{R}{U}\right)^3\left(f^{-1} - \left(2\pi\alpha'\mathcal{A}_0'\right)^2\right)\right]^{\frac{1}{2}}, \quad (3.1)$$

where $\mathcal{A}_0' = \frac{d\mathcal{A}_0}{dU}$ and the Chern-Simons action vanishes. The equations of motion for $\tau(U)$ and $\mathcal{A}_0(U)$ are [50]

$$\frac{d}{dU}\left[\frac{U^4 f\,\tau'}{\sqrt{f\left(\tau'\right)^2 + \left(\frac{R}{U}\right)^3\left(f^{-1} - \left(2\pi\alpha'\mathcal{A}_0'\right)^2\right)}}\right] = 0,$$

$$\frac{d}{dU}\left[\frac{U^4\left(\frac{R}{U}\right)^3\mathcal{A}_0'}{\sqrt{f\left(\tau'\right)^2 + \left(\frac{R}{U}\right)^3\left(f^{-1} - \left(2\pi\alpha'\mathcal{A}_0'\right)^2\right)}}\right] = 0.$$

In this paper we consider only the case $\tau' = 0$, Sakai-Sugimoto's original embedding [28, 29], where the D8-branes configuration in the τ coordinate is not affected by the existence of background $\mathcal{A}_0$. This corresponds to $\tau = \frac{\delta\tau}{4}$, the maximal asymptotic separation between D8 and $\overline{\rm D8}$ branes.

To compare with [28, 29] we change the variable U to z through

$$U \equiv (U_{\rm KK}^3 + U_{\rm KK} z^2)^{1/3} \quad (3.2)$$

The action (3.1) is then

$$S_{\rm D8} = -N_f\widetilde{T}\int d^4x\int_0^\infty dz\, U^2\sqrt{1 - (2\pi\alpha')^2\frac{9}{4}\frac{U_z}{U_{\rm KK}}(\partial_z\mathcal{A}_0)^2}\,, \quad (3.3)$$

where we used $\tau' = 0$ and $\widetilde{T} \equiv \frac{N_c M_{\rm KK}}{216\pi^5\alpha'^3}$. It is useful to define the dimensionless

quantities

$$Z \equiv \frac{z}{U_{\rm KK}}, \quad K(U) \equiv 1 + Z^2 = \left(\frac{U}{U_{\rm KK}}\right)^3 , \tag{3.4}$$

in terms of which the action is written as[1]

$$S_{\rm D8} = -a \int d^4x \int dZ\, K^{2/3} \sqrt{1 - bK^{1/3}(\partial_Z \mathcal{A}_0)^2} , \tag{3.5}$$

where

$$a \equiv \frac{N_c N_f \lambda^3 M_{\rm KK}^4}{3^9 \pi^5} , \qquad b \equiv \frac{3^6 \pi^2}{4\lambda^2 M_{\rm KK}^2} . \tag{3.6}$$

Now we introduce the baryon source coupled to $\mathcal{A}_0$ through the Chern-Simons term [14, 30, 76] as mentioned before. We assume that baryons are uniformly distributed over $\mathbb{R}^3$ space whose volume is V. For large λ, the instanton size is $1/\sqrt{\lambda}$ [30, 33]. It can be treated as a static delta function source at large N_c. For a uniform baryon distribution, the source is

$$S_{\rm source} = N_c n_B \int d^4x \int dZ\, \delta(Z) \mathcal{A}_0(Z). \tag{3.7}$$

The equation of motion of $\mathcal{A}_0$ is

$$\frac{d}{dZ} \frac{\partial \mathcal{L}}{\partial(\partial_Z \mathcal{A}_0)} = n_q \delta(Z) , \tag{3.8}$$

which yields

$$\frac{\partial \mathcal{L}}{\partial(\partial_Z \mathcal{A}_0)} = \frac{1}{2} n_q \, \mathrm{sgn}(Z) , \tag{3.9}$$

where $n_q = N_c n_B$ is the quark density and the step function $\mathrm{sig}(Z)$ is determined by the symmetry between D8 ($Z > 0$) and $\overline{\rm D8}$($Z < 0$). By integrating

[1]The integral is extended to $(-\infty, \infty)$ to take into account $\overline{\rm D8}$ branes as well as D8 branes.

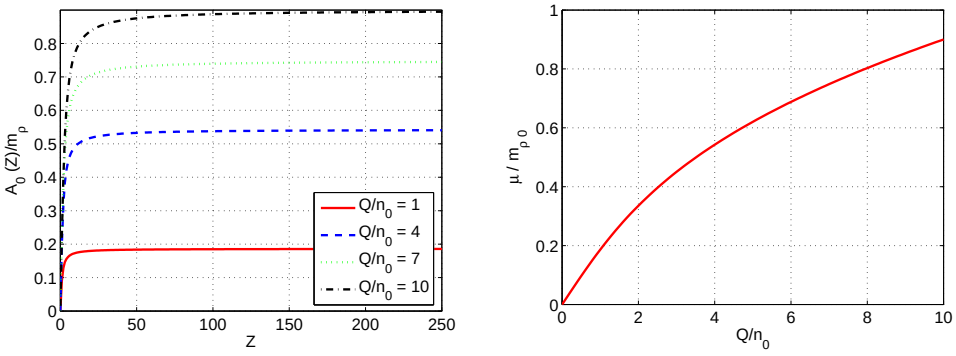

(a) (b)

Figure 3.1: (a) The profile of $\mathcal{A}_0(Z)$, (b) Chemical potential vs baryon charge ($\frac{\mu}{m_\rho}$ vs $\frac{Q}{n_0}$, where $Q \equiv n_q/2$).

once more we get the classical solution $\mathcal{A}_0$

$$\mathcal{A}_0(Z;n_q) = \mathcal{A}_0(0) + \int_0^Z dZ \frac{n_q/2}{\sqrt{(ab)^2K^2 + bK^{1/3}n_q^2/4}} \ . \tag{3.10}$$

We introduce the "baryon charge chemical potential of a quark", μ, by [73, 74]

$$\mu(n_q) \equiv \lim_{|Z|\to\infty} \mathcal{A}_0(Z;n_q) \ . \tag{3.11}$$

This relation also defines μ as a function of n_q and vice versa. Furthermore we define the baryon chemical potential as

$$\mu_B = m_B + N_c\mu \ . \tag{3.12}$$

In Fig.(3.1a) we plot the profile of $\mathcal{A}_0(Z)$ in the Z coordinate and in Fig.(3.1b) we show μ for various baryon densities. Since we work in the canonical formalism μ is more like a Lagrange constraint.

Throughout, the numerics will be carried using the following values [28, 29]: $N_f = 2$, $N_c = 3$, $f_\pi = 92.6$MeV, and $m_\rho = 776$MeV. The smallest eigenvalue was calculated to be $\lambda_1 = 0.669$. Using these five values we can estimate $M_{\rm KK}$,

λ, κ, a, and b:

$$M_{\rm KK} = \frac{m_\rho}{\sqrt{\lambda_1}} \simeq 950 MeV, \quad \lambda \equiv g_{YM}^2 N_c = f_\pi^2 \frac{54\pi^4}{N_c M_{\rm KK}^2} \simeq 16.71,$$
$$\kappa \equiv \frac{\lambda N_c}{216\pi^3} \simeq 0.0075, \tag{3.13}$$

and

$$a = 3.76 \cdot 10^9 MeV^4, \quad b = 7.16 \times 10^{-6} MeV^{-2}. \tag{3.14}$$

The definition of κ and λ are different from [28, 29] by a factor of 2, but it is consistent with [30]. In all figures n_B is normalized to $\frac{n_B}{n_0}$, with n_0 the nuclear matter density,

$$n_0 = 0.17 fm^{-3} \simeq 1.3 \times 10^6 MeV^3. \tag{3.15}$$

3.1.3 Thermodynamics

Consider the action (3.5) with the source term (3.8),

$$S = \int d^4x \int_{-\infty}^{+\infty} dZ \, \mathcal{L}$$
$$\text{with} \quad \mathcal{L} \equiv -aK^{2/3} \sqrt{1 - bK^{1/3} (\partial_Z \mathcal{A}_0)^2} + n_q \delta(Z) \mathcal{A}_0(Z) \, . \tag{3.16}$$

The $\mathcal{A}_0$ is an auxillary field with no time-dependence. It can be eliminated by the equation of motion (3.9) and (3.10). The energy is

$$\begin{aligned} U(n_q) &= \int dx^3 \int_{-\infty}^{+\infty} dZ \, (-\mathcal{L}) \\ &= aV \int_{-\infty}^{+\infty} dZ \, K^{2/3} \sqrt{1 + \frac{n_q^2}{4a^2 b} K^{-5/3}} - n_q \mu \, , \end{aligned} \tag{3.17}$$

where V is short for $\int dx^3$ and we may set $\mu = 0$. The chemical potential μ is constrained by the Gibbs relation $\mu = \frac{\partial F(n_q)}{\partial n_q}$ where $F(n_q)$ is the Helmholtz free energy which is $U(n_q)$ at zero temperature. Thus

$$\mu = \int_{-\infty}^{\infty} dZ \frac{n_q/4}{\sqrt{(ab)^2 K^2 + bK^{1/3} n_q^2/4}} \quad , \tag{3.18}$$

which is in agreement with the solution (3.10) for $A_0(0) = 0$. We note that this construction is consistent with [14, 50, 73] where the grand potential is identified with the DBI action at finite μ.

In terms of the baryon number density n_B (n_q/N_c) the regularized Helmholtz free energy is

$$\frac{F_{\rm reg}(n_B)}{aV} \equiv \int_{-\infty}^{\infty} dZ K^{2/3} \left[\sqrt{1 + \frac{(N_c n_B)^2}{4a^2 b} K^{-5/3}} - 1 \right] , \qquad (3.19)$$

after subtracting the vacuum value. The regularized internal energy U, pressure p and grand potential Ω as a function of baryon number density n_B or the baryon chemical potential μ_B are

$$\begin{aligned}
\frac{U_{\rm reg}(n_B)}{aV} &= \int_{-\infty}^{\infty} dZ K^{2/3} \left[\sqrt{1 + \frac{(N_c n_B)^2}{4a^2 b} K^{-5/3}} - 1 \right] , \\
\frac{p(n_B)_{\rm reg}}{a} &= \int_{-\infty}^{\infty} dZ\, K^{2/3} \left[1 - \frac{1}{\sqrt{1 + \frac{(N_c n_B)^2}{4a^2 b} K^{-5/3}}} \right] , \\
\frac{\Omega_{\rm reg}(\widetilde{\mu_B})}{aV} &= \int_{-\infty}^{\infty} dZ\, K^{2/3} \left[\frac{1}{\sqrt{1 + \frac{(N_c n_B(\widetilde{\mu_B}))^2}{a^2 b} K^{-5/3}}} - 1 \right] , \\
\widetilde{\mu_B} &= N_c \int_{-\infty}^{\infty} dZ \frac{N_c n_B/4}{\sqrt{(ab)^2 K^2 + b K^{1/3} (N_c n_B/2)^2}} ,
\end{aligned} \qquad (3.20)$$

where $\widetilde{\mu_B} \equiv \mu_B - m_B = N_c \mu$.

In Fig.(3.2) we present the numerical plots of these thermodynamic functions with the numerical inputs in section 3.1. For small baryon densities the energy density is quadratic in n_B/n_0 (or μ/m_ρ). At large baryon densities it is of order $(n_B/n_0)^{1.4}$. The small density limit can be qualitatively understood by noting that in bulk the $\mathcal{A}_0$ configuration for fixed charge is obtained by minimizing the induced DBI action of D8-$\overline{\rm D8}$. Thus only flavor-meson mediated interactions between the point-like baryons are included. At large N_c the $D4$ mediated correlated gravitons (glueballs on the boundary) are heavy and decouple. Since our point baryonic vertices in bulk map on infinite size skyrmions at the boundary this implies that only ω exchanges survive at large N_c. Rho and pion exchange relies on skyrmion gradients which are zero. At

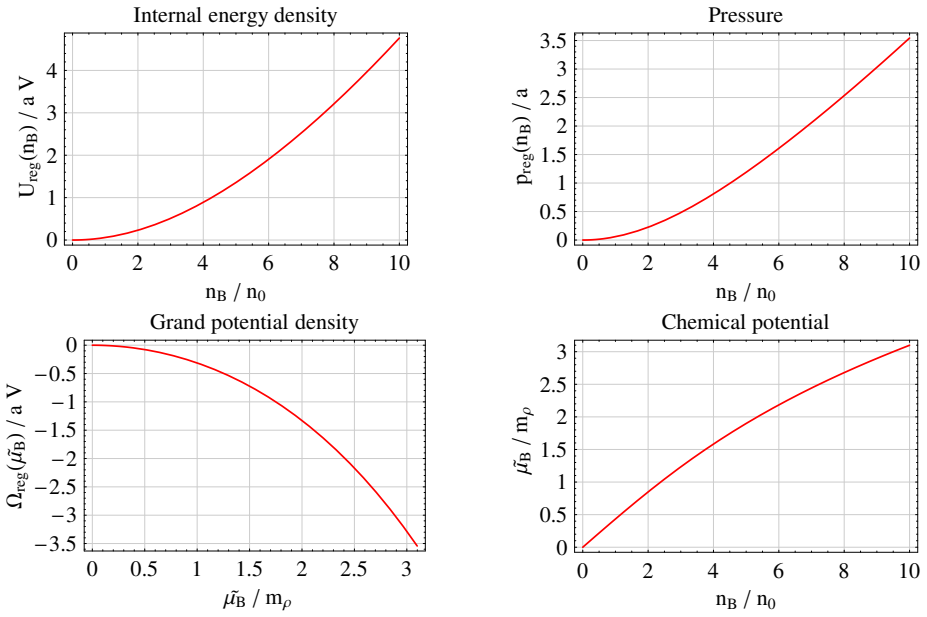

Figure 3.2: Numerical behaviour of the thermodynamic functions: See Eq.(3.20)

low baryon densities, the dominant Skyrmion-omega-Skyrmion interaction is two-body and repulsive. Thus the energy density is positive and quadratic in the baryon density. The baryonic matter is prevented from flying apart by the container V. At large baryon densities, the energy density softens as the quark chemical potential is seen to saturate to $(n_B/n_0)^{0.4}$ numerically. We recall that the baryons are fixed sources so no Fermi motion is involved to this order. The pressure behaves as $(n_B/n_0)^2$ at low baryon densities, and again softens to $(n_B/n_0)^{7/5}$ at large baryon densities from the plot. We sum-

Thermodynamic function	$n_B/n_0 \sim 0$	$n_B/n_0 \sim 10$	$n_B/n_0 \to \infty$
Internal energy	$(n_B/n_0)^2$	$(n_B/n_0)^{1.85}$	$(n_B/n_0)^{1.4}$
Pressure	$(n_B/n_0)^2$	$(n_B/n_0)^{1.45}$	$(n_B/n_0)^{1.4}$
Chemical potential	$(n_B/n_0)^1$	$(n_B/n_0)^{0.67}$	$(n_B/n_0)^{0.4}$
Grand potential	$-(\widetilde{\mu_B}/m_\rho)^2$	$-(\widetilde{\mu_B}/m_\rho)^{2.16}$	$-(\widetilde{\mu_B}/m_\rho)^{3.5}$

Table 3.1: Numerical behaviour of the thermodynamic functions: See Eq.(3.20)

marize the behaviour of the thermodynamic functions obtained numerically in Table.(3.1). In this paper we do not consider the back reaction of gravity for baryons or D8 brane, therefore the behaviour at higher densities, say $n_B/n_0 \gg 10$, is not justified.

3.1.4 Conclusions

We have considered a generalization of the chiral model proposed by Sakai and Sugimoto to finite baryon density. The baryon vertices in bulk are attached equally to the D8-$\overline{\text{D8}}$ branes and correspond to S^4 in $D8$. They are treated as stable and point like in $\mathbb{R}^3$ and act as uniform sources of baryon density. Their point-like nature at large N_c and coupling λ imply that their interactions as induced by D8-$\overline{\text{D8}}$ is mostly repulsive through the exchanges of omega mesons.

The bulk energy density grows quadratically with the baryon density before softening at asymptotic densities. The quadratic and repulsive growth is expected from the exchange of omega mesons. The softening reflects on the fact that at asymptotic densities the repulsive baryons form an instable but regular array for fixed volume V. If V acting as a container is removed, the baryons fly away in this version of the SS model. We note that the energy density scales as N_c since $N_c/\sqrt{a}$ is of order 1 as expected from standard large N_c arguments. The DBI action resums (partially) the strong NN-interactions while keeping the leading N_c result unchanged. Since the instanton size is of order $1/\sqrt{\lambda}$ we also note that the resummed contributions are of order λ^0 since the bulk instanton density $\sqrt{\lambda}n_B$ is of order λ^2 (The additional $\sqrt{\lambda}$ here stems from the rescaling of $z \to z/\sqrt{\lambda}$ in the delta-function source at $z = 0$).

The current approach needs to be improved in a number of ways to accomodate the baryon physics expected in the real world. First, the point-like nature of the sources need to be relaxed. This is possible by constructing the pertinent instanton vertex. Also, the point-like limit suggests that the DBI results quoted here are only indicative since higher derivative corrections to the DBI effective action are expected to contribute (see also [28–30] for further comments on this point)). Second, the Fermi motion of the sources need to be included. This can be achieved through a select quantization of the collective variables associated to the baryon vertex insertion. Some of these issues will be addressed in later work.

3.2 Inhomogeneous matter

3.2.1 Introduction

Cold and dense hadronic matter in QCD is difficult to track from first principles in current lattice simulations owing to the sign problem. In large N_c QCD baryons are solitons and a dense matter description using Skyrme's chiral model [78–80] was originally suggested by Skyrme and others [81]. At large N_c and high density matter consisting of solitons crystallizes, as the ratio of potential to kinetic energy $\Gamma = V/K \approx N_c^2$ is much larger than 1. QCD matter at large N_c was recently revisited in [82].

The many-soliton problem can be simplified in the crystal limit by first considering all solitons to be the same and second by reducing the crystal to a single cell with boundary conditions much like the Wigner-Seitz approximation in the theory of solids. A natural way to describe the crystal topology is through T^3 with periodic boundary conditions. In so far, this problem can only be addressed numerically. A much simpler and analytically tractable approximation consists of treating each Wigner-Seitz cell as S^3 with no boundary condition involved. The result is dense Skyrmion matter on S^3 [83–85]. Interestingly enough, the energetics of this phase is only few percent above the energetics of a more involved numerical analysis based on T^3. Skyrmions on S^3 restore chiral symmetry on the average above a critical density. While Skyrmions on S^3 are unstable against T^3, they still capture the essentials of dense matter and chiral restoration in an analytically tractable framework.

Cold dense matter in holographic QCD is a crystal of instantons with $\Gamma = \sqrt{\lambda}/v_F \gg 1$ where $v_F \approx 1/N_c$ is the Fermi velocity. (In contrast hot holographic QCD has $\Gamma = \sqrt{\lambda} \gg 1$). When the wigner-Seitz cell is *approximated* by S^3, the pertinent instanton is defined on $S^3 \times R$. In this chpater, we investigate cold QCD matter using instantons on $S^3 \times R$ in bulk. As a result the initial D4 background is *deformed* to accomodate for the S^3 which is just the back reaction of the flavour crystal structure on the pure gauge theory. Holographic dense matter can be organized in $1/\lambda$ at large N_c. In our model the baryon density is uniform while the chiral condensate is p-wave over a cell.

However, the chiral condensation is averaged to be zero over a cell so that the chiral symmetry is effectively restored in long wavelength limit. We will show that as the average density goes up, it approaches to uniform distribution while the chiral condensate approaches to p-wave over a cell. The energy density in dense medium varies as $n_B^{5/3}$, which is the expected power for non-relativistic fermion. This shows that the Pauli exclusion effect in boundary is encoded in the Coulomb repulsion in the bulk.

In section 2, we define this deformation and discuss the D8 brane embedding structure. The instantons on $S^3 \times R$ in the flavour D8 brane is discussed in section 3. In section 4,5,6,7 we derive the equation of state of cold holographic matter using the small size instanton expansion and in general. In section 8 we show how the holographic small instantons in bulk transmute large size Skyrmions on the boundary. The comparison to other models of nuclear matter is carried in section 9. Our conclusions are in section 10.

3.2.2 D8 brane action

We consider crystallized skyrmions at finite density in the Wigner Seitz approximation. Spatial R^3 is naturally converted to T^3 with periodic boundary conditions. As a result the D4 background geometry is deformed. The baryons are then instantons on $T^3 \times R$. Most solutions are only known numerically on the lattice. A simpler and analytically tractable analysis that captures the essentials of dense matter is to substitute T^3 by S^3 in bulk with no boundary conditions altogether. As a result, the D4 background dual to the crystal is modified with the boundary special space as S^3. Specifically, the 10 dimensional space is that of $(R^1 \times S^3) \times R^1 \times S^4$. The ensuing metric on D4 is therefore

$$ds^2 = \left(\frac{U}{R}\right)^{3/2} \left(-dt^2 + \mathcal{R}^2 d\Omega_3^2 + f(U) d\tau^2\right) + \left(\frac{R}{U}\right)^{3/2} \left(\frac{dU^2}{f(U)} + U^2 d\Omega_4^2\right) , \tag{3.21}$$

$$d\Omega_3 \equiv d\psi^2 + \sin^2\psi \; d\theta^2 + \sin^2\psi \sin^2\theta \; d\phi^2 , \quad f(U) \equiv 1 - \frac{U_{\rm KK}^3}{U^3} , \tag{3.22}$$

$$e^{\phi} = g_s \left(\frac{U}{R}\right)^{3/4} , \; F_4 \equiv dC_3 = \frac{2\pi N_c}{V_4} \epsilon_4 , \tag{3.23}$$

While this compactified metric is not an exact solution to the general relativity (GR) equations for small size S^3, it can be regarded as an approximate solution for large size S^3. Indeed, in this case, the GR equations are seen to be sourced by terms wich are down by the size of S^3. Here, (3.23) can be regarded as an approximation to the stable metric with T^3 for a dense matter analysis. Clearly, the former is unstable against decay to the latter, which will be reflected by the fact that the energy of dense matter on S^3 is higher than that on T^3. As indicated in the introduction, the Skyrmion analysis shows that the energy on S^3 is only few percent that of T^3. So we expect the current approximation to capture the essentials of dense matter in holographic QCD. Specifically, the nature and strength of the attraction and repulsion in dense matter. Indeed, this will be the case as we will detail below.

Now, consider N_f probe D8-branes in the N_c D4-branes background. With $U(N_f)$ gauge field A_M on the D8-branes, the effective action consists of the DBI action and the Chern-Simons action

$$\begin{aligned} S_{\rm D8} &= S_{\rm DBI} + S_{\rm CS} \ , \\ S_{\rm DBI} &= -T_8 \int d^9x \ e^{-\phi} \ {\rm tr} \sqrt{-{\rm det}(g_{MN} + 2\pi\alpha' F_{MN})} \ , \qquad (3.24) \\ S_{\rm CS} &= \frac{1}{48\pi^3} \int_{D8} C_3 {\rm tr} \, F^3 \ . \qquad (3.25) \end{aligned}$$

where $T_8 = 1/((2\pi)^8 l_s^9)$, the tension of the D8-brane, $F_{MN} = \partial_M A_N - \partial_N A_M - i\,[A_M, A_N]$ $(M, N = 0, 1, \cdots, 8)$, and g_{MN} is the induced metric on the D8-branes

$$\begin{aligned} ds^2_{D8} &= \left(\frac{U}{R}\right)^{3/2} (-dt^2 + \Re^2 d\Omega_3^2) + g_{\sigma\sigma} d\sigma^2 + \left(\frac{R}{U}\right)^{3/2} U^2 d\Omega_4^2 \ , \qquad (3.26) \\ g_{\sigma\sigma} &\equiv G_{\tau\tau} \partial_\sigma \tau \partial_\sigma \tau + G_{UU} \partial_\sigma U \partial_\sigma U \ , \qquad (3.27) \end{aligned}$$

where G_{MN} refer to the background metric (3.21) and the profile of the D8 brane is parameterized by $U(\sigma)$ and $\tau(\sigma)$.

The gauge field A_M has nine components, $\mathcal{A}_0$, $A_i = A_{1,2,3}$, $A_\sigma (= A_4)$, and

$A_\alpha (\alpha = 5, 6, 7, 8$, the coordinates on the S^4). We assume

$$\mathcal{A}_0 = \mathcal{A}_0(\sigma) \in U(1) \ , \tag{3.28}$$

$$(A_i = A_i(x^i, \sigma), \quad A_\sigma = A_\sigma(x^i, \sigma)) \in SU(N_f) \ , \tag{3.29}$$

$$A_\alpha = 0 \ . \tag{3.30}$$

Then the action becomes 5-dimensional:

$$\begin{aligned} S_{\rm DBI} = &-\frac{8\pi^2 T_8 R^3}{3g_s} \ {\rm tr} \int dt \epsilon_3 d\sigma \ U \\ &\Bigg[\ \left\{ \left(\frac{U}{R}\right)^{3/2} g_{\sigma\sigma} - (2\pi\alpha')^2 (\partial_\sigma \mathcal{A}_0)^2 \right\} \left\{ \left(\frac{U}{R}\right)^3 + \frac{1}{2}(2\pi\alpha')^2 F_{ij} F^{ij} \right\} \\ &+ \left(\frac{U}{R}\right)^3 (2\pi\alpha')^2 F_{\sigma i} F_\sigma{}^i + \frac{1}{4}(2\pi\alpha')^4 (\epsilon_{ijk} F_{i\sigma} F_{jk})(\epsilon_{ijk} F^i{}_\sigma F^{jk}) \ \Bigg]^{1/2} \ , \end{aligned} \tag{3.31}$$

$$S_{\rm CS} = \frac{N_c}{24\pi^2} {\rm tr} \int \mathcal{A} \wedge F \wedge F \ , \tag{3.32}$$

where ϵ_3 is the volume form of S^3 space and the indices $i, j, k (\in \{\psi, \theta, \phi\})$ are raised by the metric $\tilde{g}^{ij}$ defined by

$$\tilde{g}^{ij} = \left(\frac{1}{\mathcal{R}^2}, \frac{1}{\mathcal{R}^2 \sin^2\psi}, \frac{1}{\mathcal{R}^2 \sin^2\psi \sin^2\theta} \right) \ . \tag{3.33}$$

3.2.3 Instanton in $S^3 \times R^1$

Only $\mathcal{A}_0$ will be determined dynamically in the given instanton background A_i, A_σ. The exact background instanton solution is unknown. Thus we start with an approximate solution which is the SU(2) Yang-Mills instanton solution in the space with metric,

$$ds^2 = d\sigma^2 + \mathcal{R}^2 d\Omega_3 \ . \tag{3.34}$$

This metric is different from our metric in (3.26) and (6.9), where there are warping factors. Furthermore our action is the nonlinear DBI action and not a Yang-Mills action. However it can be shown that the Yang-Mills instanton in the space (3.34) is the leading order solution of $1/\lambda$ expansion of the full

metric and the DBI action as shown in [30] . So the solution can be used in the leading order calculation.

We summarize here the (anti) self dual instanton solution obatained in [86]. Using the ansatz ,

$$A = f(\sigma)U^{-1}dU \ , \qquad U \equiv \cos\psi + i\tau_a \hat{r}^a(\theta,\phi)\sin\psi \ , \tag{3.35}$$

we get the field strength, in terms of vielbein whose relation to the coordinate ψ, θ, ϕ, is specified in [86],

$$F = \frac{(\partial_\sigma f)\tau_a}{\mathcal{R}} \ e^0 \wedge e^a + \frac{1}{2}\left[\frac{2(f^2-f)\tau_d \epsilon^d{}_{bc}}{\mathcal{R}^2}\right] \ e^b \wedge e^c \ , \tag{3.36}$$

where we used $L_a = U^{-1}\partial_a U = \tau_a/\mathcal{R}$. If we require (anti) self-duality,

$$\partial_\sigma f = \pm\frac{2(f^2-f)}{\mathcal{R}} \ , \tag{3.37}$$

then f is determined as

$$f_\pm \equiv \frac{1}{1+e^{\mp 2(\sigma-\sigma_0)/\mathcal{R}}} \ , \tag{3.38}$$

so the field strength of one (anti) instanton solution is

$$F^\pm = (\partial_\sigma f_\pm)\frac{\tau_a}{\mathcal{R}}(e^0 \wedge e^a \pm \frac{1}{2}\epsilon^a{}_{bc}e^b \wedge e^c) \ . \tag{3.39}$$

3.2.4 D8 brane plus Instanton

Now that we have the background instanton configurations, the remaining dynamical variables are τ and $\mathcal{A}_0$. However it can be shown that $\partial_\sigma \tau(\sigma) = 0$ is always a solution of the Euler-Lagrange equation regardless of the gauge field. For simplicity we will work with this specific configuration so that the only dynamical variable is $\mathcal{A}_0$. Let us parameterize $\mathcal{A}_0$ by Z defined as

$$\begin{aligned} U &\equiv (U_{\rm KK}^3 + U_{\rm KK}\sigma^2)^{1/3} \ , \\ Z &\equiv \frac{\sigma}{U_{\rm KK}} \ , \quad K \equiv 1+Z^2 \ . \end{aligned} \tag{3.40}$$

Then the field strength is expressed in terms of Z and the dimensionless radius $\widehat{\mathcal{R}} \equiv \mathcal{R}/U_{\rm KK}$,

$$
\begin{aligned}
F_{Za} &= \frac{1}{U_{\rm KK}} f' \, \frac{\tau_a}{\widehat{\mathcal{R}}} \ , \\
F_{ab} &= \frac{1}{U_{\rm KK}^2} f' \, \frac{\epsilon_{ab}{}^c \tau_c}{\widehat{\mathcal{R}}} \ ,
\end{aligned}
\tag{3.41}
$$

where $f' \equiv \partial_Z f$. The instanton configuration is

$$
f_\pm = \frac{1}{1 + e^{\mp 2(Z - Z_0)/\widehat{\mathcal{R}}}} \ . \tag{3.42}
$$

The DBI action reads

$$
\begin{aligned}
S_{\rm DBI} = -\frac{8\pi^2 T_8 R^3}{3 g_s} \ {\rm tr} \int dt \epsilon_3 dZ K^{1/3} \\
\Bigg[\ \left\{ \left(\frac{4}{9}\right) U_{\rm KK}^2 K^{-1/3} - (2\pi\alpha')^2 (\mathcal{A}_0')^2 \right\} \left\{ K \left(\frac{U_{\rm KK}}{R}\right)^3 + \frac{1}{2} (2\pi\alpha')^2 F_{ab}^2 \right\} \\
+ K \left(\frac{U_{\rm KK}}{R}\right)^3 (2\pi\alpha')^2 F_{Za}^2 + \frac{1}{4} (2\pi\alpha')^4 (\epsilon_{abc} F_{aZ} F_{bc})^2 \ \Bigg]^{1/2} \ ,
\end{aligned}
\tag{3.43}
$$

where $\mathcal{A}_0' \equiv \partial_Z \mathcal{A}_0$. We are using the same vielbein coordinates as (3.36). Since the instanton size ($\mathcal{R}$) is of order $\mathcal{O}(\lambda^{-1/2})$ we define a new dimensionless parameter $\widetilde{\mathcal{R}}$, which is order of (λ^0), as

$$
\widetilde{\mathcal{R}} \equiv \sqrt{\lambda} \widehat{\mathcal{R}} = \sqrt{\lambda} \frac{\mathcal{R}}{U_{\rm KK}} \ . \tag{3.44}
$$

Furthermore we rescale the coordinate and the instanton field strength for a systematic $1/\lambda$ expansion

$$
\begin{aligned}
& x^a \to \lambda^{-1/2} x^a \ , \quad Z \to \lambda^{-1/2} Z \ , \quad t \to t \ , \\
& F_{ab} \to \lambda F_{ab} \ , \quad F_{aZ} \to \lambda F_{aZ} \ , \quad \mathcal{A}_0 \to \mathcal{A}_0 \ , \\
& K = (1 + Z^2) \to \left(1 + \frac{1}{\lambda} Z^2\right) \equiv K_\lambda ,
\end{aligned}
\tag{3.45}
$$

so all coordinates and gauge fields become of order of $\mathcal{O}(\lambda^0)$.

By using the instanton solution (3.42) we get

$$
\begin{aligned}
S_{\rm DBI} = & -\frac{N_c\lambda}{3^9\pi^5 U_{\rm KK} M_{\rm KK}^{-3}}\ {\rm tr}\int dt\epsilon_3 dZ K_\lambda^{1/3} \\
& \Bigg[\quad \left\{1+\frac{3^7\pi^2}{4M_{\rm KK}^2U_{\rm KK}^2}K_\lambda^{1/3}\frac{f'^2}{\widetilde{\mathcal{R}}^2}-\frac{1}{\lambda}\frac{3^6\pi^2}{4M_{\rm KK}^2}K_\lambda^{1/3}(\mathcal{A}_0')^2\right\} \\
& \left\{M_{\rm KK}^2U_{\rm KK}^2K_\lambda^{4/3}+\frac{3^7\pi^2}{4M_{\rm KK}^2U_{\rm KK}^2}K_\lambda^{1/3}\frac{f'^2}{\widetilde{\mathcal{R}}^2}\right\} \quad \Bigg]^{1/2}
\end{aligned}
\tag{3.46}
$$

If we let $U_{\rm KK}=M_{\rm KK}^{-1}$ for simplicity, then the DBI action yields

$$
\begin{aligned}
S_{\rm DBI} &= -dN_c\lambda\int dt\epsilon_3 dZ\ \sqrt{\left\{1+K_\lambda^{1/3}\widetilde{F}^2-\frac{1}{\lambda}K_\lambda^{1/3}(\widetilde{\mathcal{A}}_0')^2\right\}\left\{K_\lambda^{3/4}+K_\lambda^{1/3}\widetilde{F}^2\right\}} \\
&= -dN_c\lambda\int dt\epsilon_3 dZ\ \left[1+\frac{3Z^2}{8\lambda}+\widetilde{F}^2+\frac{Z^2}{3\lambda}\widetilde{F}^2-\frac{1}{2\lambda}(\widetilde{\mathcal{A}}_0')^2+\mathcal{O}((1/\lambda)^2)\right]\ ,
\end{aligned}
\tag{3.47}
$$

where

$$
\begin{aligned}
& d\equiv\frac{2M_{\rm KK}^4}{3^9\pi^5}\ , \quad \widetilde{\mathcal{A}}_0\equiv\frac{3^3\pi}{2M_{\rm KK}}\mathcal{A}_0\ , \quad \widetilde{F}^2\equiv\frac{3^7\pi^2}{4}J\ , \\
& J\equiv\frac{f'^2}{\widetilde{\mathcal{R}}^2}=\frac{{\rm sech}^4(Z/\widetilde{\mathcal{R}})}{4\widetilde{\mathcal{R}}^4}\sim\frac{1}{3\widetilde{\mathcal{R}}^3}\delta(Z)\ , \\
& \partial_Z\mathcal{K}\equiv\partial_Z\frac{1}{6\widetilde{\mathcal{R}}^3}\left[\tanh(Z/\widetilde{\mathcal{R}})\left(1+\frac{1}{2}{\rm sech}^2(Z/\widetilde{\mathcal{R}})\right)\right]\sim\frac{1}{6\widetilde{\mathcal{R}}^3}{\rm sgn}(Z)\ .
\end{aligned}
\tag{3.48}
$$

The Chern-Simons action does not change by the recaling (8.50) , and it is order of λ^0. With the instanton solution (3.42) the Chern-Simons action reduces to

$$
\begin{aligned}
S_{\rm CS} &= \frac{N_c}{24\pi^2}{\rm tr}\int\mathcal{A}\wedge F\wedge F=\frac{N_c}{8\pi^2}{\rm tr}\int dt\epsilon_3 dZ\mathcal{A}_0\frac{1}{2}\left(24M_{\rm KK}^3\frac{f'^2}{\widetilde{\mathcal{R}}^2}\right) \\
&= cN_c\int dt\epsilon_3 dZ\widetilde{\mathcal{A}}_0\widetilde{F}^2\ ,
\end{aligned}
\tag{3.49}
$$

where

$$
c\equiv\frac{4M_{\rm KK}^4}{3^9\pi^5}\ .
\tag{3.50}
$$

It also can be written as

$$S_{\rm CS} = 3N_c\widetilde{\mathcal{R}}^3 \int dZ\mathcal{A}_0\partial_Z\mathcal{K} \to N_c \ , \qquad \text{for } \mathcal{A}_0 = 1 \ , \tag{3.51}$$

which confirms that the field configuration (3.41), and (3.42) describe the single (anti) self dual instanton since $S_{\rm CS}$ corresponds to $N_c \times$ the Pontryagin index when $\mathcal{A}_0 = 1$.

3.2.5 Equation of State in $1/\lambda$

The equation of state of cold holographic matter is the energy following from the action functional. The total action up to order of λ^0 is

$$\begin{aligned} S &\equiv \int dt\epsilon_3 dZ(\mathcal{L}_{\rm DBI} + \mathcal{L}_{\rm CS}) \\ &= -dN_c \int dt\epsilon_3 dZ \left[\lambda\widetilde{F}^2 + \frac{Z^2}{3}\widetilde{F}^2 - \frac{1}{2}(\widetilde{\mathcal{A}}_0')^2\right] + cN_c \int d^4x dZ \widetilde{\mathcal{A}}_0\widetilde{F}^2 \end{aligned} \tag{3.52}$$

where $\mathcal{A}_0$ is an auxillary field with no time-dependence that can be eliminated by the equation of motion or Gauss law,

$$\Pi' = cN_c\widetilde{F}^2 \ , \tag{3.53}$$

with

$$\Pi \equiv \frac{\partial\mathcal{L}}{\partial\widetilde{\mathcal{A}}_0'} = dN_c\widetilde{\mathcal{A}}_0' \ , \tag{3.54}$$

The integral of the equation of motion with $\widetilde{F}^2$ in (3.48) is

$$\begin{aligned} \Pi(Z) &= \Pi(\infty)\left[\tanh(Z/\widetilde{\mathcal{R}})\left(1 + \frac{1}{2}\mathrm{sech}^2(Z/\widetilde{\mathcal{R}})\right)\right] \ , \\ \Pi(\infty) &= \frac{M_{\rm KK}^4}{54\pi^3}\frac{N_c}{\widetilde{\mathcal{R}}^3} \ , \end{aligned} \tag{3.55}$$

where we have set $\Pi(0) = 0$.

The energy of one cell is

$$\begin{aligned}
\mathcal{E}_{\rm cell} &= -\int \epsilon_3 dZ(\mathcal{L}_{\rm DBI}+\mathcal{L}_{\rm CS}) \\
&= dN_c \int \epsilon_3\, dZ\, \left[\lambda\widetilde{F}^2+\frac{Z^2}{3}\widetilde{F}^2-\frac{1}{2}\frac{\Pi^2}{(dN_c)^2}\right]-\int \epsilon_3\, dZ\widetilde{\mathcal{A}}_0\Pi' \ , \\
&= dN_c \int \epsilon_3\, dZ\, \left[\lambda\widetilde{F}^2+\frac{Z^2}{3}\widetilde{F}^2+\frac{1}{2}\frac{\Pi^2}{(dN_c)^2}\right]-\int \epsilon_3\, \widetilde{\mathcal{A}}_0(Z)\Pi(Z)\Big|_{-\infty}^{\infty} \ .
\end{aligned}$$

Thus the energy density (ε) of the crystalline structure is

$$\begin{aligned}
\varepsilon &\equiv \frac{N\mathcal{E}_{\rm cell}}{V}\approx\frac{\mathcal{E}_{\rm cell}}{\int\epsilon_3} \\
&= dN_c\int dZ\, \left[\lambda\widetilde{F}^2+\frac{Z^2}{3}\widetilde{F}^2+\frac{1}{2}\frac{\Pi^2}{(dN_c)^2}\right]-\widetilde{\mathcal{A}}_0(Z)\Pi(Z)\Big|_{-\infty}^{\infty} \ , \quad (3.56)
\end{aligned}$$

where N is the total number of baryons(cells) and V is the total volume which is approximated by $N\int\epsilon_3$. Interestingly the second term in (3.56) is equal to $\mu_B n_B$ since the density and the baryon chemical potential is given by

$$n_B=\frac{1}{\int\epsilon_3}=\frac{1}{2\pi^2(U_{\rm KK}\widetilde{\mathcal{R}})^3}=\frac{1}{2\pi^2(\sqrt{\lambda}\mathcal{R})^3} \ , \qquad \mu_B\equiv N_c\mathcal{A}_0(\infty) \ . \quad (3.57)$$

respectively and because

$$\widetilde{\mathcal{A}}_0(Z)\Pi(Z)\Big|_{-\infty}^{\infty}=2\widetilde{\mathcal{A}}_0(\infty)\Pi(\infty)=N_c\mathcal{A}_0(\infty)\frac{1}{2\pi^2(U_{\rm KK}\widetilde{\mathcal{R}})^3}=\mu_B n_B \ , \quad (3.58)$$

Notice that $\widetilde{\mathcal{R}}$ is of order of $(\lambda)^0$ from (3.44) so the baryon density is of order $(N_c\lambda)^0$. Since the action is finite and concentrated in a finite size, we can restrict the integral to the region $Z\le Z_c$ and expand the action in $1/\lambda$.

$$\begin{aligned}
\varepsilon &= dN_c\int_0^{Z_c} dZ\, \left[\lambda\widetilde{F}^2+\frac{Z^2}{3}\widetilde{F}^2+\frac{1}{2}\frac{\Pi^2}{(dN_c)^2}\right] \quad (3.59) \\
&= M_0\left[n_B+\frac{a}{\lambda}n_B^{1/3}+\frac{b}{\lambda}Z_c\, n_B^2\right] \ , \quad (3.60)
\end{aligned}$$

where

$$M_0 \equiv 8\pi^2\kappa M_{\rm KK} \ , \quad \kappa \equiv \frac{\lambda N_c}{216\pi^3} \ ,$$
$$a \equiv \frac{(\pi^2-6)M_{\rm KK}^2}{36(2\pi^2)^{2/3}} \ , \quad b \equiv \frac{3^6\pi^4}{2M_{\rm KK}^3} \ , \tag{3.61}$$

A few remarks are in order.

1. Z_c is introduced as an arbitrary cut-off which is bigger than the instanton size. However in section 8, we will argue that Z_c should be identified as baryon size by explicitly contructing the Skyrmion out of the instanton Therefore it is not an arbitrary number.

2. Even in the case the instanton size is small, the baryon size on the boundary is not. It is of order $(N_c\lambda)^0$ and large in units of M_{KK}. This point is important. While the instanton size in bulk is of the order of the string length and thus small as $1/\sqrt{\lambda}$ in units of M_{KK}, its image on the boundary is a large Skyrmion.

3. The position of the instanton Z_0 in the conformal direction is set to zero by parity.

The various density contributions in (3.60) can be understood from the zero density and finite instanton calculation discussed by Sakai and Sugimoyo to order $N_c\lambda^0$. For that, we recall that the energy balance for a holographic instanton with flat $\mathbb{R}^3$ directions reads schematically as [30]

$$N_c\left(\mathbf{A}\,\lambda\,\rho^2 + \mathbf{B}\,\frac{1}{\lambda\,\rho^2}\right) \tag{3.62}$$

leading to an instanton size in bulk of order $\rho \sim (\mathbf{B}/\mathbf{A})^{1/4}/\sqrt{\lambda}$. The Coulomb repulsion $\mathbf{B}$ is 10^4 times the gravitational attraction $\mathbf{A}$ resulting into a size that is of order $\rho \sim 10/\sqrt{\lambda}$. This parametrically huge repulsion results in a stiffer equation of state in holographic QCD.

The linear term in n_B in (3.60) is just the topological winding of the $U(N_f)$ flavored instanton in D8 on S^4 due to the self duality of the instanton configuration. It is leading and of order $N_c\lambda$. Geometry is unaffected by matter. A point-like instanton in bulk corresponds to a very large Skyrmion on the

boundary. The term of order $n_B^{1/3}$ is of order $N_c\lambda^0$. It corresponds to the *attraction* due to gravity in bulk at finite size. Indeed, the energy of this term is of order $\lambda\rho^2 = \widetilde{\mathcal{R}}^2$, as in (3.62) favoring smaller and smaller instanton. The energy per volume for this term is of order $1/\widetilde{\mathcal{R}}$. Since in matter the cell size is of the order of the interparticle distance $1/n_B^{1/3}$, the $n_B^{1/3}$ follows. The term of order n_B^2 is also of order $N_c\lambda^0$. It stems from the Coulomb repulsion in bulk which is of order $1/\lambda\rho^2 = 1/\widetilde{\mathcal{R}}^2$ since the instanton is static in 4-space (space-plus-conformal). This contribution is *repulsive* and favors larger size instanton. The corresponding energy per cell is of order $(Z_c/\widetilde{\mathcal{R}})(1/\widetilde{\mathcal{R}}^5)$, since the warping in the conformal direction is subleading in $1/\lambda$. The n_B^2 contribution follows.

For a Skyrmion with a size $Z_c \ll \widetilde{\mathcal{R}}$, (3.60) describes the low density regime. In this regime the use of the $S^3\times\mathbb{R}$ instanton is likely to give higher energy than a localized but flat instanton at the pole of S^3 say. Dilute holographic matter is made out of flat $\mathbb{R}^3$ instantons with (3.60) providing an upper bound on the energy per unit volume. This phase breaks spontaneously chiral symmetry. In the point particle limit, the equation of state at low density was discussed in [15]

$$\epsilon_{\rm p} \sim N_c \frac{27\pi^4}{4M_{\rm KK}^2} n_B^2 \tag{3.63}$$

for low densities after re-scaling $\sqrt{\lambda}n_B/\lambda^{3/2} \to n_B$ [15]. The point-like and flat space instanton contribution (3.63) at low density is lower in energy than (3.60) and therefore favored. This will be made more explicit below. The $n_B^{1/3}$ is absent in the point like limit (finite size effect).

As the density is increased (or equivalently as $\widetilde{\mathcal{R}}$ approaches down to Z_c), there is a change in the equation of state (3.60). For $Z_c = \widetilde{\mathcal{R}}$,

$$\varepsilon = M_0 \left[n_B + \frac{a}{\lambda} n_B^{1/3} + \frac{b'}{\lambda} n_B^{5/3} \right] , \tag{3.64}$$

with b changing to b'

$$b' \equiv \frac{3^6 (2\pi^2)^{5/3}}{2^3 M_{\rm KK}^2} . \tag{3.65}$$

The softening of the equation of state at higher density from n_B^2 to $n_B^{5/3}$ follows from a transition from a dilute gas/liquid phase to a dense solid/crystal phase. This transition effectively restores chiral symmetry as we will show later. An estimate of the chiral transition density follows by comparing the n_B^2 term from (3.63) to the leading $n_B^{5/3}$ in (3.64)

$$\epsilon_{\rm s} \sim N_c \frac{27\pi^{7/3}}{2^{4/3} M_{\rm KK}} n_B^{5/3} \tag{3.66}$$

By setting $\epsilon_p = \epsilon_s$, the critical transition density follows

$$n_B^c = \frac{4 M_{\rm KK}^3}{\pi^5} \ . \tag{3.67}$$

3.2.6 Numbers

To give some estimates of the numbers emerging from the current discussion, we first recall that in holographic QCD the mass of one baryon at next to leading order is not unique. We refer to [30] for a more thorough discussion. In particular, the baryon mass to order $N_c \lambda^0$ is

$$M_B = M_0 \left(1 + \frac{c}{\lambda}\right) \ , \tag{3.68}$$

where $c = 27\pi\sqrt{2/15}$. Thus the interaction energy per unit volume for the dilute case is

$$E_{\rm int}^{\rm Dilute} \equiv \varepsilon - n_B M_B = \frac{M_0}{\lambda} \left(a n_B^{1/3} - c n_B + b\, Z_c\, n_B^2 \right) \ , \tag{3.69}$$

while for the denser case it is ,

$$E_{\rm int}^{\rm Dense} \equiv \varepsilon - n_B M_B = \frac{M_0}{\lambda} \left(a n_B^{1/3} - c n_B + b'\, n_B^{5/3} \right) \ . \tag{3.70}$$

For numerical estimates, we use $M_{\rm KK} = 500$ MeV and $M_0 = 940$ MeV for $N_c = 3$ [**?**]. Our parameters are

$$\lambda \sim 53.2 \ , \quad a \sim 0.095\,{\rm fm}^{-2} \ , \quad b \sim 2172\,{\rm fm}^3 \ , \quad b' \sim 2039\,{\rm fm}^2 \ , \quad c \sim 31 \ .$$

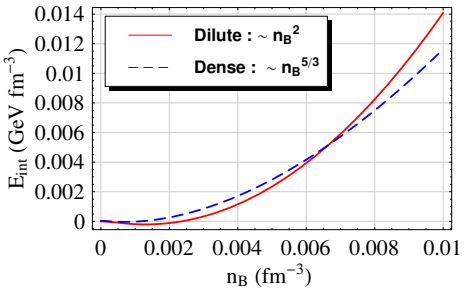

Figure 3.3: The energy per unit volume: $Z_c = 5$ (red) and $Z_c = \widetilde{\mathcal{R}}$ (blue). See text.

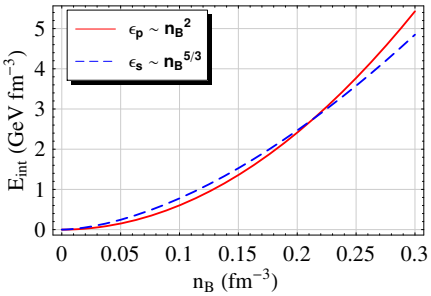

Figure 3.4: The energy per unit volume: $Z_c = \infty$ (red) and $Z_c = \widetilde{\mathcal{R}}$ (blue). See text.

The interaction energies are then

$$S^3 \ : E_{\rm int}^{\rm Dilute}({\rm GeV\,fm^{-3}}) = 0.00168 n_B^{1/3} - 0.548 n_B + 192 n_B^2 \ , \quad (3.71)$$

$$S^3 \ : E_{\rm int}^{\rm Dense}({\rm GeV\,fm^{-3}}) = 0.00168 n_B^{1/3} - 0.548 n_B + 36.0\, n_B^{5/3} \ , \quad (3.72)$$

$$R^3 \ : E_{\rm int}^{\rm Dilute,P}({\rm GeV\,fm^{-3}}) = \qquad -0.548 n_B + 60.3\, n_B^2 \quad (3.73)$$

where we used $Z_c = 5$. Notice that due to the smallness of the coefficients of the first two terms, the last term is dominant even in the relatively small baryon density if it is not much smaller than $10^{-2}{\rm fm}^{-3}$.

The results on S^3: $E_{\rm int}^{\rm Dilute}$ and $E_{\rm int}^{\rm Dense}$ are compared in Fig.(3.3) for $Z_c = 5$ ($Z_c = 5/M_{\rm KK} = 1\,{\rm fm}$ with restored dimensions). The results on S^3 and R^3 are compared in Fig. (3.4). In R^3 the instantons are point-like or $Z_c \sim \infty$ [15]. The crossing from R^3 to S^3 occurs at relatively small densities $n_B^c \approx 1.26\, n_0$ with $n_0 = 0.17\,{\rm fm}^{-1/3}$ the nuclear matter density.

3.2.7 Equation of State in General

The approximation of T^3 by S^3 suggested at the beginning of the paper was justified in way in the dilute limit or for small densities. Phenomenologically, we have found that the chiral phase transition from R^4 to $S^3 \times R$ occurs at few times nuclear matter density in holographic QCD, which is reasonable. The small size instantons dominate dense matter. This means that higher order corrections to both the DBI action and the starting D4 metric are important. While we do not know how to assess them, we now suggest that they may conspire to be small. Indeed, if we were not to expand the DBI plus CS actions, that is if we were to include only these class of higher order corrections our numerical results change only mildly.

Consider, the total (DBI + CS) action is written as

$$S = -dN_c\lambda \int d^4x dZ \sqrt{A - \frac{1}{\lambda} B(\mathcal{A}_0')^2} + \widetilde{c} N_c \int d^4x dZ J \mathcal{A}_0 \ , \tag{3.74}$$

where

$$\begin{aligned}
A &\equiv K_\lambda^{4/3} + \frac{3b}{M_{\rm KK}^2 U_{\rm KK}^4} K_\lambda^{1/3} J + \frac{3b}{U_{\rm KK}^2} K_\lambda^{5/3} J + \frac{9b^2}{M_{\rm KK}^2 U_{\rm KK}^6} K_\lambda^{2/3} J^2 \ , \\
B &\equiv b K_\lambda^{5/3} + \frac{3b^2}{M_{\rm KK}^2 U_{\rm KK}^4} K_\lambda^{2/3} J \ , \qquad J = \frac{\mathrm{sech}^4(Z/\widetilde{\mathcal{R}})}{4\widetilde{\mathcal{R}}^4} \ , \\
b &\equiv \frac{3^6\pi^2}{4M_{\rm KK}^2} \ , \qquad \widetilde{c} \equiv \frac{3}{2\pi^2 U_{\rm KK}^3} \ , \qquad d = \frac{2M_{\rm KK}^4}{3^9\pi^5} \ .
\end{aligned}$$

The equation of motion is

$$\widetilde{\Pi}' = \widetilde{c} N_c J \ , \tag{3.75}$$

with

$$\widetilde{\Pi} \equiv \frac{\partial \mathcal{L}}{\partial \mathcal{A}_0'} = \frac{dN_c B \mathcal{A}_0'}{\sqrt{A - \frac{1}{\lambda} B(\mathcal{A}_0')^2}} \ . \tag{3.76}$$

The integral of of motion is

$$\widetilde{\Pi}(Z) = \widetilde{\Pi}(\infty)\left[\tanh(Z/\widetilde{\mathcal{R}})\left(1+\frac{1}{2}\mathrm{sech}^2(Z/\widetilde{\mathcal{R}})\right)\right] ,$$
$$\widetilde{\Pi}(\infty) \equiv \frac{\widetilde{c}N_c}{6\widetilde{\mathcal{R}}^3} = \frac{N_c}{4\pi^2(U_{\rm KK}\widetilde{\mathcal{R}})^3} = \sqrt{b}\Pi(\infty) . \qquad (3.77)$$

The energy per cell is

$$\begin{aligned}\mathcal{E}_{\rm cell} &= -\int \epsilon_3 dZ(\mathcal{L}_{\rm DBI}+\mathcal{L}_{\rm CS}) \\ &= dN_c\lambda\int \epsilon_3\, dZ\,\sqrt{\frac{A}{B+\frac{\widetilde{\Pi}^2}{\lambda d^2 N_c^2}}} - \int \epsilon_3\, dZ\mathcal{A}_0\widetilde{\Pi}' \\ &= dN_c\lambda\int \epsilon_3\, dZ\,\sqrt{A+\frac{A\widetilde{\Pi}^2}{\lambda N_c^2 d^2 B}} - \int \epsilon_3\,\mathcal{A}_0(Z)\widetilde{\Pi}(Z)\Big|_{-\infty}^{\infty} . \qquad (3.78)\end{aligned}$$

The energy density (ε) of the crystalline structure is then

$$\begin{aligned}\varepsilon &\equiv \frac{N\mathcal{E}_{\rm cell}}{V} \approx \frac{\mathcal{E}_{\rm cell}}{\int\epsilon_3} \\ &= dN_c\lambda\int dZ\,\sqrt{A+\frac{A\widetilde{\Pi}^2}{\lambda N_c^2 d^2 B}} - \mathcal{A}_0(Z)\widetilde{\Pi}(Z)\Big|_{-\infty}^{\infty} , \qquad (3.79)\end{aligned}$$

where N is the total number of baryons (cells) and V is the total volume which is approximated by $N\int\epsilon_3$. The second term in (3.56) is

$$\mathcal{A}_0(Z)\widetilde{\Pi}(Z)\Big|_{-\infty}^{\infty} = 2\mathcal{A}_0(\infty)\widetilde{\Pi}(\infty) = N_c\mathcal{A}_0(\infty)\frac{1}{2\pi^2(U_{\rm KK}\widetilde{\mathcal{R}})^3} = \mu_B n_B , \qquad (3.80)$$

where

$$n_B = \frac{1}{\int\epsilon_3} = \frac{1}{2\pi^2(U_{\rm KK}\widetilde{\mathcal{R}})^3} = \frac{1}{2\pi^2(\sqrt{\lambda}\mathcal{R})^3} , \qquad \mu_B \equiv N_c\mathcal{A}_0(\infty) . \qquad (3.81)$$

Since n_B is fixed we may set $\mu_B = 0$. Then the energy density is

$$\varepsilon = dN_c\lambda\int dZ\,\left(\sqrt{A+\frac{A\widetilde{\Pi}^2}{\lambda N_c^2 d^2 B}} - K_\lambda^{2/3}\right) , \qquad (3.82)$$

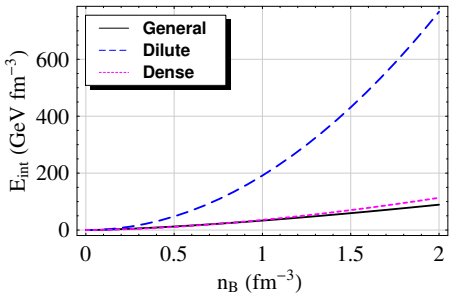

Figure 3.5: The energy per unit volume.

where we subtracted the vacuum value. Thus the interaction energy per unit volume is

$$E_{\rm int} \equiv \varepsilon - n_B M_B \ . \tag{3.83}$$

In Fig.(3.5) we show the equation of state for the expanded and unexpanded actions. As expected the corrections are of order $1/\lambda$ for a finite and small size instanton. The unexpanded energy is finite for any size of the instanton due to the gravitational warping factors which are subleading in $1/\lambda$ after rescaling. The unexpanded results are similar to the expanded ones in the range of densities explored as it should. For extremely small n_B, $E_{\rm int} \sim 0.00251 n_B^{1/3}$, however for reasonably large density $n_B \sim 1{\rm fm}^{-3}$, $E_{\rm int} \sim 33.9\, n_B^{5/3}$. This power is consistent and expected from the expansion in eq.(3.64).

All general expressions in this section are consistent with the results quoted above to order $\mathcal{O}(\lambda^0)$. Indeed, if for simplicity we set $U_{\rm KK} = M_{\rm KK}^{-1}$ with $M_{\rm KK} = 1$, then A and B reduce to

$$\begin{aligned} A &= (1+3bJ)^2 + \frac{1}{\lambda}\frac{2Z^2}{3}(1+3bJ)(2+3bJ) + \mathcal{O}(\lambda^{-2}) \ , \\ B &= b(1+3bJ) + \mathcal{O}(\lambda^{-1}) \ , \end{aligned} \tag{3.84}$$

For example, by considering $3bJ = \widetilde{F}^2$ and $\widetilde{\Pi} = \sqrt{b}\Pi$, we can readily show that (3.82) reduces to (8.51)

$$\varepsilon \ = \ dN_c \int dZ \ \left[\lambda \widetilde{F}^2 + \frac{Z^2}{3}\widetilde{F}^2 + \frac{1}{2}\frac{\Pi^2}{(dN_c)^2} \right] \ .$$

3.2.8 Holographic Skyrmions from Instantons

The $S^3 \times R$ instanton used in bulk has a very simple Skyrmion picture on the boundary. From (3.35) it follows that the gauge field at the boundary is $A(\infty, \vec{x}) = U^{-1}dU$. Following [30] we note that $U(\vec{x})$ is just the pion field at the boundary. When we have a cut-off in Z, we replace $A(\infty, \vec{x})$ by $A(Z_c, \vec{x})$. U is the boundary Skyrmion field originating from the bulk instanton. Thus U is just the *holonomy of the bulk instanton along the conformal direction*:

$$U(x; Z_c) = P \exp[i \int_0^{Z_c} dZ A_Z^{(instanton)}(Z)] \tag{3.85}$$

When the density is large and $Z_c \sim \mathcal{R}$, the instanton has a support covering the whole three sphere, therefore the resulting Skyrmion should be

$$U(\vec{x}) \simeq \sigma(\vec{x}) + i\tau_a \Pi^a(\vec{x}) = e^{i\tau_a \hat{r}^a(\theta,\phi)\,\psi} \ , \tag{3.86}$$

which is the identity map as (ψ, θ, ϕ) are the canonical angles for the unit S^3. The local Jacobian matrix for this map from S^3 to S^3 is $J^{ai} = \partial\Pi^a/\partial x_i = \mathbf{1}^{ai}/R$, proportional to the identity. The baryon density for this map is $\mathrm{detJ/volS^3} = 1/(2\pi^2 R^3)$ in agreement with bulk holography. The scalar field $\sigma(\vec{x}) = \cos\psi$ measures the *chiral condensate* and averages to zero on S^3

$$\frac{< \overline{q}q >_{S^3}}{< \overline{q}q >_{R^3}} =< \sigma(x) >_{S^3} = \frac{2}{\pi} \int_0^{\pi} d\psi \sin^2\psi \cos\psi = 0 \ . \tag{3.87}$$

The $S^3 \times R$ instanton in (3.35) corresponds to a boundary Skyrmion on S^3 with restored chiral symmetry on the average. We should notice that the chiral condensation is p-wave over a cell while the density in this case is approximately constant over a cell. But it is certainly not a constant. In fact this is a result consistent with ref. [52] where it was argued that there can not be an uniform distribution. In Fig.(3.6), we show schematically how a Skyrmion of size Z_c looks on S^3 as a function of $\mathcal{R}$. (a) corresponds to the dilute phase with broken chiral symmetry, while (b) describes the dense phase with restored chiral symmetry.

In previous section, Z_c was introduced as a cut-off of the action bigger than the instanton size. Here we give interpretation of Z_c as the size of the

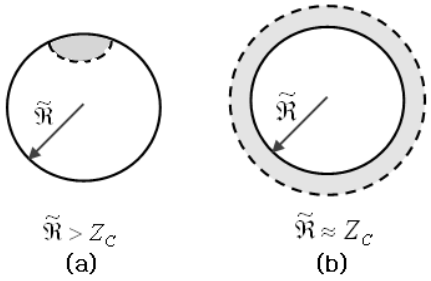

Figure 3.6: Holographic Skyrmion on S^3 on the boundary

Skyrmion on the boundary. Note that the R^4 BPS instanton used in bulk in [**?**] for the description of a single baryon, yields a boundary Skyrmion as

$$U(\vec{x}) = Z_c/\xi_c - i\vec{\tau}\cdot\vec{x}/\xi_c \tag{3.88}$$

with $\xi_c^2 = Z_c^2 + \vec{x}^2 + \rho^2$ and this is the analogue of the unit map (3.86) with $\tan\psi = x/\xi_c$. Notice that *while the size of the instanton is ρ, the size of the Skyrmion is* $\sqrt{Z_c^2+\rho^2}$. If $\rho \ll Z_c$, Z_c itself is the size of the Skyrmion, hence our interpretation above comes. Holography transmutes a small size instanton ρ in bulk to a large size Skyrmion on the boundary.

At small densities with $\widetilde{\mathcal{R}} \gg Z_c$, one can replace the spherical cell by a flat space and the map (3.88) is relevant, while at high density $\widetilde{\mathcal{R}} \leq Z_c$ the map (3.86) is relevant. On S^3 this is pictorially depicted in Fig.(3.6). Notice also that (a) has broken chiral symmetry while (b) has restored chiral symmetry effectively(See eq. (3.87)) . Again, in this case, our $S^3 \times R$ instanton in bulk describes the high density phase in holographic QCD with restored chiral symmetry. At low densities the energy density is about n_B^2 as discussed by many in qualitative agreement with our figure here. The n_B^2 term is sourced by Coulomb's repulsion in both cases. The description on S^3 carries larger energy density than on R^3 and is therefore unfavorable energitically. It is favorable at higher densities. The transition occurs at about $\mathcal{R} = Z_c$, or $n_B^c = 1/(2\pi^2\, Z_c)$, resulting into an energy density of $n_B^{5/3}$. The value of n_B^c was estimated above.

The determination of Z_c or equivalently the critical size of $\widetilde{\mathcal{R}}$ depends on the energetics of the SS model. It is worth pointing that the single baryon mass analysis on S^3 as discussed in [83] allows a considerable simplification of

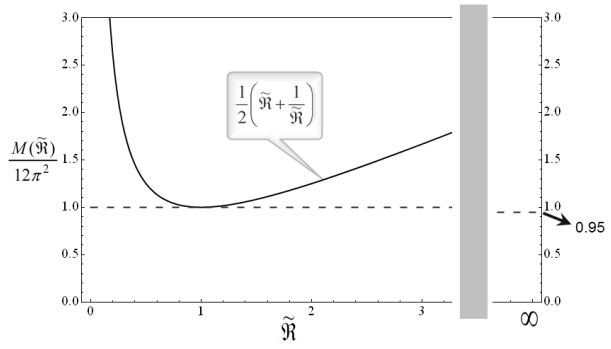

Figure 3.7: Holographic Skyrmion mass on S^3: order λ

this issue when the Skyrme model is used. We now note that this is justified in holographic QCD as small size instantons in bulk with $\rho = \widetilde{\mathcal{R}}/\sqrt{\lambda}$ map onto a large size Skyrmion on the boundary with $Z_c \gg \rho$. So the small size instanton expansion in bulk maps onto the gradient expansion in $1/Z_c$ on the boundary. Limiting the SS model on the boundary to the Skyrme model with f_π and e_S fixed by holography yields the specifics of the Skyrmion on the boundary to order λ.

In Fig. (3.7) we show how the holgraphic Skyrmion mass on S^3 to order λ changes with $\widetilde{\mathcal{R}}$ the radius of S^3 following [83]. The units of mass and length are respectively [30]

$$\begin{aligned} \frac{f_\pi}{2\sqrt{2}e_S} &= (\lambda N_c)\, M_{\rm KK}\, \frac{\sqrt{\mathbf{b}/2\pi}}{54\pi^5} \\ \frac{\sqrt{2}}{e_S f_\pi} &= (1/M_{\rm KK})\, \sqrt{8\mathbf{b}}/\pi^3 \ . \end{aligned} \tag{3.89}$$

with $\mathbf{b} = 15.25$ and $L = \mathcal{R}$. We note that the mass $M_0 = 8\pi^2\kappa M_{\rm KK}$ corresponds to the point 0.95 at $\widetilde{\mathcal{R}} = \infty$ which matches the unit map result as expected. In Fig. (3.8) we show the same curve to order $1/\lambda$. Here the energetics is determined in bulk as the chiral Lagrangian in the SS model is not known beyond the order λ. Specifically,

$$\frac{M_0}{\lambda}\left(\mathbf{A}\widetilde{\mathcal{R}}^2 + \frac{\mathbf{B}}{\widetilde{\mathcal{R}}^2}\right) \tag{3.90}$$

with $\mathbf{A} = (\pi^2 - 6)/36 \sim 0.11$ and $\mathbf{B} = (3^6\pi^2)/4 \sim 1799$. The units of mass

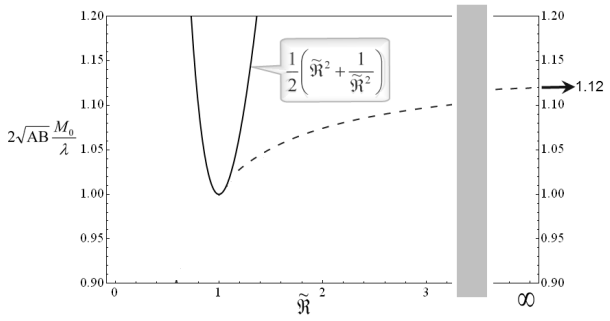

Figure 3.8: Holographic Skyrmion mass on S^3: order λ^0

and lengths are

$$\begin{aligned} (\mathbf{B}/\mathbf{A})^{1/4} &\sim 11.4 \\ 2\sqrt{\mathbf{AB}} &\sim 27.8 \end{aligned} \tag{3.91}$$

The point 1.12 is the $1/\lambda$ corrected mass (3.68) in these units. Finally, it is interesting to note that the holographic Skyrme model on S^3 yields *naively* the following equation of state

$$\varepsilon = M_0(n_B + a_S\, n_B^{2/3} + b_S\, n_B^{4/3}) \ , \tag{3.92}$$

as first noted in the context of the canonical Skyrme model [87]. The $n_B^{2/3}$ for the Skyrmion stems from the universal current algebra $(\nabla\Pi)^2$ term which is attractive and scales as $1/\rho^2$ as opposed to $1/\rho$ from the finite size instanton in bulk. The $n_B^{4/3}$ for the Skyrmion stems from the repulsive Coulomb contribution per unit 3-volume $(1/\rho)/\rho^3$ from the Skyrme term as opposed to the repulsive Coulomb contribution per unit 3-volume $(1/\rho^2)/\rho^3$ in the instanton in bulk. We recall that Coulomb's law in 1+D dimensions is $1/\rho^{D-2}$.

At high density the *naive* scalings in (3.92) obtained at the boundary differs from (3.64) obtained in bulk in two essential ways: i) a_S and b_S are of order $N_c^0\lambda^0$ on the boundary while their bulk contributions are of order N_c^0/λ; ii) the scaling with n_B appears to differ by an extra (spatial) dimension, $D = 3$ on the boundary and $D = 4$ in bulk. These differences can be understood by noting that the size of the holographic Skyrmion is Z_c. This means that the chiral gradients $L_i = U^{-1}\partial_i U$ are nearly zero on the boundary with $U \sim \mathbf{1}$, except on

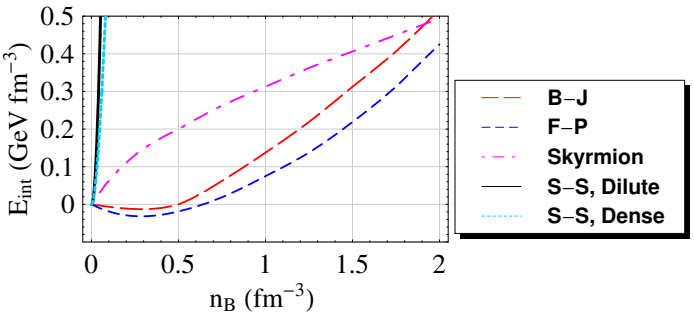

Figure 3.9: The energy per unit volume as a function of baryon density, for pure skyrmions, for the calculations of Bethe and Johnson [87, 88] and of Friedman and Pandharipande [87, 89], and for our instanton model based on Sakai-Sugimoto model for dilute and dense case.

an the shell $|\vec{x}| \approx Z_c$ of thickness $1/\sqrt{\lambda}$ to ensure that the topological baryon charge is finite [2]. This renders a_S and b_S in (3.92) effectively of order $1/\lambda$ as noted in bulk.

3.2.9 Comparison with Nuclear Models

In Fig.(3.9) we compare the interaction energy (3.69) and (3.70) with other hadronic models including Skyrme's chiral model. Holographic matter is substantially stiffer as explained through the energy budget in (3.62). The reason can be traced back to the fact that for a *single* baryon the repulsion already dwarfs the attraction in holographic QCD

At high densities ε in (3.70) is approximated as

$$\varepsilon \;\sim\; \frac{N_c 3^3 (2\pi^2)^{5/3}}{2^3 \pi M_{\rm KK}}\, n_B^{5/3} \quad\sim\quad 36 n_B^{5/3}\ ({\rm GeV\,fm^{-3}}) \quad \text{for } N_c = 3\ , \qquad (3.93)$$

and whatever N_f since the flavoured instanton in bulk is always 2×2. This behaviour is different from that of free massless quarks in $D = 3$ (ε_3) but

[2] We note that for $U \sim \mathbf{1}$ the Skyrmion obeys the Faddeev-Bogomolnyi bound since the classical equations of motion are fulfilled.

similar to *massive* quarks in $D = 3$ (ε_3'). Specifically,

$$\varepsilon_3 = \frac{N_c}{N_f^{1/3}} \frac{3^{4/3}\pi^{2/3}}{4} n_B^{4/3} \quad \sim \quad 5.52\, n_B^{4/3} (\text{GeV fm}^{-3}) \quad \text{for } N_c = 3, N_f = 2 \ ,$$
$$\varepsilon_3' = \frac{N_c}{N_f^{2/3}} \frac{3^{3/5}\pi^{4/3}}{10} \frac{1}{m} n_B^{5/3} \quad \sim \quad 1.68 \frac{1}{m}\, n_B^{5/3} (\text{GeV fm}^{-3}) \quad \text{for } N_c = 3, N_f = 2 \ .$$

So at strong coupling

$$\frac{\varepsilon}{\varepsilon_3'} = N_f^{2/3} \left(\frac{9^{6/5}5}{2^{1/3}} \right) \frac{m}{M_{\rm KK}} \quad \sim \quad \frac{88m}{M_{\rm KK}} \quad \text{for } N_f = 2 \ , \tag{3.94}$$

independently of λ and N_c. As chiral symmetry is restored in the high density phase, the comparison to the the free massive quark phase in $D = 3$ suggests that the mass $m \sim M_{\rm KK}/88$ is a chirally symmetric screening mass. While the chiral transition restores chiral symmetry it still confines baryons.

3.2.10 Conclusions

We have provided a holographic description of dense and cold hadronic matter using the brane model put forward by Sakai and Sugimoto [30]. At large N_c the matter crystallizes and can be treated in the Wigner-Seitz approximation on T^3. For simplicity, the Wigner-Seitz cell was further approximated by S^3 in space leading to a simple instanton configuration on $S^3 \times R$ with R the conformal space. The resulting equation of state at next to leading order in λ shows a free quark behavior at high density, although the overall coefficient is cutoff sensitive and large resulting into a stiff euation of state.

At high densities the gauge gradients are of order $\sqrt{\lambda}$ so the DBI action may not be enough to fix the brane dynamics at order $N_c\lambda^0$ [30]. Also our simplification of T^3 by S^3 while justified at low density, involves curvature corrections at high densities. However, we believe that the essentials of dense matter in holographic QCD are already exposed on S^3 with a small attraction leading $n_B^{1/3}$ and a large Coulomb repulsion leading $n_B^{5/3}$, where $5/3$ is the power of non-relativistic fermion. It is interesting to notice that the coulomb interaction in the bulk counts the fermi statistics in the boundary. The repulsion is 10^4 times the attraction resulting into a very stiff equation of state. Changing

S^3 to T^3 will not affect the outcome quantitativaly we believe. Indeed, this is the case for dense Skyrmions [83].

The present work expands on the original ideas developed in [51, 52]. Our calculations with finite size instantons are closer to those presented in reference [52] where finite size and homogeneous instantons were used through a variational estimate in $R^3 \times R$. Their arguments yield n_B instead of the $n_B^{1/3}$ we have reported in the equation of state at next to leading order with our $S^3 \times R$ instanton.

The inhomegeneous $S^3 \times R$ description of the crystal suggests that at high density, chiral symmetry is restored on the average. Indeed, since the dual of the instanton cell is the Skyrmion cell with a pion field restricted to S^3 in space. High density matter corresponds to small size S^3 where the pion field becomes just the unit map [83]. The corresponding chiral condensate on S^3 is seen to vanish as half of S^3 carries positive chiral condensate, while the other half carries negative chiral condensate so that on the average the chiral condensate is zero. This restoration of chiral symmetry is due to the formation of the crystal in the spatial direction in holographic QCD even though the D8-$\overline{\text{D8}}$ configuration is still attached. In other words, the left and right D8 branes cease to talk to each other through the spatial directions not the conformal direction when they *crystallize at large* N_c.

The present crystal analysis is classical in bulk. A quantum analysis including vibrational and rotational motion is needed. These corrections are subleading in $1/N_c$ and should be estimated for a more thorough phenomenological discussion. Also, the inhomogeneous phase can be probed approximatly by a dilute gas of instantons on T^3 allowing for a lower energetics than on S^3. These issues and others will be discussed elsewhere.

Chapter 4

Conductivity of Dense Matter

4.1 Introduction

In this chapter we would like to continue our investigation of the model at baryon finite density and temperature but in the presence of a finite baryonic electric field as recently discussed by Karch and O'Bannon [90] in a non-chiral model, as a prelude to understand transport phenomena. There are many works have been done in this line [18, 91–95]. In section 2, the DBI action at finite baryon density is streamlined for both the KK and BH metrics. In section 3, we discuss Ohm's law in the confined or KK metric. Above a critical value of the baryon electric field $E > E_c$ the vacuum and the dense state are unstable against quark pair creation. In section 4, we show how this pair creation translates to a vacuum persistence function thereby generalizing Schwinger's QED result to hQCD both in the vacuum and at finite density. In section 5, we derive Ohm's law in the BH background, thereby extending a recent result by Karch and Bannon [90] to the chiral case. The vacuum instability is dwarfed by thermal pair creation in the incoherent statistical averaging with a treshold value for the baryonic electric field starting at zero. Our conclusions are in section 6.

4.2 DBI action

We will use the abstract metric notations (2.18) to treat the confined (2.20) and deconfined (2.21) coherently in formal evaluation here. In the next section

we will plug in the specific embedding and metric form.

To accommodate a static baryonic electric field on D8 branes both in vacuum and matter, we follow [90] to define

$$A_t = A_t(U) \ , \quad A_x = -Et + h_x(U) \ . \tag{4.1}$$

With the induced metric (2.18) and the guage fields (4.1) the DBI action is written as

$$\begin{aligned} S_{\rm DBI} &\equiv \int d^4x dU \mathcal{L}_{\rm DBI} \\ &= -\mathcal{N} \int dU \ e^{-\phi} g_{SS}^2 g_{xx} \times \\ &\sqrt{|g_{tt}| g_{xx} g_{UU} - (2\pi\alpha')^2 \left(g_{xx} (A_t')^2 + g_{UU} (\dot{A}_x)^2 - |g_{tt}| (A_x')^2 \right)} \end{aligned} \tag{4.2}$$

where $\mathcal{N} \equiv (2N_f) T_8 V_4$. $2N_f$ comes from the fact that we consider N_f branes and anti-branes and $V_4 (= 8/3\pi^2)$ is the volume of the unit S^4 which is due to the trivial integral over S^4. $'$ is the derivative with respect to U and $\dot{}$ is the derivative with respect to t. Since (5.10) is purely kinetic, the conjugate momenta D and B are conserved. Specifically,

$$\begin{aligned} D &\equiv \frac{\partial \mathcal{L}_{\rm DBI}}{\partial A_t'} \\ &= e^{-\phi} g_{SS}^2 g_{xx} \frac{-\mathcal{N} (2\pi\alpha')^2 g_{xx} A_t'}{\sqrt{|g_{tt}| g_{xx} g_{UU} - (2\pi\alpha')^2 \left(g_{xx} A_t'^2 + g_{UU} E^2 - |g_{tt}| h_x'^2 \right)}} \end{aligned} \tag{4.3}$$

$$\begin{aligned} B &\equiv \frac{\partial \mathcal{L}_{\rm DBI}}{\partial A_x'} \\ &= e^{-\phi} g_{SS}^2 g_{xx} \frac{\mathcal{N} (2\pi\alpha')^2 |g_{tt}| h_x'}{\sqrt{|g_{tt}| g_{xx} g_{UU} - (2\pi\alpha')^2 \left(g_{xx} A_t'^2 + g_{UU} E^2 - |g_{tt}| h_x'^2 \right)}} \end{aligned} \tag{4.4}$$

By rewriting A_t' and h_x' in terms of B, D and E, we have

$$\begin{aligned} & g_{xx} A_t'(U)^2 \\ &= \frac{1}{(2\pi\alpha')^2} |g_{tt}| D^2 \frac{g_{UU} (|g_{tt}| g_{xx} - (2\pi\alpha')^2 E^2)}{\mathcal{N}^2 (2\pi\alpha')^2 |g_{tt}| g_{xx}^3 e^{-2\phi} g_{SS}^4 + |g_{tt}| D^2 - g_{xx} B^2} \end{aligned} \tag{4.5}$$

$$
\begin{aligned}
&|g_{tt}|h_x'(U)^2 \\
&\quad = \frac{1}{(2\pi\alpha')^2} g_{xx} B^2 \frac{g_{UU}(|g_{tt}|g_{xx} - (2\pi\alpha')^2 E^2)}{\mathcal{N}^2 (2\pi\alpha')^2 |g_{tt}| g_{xx}^3 e^{-2\phi} g_{SS}^4 + |g_{tt}| D^2 - g_{xx} B^2}
\end{aligned} \tag{4.6}
$$

The DBI action reduces to

$$
\begin{aligned}
S_{\rm DBI} = -\mathcal{N} \int d^4x dU \left[e^{-2\phi} g_{SS}^4 g_{xx}^{5/2} |g_{tt}|^{1/2} g_{UU}^{1/2} \right] \times \\
\sqrt{\frac{(|g_{tt}|g_{xx} - (2\pi\alpha')^2 E^2)}{|g_{tt}| g_{xx}^3 e^{-2\phi} g_{SS}^4 + \frac{|g_{tt}| D^2 - g_{xx} B^2}{\mathcal{N}^2 (2\pi\alpha')^2}}}
\end{aligned} \tag{4.7}
$$

Notice that g_{tt}, g_{xx}, g_{SS} have nothing to do with the D8 branes embedding. They carry information of D4 branes. Only g_{UU} carries information of the $x^4(U)$. It is positive for all U. Thus the factors outside the square root are real for all U. In contrast, the argument of square root may change the sign for varying U. As we will discuss below, this change in sign is the signal of a ground state instability or decay for large E fields.

4.3 Ohm's law: KK

This decay is captured by a non-linear form of Ohm's law. For that, it is useful to change variable

$$
U = U_0 (1 + Z^2)^{1/3} \ , \tag{4.8}
$$

where U_0 is the coordinate of the tip of D8-$\overline{\rm D8}$ branes' cigar-shaped configuration, which is different from $U_{\rm KK}$ in general. The range of Z is $(0, \infty)$ contrary to U whose range is (U_0, ∞). Also this range can be extended to $(-\infty, \infty)$ if we consider $\overline{\rm D8}$ branes $(-\infty, 0)$ together with D8 branes $(0, \infty)$ in a natural way. It enables us to deal with the ADHM instanton solution in $\mathbb{R}^4$ [30]. It also makes the parity property of the meson fields explicit [28]. For completeness, we note the following useful relations

$$
K \equiv 1 + Z^2 \ , \quad U = U_0 K^{1/3} \ , \quad dU = \frac{2U_0}{3} \frac{Z}{K^{2/3}} dZ \ , \ . \tag{4.9}
$$

$$f = 1 - \left(\frac{U_{\rm KK}}{U_0}\right)^3 \frac{1}{K} \ . \tag{4.10}$$

From here on and for simplicity, we follow Sakai and Sugimoto [28] and choose $U_0 = U_{\rm KK}$. The DBI action then simplifies to

$$S_{\rm DBI} = -a \int d^4x dZ K^{1/6} \sqrt{\frac{K - \frac{b}{M_{\rm KK}^2} E^2}{1 + \frac{D^2 - B^2}{a^2 b} K^{-5/3}}} \ , \tag{4.11}$$

where

$$a \equiv \frac{N_c N_f \lambda^3 M_{\rm KK}^4}{3^9 \pi^5} \ , \qquad b \equiv \frac{3^6 \pi^2}{4 \lambda^2 M_{\rm KK}^2} \ . \tag{4.12}$$

In dense hQCD baryons are sourced by BPST instantons in bulk with a size of order $1/\sqrt{\lambda}$. They are point-like at $\lambda \to \infty$. Thus the DBI action and the matter sources read

$$\mathcal{L}_{\rm tot} = \mathcal{L}_{\rm DBI} + n_B \delta(Z) A_t(Z) + \widetilde{n}_B v_x \delta(Z) A_x(t, Z) \ , \tag{4.13}$$

where n_B is the baryon - anti baryon density and $\widetilde{n}_B$ is baryon + anti baryon density. The first source contribution is that of static BPST instantons at $Z = 0$ as initially discussed in [15]. The second term is their corresponding current with a velocity $v_x \sim 1/\lambda N_c$ with a baryon mass $M_B \sim N_c \lambda M_{KK}$. Note that we have renormalized the A_μ field here by $1/N_c$ and identified the baryon chemical potential as $A_\mu(\infty) = \mu_B - m_B$ [15].

The equations of motion are

$$D' = n_B \ \delta(Z) \ , \qquad B' = \widetilde{n}_B v_x \delta(Z) \ . \tag{4.14}$$

Thus

$$D = \frac{1}{2} n_B {\rm sgn}(Z), \qquad B = \frac{1}{2} \widetilde{n}_B v_x {\rm sgn}(Z) \ , \tag{4.15}$$

where ${\rm sgn}(Z)$ reflects the symmetry of D8 and $\overline{\rm D8}$ branes (chirality). We note that the conserved momenta D, B are odd functions of Z since the baryonic field A_μ is an even function of Z.

For a finite baryonic electric field E, the current contribution in (7.84) is seen to increase linearly with time in the action. This is expected since the static electric field pumps energy in the system. For times $t \sim M_B \sim N_c\lambda$ the present stationary (time-independent) surface analysis is flawed. This notwithstanding, the action variation with respect to A_t yields

$$\begin{aligned}\delta_{A_t} S_{\rm tot} &= \int dZ \left[\frac{\delta\mathcal{L}}{\delta(\partial_Z A_t)}\partial_Z(\delta A_t) + n_B\delta(Z)\delta A_t(Z)\right] \\ &= \int dZ \left(\frac{1}{2}n_B {\rm sgn}(Z)\partial_Z(\delta A_t)\right) + n_B\delta A_t(0) \\ &= n_B\delta A_t(\infty)\ . \end{aligned} \tag{4.16}$$

where we used the on-shell condition and $A_t(\infty) = A_t(-\infty) = \mu_B - m_B$. Note that the contribution from the source term is cancelled by the boundary contribution of the DBI action at $Z = 0$. As a result the on-shell action may be considered as a functional of $A_t(\infty)$ only and we may set $A_t(0) = 0$. Similarly for $A_x(t, 0) = 0$,

$$\delta_{A_t} S_{\rm tot} = \widetilde{n}_B\, v_x \delta A_x(t, \infty)\ . \tag{4.17}$$

The former is the charge, while the latter is the current. At finite density $S_{\rm tot}$ plays the role of the grand potential. Thus

$$\bar{S} = -a\int d^4x dZ K^{1/6}\sqrt{\frac{K - \frac{b}{M_{\rm KK}^2}E^2}{1 + \frac{n_B^2 - \widetilde{n}_B^2 v_x^2}{4a^2 b}K^{-5/3}}}, \tag{4.18}$$

on shell. For $v_x = E = 0$ this result is consistent with our previous result i.e. Eq.(30) in [**?**] which is indeed the grand potential.

For $0 < E \leq E_c \equiv \frac{M_{\rm KK}}{\sqrt{b}}$, $J_x(= \widetilde{n}_B v_x)$ is bounded,

$$J_x < \sqrt{4a^2 b + n_B^2}\ , \tag{4.19}$$

for $\bar{S}$ to be real. For $E > E_c$, the numerator of (4.18) flips sign at

$$K_* = \frac{b}{M_{\rm KK}^2}E^2\ , \qquad Z_* = \pm\sqrt{bE^2 - 1}\ . \tag{4.20}$$

We demand that this flip is compensated by the denominator for arbitrary v_x. Using Z_* in the denominator we get

$$\begin{aligned} J_x^2 &= 4a^2 b K_*^{5/3} + n_B^2 \\ &= \frac{1}{2^{10/3}3^2\pi^{14/3}} N_f^2 N_c^2 \left(\frac{\lambda}{M_{\rm KK}}\right)^{2/3} E^{10/3} + n_B^2\ \theta(E)\ . \end{aligned} \tag{4.21}$$

In the unstable vacuum, the ensuing Ohmic's conductivity is

$$\sigma \equiv \frac{J_x}{E} = \frac{1}{2^{5/3}3\pi^{7/3}} N_c N_f \left(\frac{\lambda}{M_{\rm KK}}\right)^{1/3} E^{2/3}\ . \tag{4.22}$$

This pair conductivity follows from quark pairs and not from baryon pairs as it scales with $N_c N_f$. E_c is strong enough to cause deconfinement of quark pairs. For $n_B \neq 0$ the second contribution in (4.21) is that of the baryons and anti baryons moving under the action of the *strong* electric field, with $\Delta v \sim Et/M_B \sim t/N_c$. Note that for $E = 0$, the minimum of (4.18) is for $v_x = 0$.

For $E > E_c$ both the vacuum with $n_B = 0$ and the dense baryonic state with $n_B \neq 0$ are unstable against pair creation of quark-antiquark states as opposed to baryon-antibaryon states. This is clearly seen from the threshold value E_c

$$E_c = \frac{M_{\rm KK}}{\sqrt{b}} = \frac{2}{27\pi} M_{\rm KK}^2 \lambda = \frac{54\pi M_B^2}{\lambda N_c^2}\ , \tag{4.23}$$

with $M_B = 8\pi^2 \kappa M_{\rm KK}$ and $\kappa = \frac{\lambda N_c}{216\pi^3}$ [30] which is much smaller than M_B^2. The baryonic electric field is strong enough to pair create quarks with *constituent masses* of order $\sqrt{\lambda} M_{KK}$ [1].

4.4 Persistence Probability

The cold and dense states described by hQCD above are unstable for $E > E_c$, meaning that they decay to multiparticle states that are likely time-dependent. Following Schwinger, we will characterize this decay through its persistence

[1] It is interesting to note that in the BH background the thermal shifts of heavy quarks is $\pi\sqrt{\lambda}T/2$ with T in the unconfined phase being the analogue of M_{KK} in the confined phase.

probability

$$|\langle 0_+|0_-\rangle|^2 = e^{-2\mathrm{Im}\bar{S}}, \tag{4.24}$$

where $\mathrm{Im}\bar{S}$ is the imaginary part of the action $\bar{S}$ (4.18). For finite n_B and $v_x = 0$, the action $\bar{S}$ reads

$$\bar{S} = -a \int d^4x dZ (1+Z^2)^{1/6} \left[\sqrt{\frac{Z^2+1-\mathcal{E}^2}{1+\mathscr{N}^2(1+Z^2)^{-5/3}}} - \sqrt{\frac{Z^2+1}{1+\mathscr{N}^2(1+Z^2)^{-5/3}}} \right], \tag{4.25}$$

with $\mathcal{E}^2 \equiv \frac{b}{M_{\mathrm{KK}}^2} E^2$, $\mathscr{N}^2 \equiv \frac{n_B^2}{4a^2 b}$ and after regularizing the action by subtracting the $\mathcal{E} = 0$ contribution. E_c corresponds to $\mathcal{E}_c = 1$. For $\mathcal{E} \leq 1$ the action $\bar{S}$ is always real, but for $\mathcal{E} > 1$ the action develops an imaginary part from the integration interval $(-Z_c, Z_c)$, where $Z_c \equiv \sqrt{\mathcal{E}^2 - 1}$. Thus

$$\mathrm{Im}\bar{S} = \pm a \int d^4x \int_{-Z_c}^{Z_c} dZ (1+Z^2)^{1/6} \sqrt{\frac{Z^2+1-\mathcal{E}^2}{1+\mathscr{N}^2(1+Z^2)^{-5/3}}} \theta(\mathcal{E}-1) \ . \tag{4.26}$$

For $\mathscr{N} = 0$ the integrals unwind analytically

$$\mathrm{Im}\bar{S} = \pm a\pi \int d^4x \left[(\mathcal{E}^2-1) \ {}_2F_1\left(-\frac{1}{6}, \frac{1}{2}, 2, 1-\mathcal{E}^2\right) \theta(\mathcal{E}-1) \right]. \tag{4.27}$$

where ${}_2F_1$ is the hypergeometric function and has the asymptotic behaviour as follows.

$$\begin{aligned} &{}_2F_1\left(-\frac{1}{6}, \frac{1}{2}, 2, 1-\mathcal{E}^2\right) \\ &\quad \sim 1 + \frac{1}{12}(\mathcal{E}-1) + \frac{1}{144}(\mathcal{E}-1)^2 + \cdots \qquad (\mathcal{E} \sim 1) \\ &\quad \sim \frac{\Gamma(2/3)}{\sqrt{\pi}\Gamma(13/6)} \mathcal{E}^{1/3} + \frac{2\Gamma(-2/3)}{\sqrt{\pi}\Gamma(-1/6)} \frac{1}{\mathcal{E}} + \cdots \qquad (\mathcal{E} \gg 1) \end{aligned} \tag{4.28}$$

The persistence function is then

$$\begin{aligned} |\langle 0_+|0_-\rangle|^2 &= e^{-a'(\varepsilon^2-1)\ {}_2F_1\left(-\frac{1}{6},\frac{1}{2},2,1-\varepsilon^2\right)\theta(\varepsilon-1)}, \\ &= 1 \qquad\qquad (\mathcal{E}\leq 1) \\ &\quad e^{-a'[2(\varepsilon-1)+1.17(\varepsilon-1)^2+\cdots]} \qquad (\mathcal{E}\sim 1) \\ &\quad e^{-a'[0.71\ \varepsilon^{7/3}+0.70\ \varepsilon+\cdots]} \qquad (\mathcal{E}\gg 1) \end{aligned} \tag{4.29}$$

with $a' \equiv a\pi\int d^4x = \frac{N_c N_f \lambda^3 M_{\rm KK}^4}{3^9\pi^4}\int d^4x$, after chosing the negative sign for decay.

4.5 Ohm's law: BH

Since the vacuum decay under large E's so does the coherent finite baryonic state. But what about the finite temperature problem? As finite temperature involves a statistical ensemble averaging, we may suggest that the unstable ground state is statistically irrelevant and proceed to analyse the effects of a baryonic field on the excited states (unstable by fiat) in the ensemble average. This will be checked a posteriori below.

In the BH background there are two possible gravitational configurations: 1/ a U-shaped (chirally broken phase) and 2/ a parallell-shape (chirally symmetric phase). The former yields U bounded from below by U_0. The combination $g_{tt}g_{xx}$ has a positive minimum so the numerator is always positive for sufficiently small E. The nature of the transition which is suggestive of a metal-insulator transition [96] will be discussed elsewhere.

For high enough temperature the stable configuration is not the U-shaped configuration but the parallel configuration which is connected to the black hole. i.e. $\frac{dx^4}{dU} = 0$. Our intial instanton sources have now drowned into the BH horizon. So the ensuing analysis is the same as in the D3/D7 model [90], with the general formula of the conductivity for Dq/Dp given ((5.7) in [90]). Here and for completeness, we compute the conductivity for the parallel D8-$\overline{\rm D8}$ branes set up in the BH background.

We only need to consider the positivity condition for the argument of square root as before. As $U \to U_T$ *both* the numerator and denominator are *negative* since $g_{tt} \to 0$. As $U \to \infty$ *both* the numerator and denominator are *positive*.

So by choosing B,D,E we can choose the numerator and denominator in (4.7) to flip sign for the same value $U = U_*$ [90]. For the numerator

$$\begin{aligned} |g_{tt}|g_{xx}\Big|_{U=U_*} &= (2\pi\alpha')^2 E^2 \\ \Rightarrow U_* &= (U_T^3 + R^3(2\pi\alpha' E)^2)^{1/3} \ . \end{aligned} \tag{4.30}$$

Inserting this value of U_* in the denominator yields the induced current

$$\begin{aligned} J_x^2 &= \left(\mathcal{N}^2(2\pi\alpha')^2|g_{tt}|g_{xx}^2 e^{-2\phi} g_{SS}^4 + \frac{|g_{tt}|}{g_{xx}} J_t^2\right)\Big|_{U=U_*} \\ &= \left(\frac{\mathcal{N}^2(2\pi\alpha')^4 R^6}{g_s^2}\left(U_T^3 + R^3(2\pi\alpha' E)^2\right)^{2/3} + \frac{(2\pi\alpha')^2}{\frac{U_T^3}{R^3} + (2\pi\alpha' E)^2} J_t^2\right) E^2 \ , \end{aligned}$$

where $J_x = B$ and $J_t = D$ $(= n_B)$ are now defined as in [90]. Setting $U_T = \frac{16\pi^2}{9} T^2 R^3$, $\lambda = g_s N_c$ yield the Ohmic conductivity for the chiral SS model

$$\sigma = \frac{J_x}{E} = \sqrt{\left(\frac{4 l_s N_f N_c \lambda T^2}{27}\right)^2 (1+e^2)^{2/3} + \frac{d^2}{1+e^2}} \ , \tag{4.31}$$

where

$$e \equiv \frac{3^3 E}{2^5 \pi^3 T^3 \lambda l_s} \ , \qquad d \equiv \frac{3^3 J_t}{2^5 \pi^3 T^3 \lambda l_s} \ , \tag{4.32}$$

which is consistent with the result in [90] for massless but non-chiral quarks. The induced thermal current sets in for any $E \geq 0$ (large or small) with a conductivity σ of order $N_c N_f \lambda T^2 l_s$ at high temperature, which involves only thermal pairs with zero treshold for E. It dwarfs the induced vacuum pairs by a factor of $\lambda^{2/3}$. The unstable vacuum state is statistically irrelevant. This is not the case at $T = 0$ and/or very large baryonic densities.

4.6 Conclusions

We have extended our recent holographic analysis of the SS model at finite density, to the case of finite temperature and finite baryonic electric field. For $E > E_c$ the stationary SS ground state breaks down by quark pair creation. This phenomenon permeates both the cold and hot states of hQCD. The vac-

uum persistence probability is derived, generalizing Schwinger's QED result to hQCD. At finite temperature, the baryonic electric field yields a thermal conductivity at finite temperature and density that is a direct generalization of Karch and Bannon's Ohm's law in the chiral model. We have argued that the vacuum instability is statistically irrelevant in hot hQCD.

Chapter 5

Baryonic Response of Dense Matter

5.1 Introduction

Solids respond to external stress elastically through their bulk and shear modulii K and μ respectively, with almost zero dissipation. Liquids on the other hand, follow the lore of hydrodynamics with bulk and shear viscosities ξ and η accounting for dissipation. In contrast to the solid, the shear modulus vanishes in the liquid. The bulk modulus does not.

This remarkable difference between solid and liquid disappears when the stress is time-dependent. Indeed, for a stress of finite frequency ω a liquid has a non-zero shear modulus much like the solid. In the long-wavelength limit, the dual description of a solid or a liquid follows from the visco-elastic equations with complex and frequency dependent elastic constants as we detail below. In this chapter we will explore some of these ideas in the context of the AdS/CFT correspondence by analyzing the baryonic response functions at finite density for both D4/D8 and D3/D7 embeddings.

Hot and dense hadronic matter in QCD is difficult to track from first principles in current lattice simulations owing to the sign problem. In large N_c QCD baryons are solitons and a dense matter description using Skyrme's chiral model [78–80] was originally suggested by Skyrme and others [81]. At large N_c and low density matter consisting of solitons crystallizes as the ratio of potential to kinetic energy $\Gamma = V/K \approx N_c^2/p_F^2 \gg 1$ is much larger than

1. The crystal melts at sufficiently high density with $\Gamma \approx N_c^2/p_F^2 \approx 1$, or sufficiently high temperature with $\Gamma \approx N_c/T \approx 1$. QCD matter at large N_c was recently revisited in [82].

The many-soliton problem can be simplified in the crystal limit by first considering all solitons to be the same and second by reducing the crystal to a single cell with boundary conditions much like the Wigner-Seitz approximation in the theory of solids. A natural way to describe the crystal topology is through T^3 with periodic boundary conditions. A much simpler and analytically tractable approximation consists of treating each Wigner-Seitz cell as S^3 with no boundary condition involved. The result is dense Skyrmion matter on S^3 [83].

At low baryonic densities holographic QCD is a crystal of instantons with the Wigner-Seitz cell *approximated* by S^3. The pertinent instanton is defined on $S^3 \times R$ [17]. At moderate densities chiral symmetry is restored on the average with an $n_B^{5/3}$ equation of state [17]. This homogenous (on the average) liquid-like phase is strongly coupled and not emmenable to standard Fermi liquid analysis.

In this chapter, we would like to follow up on the transport properties in the homogeneous phase originally discussed in [17] using D4/D8 to contrast them with some recent studies in [97] using D3/D7. In section 2, we recall the bulk characteristics of the homogeneous phase in D4/D8 and suggest that it may be identified with a strongly coupled holographic liquid prior to the restoration of chiral symmetry. In section 3, we derive the general formulae for the holographic currents induced by an external baryonic field in the linear response approximation for both D4/D8 and D3/D7. In section 4 we show that the transverse baryonic current for cold D4/D8 is saturated by medium modified vector mesons in leading N_c in agreement with [18]. The bulk static conductivity is zero. Large N_c D4/D8 is an insulator. In section 5, we develop the quasi-normal mode approach for hot and dense D4/D8 and D3/D7, both of which are conductors at large N_c. For completeness we also discuss cold D3/D7 in light of a recent result [97]. In section 6, we suggest a unified visco-elastic framework for interpreting gapless excitations in dense media in both the elastic (collisionless) and hydrodynamic (collision) regimes. We argue that cold D3/D7 exhibits such a mode at large N_c with zero bulk viscosity and

finite shear viscosity. In section 7, we suggest that the leading $1/N_c$ correction to the baryonic currents in cold D4/D8 can be extracted from an effective baryonic theory using the Random Phase Approximation. Our conclusions and prospects are in section 8. A number of points pertaining to transport in dense holographic media are discussed in the Appendices.

5.2 Homogeneous dense matter

The interaction energy density $\epsilon_{\rm int}$, pressure P, grand potential Ω, and the baryon chemical potential μ_B have been computed in [15],

$$\epsilon_{\rm int} \equiv \frac{\Delta E}{V} = a\int_{-\infty}^{\infty} dZ K^{2/3}\left[\sqrt{1+\frac{(N_c n_B)^2}{4a^2 b}K^{-5/3}}-1\right] , \tag{5.1}$$

$$P=-\frac{\Omega}{V} = a\int_{-\infty}^{\infty} dZ\, K^{2/3}\left[1-\frac{1}{\sqrt{1+\frac{(N_c n_B)^2}{4a^2 b}K^{-5/3}}}\right] , \tag{5.2}$$

$$\mu_B = m_B + N_c\int_{-\infty}^{\infty} dZ \frac{N_c n_B/4}{\sqrt{(ab)^2K^2+bK^{1/3}(N_c n_B/2)^2}} , \tag{5.3}$$

where V is the volume and Ω is understood as a function of μ_B. At low densities they translate to

$$\epsilon_{\rm int} \sim \frac{27\pi^3}{2}\frac{N_c}{N_f\lambda}\frac{1}{M_{\rm KK}^2}n_B^2 , \tag{5.4}$$

$$P=-\frac{\Omega}{V} \sim \frac{27\pi^3}{2}\frac{N_c}{N_f\lambda}\frac{1}{M_{\rm KK}^2}n_B^2 , \tag{5.5}$$

$$\mu_B \sim m_B + 27\pi^3\frac{N_c}{N_f\lambda}\frac{1}{M_{\rm KK}^2}n_B . \tag{5.6}$$

The baryonic contributions appear through the combination $N_c/\lambda N_f$. The large N_c and large λ limit are not compatible in the homogeneous phase. Compatibility with solitonic physics suggests that the large N_c limit be taken first followed by the large λ limit, which is also consistent with holography. This will be assumed throughout, unless specified otherwise. The homogeneous phase described by (5.2) breaks spontaneously chiral symmetry with density dependent vacuum-like modes [15]. In Fig. (5.1) we sketch the various phases of dense holographic matter at zero temperature. The low density part

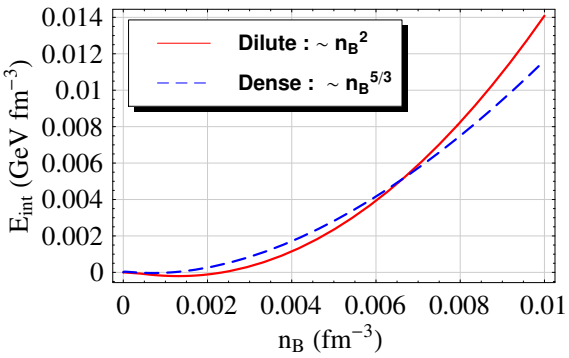

Figure 5.1: Sketch of the phases of cold D4/D8.

is inhomogeneous (solid) with spontaneously broken chiral symmetry, while the high density phase is homogeneous (gas) with restored chiral symmetry. Intermediate between the two is a possible liquid phase. Here we suggest that (5.2) may capture some aspects of the liquid phase still in the spontaneously broken phase using holography. The solid phase binds with an energy density $\epsilon_{\rm int} \approx a_M\, n_B$ where a_M is the Madelung constant for the pertinent crystallization provided that the baryons are semiclassically quantized to account for the pion-interaction through the mesonic cloud [19]. The gas phase is homogeneous with $\epsilon_{\rm int} \approx n_B^{5/3}$ and restored chiral symmetry [17]

5.2.1 Compressibility

Holographic QCD at large N_c and large λ is umcompressible. Indeed, under small scalar or longitudinal vector stress the baryonic density n_B is expected to change locally to $n_B + \delta n_B$ so that the constitutive equations read

$$M n_B \dot{\vec{v}} = -\vec{\nabla} p \ , \tag{5.7}$$

$$\partial_t \delta n_B + n_B \vec{\nabla} \cdot \vec{v} = 0 \ , \tag{5.8}$$

by the Newtonian equation of motion (5.7) and baryon current conservation (5.8). The baryonic charges move with an acceleration $(\partial P/\partial n_B)/m_B \approx 1/\lambda$ which is suppressed at large λ since $m_B = 8\pi\lambda N_c$ [30]. Another way to say this is to note that (5.8) implies $(\partial_t^2 - c_1^2\nabla^2)\delta n_B = 0$, with the speed of the first or thermodynamic sound $c_1 = \sqrt{\partial P/\partial n_B/m_B}$. For the confined D4/D8

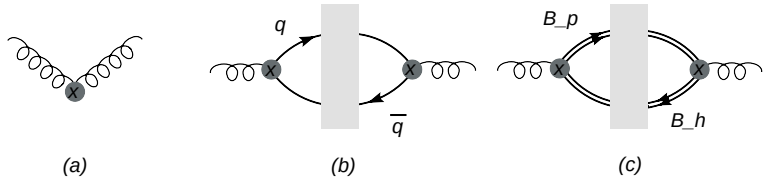

Figure 5.2: Typical contributions to the baryonic response in D4/D8. (a) Direct N_c^0 (b) Vector mesons N_c^0 and (c) Fermi (baryon) contributions N_c^{-1}

configuration

$$c_1 = \left(\frac{27\pi}{8} \frac{n_B}{\lambda^2 N_f} \int dZ \frac{1}{K} \frac{1}{\sqrt{1 + \frac{N_c^2 n_B^2}{4a^2 b} K^{-5/3}}^3} \right)^{1/2} , \tag{5.9}$$

after using (5.2). The bulk modulus is $\mathbf{K} = n_B \partial P / \partial n_B \approx n_B^2 (N_c/\lambda)$, with the compressibility $\chi = 1/\mathbf{K} \approx (\lambda/N_c)/n_B^2$. Holographic QCD is uncompressible at large N_c.

5.3 Holographic Baryonic Currents

Baryon transport in confined D4/D8 occurs explicitly through $1/N_c$ effects. Contributions to the baryonic current to order N_c^0 are shown in Fig.5.2. They follow from direct (a) or vector meson (b) such as the ω meson. All density effects in holography are suppressed at large N_c and large λ. To illustrate these points, we streamline the dense analysis given in [15] using general notations to extend the results to finite temperature and also other brane embeddings. With the induced metric (2.18) and the pertinent guage fields, the general DBI action follows as

$$\begin{aligned} S_{\rm DBI} = -\mathcal{N}\ {\rm tr} \int d^4x dU\ e^{-\phi} g_{SS}^2 \Big[& - g_{00} g_{xx}^3 g_{UU} - g_{xx}^3 F_{0U} F_{0U} \\ & - g_{xx}^2 g_{UU} \sum_i F_{0i} F_{0i} - g_{00} g_{xx}^2 \sum_i F_{iU} F_{iU} \\ & - g_{00} g_{xx} g_{UU} \sum_{i>j} F_{ij} F_{ij} - g_{xx} \sum_{i>j} F_{ij} F_{ij} F_{U0} F_{U0} + \cdots \Big]^{1/2} \end{aligned} \tag{5.10}$$

where $e^{-\phi} = g_s(U/R)^{3/4}$ and $\mathcal{N} \equiv T_8\Omega_4$. The D_8 brane tension is T_8 and Ω_4 is the volume of a unit S^4. [1] The F^3 and F^5 terms cancel by symmetry. Among the F^4 terms we only retained the relevant term for our discussion below. If we consider the fluctuation $(A_\alpha(x^\alpha))$ around the classical configuration $\mathbb{A}_0$, which is due to homogeneous matter at $Z = 0$, the action can be expanded as

$$\frac{R^{2/3}\mathcal{N}}{2g_s}(2\pi\alpha')^2\mathrm{tr}\int dU U^{5/2}\frac{1}{\sqrt{-\alpha\gamma}}\left[\frac{2\alpha\gamma\Delta^{-1}}{(2\pi\alpha')^2} + 2\Delta(\partial_U\mathbb{A}_0)F_{U0} + \Delta^3 F_{U0}F_{U0}\right.$$
$$\left. +\Delta\alpha\sum_i F_{iU}F_{iU} + \Delta\gamma\left(\frac{R}{U}\right)^3\sum_i F_{0i}F_{0i} + \Delta^{-1}\alpha\gamma\left(\frac{R}{U}\right)^3\sum_{i>j}F_{ij}F_{ij}\right] ,$$

up to quadratic terms. $F_{\alpha\beta} \equiv \partial_\alpha A_\beta - \partial_\beta A_\alpha - i[A_\alpha, A_\beta]$ and

$$\Delta \equiv \frac{1}{\sqrt{1 + \frac{(2\pi\alpha')^2}{\alpha\gamma}(\mathbb{A}_0')^2}} \quad . \tag{5.11}$$

It is useful to change variable

$$U = U_0(1 + Z^2)^{1/3} , \tag{5.12}$$

where U_0 is the coordinate of the tip of the D8-$\overline{\mathrm{D8}}$ cigar-shaped configuration in the confining background and the position of the horizon U_T in the black hole background. The range of Z is $(0, \infty)$ contrary to U whose range is (U_0, ∞). Also this range can be extended to $(-\infty, \infty)$ if we consider $\overline{\mathrm{D8}}$ branes $(-\infty, 0)$ together with D8 branes $(0, \infty)$ in a natural way. For convenience, we note the following useful relations

$$K \equiv 1 + Z^2 , \quad U = U_0 K^{1/3} , \quad dU = \frac{2U_0}{3}\frac{Z}{K^{2/3}}dZ , \quad f = 1 - \left(\frac{U_*}{U_0}\right)^3\frac{1}{K} ,$$

where U_* is U_T for the black hole background. For the confining background, from here on and for simplicity, we follow Sakai and Sugimoto [**?**] and choose

[1] We absorb $2\pi\alpha'$ into the gauge field for notational convenience. It will be recalled in the final physical quantities.

	N	k_1	k_2	k_3
D4/D8$_{\rm con}$	$\kappa \equiv \frac{\lambda N_c}{216\pi^3}$	K	$K^{-4/3}M_{\rm KK}^{-2}$	-1
D4/D8$_{\rm dec}$	$\frac{\lambda N_c T^3}{54\pi}$	$\frac{K^{3/2}}{\sqrt{K-1}}$	$K^{-4/3}(2\pi T)^{-2}$	$-\frac{K-1}{K}$
D3/D7	$\frac{\lambda N_f N_c}{2(2\pi)^4}$	Z^3	$Z^{-4}f^{-1}$	$-f$

	$2\pi\alpha'\mathbb{A}_0'$	Δ
D4/D8$_{\rm con}$	$\frac{d}{\sqrt{b}\sqrt{K^2+K^{1/3}d^2}}$	$\sqrt{1+d^2K^{-5/3}}$
D4/D8$_{\rm dec}$	$\frac{d}{\sqrt{K^{5/3}+d^2}}$	$\sqrt{1+d^2K^{-5/3}}$
D3/D7	$\frac{d}{\sqrt{Z^6+d^2}}$	$\sqrt{1+d^2Z^{-6}}$

Table 5.1: Parameters of the different embeddings in (5.13). See text.

$U_* = U_{\rm KK}$. In terms of Z the action reads

$$S = N{\rm tr}\int d^4x dZ k_1\Big[2\Delta\mathbb{A}_0' F_{Z0} + \Delta^3 F_{Z0}F_{Z0} + \Delta k_2\sum_i F_{0i}F_{0i} + \Delta k_3\sum_i F_{iZ}F_{iZ} + \Delta^{-1}k_2k_3\sum_{i>j}F_{ij}F_{ij}\Big] \quad ,(5.13)$$

where we dropped the fluctuation independent part and the parameters (k_1, k_2, k_3, Δ, N) are different for each of the brane embeddings. They are summarized in Table 1. The case $D3/D7$ is separatly discussed below (section 5.5.3). We note that the dimensionless densities are $d = \frac{3^6\pi^4}{\lambda^2 N_f M_{\rm KK}^3}n_B$ for D4/D8$_{\rm con}$, $d = \frac{3^5\pi^2}{2^5 N_c N_f \lambda T^5 l_s^2}n_B$ for D4/D8$_{\rm dec}$, and $d = \frac{(2\pi)^3}{\sqrt{\lambda}N_f N_c}n_q$ for D3/D7 with $f = 1-\frac{Z_H^4}{Z^4}$. This explicitly shows that the density effects are subleading at large λ and large N_c for fixed N_f.

Now consider an abelian fluctuation in the $A_Z = 0$ gauge

$$A_\mu = a_\mu(x^0, x^3, Z) + \mathcal{V}_\mu(x^0, x^3) \ , \quad (5.14)$$

where a_μ vanishes at the boundary i.e. $a_\mu(x^0, x^3, \infty) = 0$, so that the boundary field is simply $\mathcal{V}_\mu(x^0, x^3)$. $\mathcal{V}_\mu(x^0, x^3)$ exists for all Z as the background. [2] With

[2]This is equivalent to the usual set up A_μ with the boundary condition $A_\mu(x^0, x^3, \infty) =$

the Fourier decomposition

$$a_\mu(Z,x^0,x^3)=\int\frac{d\omega dq}{(2\pi)^2}e^{-i\omega x^0+iqx^3}a_\mu(Z,\omega,q)\ , \tag{5.15}$$

$$\mathcal{V}_\mu(Z,x^0,x^3)=\int\frac{d\omega dq}{(2\pi)^2}e^{-i\omega x^0+iqx^3}\mathcal{V}_\mu(\omega,q)\ , \tag{5.16}$$

the quadratic action can be rewritten as [3]

$$\begin{aligned}S=N\int\frac{d\omega dq}{(2\pi)^2}dZ\Big[&a_L\mathcal{D}_La_L-2f_L\mathcal{V}_La_L-f_L\mathcal{V}_L\mathcal{V}_L-2g_La_L\\&+a_T\mathcal{D}_Ta_T-2f_T\mathcal{V}_Ta_T-f_T\mathcal{V}_T\mathcal{V}_T\Big]\ ,\end{aligned}$$

where we introduced the gauge invariant variables

$$\begin{array}{rll}\text{Longitudinal mode}: & a_L\equiv qa_0+\omega a_3, & \mathcal{V}_L\equiv q\mathcal{V}_0+\omega\mathcal{V}_3\ ,\\ \text{Transverse mode}: & a_T\equiv\omega a_1, & V_T\equiv\omega\mathcal{V}_1\ ,\end{array} \tag{5.17}$$

with $a_2=0$ and used Gauss constraint $\Delta^2\omega a_0'+k_3qa_3'=0$. $a_2=0$ is a consistent choice since the transversal equation of motion decouples from the others.

The differential operators $\mathcal{D}_{L/T}$ are defined as

$$\mathcal{D}_L\equiv\partial_Z\frac{-k_1k_3\Delta^3}{\Delta^2\omega^2+k_3q^2}\partial_Z+k_1k_2\Delta\ , \tag{5.18}$$

$$\mathcal{D}_T\equiv\frac{1}{\omega^2}\Big(\partial_Zk_1k_3\Delta\partial_Z-k_1k_2(\Delta\omega^2+\Delta^{-1}k_3q^2)\Big)\ , \tag{5.19}$$

and the coefficient functions are

$$f_L\equiv-k_1k_2\Delta\ ,\qquad g_L\equiv\frac{k_3q\mathbb{A}_0'}{\Delta^2\omega^2+k_3q^2}\ , \tag{5.20}$$

$$f_T\equiv\frac{k_1k_2(\Delta\omega^2+\Delta^{-1}k_3q^2)}{\omega^2}\ . \tag{5.21}$$

$\mathcal{V}_\mu(x^0,x^3)$. The difference is in the equations of motion. The equation for A_μ is homogeneous but the equation for a_μ is inhomogeneous and sourced by $\mathcal{V}_\mu$ as shown in (5.22).

[3]For simplicity we omitted the argument of the functions. Each quadratic term is a function of (ω,q) (first) and $(-\omega,-q)$ (second). We dropped the surface terms since they vanish on shell when the source is explicitly present.

The equations of motion is

$$\mathcal{D}_L a_L = f_L \mathcal{V}_L + g_L \ , \qquad \mathcal{D}_T a_T = f_T \mathcal{V}_T. \tag{5.22}$$

With the formal solutions

$$a_L = \mathcal{D}_L^{-1}(f_L \mathcal{V}_L + g_L) \ , \qquad a_T = \mathcal{D}_T^{-1}(f_T \mathcal{V}_T) \ , \tag{5.23}$$

the on-shell action reads

$$S = -N \int \frac{d\omega dq}{(2\pi)^2} dZ \Big(\mathcal{V}_L f_L [\mathcal{D}_L^{-1}(f_L \mathcal{V}_L) + \mathcal{V}_L] + \mathcal{V}_L [2 f_L \mathcal{D}_L^{-1} g_L] \\ + g_L \mathcal{D}_L^{-1} g_L + \mathcal{V}_T f_T [\mathcal{D}_T^{-1}(f_T \mathcal{V}_T) + \mathcal{V}_T] \Big) \ . \tag{5.24}$$

The induced baryonic currents follow to leading order in large N_c and large λ as

$$J_L(\omega, q) = 2N\omega \int dZ f_L [\mathcal{D}_L^{-1}(f_L \mathcal{V}_L + g_L) + \mathcal{V}_L] \ , \tag{5.25}$$

$$J_T(\omega, q) = 2N\omega \int dZ f_T [\mathcal{D}_T^{-1}(f_T \mathcal{V}_T) + \mathcal{V}_T] \ , \tag{5.26}$$

where $\mathcal{D}_L^{-1}$ and $\mathcal{D}_T^{-1}$ are understood with the retarded prescription $\omega \to \omega + i0$. f_L, f_T, g_L are all recorded in (5.21). The longitudinal current involves g_L independently of $\mathcal{V}_L$ as g_L is triggered by the *gradient* of the baryonic profile $\mathbb{A}_0'$. This is the analogue of Fick's law (baryonic charge diffusion). The terms involving $\mathcal{V}_{L,T}$ correspond to $\sigma_{L,T}$ the longitudinal and transverse Fourier transforms of the space-time conductivities. The arguments (ω, q) are subsumed.

5.4 Baryonic current: D4/D8: Cold

In the confined phase, the operators $\mathcal{D}_{L,T}$ are hermitian modulo the retarde prescription in frequency space. They can be diagonalized using eigenmodes as discussed in [15]. Throughout the prescription $\omega \to \omega + i0$ is subsumed.

5.4.1 Longitudinal Mode

The longitudinal operator ($\mathcal{D}_L$) is

$$\mathcal{D}_L \equiv \partial_Z \frac{K\Delta^3}{\Delta^2\omega^2 - q^2}\partial_Z + K^{-1/3}\Delta \ . \tag{5.27}$$

When $q = 0$ or $\omega = 0$ it is easily diagonalized, since

$$\begin{aligned} \mathcal{D}_L(q=0) &= \frac{1}{\omega^2}\partial_Z K\Delta\partial_Z + K^{-1/3}\Delta \ , \\ \mathcal{D}_L(\omega=0) &= -\frac{1}{q^2}\partial_Z K\Delta^3\partial_Z + K^{-1/3}\Delta \ . \end{aligned} \tag{5.28}$$

The Green's function ($\mathcal{D}_L^{-1}$) may be expanded in terms of the complete set of eigenvalues that diagonalize

$$\begin{aligned} \mathcal{D}_L(q=0)f &= \left(\frac{K^{-1/3}\Delta}{\omega^2}\right)\lambda f \ , \\ \mathcal{D}_L(\omega=0)f &= \left(\frac{K^{-1/3}\Delta}{q^2}\right)\lambda f \ , \end{aligned} \tag{5.29}$$

where $\frac{K^{-1/3}\Delta}{\omega^2}$ and $\frac{K^{-1/3}\Delta}{q^2}$ are weight factors. Using the complete sets,

$$\begin{aligned} (\partial_Z K\Delta\partial_Z)\,\chi_n &= -(K^{-1/3}\Delta)\,(\lambda_n^\chi)^2\,\chi_n \ , \\ (\partial_Z K\Delta^3\partial_Z)\,\xi_n &= -(K^{-1/3}\Delta)\,(\lambda_n^\xi)^2\,\xi_n \ , \end{aligned} \tag{5.30}$$

we have

$$\langle Z|\mathcal{D}_L^{-1}(q=0)|Z'\rangle = \sum_{n\in\mathbb{N}} \frac{\chi_n(Z)\chi_n(Z')}{-\omega^2 + (\lambda_n^\chi)^2} + \frac{\chi_0(Z)\chi_0(Z')}{-\omega^2} \ , \tag{5.31}$$

$$\langle Z|\mathcal{D}_L^{-1}(\omega=0)|Z'\rangle = \sum_{n\in\mathbb{N}} \frac{\xi_n(Z)\xi_n(Z')}{q^2 + (\lambda_n^\xi)^2} + \frac{\xi_0(Z)\xi_0(Z')}{q^2} \ , \tag{5.32}$$

which are the results of [15]. Typical behaviors of χ_n and ξ_n are shown in Fig.(5.3).

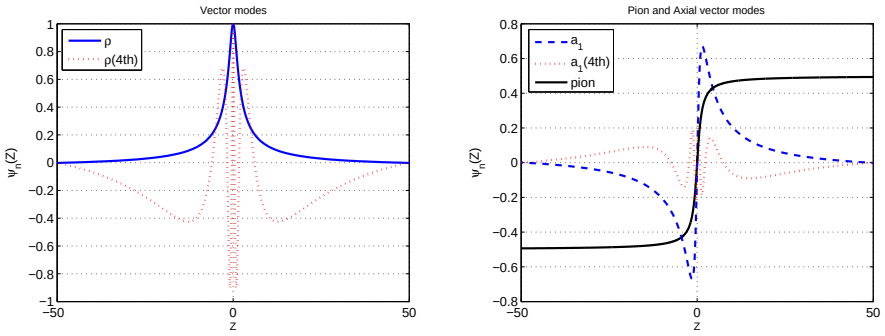

Figure 5.3: Vector mode functions (Left) and axial-vector and pion mode functions (Right)

For small ω, q we may write without loss of generality,

$$\begin{aligned}\langle Z|\mathcal{D}_L^{-1}(\omega\approx q\approx 0)|Z'\rangle \;\approx\; & \sum_{n\in 2\mathbb{N}}\frac{\varphi_n(Z)\varphi_n(Z')}{-\omega^2+c_n^2q^2+(\lambda_n^\chi)^2}+\frac{\varphi_0(Z)\varphi_0(Z')}{-\omega^2+c_\pi^2q^2}\\ & +\sum_{n\in 2\mathbb{N}+1}\frac{\varphi_n(Z)\varphi_n(Z')}{-\omega^2+c_n^2q^2+(\lambda_n^\chi)^2}\ .\end{aligned}\tag{5.33}$$

The first contribution is from the density dependent axial-vector mode, the second contribution is from the density dependent pion mode (strictly speaking its U(1) partner at large N_c), and the last contribution is from the density dependent vector mode. The denominators are the dispersive modes, while the numerators capture their residues. The even-odd in the labelling of the modes translates into odd-even in the parity of $\varphi_n(Z)$. The baryonic current reads

$$J_L=2N\omega\int dZK^{-1/3}\Delta\left[\mathcal{D}_L^{-1}(K^{-1/3}\Delta\mathcal{V}_L+g_L)+\mathcal{V}_L\right]\ .\tag{5.34}$$

The Z-integration picks only the vector or even-modes of (5.31) since $\mathcal{V}_L$ is trivially even. The longitudinal baryonic conductivity in the confined case is

$$\sigma_L=2N\omega\int dZK^{-1/3}\Delta\left[1+\mathcal{D}_L^{-1}K^{-1/3}\Delta\right]\ .\tag{5.35}$$

The longitudinal mesonic propagator $\mathcal{D}_L^{-1}$ admits the mode decomposition

(5.33). From (5.30) it follows that

$$\int dZ f_L \chi_n = \frac{1}{\lambda_n^2} \int dZ \left(\partial_Z K \Delta \partial_Z\right) \chi_n = \frac{1}{\lambda_n^2} \left(K \Delta \partial_Z \chi_n\right)_{-\infty}^{+\infty} = 0$$

is a zero boundary term. The longitudinal baryonic conductivity simplifies

$$\sigma_L = -2N\omega \int dZ f_L \ , \tag{5.36}$$

and so does the longitudinal current. The longitudinal conductivity vanishes at $\omega = 0$. Confined holographic QCD is a static insulator at large N_c and large λ in agreement with our recent analysis [18].

We now note that

$$c_n \equiv \frac{\lambda_n^\chi}{\lambda_n^\xi} \ , \qquad c_\pi \equiv \frac{f_\pi^S}{f_\pi^T} = \sqrt{\frac{\int dZ K^{-1} \Delta^{-3}}{\int dZ K^{-1} \Delta^{-1}}}, \tag{5.37}$$

where f_π^S and f_π^T have been derived in [15]. At high density the pion speed vanishes as $c_\pi \approx 1/n_B$. The propagation of the axial charge stalls in very dense matter. For small momenta q the poles develop at

$$\omega_n \approx \sqrt{(c_n^2 q^2 + \lambda_n^{\chi})^2} \approx \lambda_n^\chi + \frac{1}{2} \frac{c_n^2 q^2}{\lambda_n^\chi} \ , \tag{5.38}$$

while for small frequencies ω

$$c_n^2(-(\lambda_n^\xi)^2) + (\lambda_n^\chi)^2 = 0 \ \Rightarrow c_n^2 = \left(\frac{\lambda_n^\chi}{\lambda_n^\xi}\right)^2 \ , \tag{5.39}$$

since $q_n^2 = -(\lambda_n^\xi)^2$ from (5.32). In the confined D4/D8 embedding, the vector and axial modes disperse through

$$\omega_n \approx \lambda_n^\chi + \frac{1}{2} \frac{\lambda_n^\chi}{(\lambda_n^\xi)^2} q^2 \ , \tag{5.40}$$

where λ_n^χ is the rest mass and $\frac{(\lambda_n^\xi)^2}{\lambda_n^\chi}$ is the kinetic mass (Fig.5.4). To this order, the imaginary parts vanish in holographic QCD [15]. Indeed, vector, axial-vector and pionic modes are expected to be absorbed by excited and/or recoiling baryons which are $1/N_c$ suppressed effects in cold and dense QCD.

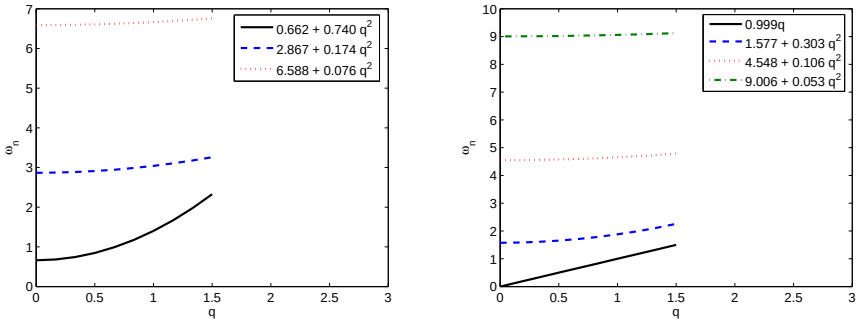

Figure 5.4: Dispersion relation for vectors (Left) and axial-vectors including the massless pion (Right), $n = 1.26 n_0$

5.4.2 Transverse Mode

The transverse operator ($\mathcal{D}_T$) is given by

$$\mathcal{D}_T \equiv -\frac{1}{\omega^2}\left(\partial_Z K \Delta \partial_Z + K^{-1/3}(\Delta\omega^2 - \Delta^{-1}q^2)\right) \ . \tag{5.41}$$

For $q = 0$ it diagonalizes trivially through

$$\mathcal{D}_T(q=0) \equiv -\frac{1}{\omega^2}\partial_Z K \Delta \partial_Z - K^{-1/3}\Delta \ , \tag{5.42}$$

The Green's function ($\mathcal{D}_L^{-1}$) may be expanded in terms of the complete set of eigenvalues that diagonalize

$$\mathcal{D}_T(q=0) f = -\left(\frac{K^{-1/3}\Delta}{\omega^2}\right)\lambda f \ , \tag{5.43}$$

by using the eigenvalues

$$\left(\partial_Z K \Delta \partial_Z\right)\chi_n = -\left(K^{-1/3}\Delta\right)\left(\lambda_n^\chi\right)^2 \chi_n \ . \tag{5.44}$$

The Green's function is then expanded as

$$\langle Z|\mathcal{D}_T^{-1}(q=0)|Z'\rangle = \sum_{n\in\mathbb{N}} \frac{\chi_n(Z)\chi_n(Z')}{-\omega^2 + (\lambda_n^\chi)^2} + \frac{\chi_0(Z)\chi_0(Z')}{-\omega^2} \ , \tag{5.45}$$

which is the same as $\mathcal{D}_L^{-1}$. A rerun of the arguments for the longitudinal current response yields

$$J_T(\omega,q) = 2N\omega \int dZ f_T[\mathcal{D}_T^{-1}(f_T\mathcal{V}_T) + \mathcal{V}_T] \ , \tag{5.46}$$

where again the retarded prescription is subsumed and

$$f_T = \frac{K^{-1/3}(\Delta\omega^2 - \Delta^{-1}q^2)}{\omega^2} \ . \tag{5.47}$$

In the confined phase, the transverse conductivity follows

$$\sigma_T = 2N\omega \int dZ f_T[1 + \mathcal{D}_T^{-1} f_T] \ . \tag{5.48}$$

Using the vector meson mode decomposition for $\mathcal{D}_T^{-1}$ (5.33) and the relation (7.98) we can simplify the transverse conductivity

$$\sigma_T = \sigma_L + 2N\omega \int dZ (f_T + f_L)[1 + \mathcal{D}_T^{-1}(f_T + f_L)] \ , \tag{5.49}$$

with

$$f_T + f_L = -\frac{q^2}{\omega^2} K^{-1/3}\Delta^{-1} \ . \tag{5.50}$$

The transverse conductivity is vector meson mediated as shown in Fig.5.2. For $q = 0$, $\sigma_T = \sigma_L$ and vanishes for $\omega \to 0$ in agreement with [18].

5.5 Quasi-normal mode analysis

we now turn our attention to the deconfined phase of dense holographic models with non-hermitean or absorptive boundary conditions. For that, the retarded prescription on the inversion of $\mathcal{D}_{L,T}$ is best captured by the quasi-normal mode analysis. The latter is enforced analytically by matching for the gapless modes and numerically for the gapped modes. We now present the general formulas pertinent to the longitudinal and transverse currents.

For $\omega \ll 1, q \ll 1$ the equations (5.18) and (5.19) are reduced to

$$\left(\partial_Z \frac{-k_1 k_3 \Delta^3}{\Delta^2 \omega^2 + k_3 q^2} \partial_Z\right) a_L = 0 \ , \tag{5.51}$$

$$(\partial_Z k_1 k_3 \Delta \partial_Z)\, a_T = 0 \ . \tag{5.52}$$

The general solutions are

$$a_L(Z) = C_L \int_Z^\infty dZ \left(\frac{\omega^2}{-k_1 k_3 \Delta} + \frac{q^2}{-k_1 \Delta^3}\right) \ , \tag{5.53}$$

$$a_T(Z) = C_T \int_Z^\infty dZ \left(\frac{1}{-k_1 k_3 \Delta}\right) = a_L(Z)(q \to 0, \omega \to 1) \ , \tag{5.54}$$

where we imposed the vanishing Dirichlet boundary condition at the boundary $Z = \infty$ i.e. $a_{L/T}(\infty) = 0$. $C_{L/T}$ will be determined by imposing incoming boundary condition at $Z = 0$ which corresponds to the location of matter (confined phase) or the black hole horizon (deconfined phase).

To constrain $C_{L/T}$ we need to know the behavior of $a_{L/T}$ around $Z = 0$. First, we solve the equations (5.18) and (5.19) near $Z = 0$ with fixed ω and q. Second, we take the limit $\omega \ll 1, q \ll 1$. $\Delta_L a_L = 0$ and $\Delta_T a_T = 0$ may be written as

$$a_L'' + \left[\frac{\Delta'(3k_3 q^2 + \omega^2 \Delta^2 (1 - k_3 (1/k_3)' \Delta/\Delta'))}{\Delta(k_3 q^2 + \omega^2 \Delta^2)} + \frac{k_1'}{k_1}\right] a_L' - k_2 \frac{\omega^2 \Delta^2 + k_3 q^2}{k_3 \Delta^2} a_L = 0 \ , \tag{5.55}$$

$$a_T'' + \left[\frac{(k_1 k_3 \Delta)'}{k_1 k_3 \Delta}\right] a_T' - k_2 \frac{\omega^2 \Delta^2 + k_3 q^2}{k_3 \Delta^2} a_T = 0 \ . \tag{5.56}$$

In this analysis the variable Z introduced in (5.12) is not convenient due to the complicated form of Δ. To make it simpler we introduce the new variable:

$$z = \frac{1}{(1 + Z^2)^{1/3}}, \tag{5.57}$$

which is nothing but U_0/U in terms of the original coordinate in (3.26). In this coordinate the boundary is $u = 0$ and the horizon or the matter location is $u = 1$.

5.5.1 D4/D8: Cold and Dense

Before analyzing the deconfined phase of D4/D8 with black-hole background absorption, it is amusing to ask whether the D4/D8 confined background with matter in the KK background could be also addressed with *absorptive* or non-hermitean boundary conditions. After all *cold* matter disperses and absorbs waves much like a black-hole. From (5.53) and (5.54) it follows that

$$a_L = C_L(\omega^2 a_\omega(z) - q^2 a_q(z)) \ , \tag{5.58}$$

$$a_T = C_T a_\omega(z) \ , \tag{5.59}$$

where

$$a_q(z) \equiv \int_0^z dz' \sqrt{\frac{z'}{(1+d^2 z'^5)^3}} \frac{1}{\sqrt{1-z'^3}} \ , \tag{5.60}$$

$$a_\omega(z) \equiv \int_0^z dz' \sqrt{\frac{z'}{1+d^2 z'^5}} \frac{1}{\sqrt{1-z'^3}} \ , \tag{5.61}$$

for $\omega, q \ll 1$. Recall that the density d is defined by $\frac{3^6\pi^4}{\lambda^2 N_f M_{\rm KK}^3} n_B$ below (5.13). At small densities we expand

$$\begin{aligned} a_L(z) = C_L \Big[& (\omega^2 - q^2) a^{(0)}(z) - \frac{d^2}{2}(\omega^2 - 3q^2) a^{(1)}(z) \\ & + \frac{3d^4}{8}(\omega^2 - 5q^2) a^{(2)}(z) \Big] + \mathcal{O}(d^6) \ , \end{aligned} \tag{5.62}$$

with

$$\begin{aligned} a^{(0)}(z) &= \int_0^z dz' \sqrt{\frac{z'}{1-z'^3}} = -\frac{2}{3}\left(\arcsin(\sqrt{1-z^3}) - \frac{\pi}{2}\right) \ , \\ a^{(1)}(z) &= \int_0^z dz' \sqrt{\frac{z'}{1-z'^3}}\ z'^5 \\ &= -\frac{1}{60}\sqrt{1-z^3}(3\sqrt{z}(7+4z^3) + 7\ {}_2F_1[1/2, 5/6; 3/2; 1-z^3]) \\ &\quad + \frac{7\sqrt{\pi}}{120}\frac{\Gamma(1/6)}{\Gamma(2/3)} \ , \\ a^{(2)}(z) &= \int_0^z dz' \sqrt{\frac{z'}{1-z'^3}}\ z'^{10} \ . \end{aligned}$$

We don't show $a^{(2)}(z)$ explicitly since it is long and not illuminating.

To impose the *incoming boundary condition* we expand the solution around $z = 1$

$$a_L(z) = C_L A + C_L B\sqrt{1-z} + \mathcal{O}((1-z)^{3/2}) \ , \tag{5.63}$$

where

$$\begin{aligned} A \equiv & -\frac{\pi}{3}(q^2-\omega^2) + \frac{7d^2\sqrt{\pi}(3q^2-\omega^2)\Gamma(1/6)}{240\Gamma(2/3)} \\ & + \frac{187d^4\sqrt{\pi}(-5q^2+\omega^2)\Gamma(5/6)}{3584\Gamma(4/3)} \ , \\ B \equiv & \frac{(-8+12d^2-15d^4)q^2 + (8-4d^2+3d^4)\omega^2}{4\sqrt{3}} \ , \end{aligned} \tag{5.64}$$

On the other hand we may first solve the equation near z=1. In general $\Delta_L a_L = 0$ and $\Delta_T a_T = 0$ are

$$\begin{aligned} & a_L'' + \left[\frac{(5d^2z^4)\{3q^2-\omega^2(1+d^2z^5)\}}{2(1+d^2z^5)\{q^2-\omega^2(1+d^2z^5)\}} - \frac{3z^2}{2(1-z^3)} - \frac{1}{2z}\right] a_L' \\ & \qquad - \frac{9\{q^2-\omega^2(1+d^2z^2)\}}{4z(1-z^3)(1+d^2z^5)} a_L = 0 \ , \end{aligned} \tag{5.65}$$

$$\begin{aligned} & a_T'' + \left[\frac{(5d^2z^4)}{2(1+d^2z^5)} - \frac{3z^2}{2(1-z^3)} - \frac{1}{2z}\right] a_L' \\ & \qquad - \frac{9\{q^2-\omega^2(1+d^2z^2)\}}{4z(1-z^3)(1+d^2z^5)} a_L = 0 \ , \end{aligned} \tag{5.66}$$

and reduce to

$$a_{L/T}'' - \frac{1}{2}\frac{1}{1-z} a_{L/T}' + \frac{3}{4}\frac{\omega^2 - \frac{q^2}{1+d^2}}{(1-z)} a_{L/T} = 0 \ , \tag{5.67}$$

near $z = 1$. The solutions are

$$a_{L/T} = C_I e^{-i\sqrt{3\gamma(1-z)}} \ , \qquad \gamma \equiv \omega^2 - \frac{q^2}{1+d^2} \ , \tag{5.68}$$

where we imposed the incoming boundary condition at $z = 1$. Their expanded

form reads

$$a_L(z) \approx C_I - iC_I\sqrt{3\gamma}\sqrt{1-z} + \mathcal{O}(1-z) \ , \tag{5.69}$$

$$\gamma = \omega^2 - q^2 + q^2d^2 - q^2d^4 + \mathcal{O}(d^6) \ . \tag{5.70}$$

A comparison of (5.63) and (5.69) yields

$$B + iA\sqrt{3\gamma} = 0 \ , \tag{5.71}$$

and the dispersion relation is

$$\omega = \pm\left[1 - \frac{d^2}{2} + \frac{3d^4}{8} + \mathcal{O}(d^6)\right] q + \mathcal{O}(d^6)q^2 + \mathcal{O}(d^6)q^3 + \mathcal{O}(q^4) \quad . \tag{5.72}$$

The latter resums to

$$\omega = \pm\frac{1}{\sqrt{1+d^2}}q \ . \tag{5.73}$$

This is consistent with the zero mode result obtained in (5.33), (5.37) and Fig.5.4 where we also found the zero mode solution odd in Z. Interestingly enough, the quasinormal mode analysis when applied to the confined and dense KK background with absorptive boundary condition, it yields a massless pole which is the pion pole with a speed $c_\pi = 1/\sqrt{1+d^2}$. Note that there is *no imaginary* part. The reason can be traced back to the + (outgoing) and − (incoming) wave assignment in (5.71), both of which solve

$$0 = B \pm iA\sqrt{3\gamma} = \left[\frac{8 - 4d^2 + 3d^4}{4\sqrt{3}}\sqrt{\gamma} \pm i\sqrt{3}\right]\sqrt{\gamma} = 0 \ , \tag{5.74}$$

for $\gamma = 0$.

For the transverse mode we may follow the same procedure with the substitution in (5.63)

$$a_T(z) = a_L(z)(q \to 0 \ , \omega \to 1) \ . \tag{5.75}$$

The relation (5.71) yields

$$\omega = i\left[\frac{2}{\pi} + \left(-\frac{1}{\pi} + \frac{7\Gamma(1/6)}{40\pi^{3/2}\Gamma(2/3)}\right) d^2 + \mathcal{O}(d^4)\right] + \mathcal{O}(q) \ , \tag{5.76}$$

which shows that there is no massless excitation. This channel is indeed gapped in the confined D4/D8 case as we discussed earlier for the case of reflecting boundary conditions.

5.5.2 D4/D8: Hot and Dense

The absorptive boundary condition is more appropriate for the deconfined BH background that we now discuss. For that, we rerun the same steps as we did in the previous section. First we solve the equations for $\mathfrak{w} \ll 1, \mathfrak{q} \ll 1$, where $\mathfrak{w} \equiv \frac{\omega}{2\pi T}$ and $\mathfrak{q} \equiv \frac{q}{2\pi T}$. From (5.53) and (5.54)

$$a_L = C_L(\mathfrak{w}^2 a_{\mathfrak{w}}(z) - \mathfrak{q}^2 a_{\mathfrak{q}}(z)) \ , \tag{5.77}$$

$$a_T = C_T a_{\mathfrak{w}}(z) \ , \tag{5.78}$$

where

$$\begin{aligned} a_{\mathfrak{q}}(z) &\equiv \int_0^z dz' \sqrt{\frac{z'}{(1+d^2 z'^5)^3}} \qquad (5.79)\\ &= \frac{2}{15} z^{3/2}\left[\frac{3}{\sqrt{1+d^2 z^5}} + 2\ {}_2F_1[3/10, 1/2; 13/10; -d^2 z^5]\right] \ , \\ a_{\mathfrak{w}}(z) &\equiv \int_0^z dz' \sqrt{\frac{z'}{1+d^2 z'^5}} \frac{1}{1-z'^3} \ . \qquad (5.80) \end{aligned}$$

Recall that the density d is defined by $\frac{3^5\pi^2}{2^5\lambda N_c N_f T^5 l_s^2} n_B$ below (5.13). To impose the incoming boundary condition we expand a_L around the horizon.

$$\begin{aligned} a_L(1-\epsilon) &= a_L(1) - \epsilon a_L'(1) + \cdots \\ &= C_L \mathfrak{w}^2 a_{\mathfrak{w}}(1) - \frac{C_L \mathfrak{w}^2}{3\sqrt{1+d^2}} - C_L \mathfrak{q}^2 a_{\mathfrak{q}}(1) + \mathcal{O}(\epsilon) \ , \end{aligned} \tag{5.81}$$

where $a_{\mathfrak{w}}(1)$ has a logarithmic divergence and $a_{\mathfrak{q}}(1)$ is finite.

In general $\Delta_L a_L = 0$ and $\Delta_T a_T = 0$ are

$$\begin{aligned} a_L'' + \Bigg[& \frac{(5d^2z^4)\{3(1-z^3)q^2 - \mathfrak{w}^2(1+d^2z^5)\}}{2(1+d^2z^5)\{(1-z^3)\mathfrak{q}^2 - \mathfrak{w}^2(1+d^2z^5)\}} \\ & + \frac{\mathfrak{w}^2(1+d^2z^5)}{(1-z^3)\mathfrak{q}^2 - \mathfrak{w}^2(1+d^2z^5)} \frac{3z^2}{1-z^3} - \frac{1}{2z} \Bigg] a_L' \\ & - \frac{9\{(1-z^3)\mathfrak{q}^2 - \mathfrak{w}^2(1+d^2z^2)\}}{4z(1-z^3)^2(1+d^2z^5)} a_L = 0 \ , \\ a_T'' + \Bigg[& \frac{(5d^2z^4)}{2(1+d^2z^5)} - \frac{3z^2}{(1-z^3)} - \frac{1}{2z} \Bigg] a_T' \\ & - \frac{9\{(1-z^3)\mathfrak{q}^2 - \mathfrak{w}^2(1+d^2z^2)\}}{4z(1-z^3)^2(1+d^2z^5)} a_T = 0 \ , \end{aligned}$$

which simplify to

$$a_{L/T}'' - \frac{1}{1-z} a_{L/T}' + \frac{\mathfrak{w}^2}{4(1-z)^2} a_{L/T} = 0 \ , \tag{5.82}$$

near the horizon with $z = 1$. The incoming wave solution near the horizon is

$$a_{L/T} = (1-z)^{-i\mathfrak{w}/2} F(z) \ , \tag{5.83}$$

with $F(z)$ a regular function near $z = 1$ or $z = 1 - \epsilon$. Assuming $\mathfrak{w} \ln \epsilon \ll 1$ we have

$$\begin{aligned} \epsilon^{-i\mathfrak{w}/2} F(1-\epsilon) &= F(1-\epsilon) - \frac{i\mathfrak{w}}{2} \ln \epsilon F(1-\epsilon) + \cdots \\ &= F(1) - \frac{i\mathfrak{w}}{2} \ln \epsilon|_{\epsilon \to 0} F(1) + \mathcal{O}(\epsilon) \ . \end{aligned} \tag{5.84}$$

By comparing the singular part of (5.81) with (5.84) we get

$$C_L = \frac{i3\sqrt{1+d^2}}{2\mathfrak{w}} F(1) \ . \tag{5.85}$$

By comparing the regular part of (5.81) with (5.84) we get the dispersive retation for the longitudinal baryonic waves

$$1 = -\frac{i\mathfrak{w}}{2} - \frac{i3a_{\mathfrak{q}}(1)\sqrt{1+d^2}}{2} \frac{\mathfrak{q}^2}{\mathfrak{w}} \ . \tag{5.86}$$

For small $\mathfrak{w}$ and $\mathfrak{q}$ but fixed $\mathfrak{q}^2/\mathfrak{w}$ the dispersion relation is

$$\begin{aligned}\omega &\approx -\frac{i3\sqrt{1+d^2}}{2}\frac{q^2}{2\pi T}\frac{2}{15}\left[\frac{3}{\sqrt{1+d^2}}+2\ {}_2F_1[3/10,1/2;13/10;-d^2]\right] \\ &\approx -i\frac{q^2}{2\pi T}\left(1+\frac{2d^2}{13}-\frac{16d^4}{299}+\cdots\right) \quad \text{(For small } d) \\ &\approx -i\frac{q^2}{2\pi T}\left(\frac{2\Gamma(1/5)\Gamma(13/10)}{5\Gamma(1/2)}d^{2/5}+\frac{\Gamma(1/5)\Gamma(13/10)}{5\Gamma(1/2)}d^{-8/5}+\cdots\right) \\ &\qquad \text{(For large } d)\ , \end{aligned} \tag{5.87}$$

where both the small and large baryon density limits are displayed explicitly. The longitudinal diffusion constant is

$$D_L \approx \frac{\sqrt{1+d^2}}{2\pi T}\left[\frac{3/5}{\sqrt{1+d^2}}+\frac{2}{5}\ {}_2F_1[3/10,1/2;13/10;-d^2]\right] . \tag{5.88}$$

For zero baryon density this is $D = 1/2\pi T$. In the deconfined phase of D4/D8 the baryonic charge diffuses whatever the density. This is expected from baryon number conservation. The presence of the BH in the deconfined phase overwhelms the Fermi effects.

A rerun of the analysis for the transverse baryonic current follows the substitution

$$a_T = a_L(\mathfrak{q} \to 0\ , \mathfrak{w} \to 1)\ . \tag{5.89}$$

Comparing the singular part of (5.81) and (5.84) gives

$$C_T = \frac{i3\mathfrak{w}\sqrt{1+d^2}}{2}F(1)\ , \tag{5.90}$$

and comparing the regular part of (5.81) and (5.84) yields

$$\mathfrak{w}^3 = i2\ . \tag{5.91}$$

Thus there is no hydrodynamic pole. The transverse baryonic current in dense and deconfined D4/D8 is still gapped. It is much like a *transverse plasmon*.

5.5.3 D3/D7: Hot and Dense

For comparison, let us consider in this case the non-chiral and non-confining embedding with D3/D7 at finite temperature and finite density. We consider the massless quark embedding where analytic solutions are available [98]. The induced metric becomes simply $AdS_5 \times S^3$ independent of the gauge field.

$$ds^2 = \frac{Z^2}{R^2}(-f dt^2 + d\vec{x}^2) + f^{-1}\frac{R^2}{Z^2}dZ^2 + R^2 d\Omega_3^2 \ , \quad f \equiv 1 - \frac{Z_H^4}{Z^4} \ , \tag{5.92}$$

where $R = 4\pi g_s N_c \alpha'^2$ is the curvature radius. We work in units of $R = 1$. $Z_H = \pi T$ where T is the temperature. SUGRA and SYM quantities will be tied by $\alpha' = 1/\sqrt{\lambda}$ with $\lambda = 4\pi g_s N_c$. With this metric, we compute the DBI action as

$$\begin{aligned} S_{\rm DBI} = -\mathcal{N}\ {\rm tr} \int d^4x dZ\ g_{SS}^{3/2} \big[& -g_{00}g_{xx}^3 g_{ZZ} - g_{xx}^3 F_{0Z}F_{0Z} \\ & -g_{xx}^2 g_{ZZ}\sum_i F_{0i}F_{0i} - g_{00}g_{xx}^2 \sum_i F_{iZ}F_{iZ} \\ & -g_{00}g_{xx}g_{ZZ}\sum_{i>j} F_{ij}F_{ij} - g_{xx}\sum_{i>j} F_{ij}F_{ij}F_{Z0}F_{Z0} + \cdots \big]^{1/2} \end{aligned} \tag{5.93}$$

The result is analogous to the D4/D8 case (5.10) with three differences: 1) $\mathcal{N} = T_7\Omega_3$; 2) there is no contribution from the dilaton; 3) $g_{SS}^{3/2}$ appears instead of $g_{SS}^{4/2}$, since the compact space is S^3 not S^4.

To consider finite baryon density (or chemical potential) we set the background vector $U(1)$ field $\mathbb{A}_0(Z)$ in bulk. Its form follows from minimizing the DBI action (5.93):

$$2\pi\alpha'\mathbb{A}_0' = \frac{d}{\sqrt{Z^6 + d^2}} \ . \tag{5.94}$$

We explicitly recalled $2\pi\alpha'$ and $d \equiv \frac{(2\pi)^3}{\sqrt{\lambda}N_f N_c} n_q$ [97, 98].

Following the analysis in D4/D8 above, we now consider mesonic fluctuations around the density background $\mathbb{A}_0$. In the general form cast in (5.13)

the quadratic action reads

$$S = N\mathrm{tr}\int d^4xdZk_1\Big[\Delta^3 F_{Z0}F_{Z0} + \Delta k_2\sum_i F_{0i}F_{0i} + \Delta k_3\sum_i F_{iZ}F_{iZ} + \Delta^{-1}k_2k_3\sum_{i>j}F_{ij}F_{ij}\Big] ,$$

where the information of the background field $\mathbb{A}_0$ is encoded in Δ and

$$N = \frac{\lambda N_f N_c}{2(2\pi)^4} , \qquad \Delta = \sqrt{1+d^2Z^{-6}} ,$$
$$k_1 = Z^3 , \qquad k^2 = Z^{-4}f^{-1} , \qquad k^3 = f^{-1}, \tag{5.95}$$

as in Table.5.1.

In this general form we can use (5.51)-(5.56). In terms of the variable $z = \frac{Z_H}{Z}$, $\mathfrak{w} = \frac{\omega}{2\pi T}$, $\mathfrak{q} \equiv \frac{q}{2\pi T}$, and $\mathbf{d} \equiv \frac{d}{(\pi T)^3}$ we have

$$a_L = C_L(\mathfrak{w}^2 a_{\mathfrak{w}}(z) - \mathfrak{q}^2 a_{\mathfrak{q}}(z)) , \tag{5.96}$$
$$a_T = C_T a_{\mathfrak{w}}(z) , \tag{5.97}$$

with

$$a_{\mathfrak{q}}(z) \equiv \int_0^z dz' \frac{z'}{\sqrt{1+\mathbf{d}^2 z'^6}^3} \tag{5.98}$$
$$= z^2({}_2F_1[3/2, 1/3; 4/3, -z^6d^2]) ,$$
$$a_{\mathfrak{w}}(z) \equiv \int_0^z dz' \frac{z'}{\sqrt{1+\mathbf{d}^2 z'^6}}\frac{1}{1-z'^4} . \tag{5.99}$$

Note that the integrand in $a_{\mathfrak{w}}$ exhibits explicitly the BH horizon at $z' = 1$ in units of temperature. At zero temperature the integrand smoothly reduces from $1/(1-z'^4)$ to 1. However, the BH singularity makes the integral logarithmically divergent at the horizon. As a result, the zero temperature limit is singular and will be considered separatly next. To impose the incoming boundary condition we expand a_L around the horizon.

$$a_L(1-\epsilon) = a_L(1) - \epsilon a_L'(1) + \cdots$$
$$= C_L\mathfrak{w}^2 a_{\mathfrak{w}}(1) - \frac{C_L\mathfrak{w}^2}{4\sqrt{1+\mathbf{d}^2}} - C_L\mathfrak{q}^2 a_{\mathfrak{q}}(1) + \mathcal{O}(\epsilon) , \tag{5.100}$$

Alternatively, the zero mode equation ($\mathcal{D}_L a_L = 0$) is

$$\partial_z^2 a_L + \left[\frac{3\mathbf{d}^2 z^5}{(1+\mathbf{d}^2 z^6)}\left(\frac{3(1-z^4)\mathfrak{q}^2 - \mathfrak{w}^2(1+\mathbf{d}^2 z^6)}{(1-z^4)\mathfrak{q}^2 - \mathfrak{w}^2(1+\mathbf{d}^2 z^6)}\right) + \frac{\mathfrak{w}^2(1+\mathbf{d}^2 z^6)}{(1-z^4)\mathfrak{q}^2 - \mathfrak{w}^2(1+\mathbf{d}^2 z^6)}\frac{4z^3}{1-z^4} - \frac{1}{z}\right]\partial_z a_L + \frac{4}{1-z^4}\left(\frac{\mathfrak{w}^2}{1-z^4} - \frac{\mathfrak{q}^2}{1+\mathbf{d}^2 z^6}\right) a_L = 0 \ , \quad (5.101)$$

$$\partial_z^2 a_T + \left[\frac{3\mathbf{d}^2 z^5}{(1+\mathbf{d}^2 z^6)} - \frac{4z^3}{1-z^4} - \frac{1}{z}\right]\partial_z a_T + \frac{4}{1-z^4}\left(\frac{\mathfrak{w}^2}{1-z^4} - \frac{\mathfrak{q}^2}{1+\mathbf{d}^2 z^6}\right) a_T = 0 \ , \quad (5.102)$$

which reduces to

$$a''_{L/T} - \frac{1}{1-z}a'_{L/T} + \frac{\mathfrak{w}^2}{4(1-z)^2}a_{L/T} = 0 \ , \quad (5.103)$$

near the horizon at $z = 1$. The incoming wave solution is of the form

$$a_{L/T} = (1-z)^{-i\mathfrak{w}/2}F(z) \ , \quad (5.104)$$

with $F(z)$ a regular function near $z = 1$. For $\mathfrak{w}\ln\epsilon \ll 1$ we have

$$\begin{aligned}\epsilon^{-i\mathfrak{w}/2}F(1-\epsilon) &= F(1-\epsilon) - \frac{i\mathfrak{w}}{2}\ln\epsilon F(1-\epsilon) + \cdots \\ &= F(1) - \frac{i\mathfrak{w}}{2}\ln\epsilon|_{\epsilon\to 0}F(1) + \mathcal{O}(\epsilon) \ . \end{aligned} \quad (5.105)$$

A comparison of the singular part of (5.100) and (5.105) yields

$$C_L = \frac{i2\sqrt{1+\mathbf{d}^2}}{\mathfrak{w}}F(1) \ , \quad (5.106)$$

and a comparison of (5.100) and (5.105) yields

$$1 = -\frac{i\mathfrak{w}}{2} - i2a_{\mathfrak{q}}(1)\sqrt{1+\mathbf{d}^2}\frac{\mathfrak{q}^2}{\mathfrak{w}} \ . \quad (5.107)$$

For small $\mathfrak{w}$ and $\mathfrak{q}$ with fixed $\mathfrak{q}^2/\mathfrak{w}$ the dispersion relation follows

$$\begin{aligned}
\omega &\approx -i\sqrt{1+\left(\frac{d}{(\pi T)^3}\right)^2}\,\frac{q^2}{2\pi T}\;{}_2F_1[3/2,1/3;4/3;-d^2] \\
&\approx -i\frac{q^2}{2\pi T}\left(1+\frac{1}{8}\left(\frac{d}{(\pi T)^3}\right)^2-\frac{1}{112}\left(\frac{d}{(\pi T)^3}\right)^4+\cdots\right) \quad \left(\frac{d}{(\pi T)^3}\ll 1\right) \\
&\approx -i\frac{q^2}{2\pi T}\left(\frac{2\Gamma(7/6)\Gamma(4/3)}{\Gamma(1/2)}\left(\frac{d}{(\pi T)^3}\right)^{1/3}\right. \\
&\qquad \left.+\frac{\Gamma(7/6)\Gamma(4/3)}{\Gamma(1/2)}\left(\frac{d}{(\pi T)^3}\right)^{-5/3}-\cdots\right)\left(\frac{d}{(\pi T)^3}\gg 1\right)\ . \qquad (5.108)
\end{aligned}$$

The longitudinal diffusion constant for hot and dense D3/D7 is

$$D_L \approx \frac{1}{2\pi T}\sqrt{1+\left(\frac{d}{(\pi T)^3}\right)^2}\;{}_2F_1[3/2,1/3;4/3;-d^2]\ . \qquad (5.109)$$

As mentioned earlier the zero temperature limit is singular owing to the occurence of the BH pole in the issuing integrals.

To analyze the transverse baryonic current [4] in the same limit of small ω, q we follow the same procedure with the substitution in (5.100)

$$a_T = a_L(q\to 0\ ,\mathfrak{w}\to 1)\ . \qquad (5.110)$$

A comparison of the singular part of (5.100) and (5.105) yields

$$C_T = i2\mathfrak{w}\sqrt{1+\mathbf{d}^2}F(1)\ , \qquad (5.111)$$

while a comparison of the regular part of (5.100) and (5.105) gives

$$\mathfrak{w}^3 = i2\ , \qquad (5.112)$$

which is incompatible with the limits. The transverse baryonic mode in hot and dense D3/D7 is gapped much like the transverse plasmon in dense matter. This reflects on the long-range nature of the transverse forces in holography. We will comment further on this point below.

[4] See [99] for related work on the dispersion relation

5.5.4 D3/D7: Cold and Dense

In a recent analysis [97] have reported the occurence of a *zero sound* mode in cold D3/D7. For completeness we now rederive their results using our general result (5.53). At zero temperature we set $Z_H = 0$ in (5.92) and change the variable to $z = 1/Z$.

For $\omega \ll 1$ and $q \ll 1$ (5.53) gives

$$a_L = C_L(\omega^2 a_\omega(z) - q^2 a_q(z)) \ , \tag{5.113}$$

$$a_T = C_T a_\omega(z) \ , \tag{5.114}$$

with

$$\begin{aligned} a_q(z) &\equiv \int_0^z dz' \frac{z'}{\sqrt{1+d^2 z'^6}^3} = \frac{1}{2} z^2 (\ {}_2F_1[3/2, 1/3; 4/3; -z^6 d^2]) \ , \\ a_\omega(z) &\equiv \int_0^z dz' \frac{z'}{\sqrt{1+d^2 z'^6}} = \frac{1}{2} z^2 (\ {}_2F_1[1/2, 1/3; 4/3; -z^6 d^2]) \ , \end{aligned} \tag{5.115}$$

Near the horizon a_L is expanded as

$$a_L = C_L A \frac{1}{z} + C_L B + \mathcal{O}\left(1/z^2\right) \ , \tag{5.116}$$

with

$$A \equiv \frac{\omega^2}{d} \ , \qquad B \equiv \frac{(q^2 - 3\omega^2) d^{-2/3} \Gamma(1/3)\Gamma(1/6)}{18\Gamma(1/2)} \ . \tag{5.117}$$

On the other hand the zero mode equations $\mathcal{D}_{L/T} a_{L/T} = 0$ are

$$\begin{aligned} \partial_z^2 a_L + \left[\frac{3d^2 z^5}{(1+d^2 z^6)}\left(1 + \frac{2q^2}{q^2 - \omega^2(1+d^2 z^6)}\right) - \frac{1}{z}\right] \partial_z a_L \\ + \left(\omega^2 - \frac{q^2}{1+d^2 z^6}\right) a_L = 0 \ , \\ \partial_z^2 a_T + \left[\frac{3d^2 z^5}{(1+d^2 z^6)} - \frac{1}{z}\right] \partial_z a_T + \left(\omega^2 - \frac{q^2}{1+d^2 z^6}\right) a_T = 0 \ . \end{aligned} \tag{5.118}$$

Near the horizon the incoming solution is

$$a_L(z) = C_I \frac{e^{iwz}}{z} \ , \tag{5.119}$$

and for $\omega z \ll 1$

$$a_L(z) = \frac{C_I}{z} + i\omega C_I \ , \tag{5.120}$$

A comparison of (5.116) with (5.120) yields

$$Ai\omega = B \ , \tag{5.121}$$

which yields the dispersion relation reported in [97]

$$\omega = \pm \frac{q}{\sqrt{3}} - \frac{iq^2}{2p\mu_0} + \mathcal{O}(q^3) \ , \tag{5.122}$$

for a massless excitation. Holographic D3/D7 at arbitrarily small temperatures is diffusive. It is not at strictly zero temperature with the occurence of a long-range collective mode. In the next section we suggest that this is a visco-elastic mode, and thereby generalize it to massive quarks. Any amount of temperature (collisions) destroy the Fermi-surface at large λ and large N_c. Indeed, while the temperature effects are of order N_c^0 through the underlying BH metric, the density effects are $1/\lambda$ and $1/N_c$ suppressed through the N_F embeddings either D7 or D8.

Finally and for completeness we note that the transverse baryonic mode follows also from (5.116) with the substitution

$$a_T = a_L(q \to 0 \ , \omega \to 1) \ . \tag{5.123}$$

From (5.121) we get

$$\omega = i \frac{d^{1/3}\Gamma(1/3)\Gamma(1/6)}{\Gamma(1/2)} \ . \tag{5.124}$$

The transverse baryonic current is gapped in cold D3/D7 much like the current is plasmon-gapped in a metal.

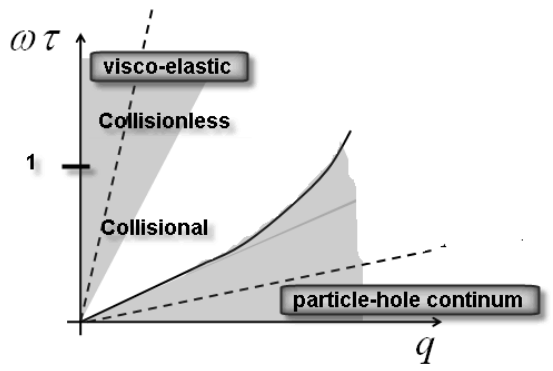

Figure 5.5: Visco-elastic domain versus the free particle-hole continuum. See text.

5.6 Visco-Elastic Analysis

The occurence of a collective mode in cold D3/D7 suggests that collectivity through the possible occurence of a Fermi surface at strong coupling maybe at work. To understand that, we propose to understand this collectivity by unifying the hydrodynamical or collision regime with the elastic or collisionless regime.

In Fig. 5.5 we show different propagating domains for a wave of frequency ω and momentum q in liquids. The dashed curves are typical wave dispersions. The free particle-hole continuum occupies the lower quadrant. τ is a typical relaxation time to equilibrium, say $\tau \approx 1/T$ (hot) and $\tau \approx 1/\mu$ (cold) for conformal and strongly coupled theories. For waves with $\omega\tau \gg 1$ and large velocities compared to the Fermi velocity v_F of a quasiparticle, we expect *collisionless* wave propagation or *elastic* regime. For waves with $\omega\tau \ll 1$ but still large velocities compared to the Fermi velocity v_F we expect *collision* wave propagation or *hydrodynamic* regime. Typical cold media behave elastically at low temperature and hydrodynamically at higher temperature. Thus, an elastic mode can be turned inelastic by just raising the temperature. This is typically what happens in liquid He^3 where the zero sound transmutes to the first or thermodynamic sound by changing its frequency or temperature to interpolate between the collisionless and collision regimes. To understand these regimes we now introduce a unified visco-elastic framework.

5.6.1 Generalities

In a homogeneous and isotropic solid, the constitutive equations for the elastic displacement field $\vec{u}(t,\vec{x})$ are discussed in the canonical book by Landau and Lifshitz on the theory of elasticity [100]. Specifically

$$m_B\, n_B \frac{\partial^2 \vec{u}}{\partial t^2} = (K + (1-2/p)\,\mu)\,\vec{\nabla}(\vec{\nabla}\cdot\vec{u}) + \mu\nabla^2\vec{u} + \vec{F}(t,\vec{x})\ , \qquad (5.125)$$

where K and μ are the bulk and shear moduli, $p=3$ is the dimensionality of space, $\vec{F}$ is an external volume force, n_B is the baryon equilibrium density and m_B is the bare baryon mass. The massless case more pertinent for D3/D7 will be deduced by inspection below. Without loss of generality, we may write

$$\vec{F}(t,\vec{x}) = n_B \frac{\partial \vec{A}(t,\vec{x})}{\partial t}\ , \qquad (5.126)$$

which is the 'baryon electric field'. Since the transverse part of $\vec{A}$ induces a 'baryon magnetic field' we expect (5.126) to also include the magnetic contribution as it plays the role of the Lorentz force. Since we are interested in the induced baryon current through $\vec{A}$, the magnetic effects are second order and will be omitted. The baryon current density is

$$\vec{j}(t,\vec{x}) = n_B \frac{\partial \vec{u}(t,\vec{x})}{\partial t}\ . \qquad (5.127)$$

Inserting (5.126) and (5.127) in (5.125) and taking the Fourier transforms yield

$$\begin{aligned} -i\omega\, m_B \vec{j}(\omega,\vec{q}) = \quad & \left(\frac{K}{n_B} + \left(1-\frac{2}{p}\right)\frac{\mu}{n_B}\right)\frac{\vec{q}\,(\vec{q}\cdot\vec{j}(\omega,\vec{q}))}{i\omega} \\ & + \frac{\mu}{n_B}\frac{q^2}{i\omega}\,\vec{j}(\omega,\vec{q}) - i\omega\, n_B \vec{A}(\omega,\vec{q})\ . \end{aligned} \qquad (5.128)$$

Decomposing the current $j = j_T + j_L$ and the potential $A = A_L + A_T$ along $\vec{q}$ and transverse to $\vec{q}$ allows the transverse and longitudinal induced currents

$$\vec{j}_T(\omega,\vec{q}) = \frac{n_B/m_B}{1-\frac{\mu}{n_B^2}\frac{n_B q^2}{m_B\omega^2}}\,\vec{A}_T(\omega,\vec{q})\ , \qquad (5.129)$$

and

$$\vec{j}_L(\omega,\vec{q}) = \frac{n_B/m_B}{1-\left(\frac{K}{n_B^2}+2\left(1-\frac{1}{p}\right)\frac{\mu}{n_B^2}\right)\frac{n_B q^2}{m_B\omega^2}}\,\vec{A}_L(\omega,\vec{q})\ . \tag{5.130}$$

j_L relates directly to the induced baryon density through the local conservation law as qj_L/ω.

The response currents (5.129) and (5.130) have a direct analogy with their counterparts in a liquid. Indeed, using hydrodynamics for the baryon current density in a liquid we can write the analogue of (5.128). In the linear response approximation

$$\begin{aligned} -i\omega\, m_B\vec{j}(\omega,\vec{q}) = \quad & \left(\frac{K}{n_B}-\frac{i\omega\zeta}{n_B}+\left(1-\frac{2}{p}\right)\frac{i\omega\eta}{n_B}\right)\frac{\vec{q}\,(\vec{q}\cdot\vec{j}(\omega,\vec{q}))}{i\omega} \\ & +\frac{i\omega\eta}{n_B}\frac{q^2}{i\omega}\,\vec{j}(\omega,\vec{q}) - i\omega\, n_B\vec{A}(\omega,\vec{q})\ , \end{aligned} \tag{5.131}$$

where the hydrostatic pressure term $\mathbf{p}$ in the Euler equation was traded with the longitudinal baryon current through the continuity equation,

$$-\vec{\nabla}\mathbf{p}(\omega,\vec{q}) = -\frac{\partial\mathbf{p}}{\partial n}\nabla n_B(\omega,\vec{q}) = \frac{\partial\mathbf{p}}{\partial n}\vec{q}\left(\frac{\vec{q}\cdot\vec{j}(\omega,\vec{q})}{i\omega}\right)\ , \tag{5.132}$$

where η and ζ are the shear and bulk viscosities; $\mathbf{p}$ is the equilibrium pressure as a function of density with $K = n_B\partial\mathbf{p}/\partial n$ the bulk modulus. (5.128) is very similar to (5.131) except for: 1/ the shear modulus in the solid becomes purely imaginary or $-i\omega\eta$ in the liquid; 2/ the bulk modulus acquires an imaginary part through $-i\omega\zeta$ in the liquid. Both imaginary parts vanish at $\omega = 0$ making the liquid insensitive to shear at zero frequency. This also means that their contributions in $j_{L,T}$ are diffusive.

The solid and liquid visco-elastic coefficients can be described in a unified manner through (5.129) and (5.130) by substituting

$$K \to \mathbf{K}(\omega) = K(\omega) - i\omega\zeta(\omega)\ , \tag{5.133}$$

$$\mu \to \mathbf{M}(\omega) = \mu(\omega) - i\omega\eta(\omega)\ , \tag{5.134}$$

as the complex and frequency dependent bulk $\mathbf{K}$ and shear $\mathbf{M}$ visco-elastic

coefficients. The solid has real $\mathbf{M}$ with a small imaginary part η (zero up to the uncertainty principle) while the liquid has imaginary $\mathbf{M}$ with a small μ and large imaginary part η. The bulk modulus K is about the same in liquid and solid, and of the same order of magnitude as the shear viscosity η.

In light of (5.134) it follows from (5.130) and (5.129) that the longitudinal current admits a gapless pole (compression mode) at

$$\begin{aligned}\omega \approx & \left(\frac{K}{m_B n_B}+2\left(1-\frac{1}{p}\right)\frac{\mu}{m_B n_B}\right)^{1/2} q \\ & -i\left(\frac{\zeta}{m_B n_B}+2\left(1-\frac{1}{p}\right)\frac{\eta}{m_B n_B}\right)\frac{q^2}{2}\ ,\end{aligned} \tag{5.135}$$

while the transverse current admits a gapless pole (shear mode) at

$$\omega \approx \sqrt{\frac{\mu}{m_B n_B}}q - i\frac{\eta}{m_B n_B}\frac{q^2}{2}\ . \tag{5.136}$$

We see that for finite frequency waves and in the long-wavelength approximation the way a solid responds to external wave-stress is similar to the way a liquid does. The difference is that in a solid $\mu \approx K$ and ζ, η are small, while in a liquid μ is close to zero and ζ, η are large. In the liquid the transverse or shear mode becomes diffusive.

5.6.2 Cold D3/D7

D3/D7 at finite density yields a gapped transverse baryonic current and a gapless longitudinal baryonic current [97]. The gapless longitudinal baryonic current can be compared with the longitudinal visco-elastic mode (5.135) with

$$\left(\frac{K}{m_B n_B}+2\left(1-\frac{1}{p}\right)\frac{\mu}{m_B n_B}\right)^{1/2} \Leftrightarrow \frac{1}{\sqrt{p}}\ , \tag{5.137}$$

$$\left(\frac{\zeta}{m_B n_B}+2\left(1-\frac{1}{p}\right)\frac{\eta}{m_B n_B}\right) \Leftrightarrow \frac{1}{p\mu_B}\ . \tag{5.138}$$

The compressibility is readily tied with the equation of state for any embedding

$$\frac{K}{m_B n_B} \equiv \left(\frac{\partial P}{\partial \epsilon}\right)_S = \frac{1}{p}\ , \tag{5.139}$$

since $\epsilon - pP = 0$ in a conformal theory. [5] The energy momentum tensor is still traceless at finite temperature and density for massless fermions. The gapless and longitudinal baryonic mode has the speed of the first sound $c_1 = 1/\sqrt{p}$ for zero shear modulus $\mu = 0$ and massless quarks. For massive quarks $\epsilon - pP \neq 0$. For D3/D7 it follows from [98] that

$$\epsilon = \frac{1}{4}\gamma N(2\pi\alpha')^4(\mu_q^2 - m_q^2)(3\mu_q^2 + m_q^2) \ , \tag{5.140}$$

$$P = \frac{1}{4}\gamma N(2\pi\alpha')^4(\mu_q^2 - m_q^2)^2 \ , \tag{5.141}$$

where $\gamma \approx 0.363$. The visco-elastic mode has a speed

$$c_1 = \sqrt{\left(\frac{\partial P}{\partial \epsilon}\right)_S} = \sqrt{\frac{\mu_q^2 - m_q^2}{3\mu_q^2 - m_q^2}} \ , \tag{5.142}$$

in agreement with the detailed quasi-normal mode analysis in [101].

Since the mode $\omega = q/\sqrt{3}$ lies within the free particle-hole continuum as shown in Fig.(5.2), it is susceptible to Landau-like damping through single particle-hole or multi-particle-multi-hole. Again, the visco-elastic analysis suggests that the bulk viscosity in cold D3/D7 with massless quarks is

$$\frac{\eta}{n_B} = \frac{\hbar}{2(p-1)} \ , \tag{5.143}$$

where we used (5.158) and (5.159). In conformal theories the shear modulus ($\mu = 0$) and bulk viscosity are zero (ζ). For $p = 3$, we have $\eta/n_B = \hbar/4$, where $\hbar$ has been restored. This is to be compared with $\hbar/6\pi$ argued in [102] using the Stokes-Einstein relation and the uncertainty principle for cold and strongly coupled Fermions.

It is worth noting that (5.143) can be rewritten as

$$\frac{\eta}{n_B} = \left(\frac{p}{p-1}\right)\frac{\hbar}{2p} = \frac{n_F k_F}{N_c N_f n_B}\frac{\hbar}{p} \ , \tag{5.144}$$

[5] p is the dimensionality of space and P is pressure.

where

$$\frac{n_F}{n_B} = \frac{N_c N_f \int_0^{k_F} \frac{d^p k}{(2\pi)^p} \frac{1}{2k}}{\int_0^{k_F} \frac{d^p k}{(2\pi)^p}} = \frac{N_c N_f}{2k_F} \frac{p}{p-1} \ , \tag{5.145}$$

is the ratio of the quark density at the Fermi surface normalized to the baryon density. For massless quarks $n_B k_F = \epsilon + P$ with $n_q = N_c N_f n_B$ so that in general

$$\frac{\eta}{\epsilon + P} = \frac{n_F}{n_q} \frac{\hbar}{p} \ . \tag{5.146}$$

This result can generalized to finite mass by noting that at zero temperature $\epsilon + P = n_B \mu_B$ and substituting $2k \to 2\sqrt{k^2 + m_q^2}$ in n_F in (5.145). Specifically,

$$\frac{n_F}{n_B} = \frac{N_c N_f \int_0^{k_F} \frac{d^p k}{(2\pi)^p} \frac{1}{2\sqrt{k^2+m_q^2}}}{\int_0^{k_F} \frac{d^p k}{(2\pi)^p}} = \frac{N_c N_f v_F}{4k_F} \ {}_2F_1(1/2, p/2; 1 + p/2; -v_F^2) \ ,$$

with $v_F = k_F/m_q$. Thus

$$\frac{\eta}{n_B} = \left(\frac{\mu_B v_F}{4k_F} \right) \ {}_2F_1(1/2, p/2; 1 + p/2; -v_F^2) \ \frac{\hbar}{p} \ . \tag{5.147}$$

The visco-elastic (5.122) for massless quarks, turn to

$$\omega = c_1 q \ - \frac{i}{p} \left(1 - \frac{1}{p} \right) \left(\frac{v_F}{k_F} \ {}_2F_1(1/2, p/2; 1 + p/2; -v_F^2) \right) \frac{q^2}{4} \ , \tag{5.148}$$

for massive quarks. c_1 is the first sound speed. For $D3/D7$ it is explicitly given in (5.142), while for arbitrary Dp/Dq it follows from the known equations of state [98].

In D3/D7 any infinitesimal temperature washes out the Fermi surface, resulting in a diffusive baryonic phase. Thermal collisions at strong coupling take over the collisions through the Fermi surface however small is the temperature. As noted earlier, this is the hallmark of strong coupling holography whereby the BH contribution is of order N_c^0 while the Fermi contributions are $1/N_c$ suppressed.

5.7 Random Phase Approximation

If cold D3/D7 exhibits collectivity at large λ and large N_c that is consistent with a constitutive visco-elastic analysis, why the cold D4/D8 results above are all gapped. The short answer is that in D4/D8 the baryons are solitons, so baryonic motion with a Pauli-blocked Fermi surface is subleading in $1/N_c$ as shown in Fig.(5.2). Baryons move semi-classically by quantizing the isorotations and rotations both of which are $1/N_c$ suppressed. To estimate some of these contributions we note that the baryons in D4/D8 are flavored instantons with core sizes of order $1/\sqrt{\lambda}$. They are heavy with $m_B = 8\pi^2 N_c \lambda$. So the semiclassical descriptive of the translational zero modes follow from the point-like effective action

$$S = \phi^+ \left(i\partial_t - \frac{(-i\vec{\nabla} - \vec{\mathcal{V}})^2}{2m_B} - \mu_B \right) \phi - \frac{1}{2}\alpha(\phi^+\phi)^2 + ... \,, \tag{5.149}$$

where the repulsive interaction $\alpha = (24\pi^4/4M_{KK}^2)(N_c/\lambda)$ is set to reproduce the energy density and pressure of the holographic matter (5.2) with $p \approx \alpha n_B^2/2$. The dotted contributions involve higher derivative terms, e.g. $(\phi^+(-i\nabla - \mathcal{V})/m_B\phi)^2$ which are suppressed by $1/N_c$. Again, note that the limit N_c and λ large do not commute for α. For fixed λ and large N_c the repulsion is strong as it should, while for fixed N_c and large λ the repulsion is weak. Here $\vec{\mathcal{V}}$ is the probing baryonic vector source. In large N_c the baryons are scalar fermions with no assigned spin to leading order in $1/N_c$. Therefore their spin degeneracy is 1.

In the RPA approximation, the zero modes in (5.149) integrate to the effective action

$$S_{RPA}(\mathcal{V}) = \frac{1}{2}\mathcal{V}_L\Delta_L\mathcal{V}_L + \frac{1}{2}\mathcal{V}_T\Delta_T\mathcal{V}_T \,, \tag{5.150}$$

with $j_L = \Delta_L\mathcal{V}_L$ and $j_T = \Delta_T\mathcal{V}_T$ for the longitudinal and transverse currents. $\omega\Delta_{L,T}$ are the longitudinal and transverse baryonic conductivities respectively. The RPA contributions as shown in Fig.(7.1) resum to

$$\Delta_L = \frac{\Pi_L}{1 - \alpha\frac{q^2}{\omega^2}\Pi_L} \,, \qquad \Delta_T = \frac{\Pi_T}{1 - \tilde{\alpha}\frac{q^2}{\omega^2}\Pi_T} \,, \tag{5.151}$$

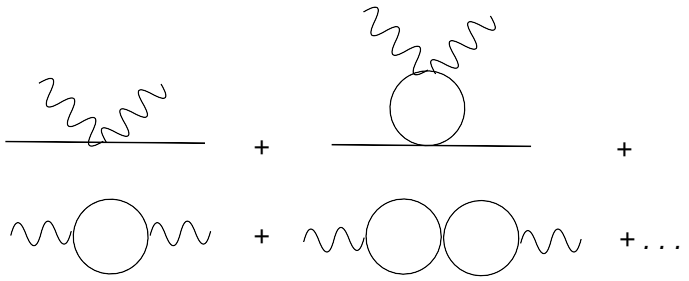

Figure 5.6: RPA contributions following from (5.149).

with

$$\Pi_{L,T} = \sum_k^F \frac{1}{m_B} + \sum_k^F \left(\frac{k_{L,T}}{m_B}\right)^2 \Delta_F(k+q)\Delta_F(k) \ . \tag{5.152}$$

The solid lines in Fig.(7.1) lie in the Fermi surface. $\tilde{\alpha}/\alpha \approx 1/N_c$. The transverse contributions follow solely from the dotted terms in (5.149). The summation is carried over the Fermi surface. Δ_F is the massive and non-relativistic fermion propagator associated to (5.149) in the presence of a Fermi surface. The first contribution in (5.152) is from the seagull term in (5.149) and the second contribution is from the particle-hole bubble. The londitudinal vector response Δ_L relates to the scalar density-density response function by current conservation. Specifically, $\Pi_L = \omega^2/q^2\Pi$ where

$$\Pi(q) = \sum_k^F \Delta_F(k+q)\Delta_F(k) \tag{5.153}$$

is the Lindhard function for scalar fermions. For $\omega, q \to 0$ but fixed $\beta = \omega/q/v_F$ it takes the form

$$\Pi(q) \approx \frac{m_B k_F}{2\pi^2}\left(-1 + \frac{\beta}{2}\ln\left|\frac{1+\beta}{1-\beta}\right|\right) - i\theta(1-|\beta|)\frac{m_B\beta k_F}{4\pi} \ . \tag{5.154}$$

The quasiparticle spectrum following from (5.153) is schematically displayed in Fig.(5.7) with massless quasiparticles of energy $\omega = v_F q$ at small k, and free massive fermions with $\omega = q^2/2m_B$ away from the Fermi surface. This description is rooted in weak coupling.

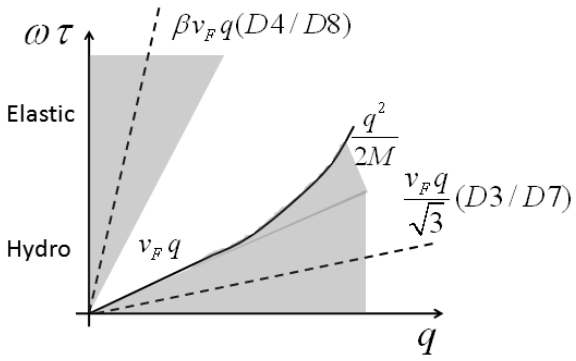

Figure 5.7: Dispersion relations (dotted lines) for D4/D8 and D3/D7.

We note that the longitudinal current in (5.151) develop a *massless* poles for strongly repulsive fermions as D4/D8. The longitudinal modes are directly tied to the Lindhard function by current conservation. They follow from $1 = \alpha\Pi$. In particular the longitudinal sound modes is stable for $\beta > 1$ above the quasiparticle cut (no imaginary part) with a speed ($\beta \gg 1$)

$$c_L = \beta\, v_F \approx \sqrt{\frac{\alpha m_B k_F}{3\pi^2}}\, v_F = \sqrt{\alpha n_B/m_B} = c_1 \ , \tag{5.155}$$

in agreement with the pressure $p \approx \alpha n_B^2/2$ in leading order in the density. For $\beta > 1$ the decay of the longitudinal baryonic in D4/D8 is not through Landau-like damping.

The transverse mode follows from the pole at $\omega^2 = \tilde{\alpha} q^2 \Pi_T$. For $\tilde{\alpha} \approx \alpha_*/(N_c q^2)$ the transverse mode is gapped since

$$\Pi_T(q) \approx \frac{n_B}{m_B} + \frac{n_B}{20 m_B \beta^2} - i\theta(1-|\beta|)\frac{3\pi n_B}{8 m_B} \ , \tag{5.156}$$

for $\omega, q \to 0$ and fixed $\beta = \omega/q/v_F$. The transverse gap is typically $\omega_T \approx \alpha_* n_B/m_B N_c$ with α_* following from a a numerical analysis of the transverse quasi-normal modes in holography. In light of the RPA analysis, the holographic result *suggests* that the transverse baryonic fluctuations are long ranged and unscreened unlike their longitudinal counterparts.

5.8 Conclusions

We have analyzed the baryonic transport in D4/D8 (chiral) and D3/D7 (nonchiral) at finite density and/or temperature. D4/D8 is a holographic model of QCD at large N_c and large 'tHooft coupling λ. The transverse baryonic current in D4/D8 is saturated by the medium modified vector mesons in the confined phase with $T < M_{KK}/\pi$. The vector spectrum is gapped since matter is uncompressible at large N_c. Confined D4/D8 matter becomes compressible to order $1/N_c$ with the occurence of a gapless longitudinal vector mode. While $1/N_c$ effects are difficult to assess in holography, we have provided an RPA argument for the speed of the gapless mode using an effective action for baryons constrained by holography. D4/D8 is diffusive in the deconfined regime.

D3/D7 is diffusive at all temperatures except zero where it is visco-elastic. This is a hallmark of holography at large N_c and large λ. Indeed, the temperature effects are mediated by the BH background and leading in $1/N_c$, while the baryonic density effects are carried by the probe branes which are N_f/N_c suppressed. At strong coupling and large N_c the thermal or collisional collision regime is dominant. The exception is D3/D7 at zero temperature but finite density as recently pointed by [97]. A Fermi surface (albeit strongly coupled) maybe at work in this case that suggests a visco-elastic regime. A longitudinal gapless mode emerges with a small width suggestive of a shear viscosity to baryon ratio $\eta/n_B = \hbar/4$ in cold but dense $D3/D7$. This mode is turned diffusive by arbitrarily small temperatures at strong coupling. Our observations extend readily to massive quarks in D3/D7.

5.9 Appendix

5.9.1 Cold Dp/Dq

It is interesting to analyze the equation of state of cold Dp/Dq embeddings. We consider Dq probe branes whose worldvolume spans an AdS_{p+2} factor and wraps the n-sphere S^n in $AdS_5 \times S^5$, where $p = q - n - 1$. For example, $q = 5, p = 2$ corresponds to $D5$ branes on $AdS_4 \times S^2$, and $q = 3, p = 1$ corresponds to $D3$ branes on $AdS_3 \times S^1$ in $AdS_5 \times S^5$.

At zero temperature and for massless quarks, the pressure P and energy

density ϵ read [97]

$$P = -\frac{\Omega}{V_p} = \frac{1}{p+1}\frac{\alpha}{\mathcal{N}_q^{1/p}}\widetilde{n}_B^{\frac{p+1}{p}} \ , \tag{5.157}$$

$$\widetilde{\mu}_B = \frac{\alpha}{\mathcal{N}_q^{1/p}}\widetilde{n}_B^{\frac{1}{p}} \ , \tag{5.158}$$

$$\epsilon = -P + \widetilde{\mu}_B\widetilde{n}_B = \frac{p}{p+1}\frac{\alpha}{\mathcal{N}_q^{1/p}}\widetilde{n}_B^{\frac{p+1}{p}} \ , \tag{5.159}$$

$$\frac{\epsilon}{\epsilon_0} = \frac{\alpha}{4\pi^{3/2}}\left(\frac{1}{\Gamma(p/2+1)\pi N_c N_f}\right)^{1/p}\left(\frac{\lambda^{\frac{p+1}{2}}}{\mathcal{N}_q}\right)^{1/p} \ , \tag{5.160}$$

$$\epsilon_0 = 2\sqrt{\pi}\left(\frac{\Gamma(p/2)p}{4N_cN_f}\right)^{1/p}\frac{p}{p+1}n_q^{(p+1)/p} \ , \tag{5.161}$$

where $\widetilde{n}_B \equiv \frac{\sqrt{\lambda}}{2\pi}n_q$, $\widetilde{\mu}_B \equiv \frac{2\pi}{\sqrt{\lambda}}\mu_q$, and $\alpha \equiv \frac{\Gamma(1/2-1/2p)\Gamma(1+1/2p)}{\Gamma(1/2)}$. $\mathcal{N}_q \equiv N_f T_{Dq} V_n$ with V_n the volume of a unit n-sphere and T_{Dq} is the Dq brane tension [98]. That is $N_7 = \lambda N_f N_c/(2\pi)^4$, $N_5 = \frac{N_f N_c\sqrt{\lambda}}{2\pi^3}$, and $N_3 = \frac{N_f N_c}{\pi}$. The ratio ϵ/ϵ_0 shows the energy density in cold Dp/Dq normalized to the free Fermi energy density:

$$\frac{\epsilon}{\epsilon_0} \approx \lambda^{1/p} \ . \tag{5.162}$$

For $Dp/Dq \equiv (D3/D7), (D2/D5), (D1/D3)$ dense Dp/Dq is unbound at large λ.

5.9.2 Fermionic Drag

Hot D3/D7

Hot D3/D7 is diffusive at all temperatures. The drag coefficient η_D is inversely proportional to the baryonic diffusion constant D_q through the Einstein formulae at strong coupling [102–105]

$$\eta_D = \frac{T}{D_q} \ , \tag{5.163}$$

and for slowly moving particles. In equilibrium, the diffusion constant ties with the baryonic conductivity σ_q (at zero frequency and momentum)

$$\Xi = \frac{< (\Delta N)^2 >}{TV_3} = \frac{\sigma_q}{D_q} \ , \tag{5.164}$$

where Ξ is the baryonic susceptibility. Thus

$$\eta_D = \frac{\Xi}{\sigma_q} T \ . \tag{5.165}$$

The conductivity σ_q has been obtained using Ohm's law in [**?**] (See also next Appendix)

$$\sigma_q = \frac{N_c N_f T}{4\pi} \sqrt{c^6 + \mathbf{d}^2} \ , \quad \mathbf{d} \equiv \frac{8 n_q}{\sqrt{\lambda} N_c N_f T^3} \ , \tag{5.166}$$

with $c \equiv \cos^6 \theta(z_*)$ and $z_* \equiv 4/(\pi^2 T^2)$ a dynamically generated value of a scalar profile at the BH horizon. Massless quarks correspond to $\theta = 0$ and infinite mass quarks to $\theta = \pi/2$. Thus

$$\eta_D = \frac{\Xi}{N_c N_f} \frac{4\pi}{\sqrt{c^6 + \mathbf{d}^2}} \ . \tag{5.167}$$

This expression expresses the drag of a quark in diffusive D3/D7 for arbitrary mass, temperature and baryon density. When $m_q = 0$

$$\eta_D = \frac{\Xi}{N_c N_f} \frac{4\pi}{\sqrt{1 + \mathbf{d}^2}} = \frac{2\pi T^2}{\sqrt{1 + \mathbf{d}^2}} \ , \tag{5.168}$$

where $\Xi = \frac{N_f N_c T^2}{2}$ [106]. When $m_q = \infty$

$$\eta_D = \frac{\Xi}{N_c N_f} \frac{4\pi}{\mathbf{d}} = \frac{\Xi}{n_q} \frac{\pi}{2} \sqrt{\lambda} T^3 \ , \tag{5.169}$$

where Ξ can be read off from Eq.(5.7) in [106].

Cold D3/D7

The zero temperature case is visco-elastic as we suggested earlier. In this regime the fermionic conductivity ties to the diffusion constant by the Kubo

formulae

$$\sigma_q = n_F D_q \ , \tag{5.170}$$

$$n_F = N_c N_f \int \frac{d^p k}{(2\pi)^p} \frac{1}{2E_k} (f(E_k) + \bar{f}(E_k)) \ , \tag{5.171}$$

where f is Boltzmann distribution function and $E_k = \sqrt{k^2 + m_q^2}$. This relation follows from the relaxation time approximation in the quark probe phase space irrespective of strong or weak coupling. Relaxation to equilibrium at strong coupling is subsumed. For infinitesimal temperatures and for finite quark mass [98, 107] (see also next Appendix)

$$\frac{\sigma_q}{T} = \frac{N_c N_f}{4\pi} \sqrt{c^6 + \mathbf{d}^2} \ . \tag{5.172}$$

From (5.163) it follows that the drag is

$$\frac{\eta_D}{n_B} = \frac{n_F}{N_c N_f n_B} \frac{4\pi}{\sqrt{c^6 + \mathbf{d}^2}} \ . \tag{5.173}$$

This is the general form of the quark drag in a cold holographic medium (Coulomb phase) with *infinitesimal* temperature. We will assume it also for $T = 0$ by continuity.

For m_q finite ($c \neq 0$) and $N_c, \lambda \to \infty$ ($\mathbf{d} \to 0$)

$$\eta_D \approx \frac{n_F}{N_c N_f} \frac{4\pi}{c^3} \ . \tag{5.174}$$

When $T = 0$ and $m_q = 0 (c = 1)$

$$\eta_D = \frac{2^{(2-p)} \pi^{(1-p/2)}}{\Gamma(p/2)} \frac{\mu_q^{p-1}}{p-1} \ , \tag{5.175}$$

where we used

$$n_F = N_c N_f \int_0^{\mu_q} \frac{d^p k}{(2\pi)^p} \frac{1}{2k} \ . \tag{5.176}$$

When $T=0$ and $m_q \neq 0 (c \neq 1)$ and $p=3$

$$\frac{\eta_D(m_q)}{\eta_D(m_q=0)} = \left[\frac{\mu_q}{\sqrt{\mu_q^2 - m_q^2}} - \frac{m_q^2}{\mu_q^2 - m_q^2} \ln \left(\frac{1 + \frac{\mu_q}{\sqrt{\mu_q^2 - m_q^2}}}{\frac{m}{\sqrt{\mu_q^2 - m_q^2}}} \right) \right] \frac{1}{c^3} \ , \quad (5.177)$$

where $n_q = \sqrt{m_q^2 + k_F^2}$.

For $m_q \to \infty (c=0)$

$$\eta_D \approx \frac{n_F}{N_c N_f} \frac{4\pi}{\mathbf{d}} = \frac{n_F}{n_q} \frac{\pi\sqrt{\lambda}}{2} T^3 = \frac{1}{2(p-2)} \pi\sqrt{\lambda} T^2 \ , \quad (5.178)$$

where $n_q = N_c N_f n_B$ and

$$\frac{n_F}{n_q} = \frac{\int d^p k \frac{1}{k^2/2m_q} e^{-k^2/2m_q T}}{\int d^p k e^{-k^2/2m_q T}} = \frac{1}{p-2} \frac{1}{T} \ . \quad (5.179)$$

For $p=3$, η_D is the drag coefficient reported in [103–105].

5.9.3 Baryonic conductivity

The baryonic conductivity σ_q in D3/D7 has been derived by various methods [98, 107, 108]. Generically, the Kubo formulae for the conductivity is

$$\sigma_q = -\lim_{\omega \to 0} \frac{1}{\omega} \mathrm{Im} G_{xx}^{\mathrm{ret}}(K) \Big|_{\omega = |\vec{k}|} \ , \quad (5.180)$$

where only the transverse response function contributes, as the longitudinal part vanishes for light-like momenta by charge conservation. For a rotationally symmetric medium, $G_{xx} = G_{yy} = G_{zz}$ are the components of the $j_x j_x$, $j_y j_y$ and $j_z j_z$ retarded baryonic current correlations.

Using AdS/CFT the transverse response can be extracted from (5.102), i.e.

$$a_T'' - \frac{u(u + \mathbf{d}^2 u(-3 + 7u^2))}{2(1-u^2)(1+\mathbf{d}^2 u^3)} a_T' + \frac{\mathfrak{w}^2 u}{(1-u^2)^2} \frac{1 + u\mathbf{d}^2}{1 + u^3 \mathbf{d}^2} a_T = 0 \ , \quad (5.181)$$

with $u \equiv z^2$. The horizon($u=1$) is a regular singular point and the solution behaves as $a_T \sim (1-u)^{\pm i\mathfrak{w}/2}$. We choose the incoming boundary

condition($a_T \sim (1-u)^{-i\mathfrak{w}/2}$) and extract the singularity at $u=1$ by substituting

$$a_T = (1-u^2)^{-i\mathfrak{w}/2} F(u)\,. \tag{5.182}$$

$F(u)$ is regular at $u=1$ and satisfies the following equation

$$F'' + \frac{u(-4+u\mathbf{d}^2(3-7u^2)) + 2i(1+u)(1+\mathbf{d}^2u^3)\mathfrak{w}}{2(1-u^2)(1+\mathbf{d}^2u^3)}F' \\ + \frac{i(1+u)(2+\mathbf{d}^2u^2(3+5u))\mathfrak{w} + (-1+u+\mathbf{d}^2u^2(4+3u+u^2))\mathfrak{w}^2}{4(1-u^2)(1+u)(1+\mathbf{d}^2u^3)}F = 0\,.$$

In the hydrodynamic region($\mathfrak{w} \ll 1$) we may expand $F(u)$ in terms of $\mathfrak{w}$ as

$$F = F_0 + \mathfrak{w}F_1 + \mathfrak{w}^2F_2 \cdots\,, \tag{5.183}$$

and unwind $F_0, F_1, F_2, \cdots$ order by order. For that consider the case with $\mathbf{d}=0$. The zeroth order equation is solved with

$$F_0' = \frac{C}{1-u^2}\,, \tag{5.184}$$

where C is an integration constant. Regularity at $u=1$ forces $C=0$. So F_0 is a constant. At next order we have

$$F_1' = \frac{i}{2(-1+u^2)}F_0 + \frac{C}{-1+u^2}\,. \tag{5.185}$$

Again regularity at $u=1$ sets the constant $C=-iF_0/2$. Thus

$$F_1' = \frac{iF_0}{2(1+u)}\,, \tag{5.186}$$

which is enough unwinding of the transverse solution for the Green's function in the zero frequency limit needed for the Kubo formulae.

To obtain the retarded Green's function we need the boundary action

$$\begin{aligned} S &= \lim_{Z\to\infty} -2\widetilde{N}\int \frac{d\omega dq}{(2\pi)^2}\Delta k_1 k_3 \frac{1}{\mathfrak{w}^2} a_T'(Z,\mathfrak{w})a_T(Z,-\mathfrak{w}) \\ &= \lim_{u\to 0} -4\widetilde{N}(\pi T)^2\int \frac{d\omega dq}{(2\pi)^2}\frac{1}{\mathfrak{w}^2} a_T'(u,\mathfrak{w})a_T(u,-\mathfrak{w}) \\ &= -4\widetilde{N}(\pi T)^2\int \frac{d\omega dq}{(2\pi)^2}\frac{1}{\mathfrak{w}^2} F'(0,\mathfrak{w})F(0,-\mathfrak{w})\,, \end{aligned}$$

where we recovered $2\pi\alpha'$ and $\widetilde{N} \equiv N(2\pi\alpha')^2 = \frac{N_c N_f}{2(2\pi)^2}$. The retarded Green function is then

$$\begin{aligned} G^{\rm ret}_{xx} &= \frac{\delta^2 S}{\delta a_x(0,\mathfrak{w})\delta a_x(0,-\mathfrak{w})} = \frac{\mathfrak{w}^2\delta^2 S}{\delta F(0,\mathfrak{w})\delta F(0,-\mathfrak{w})} \\ &= -8\widetilde{N}(\pi T)^2\frac{F'(0,\mathfrak{w})}{F(0,\mathfrak{w})} \ , \end{aligned} \tag{5.187}$$

and the conductivity is

$$\begin{aligned} \sigma_q &= -\lim_{\omega\to 0}\frac{1}{\omega}{\rm Im}G^{\rm ret}_{xx}(K)\Big|_{\omega=|\vec{k}|} \\ &= 8\widetilde{N}(\pi T)^2\lim_{\omega\to 0}\frac{1}{\omega}{\rm Im}\left(\frac{F_1'(0,\mathfrak{w})\mathfrak{w}}{F_0}+\mathcal{O}(\omega^2)\right) \\ &= \frac{N_c N_f T}{4\pi} \ . \end{aligned} \tag{5.188}$$

Extending the procedure to finite density yields [107]

$$\sigma_q = \frac{N_c N_f T}{4\pi}\sqrt{1+\mathbf{d}^2} \ , \tag{5.189}$$

where $\mathbf{d} = \frac{d}{(\pi T)^3} = \frac{8n_q}{N_c N_f\sqrt{\lambda}T^3}$, which is (5.166) with $c=1$.

5.9.4 D4/D8 Deconfined phase

In this section we enforce an eigenmode analysis on the longitudinal and transverse vector currents in the deconfined hot and dense D4/D8. The eigenmode analysis parallels the one for cold and dense D4/D8 with reflective boundary conditions at the BH horizon. No imaginary parts arise from this analysis. In a way, in D4/D8 we may still entertain the possibility of stationary solutions between the Left-pending and Right-pending branes to mock up existing light bound states. Of course, this is a formal suggestion.

The longitudinal operator ($\mathcal{D}_L$) is

$$\mathcal{D}_L \equiv \partial_Z\frac{\sqrt{K(K-1)}\Delta^3}{\Delta^2\omega^2-\frac{K-1}{K}q^2}\partial_Z + \frac{K^{1/6}}{\sqrt{K-1}}\Delta \ . \tag{5.190}$$

When $q = 0$ or $\omega = 0$ it is easily diagonalized, since

$$\begin{aligned}\mathcal{D}_L(q=0) &= \frac{1}{\omega^2}\partial_Z\sqrt{K(K-1)}\Delta\partial_Z + \frac{K^{1/6}}{\sqrt{K-1}}\Delta \ , \\ \mathcal{D}_L(\omega=0) &= -\frac{1}{q^2}\partial_Z\frac{K^{3/2}}{\sqrt{K-1}}\Delta^3\partial_Z + \frac{K^{1/6}}{\sqrt{K-1}}\Delta \ .\end{aligned}$$

The Green's function ($\mathcal{D}_L^{-1}$) may be expanded in terms of the complete set of eigenvalues that diagonalize

$$\mathcal{D}_L(q=0)f = \left(\frac{K^{1/6}}{\omega^2\sqrt{K-1}}\Delta\right)\lambda f \ , \tag{5.191}$$

$$\mathcal{D}_L(\omega=0)f = \left(\frac{K^{1/6}}{q^2\sqrt{K-1}}\Delta\right)\lambda f \ , \tag{5.192}$$

where $\frac{K^{1/6}}{\omega^2\sqrt{K-1}}\Delta$ and $\frac{K^{1/6}}{q^2\sqrt{K-1}}\Delta$ are weight factors. Using the complete sets,

$$\begin{aligned}(\partial_Z\sqrt{K(K-1)}\Delta\partial_Z)\,\chi_n &= -\left(\frac{K^{1/6}}{\omega^2\sqrt{K-1}}\Delta\right)\,(\lambda_n^\chi)^2\,\chi_n \ , \\ \left(\partial_Z\frac{K^{3/2}}{\sqrt{K-1}}\Delta^3\partial_Z\right)\,\xi_n &= -\left(\frac{K^{1/6}}{\omega^2\sqrt{K-1}}\Delta\right)\,(\lambda_n^\xi)^2\,\xi_n \ ,\end{aligned}$$

we have

$$\langle Z|\mathcal{D}_L^{-1}(q=0)|Z'\rangle = \sum_{n\in\mathbb{N}}\frac{\chi_n(Z)\chi_n(Z')}{-\omega^2+(\lambda_n^\chi)^2} + \frac{\chi_0(Z)\chi_0(Z')}{\omega^2} \ , \tag{5.193}$$

$$\langle Z|\mathcal{D}_L^{-1}(\omega=0)|Z'\rangle = \sum_{n\in\mathbb{N}}\frac{\xi_n(Z)\xi_n(Z')}{q^2+(\lambda_n^\xi)^2} + \frac{\xi_0(Z)\xi_0(Z')}{q^2} \ . \tag{5.194}$$

The transversal operator ($\mathcal{D}_T$) is

$$\mathcal{D}_T \equiv -\frac{1}{\omega^2}\left(\partial_Z\sqrt{K(K-1)}\Delta\partial_Z + \frac{K^{1/6}}{\sqrt{K-1}}\left(\Delta\omega^2 - \Delta^{-1}\frac{K-1}{K}q^2\right)\right) \ .$$

When $q = 0$ it is easily diagonalized as

$$\mathcal{D}_T(q=0) \equiv -\frac{1}{\omega^2}\partial_Z\sqrt{K(K-1)}\Delta\partial_Z - \frac{K^{1/6}}{\sqrt{K-1}}\Delta \ . \tag{5.195}$$

With the eigenfunctions and eigenvalues:

$$(\partial_Z \sqrt{K(K-1)}\Delta\partial_Z)\,\zeta_n = -\frac{K^{1/6}}{\sqrt{K-1}}\Delta\,(\lambda_n^\zeta)^2\,\zeta_n\ ,$$

the Green's function is expanded as

$$\langle Z|\mathcal{D}_T^{-1}(q=0)|Z'\rangle = \sum_{n\in\mathbb{N}} \frac{\zeta_n(Z)\zeta_n(Z')}{\omega^2+(\lambda_n^\zeta)^2} + \frac{\zeta_0(Z)\zeta_0(Z')}{\omega^2}\ . \tag{5.196}$$

Chapter 6

Meson

In [28, 29] the meson spectrum and coupling was studied at zero baryon density by analyzing the DBI action of D8-$\overline{\text{D8}}$ branes with the fluctuating gauge field A_M. We want to extend the analysis to *finite baryon density* or $n_B \neq 0$. For this purpose we streamline in this section the construction in [28, 29] for notational purposes and completeness. In the next two sections we add the background $U(1)_V$ field $\mathcal{A}_0$ to the fluctuating gauge field A_M. It will enable us to study meson properties at finite baryon density.

In section 2, we summarize the construction of the chiral effective action for pions, vectors and axials at zero density. In section 3, we show how this chiral effective action is modified by the finite "charges" in bulk. A number of meson properties are discussed as a function of the identified baryon number. Our conclusions are in section 4. In the appendix we discuss the effective action using vacuum mode.

6.1 Effective meson action: $n_B = 0$

6.1.1 Mode decomposition of A_M

The gauge field A_M has nine components, $A_\mu = A_{1,2,3,4}$, $A_z (\equiv A_5)$, and $A_\alpha (\alpha = 5, 6, 7, 8$, the coordinates on the $S^4)$. We assume that $A_\alpha = 0$, and A_μ and A_z are independent of the coordinate on S^4. We further assume that A_M can be

expanded in terms of complete sets, $\psi_n(z)$ and $\phi_n(z)$ as

$$A_\mu(x^\mu, z) = \sum_{n=1}^{\infty} B_\mu^{(n)}(x^\mu)\psi_n(z) \ , \tag{6.1}$$

$$A_z(x^\mu, z) = \varphi^{(0)}(x^\mu)\phi_0(z) + \sum_{n=1}^{\infty} \varphi^{(n)}(x^\mu)\phi_n(z) \ , \tag{6.2}$$

where $B_\mu^{(n)}$ is identified with vector and axial vector mesons and $\varphi^{(0)}$ with pions. $\varphi^{(n)}$ can be absorbed into $B_\mu^{(n)}$ through the gauge transformation (section 6.1.2). ψ_n satisfies the eigenvalue equation,

$$-K^{1/3}\,\partial_Z\left(K\,\partial_Z\psi_n\right) = \lambda_n\psi_n \ , \tag{6.3}$$

with the boundary condition $\partial_Z\psi_n(0) = 0$ (vector meson) or $\psi_n(0) = 0$ (axial vector meson) at $Z = 0$. They are normalized by

$$\kappa \int dZ\, K^{-1/3}\psi_n\psi_m = \delta_{nm} \ , \tag{6.4}$$

where $\kappa \equiv \widetilde{T}(2\pi\alpha')^2R^3 = \frac{\lambda N_c}{216\pi^3}$, and (6.3) and (6.4) implies

$$\kappa \int dZ\, K(\partial_Z\psi_n)(\partial_Z\psi_m) = \lambda_n\delta_{nm} \ . \tag{6.5}$$

The $\phi_n(Z)$ are chosen such that

$$\phi_n(Z) = \frac{1}{\sqrt{\lambda_n}M_{\rm KK}U_{KK}}\partial_Z\psi_n(Z) \quad (n \geq 1) \ , \tag{6.6}$$

$$\phi_0(Z) = \frac{1}{\sqrt{\pi\kappa}M_{kk}U_{KK}}\frac{1}{K} \ , \tag{6.7}$$

with the normalization condition:

$$(\phi_m, \phi_n) \equiv \kappa M_{\rm KK}^2U_{\rm KK}^2 \int dZ\, K\,\phi_m\phi_n = \delta_{mn} \ , \tag{6.8}$$

which is compatible with (6.5).

6.1.2 Effective meson action

With the gauge field $A_\mu(x^\mu, z)$ and $A_z(x^\mu, z)$ the DBI action of the D8-$\overline{\text{D8}}$-branes becomes 5-dimensional [1]:

$$S^{DBI}_{\text{D8-}\overline{\text{D8}}} = -\widetilde{T}\int d^4x dz\, U^2$$
$$\text{tr}\sqrt{1+(2\pi\alpha')^2\frac{R^3}{2U^3}F_{\mu\nu}F^{\mu\nu}+(2\pi\alpha')^2\frac{9}{4}\frac{U}{U_{\text{KK}}}F_{\mu z}F^{\mu z}+[F^3]+[F^4]+[F^5]}\,, \tag{6.9}$$

where $\widetilde{T} = \frac{N_c}{216\pi^5}\frac{M_{KK}}{\alpha'^3}$, U is a function of z, and the indices are contracted by the metric $(-,+,+,+,+)$. $[F^3], [F^4]$, and $[F^5]$ are short for the terms of F^3, F^4, and F^5 respectively. Notice that the range of z is extended from $[0,\infty]$ to $[-\infty,\infty]$ to account for both $D8$ and $\overline{\text{D8}}$.

Inserting (6.1) and (6.2) into (6.9) and using the orthonomality of ψ_n and ϕ_n ((6.4)$\sim$(6.8)), we have [28, 29]

$$\begin{aligned} S^{DBI}_{\text{D8-}\overline{\text{D8}}} \;\sim\; \int d^4x\,\text{tr}\Bigg[&(\partial_\mu\varphi^{(0)})^2+\sum_{n=1}^{\infty}\Big(\frac{1}{2}(\partial_\mu B^{(n)}_\nu-\partial_\nu B^{(n)}_\mu)^2 \\ &+\lambda_n M^2_{KK}(B^{(n)}_\mu-\lambda_n^{-1/2}\partial_\mu\varphi^{(n)})^2\Big)\Bigg] \\ &+(\text{interaction terms})\,. \end{aligned} \tag{6.10}$$

Here $\varphi^{(0)}$ and $B^{(n)}_\mu$ are interpreted as a masseless pion field and an infinite tower of vector (or axial) vector meson fields with masses $m_n^2(\equiv\lambda_n M^2_{\text{KK}})$. The lightest vector meson ρ is identified with $B^{(1)}_\mu$. $\varphi^{(n)}$ are absorbed into $B^{(n)}_\mu$. In the expansion (6.1) and (6.2), we have implicitly assumed that the gauge fields are zero asymptotically, i.e. $A_M(x^\mu, z)\to 0$ as $z\to\pm\infty$. The residual gauge transformation that does not break this condition is obtained by a gauge function $g(x^\mu, z)$ that asymptotes a constant $g(x^\mu, z)\to g_\pm$ at $z\pm\infty$. (g_+, g_-) are interpreted as elements of the chiral symmetry group $U(N_f)_L\times U(N_f)_R$ in QCD with N_f massless flavors.

[1] The gauge group generators t^a are normalized as $\text{tr}\, t^a t^b = \delta_{ab}/2$

6.1.3 $A_z = 0$ gauge and pion effective action

In the previous subsection we worked in the gauge $A_M(x^\mu, z) \to 0$ as $z \to \pm\infty$. However the $A_z = 0$ gauge can be achieved by applying the gauge transformation $A_M \to g A_M g^{-1} + g\partial_M g^{-1}$ with the gauge function

$$g^{-1}(x^\mu, z) = P \exp\left\{ -\int_0^z dz'\, A_z(x^\mu, z') \right\} . \tag{6.11}$$

Then the asymptotic values of $A_\mu(z \to \infty)$ do not vanish and change to

$$A_\mu(x^\mu, z) \to \xi_\pm(x^\mu)\partial_\mu \xi_\pm^{-1}(x^\mu) \qquad \text{as} \quad z \to \pm\infty , \tag{6.12}$$

where $\xi_\pm(x^\mu) \equiv \lim_{z\to\pm\infty} g(x^\mu, z)$. The gauge fields can be expanded as

$$\begin{aligned} A_\mu(x^\mu, z) &= \xi_+(x^\mu)\partial_\mu \xi_+^{-1}(x^\mu)(x^\mu)\psi_+(z) + \xi_-(x^\mu)\partial_\mu \xi_-^{-1}(x^\mu)\psi_-(z) \\ &\quad + \sum_{n=1}^{\infty} B_\mu^{(n)}(x^\mu)\psi_n(z) , \\ A_z(x^\mu, z) &= 0 , \end{aligned} \tag{6.13}$$

where $\psi_\pm$ is the non-normalizable zero mode of (6.3) with the appropriate boundary condition to yield (6.12):

$$\begin{aligned} \psi_\pm &= \frac{1}{2} \pm \widehat{\psi}_0 , \\ \widehat{\psi}_0 &= \frac{1}{\pi}\arctan(Z) \end{aligned}$$

There is a residual gauge symmetry which maintains $A_z = 0$. It is given by the z-independent gauge transformation $h(x^\mu)$,

$$A_M(x^\mu, z) \to h(x^\mu) A_M(x^\mu, z) h^{-1}(x^\mu) + h(x^\mu)\partial_M h^{-1}(x^\mu) , \tag{6.14}$$

which acts on the component fields as

$$\xi_\pm \to h\, \xi_\pm\, g_\pm^{-1} , \tag{6.15}$$

$$B_\mu^{(n)} \to h\, B_\mu^{(n)}\, h^{-1} , \tag{6.16}$$

where we considered chiral symmetry $g_\pm$ together. Then $\xi_\pm(x^\mu)$ are interpreted

as the $U(N_f)$ valued fields $\xi_{L,R}(x^\mu)$ which carry the pion degrees of freedom in the hidden local symmetry approach . Indeed the transformation property (6.15) is the same as that for $\xi_{L,R}(x^\mu)$ if we interpret $h(x^\mu) \in U(N_f)$ as the hidden local symmetry. They are related to the $U(N_f)$ valued pion field $U(x^\mu)$ in the chiral Lagrangian by

$$\xi_+^{-1}(x^\mu)\xi_-(x^\mu) = U(x^\mu) \equiv e^{2i\Pi(x^\mu)/f_\pi} \ . \tag{6.17}$$

The pion field $\Pi(x^\mu)$ is identical to $\varphi^{(0)}(x^\mu)$ in (6.2) in leading order. A convenient gauge choice is

$$\xi_-(x^\mu) = 1, \quad \xi_+^{-1}(x^\mu) = U(x^\mu) = e^{2i\Pi(x^\mu)/f_\pi} \tag{6.18}$$

which expresses the gauge fields as,

$$A_\mu(x^\mu, z) = U^{-1}(x^\mu)\partial_\mu U(x^\mu)\psi_+(z) + \sum_{n\geq 1} B_\mu^{(n)}(x^\mu)\psi_n(z) \tag{6.19}$$

In this gauge, after omitting the vector meson fields $B_\mu^{(n)}$, the effective action reduces to the Skyrme model

$$\begin{aligned} &S^{DBI}_{\text{D8-}\overline{\text{D8}}}\Big|_{B_\mu^{(n)}=0} \\ &= \int d^4x \left(\frac{\kappa M_{\text{KK}}^2}{\pi} \text{tr} \left(U^{-1}\partial_\mu U\right)^2 + \frac{1}{32e_S^2} \text{tr} \left[U^{-1}\partial_\mu U, U^{-1}\partial_\nu U\right]^2 \right) \ , \end{aligned} \tag{6.20}$$

where $e_S^{-2} \equiv \kappa \int dz\, K^{-1/3}(1-\psi_0^2)^2$ and the pion decay constant f_π is fixed by the comparison with the Skyrme model:

$$f_\pi^2 \ \equiv \ \frac{4}{\pi}\kappa M_{\text{KK}}^2 = \frac{1}{54\pi^4} M_{\text{KK}}^2 \lambda N_c \ , \tag{6.21}$$

Another gauge we will consider below is

$$\xi_+^{-1}(x^\mu) = \xi_-(x^\mu) = e^{i\Pi(x^\mu)/f_\pi} \ . \tag{6.22}$$

in terms of which the gauge fields are written as

$$
\begin{aligned}
A_\mu(x^\mu, z) &= \alpha_\mu(x^\mu)\widehat{\psi}_0(z) + \beta_\mu(x^\mu) + \sum_{n=1}^{\infty} B_\mu^{(n)}(x^\mu)\psi_n(z) \ , \qquad (6.23)\\
\alpha_\mu(x^\mu) &= \{\xi^{-1}, \partial_\mu \xi\} = \frac{2i}{f_\pi}\partial_\mu \Pi + [[\partial_\mu \Pi^3]] + \mathcal{O}(\Pi^4) \ ,\\
\beta_\mu(x^\mu) &= \frac{1}{2}[\xi^{-1}, \partial_\mu \xi] = \frac{1}{2f_\pi^2}[\Pi, \partial_\mu \Pi] + \mathcal{O}(\Pi^4) \ ,
\end{aligned}
$$

where $[[\partial_\mu \Pi^3]] \equiv -\frac{i}{3f_\pi^3}((\partial_\mu \Pi)\Pi^2 + \Pi^2 \partial_\mu \Pi - 2\Pi(\partial_\mu \Pi)\Pi)$.

6.2 Effective meson action: $n_B \neq 0$

We now extend the previous analysis to finite baryon density for $n_B = 0$. This is achieved by adding the background $U(1)_V$ field $\mathcal{A}_0$ to the fluctuating gauge field A_M. Since, the vacuum modes $\{\psi_n, \phi_n\}$ are not mass eigenmodes in matter, we may choose more pertinent eigenmodes in matter. Two basis set are possible: (1) medium mass eigenmodes $\psi_n \sim e^{-imt} f_n(z)$; (2) screening eigenmodes $\psi \sim e^{i\vec{k}\cdot\vec{x}} f_n(z)$. With this in mind, we have the following gauge fields decomposition

$$
\begin{aligned}
A_0(x^\mu, z) &= \mathcal{A}_0(z) + \sum_{n=1}^{\infty} B_0^{(n)}(x^\mu)\omega_n(z) \ , \qquad (6.24)\\
A_i(x^\mu, z) &= \sum_{n=1}^{\infty} B_i^{(n)}(x^\mu)\psi_n(z) \ , \qquad (6.25)\\
A_z(x^\mu, z) &= \sum_{n=0}^{\infty} \varphi^{(n)}(x^\mu)\phi_n(z) \, . \qquad (6.26)
\end{aligned}
$$

$\mathcal{A}_0(z)$ is the background gauge field. The time component modes $(\omega_n(z))$ and the space component $(\psi_n(z))$ are not necessarily the same as Lorentz symmetry does not hold in the matter rest frame. Note that $F_{\mu z}$ is modified by $\mathcal{A}_0$ while $F_{\mu\nu}$ is not.

In order to compute the DBI action (6.9),

$$S^{DBI}_{\text{D8-}\overline{\text{D8}}} = -\widetilde{T}\int d^4x dz\, U^2$$
$$\text{tr}\sqrt{1+(2\pi\alpha')^2\frac{R^3}{2U^3}F_{\mu\nu}F^{\mu\nu}+(2\pi\alpha')^2\frac{9}{4}\frac{U}{U_{\text{KK}}}F_{\mu z}F^{\mu z}+[F^3]+[F^4]+[F^5]}\ ,$$

we need to know $F_{\mu\nu}F^{\mu\nu}, F_{\mu z}F^{\mu z}, [F^3], [F^4]$, and $[F^5]$, which are involved in general. To quadratic order (ignoring $\mathcal{O}((B_\mu,\varphi)^3)$), the contributions are greatly simplified because of: 1) cyclic property of the trace, 2) antisymmetry of $F_{\mu,\nu}$, 3) parity of mode functions. Then there is no contribution from $[F^3]$ and $[F^5]$. $[F^4]$ has important terms that will modify $F_{\mu\nu}F^{\mu\nu}$:

$$[F^4] = (2\pi\alpha')^4\frac{9}{8}\frac{U}{U_{\text{KK}}}\left(\frac{R}{U}\right)^3 F_{0z}F^{0z}F_{ij}F^{ij}+\mathcal{O}((B_\mu,\varphi)^4)\ . \tag{6.27}$$

Table (6.1) lists all the relevant terms, where we have introduced f_{ij} defined as

$$f_{ij}\equiv\partial_i v_j-\partial_j v_i\ , \tag{6.28}$$

with $i,j=1,2,3$. Table (6.1) should be understood in the integral and trace operation. We omitted some terms vanishing in those operations and rearranged some terms by using the cyclicity of the trace.

In terms of the definitions on the RHS of the Table (6.1) , the action reads

$$S^{DBI}_{\text{D8-}\overline{\text{D8}}} = -\widetilde{T}\int d^4x dz\, U^2\,\text{tr}\,\sqrt{P_0+P_1}\ , \tag{6.29}$$

with

$$P_0 \equiv 1-(2\pi\alpha')^2\frac{9}{4}\frac{U}{U_{\text{KK}}}\,\beta_0 = 1-bK^{\frac{1}{3}}(\partial_Z\mathcal{A}_0)^2\ , \tag{6.30}$$

$$\begin{aligned}P_1 &\equiv (2\pi\alpha')^2\frac{R^3}{2U^3}(\alpha_2)+(2\pi\alpha')^2\frac{9}{4}\frac{U}{U_{\text{KK}}}(\beta_1+\beta_2)\\ &+ (2\pi\alpha')^4\frac{9}{8}\frac{R^3}{U_{KK}U^2}(\gamma_2)\ ,\end{aligned} \tag{6.31}$$

where P_0 does not contain meson fields but involves the baryon density. Ex-

$F_{\mu\nu}F^{\mu\nu}$	$\to$	$\Big[\ 2\partial_0 B_i^{(n)}\partial^0 B^{(m)i}\psi_n\psi_m + 2\partial_i B_0^{(n)}\partial^j B^{(m)0}\omega_n\omega_m$		
		$-2\partial_0 B_i^{(n)}\partial^i B^{(m)0}\psi_n\psi_m$		
		$+(\partial_i B_j^{(n)} - \partial_j B_i^{(n)})(\partial^i B^{(m)j} - \partial^j B^{(m)i})\psi_n\psi_m\ \Big]$	$\equiv$	α_2
$F_{\mu z}F^{\mu z}$	$\to$	$-(\dot{\mathcal{A}}_0)^2$	$\equiv$	β_0
		$+2\dot{\mathcal{A}}_0\Big[\partial^0\varphi^{(n)}\phi_n - B^{0(n)}\dot{\omega}_n + [B^{(n)0},\varphi^{(m)}]\omega_n\phi_m\Big]$	$\equiv$	β_1
		$+\Big[\partial_0\varphi^{(n)}\partial^0\varphi^{(m)}\phi_n\phi_m + B_0^{(n)}B^{(m)0}\dot{\omega}_n\dot{\omega}_m$		
		$-2\partial_0\varphi^{(n)}B^{(m)0}\phi_n\dot{\omega}_m + \partial_i\varphi^{(n)}\partial^i\varphi^{(m)}\phi_n\phi_m$		
		$+B_i^{(n)}B^{(m)i}\dot{\psi}_n\dot{\psi}_m - 2\partial_i\varphi^{(n)}B^{(m)i}\phi_n\dot{\psi}_m\Big]$	$\equiv$	β_2
$[F^4]$	$\to$	$f_{ij}f^{ij}(\dot{\mathcal{A}}_0)^2\psi_1^2$	$\equiv$	γ_2

Table 6.1: The relevant terms in evaluating the DBI action up to quadratic order in the fields (B_μ, φ). The upper dot stands for the derivative with respect to z. The terms should be understood in the integral and trace operation.

panding the action for small fields we have

$$\begin{aligned} S^{DBI}_{\text{D8-}\overline{\text{D8}}} &= -\widetilde{T}\int d^4x dz\, U^2\,\text{tr}\,\left[\sqrt{P_0} + \frac{1}{2}\frac{P_1}{\sqrt{P_0}} - \frac{1}{8}\frac{P_1^2}{\sqrt{P_0}^3}\right] + \mathcal{O}((B_\mu,\varphi)^3) \\ &= S_1 + S_2 + \mathcal{O}((B_\mu,\varphi)^3)\ , \end{aligned} \tag{6.32}$$

with

$$S_1 \equiv -\widetilde{T}\int d^4x dz\, U^2\text{tr}\ \Delta^{-1}\ , \tag{6.33}$$

$$S_2 \equiv -\widetilde{T}\int d^4x dz\, U^2\text{tr}\ \left[\frac{1}{2}\Delta P_1 - \frac{1}{8}\Delta^3 P_1^2\right]\ , \tag{6.34}$$

where the modification factor $\Delta(n_B)$ is

$$\Delta(n_B) \equiv \frac{1}{\sqrt{P_0}} = \frac{1}{\sqrt{1 - bK^{\frac{1}{3}}(\partial_Z \mathcal{A}_0)^2}} = \sqrt{1 + \frac{n_B^2}{4a^2 b} K^{-5/3}} \ .$$

$-S_0$ is the grand potential discussed in section 3.1.3, and S_2 will be reduced to [2]

$$\begin{aligned}
S_2 = -\mathrm{tr} \int d^4x \Bigg\{ & \\
& \left[\int dZ K^{-1/3} \Delta \ \Psi_n \Psi_m \right] \partial_0 B_i^{(m)} \partial^0 B^{(n)i} \\
& + \left[\int dZ K^{-1/3} \Delta \ \Omega_n \ \Omega_m \right] \partial_i B_0^{(n)} \partial^i B^{(m)0} \\
& - \left[\int dZ K^{-1/3} \Delta \ \Psi_n \ \Omega_m \right] 2\partial_0 B_i^{(n)} \partial^i B^{(m)0} \\
& + \left[\int dZ K^{-1/3} \Delta^{-1} \Psi_n \Psi_m \right] \frac{1}{2} (\partial_i B_j^{(n)} - \partial_j B_i^{(n)}) (\partial^i B^{(m)j} - \partial^j B^{(m)i}) \\
& + \left[M_{\mathrm{KK}}^2 \int dZ K \Delta^3 \ \partial_Z \Omega_n \ \partial_Z \Omega_m \right] B_0^{(n)} B^{(m)0} \\
& + \left[M_{\mathrm{KK}}^2 \int dZ K \Delta \ \partial_Z \Psi_n \partial_Z \Psi_m \right] B_i^{(n)} B^{(m)i} \\
& + \left[M_{\mathrm{KK}}^2 \int dZ K \Delta^3 \Phi_n \Phi_m \right] \partial_0 \varphi^{(n)} \partial^0 \varphi^{(m)} \\
& + \left[M_{\mathrm{KK}}^2 \int dZ K \Delta \Phi_n \Phi_m \right] \partial_i \varphi^{(n)} \partial^i \varphi^{(m)} \\
& - \left[M_{\mathrm{KK}}^2 \int dZ K \Delta^3 \Phi_n \partial_Z \Omega_m \right] 2\partial_0 \varphi^{(n)} B^{(m)0} \\
& - \left[M_{\mathrm{KK}}^2 \int dZ K \Delta \Phi_n \partial_Z \Psi_m \right] 2\partial_i \varphi^{(n)} B^{(m)i} \Bigg\} \ ,
\end{aligned} \tag{6.35}$$

where we defined the scaled eigenfounctions as

$$\Omega_n \equiv \sqrt{\kappa} \omega_n \ , \quad \Phi_n \equiv \sqrt{\kappa} \psi_n \ , \quad \Phi_n \equiv \sqrt{\kappa} U_{\mathrm{KK}} \phi_n \ . \tag{6.36}$$

[2]Note that the pattern: Δ, Δ^{-1}, and Δ^3. This pattern appears also when we consider higher order terms including couplings. The origin is explained in Appendix A.

At zero density $\Delta = 1$, so $\Phi_n = \Omega_n$ and the action reduces to the (6.10) by the same mode function in (6.3) $\sim$ (6.8). However at finite density the eigen modes Ω_n, Ψ_n, and Φ_n cannot be determined uniquely. In other words there is no mode decomposition which makes the action completly diagonal. So we consider the space-like and time-like separatly: (1) $A_M = A_M(x^i, z)$ and (2) $A_M = A_M(x^0, z)$.

6.2.1 Space-like fields $A_M = A_M(x^i, z)$

First we consider time-independent gauge fields. Up to quadratic order the action is

$$\begin{aligned} S_2 = -\mathrm{tr} \int d^4x \Bigg\{ & \left[\int dZ K^{-1/3} \Delta \; \Omega_n \; \Omega_m \right] \partial_i B_0^{(n)} \partial^i B^{(m)0} \\ & + \left[\int dZ K^{-1/3} \Delta^{-1} \Psi_n^S \Psi_m^S \right] \frac{1}{2} (\partial_i B_j^{(n)} - \partial_j B_i^{(n)})(\partial^i B^{(m)j} - \partial^j B^{(m)i}) \\ & + \left[M_{\mathrm{KK}}^2 \int dZ K \Delta^3 \; \partial_Z \Omega_n \; \partial_Z \Omega_m \right] B_0^{(n)} B^{(m)0} \\ & + \left[M_{\mathrm{KK}}^2 \int dZ K \Delta \; \partial_Z \Psi_n^S \partial_Z \Psi_m^S \right] B_i^{(n)} B^{(m)i} \\ & + \left[M_{\mathrm{KK}}^2 \int dZ K \Delta \Phi_n^S \Phi_m^S \right] \partial_i \varphi^{(n)} \partial^i \varphi^{(m)} \\ & - \left[M_{\mathrm{KK}}^2 \int dZ K \Delta \Phi_n^S \partial_Z \Psi_m^S \right] 2 \partial_i \varphi^{(n)} B^{i(m)} \Bigg\} , \end{aligned} \tag{6.37}$$

where we have defined the scaled eigenfunctions as

$$\Omega_n \equiv \sqrt{\kappa} \omega_n \; , \quad \Psi_n^S \equiv \sqrt{\kappa} \psi_n \; , \quad \Phi_n^S \equiv \sqrt{\kappa} U_{\mathrm{KK}} \phi_n \; . \tag{6.38}$$

To diagonalize the action we choose Ψ_n^S as the eigenfunction satisfying

$$-K^{1/3} \Delta^{-1} \partial_Z \left(K \Delta^3 \; \partial_Z \Omega_n \right) = \lambda_n^\Omega \Omega_n \; , \tag{6.39}$$

$$-K^{1/3} \Delta \; \partial_Z \left(K \Delta \; \partial_Z \Psi_n^S \right) = \lambda_n^S \Psi_n^S \; , \tag{6.40}$$

with the normalization conditions,

$$\int dZ K^{-1/3} \Delta \ \Omega_n \ \Omega_m = \delta_{nm} \ , \tag{6.41}$$

$$\int dZ K^{-1/3} \Delta^{-1} \Psi_n^S \Psi_m^S = \delta_{nm} \ , \tag{6.42}$$

which imply

$$\int dZ K \Delta^3 \ \partial_Z \Omega_n \ \partial_Z \Omega_m = \lambda_n^\Omega \delta_{nm} \ , \tag{6.43}$$

$$\int dZ K \Delta \ \partial_Z \Psi_n^S \partial_Z \Psi_m^S = \lambda_n^S \delta_{nm} \ . \tag{6.44}$$

If we choose Φ_n^S as

$$\Phi_n^S = \frac{1}{M_{\rm KK}\sqrt{\lambda_n^S}} \partial_Z \Psi_n^S \ \ (n \geq 1) \ , \quad \Phi_0^S = \frac{1}{M_{\rm KK}} \frac{1}{\sqrt{\int dZ (K^{-1}\Delta^{-1})}} \ \frac{1}{K\Delta} \ , \tag{6.45}$$

then $\partial_i \varphi^{(n)}$ $(n \geq 1)$ can be absorbed into $B_i^{(n)}$ through the gauge transformation

$$B_i^{(n)} \to B_i^{(n)} + \frac{1}{M_{\rm KK}\sqrt{\lambda_n^S}} \partial_i \varphi^{(n)} \ . \tag{6.46}$$

These choices of mode functions reduces the action to

$$\begin{aligned} S_2 = -{\rm tr} \int d^4x \Big\{ & \partial_i \varphi^{(0)} \partial^i \varphi^{(0)} \\ & + \partial_i B_0^{(n)} \partial^i B^{(n)0} + \frac{1}{2} f_{ij}^{(n)} f^{(n)ij} + \mathcal{M}_n^{\shortparallel 2} B_0^{(n)} B^{(n)0} + \mathcal{M}_n^{\perp 2} B_i^{(n)} B^{(n)i} \Big\} \ , \end{aligned}$$

where we have defined longitudinal screening masses $\mathcal{M}_n^{\shortparallel}$ and transverse screening masses $\mathcal{M}_n^\perp$ as

$$\mathcal{M}_n^{\shortparallel} \equiv \sqrt{\lambda_n^\Omega} M_{\rm KK} \ , \qquad \mathcal{M}_n^\perp \equiv \sqrt{\lambda_n^S} M_{\rm KK} \ . \tag{6.47}$$

6.2.2 Time-like fields $A_M = A_M(x^0, z)$

For spacially homogeneous gauge fields the action reads

$$\begin{aligned} S_2 = -\mathrm{tr} \int d^4x \Bigg\{ & \left[\int dZ K^{-1/3} \Delta \ \Psi_n^T \Psi_m^T \right] \partial_0 B_i^{(m)} \partial^0 B^{(n)i} \\ & + \left[M_{\mathrm{KK}}^2 \int dZ K \Delta \ \partial_Z \Psi_n^T \partial_Z \Psi_m^T \right] B_i^{(n)} B^{(m)i} \\ & + \left[M_{\mathrm{KK}}^2 \int dZ K \Delta^3 \ \partial_Z \Omega_n \ \partial_Z \Omega_m \right] B_0^{(n)} B^{(m)0} \\ & + \left[M_{\mathrm{KK}}^2 \int dZ K \Delta^3 \Phi_n^\Omega \Phi_m^\Omega \right] \partial_0 \varphi^{(n)} \partial^0 \varphi^{(m)} \\ & - \left[M_{\mathrm{KK}}^2 \int dZ K \Delta^3 \Phi_n^\Omega \partial_Z \Omega_m \right] 2 \partial_0 \varphi^{(n)} B^{0(m)} \Bigg\} , \end{aligned} \tag{6.48}$$

where we have defined the scaled eigenfunctions

$$\Omega_n \equiv \sqrt{\kappa} \omega_n \ , \quad \Psi_n^T \equiv \sqrt{\kappa} \psi_n \ , \quad \Phi_n^\Omega \equiv \sqrt{\kappa} U_{\mathrm{KK}} \phi_n \ . \tag{6.49}$$

We choose Ψ_n^S as the eigenfunction satisfying

$$-K^{1/3} \Delta^{-1} \partial_Z \left(K \Delta \ \partial_Z \Psi_n^T \right) = \lambda_n^T \Psi_n^T \ , \tag{6.50}$$

$$-K^{1/3} \Delta^{-1} \partial_Z \left(K \Delta^3 \ \partial_Z \Omega_n \right) = \lambda_n^\Omega \Omega_n \ , \tag{6.51}$$

with the normalization conditions,

$$\int dZ K^{-1/3} \Delta \ \Psi_n^T \Psi_m^T = \delta_{nm} \ , \tag{6.52}$$

$$\int dZ K^{-1/3} \Delta \ \Omega_n \ \Omega_m = \delta_{nm} \ , \tag{6.53}$$

which imply

$$\int dZ K \Delta \ \partial_Z \Psi_n^T \partial_Z \Psi_m^T = \lambda_n^T d_{nm} \ , \tag{6.54}$$

$$\int dZ K \Delta^3 \ \partial_Z \Omega_n \ \partial_Z \Omega_m = \lambda_n^\Omega \delta_{nm} \ , \tag{6.55}$$

If we choose Φ_n^S as

$$\Phi_n^\Omega = \frac{1}{M_{\rm KK}\sqrt{\lambda_n^\Omega}}\partial_Z \Psi_n^\Omega \ , \quad \Phi_0^\Omega = \frac{1}{M_{\rm KK}} \frac{1}{\sqrt{\int dZ (K^{-1}\Delta^{-3})}} \ \frac{1}{K\Delta^3} \ , \tag{6.56}$$

then $\partial_0 \varphi^{(n)}$ $(n \geq 1)$ can be absorbed into $B_0^{(n)}$ through the gauge transformation

$$B_0^{(n)} \to B_0^{(n)} + \frac{1}{M_{\rm KK}\sqrt{\lambda_n^\Omega}} \partial_0 \varphi^{(n)} \ . \tag{6.57}$$

The action is reduced to

$$\begin{aligned} S_2 = -{\rm tr} \int d^4x \Big\{ & \partial_0 \varphi^{(n)} \partial^0 \varphi^{(n)} + \partial_0 B_i^{(n)} \partial^0 B^{(n)i} \\ & + m_n^2 B_i^{(n)} B^{(n)i} + M_{\rm KK}^2 \lambda_n^\Omega B_0^{(n)} B^{(n)0} \Big\} \ , \end{aligned} \tag{6.58}$$

where we have defined the mass

$$m_n = \sqrt{\lambda_n^T} M_{\rm KK} \ . \tag{6.59}$$

6.2.3 Pion effective action

In this subsection we work in the $A_z = 0$ gauge following the procedure in section 6.1.3.

Time-like field ($A_M = A_M(x^0, z)$)

First consider the case $A_M = A_M(x^0, z)$. By the gauge transformation $A_M \to g A_M g^{-1} + g \partial_M g^{-1}$ with the gauge function

$$g^{-1}(x^0, z) = P \exp \left\{ - \int_0^z dz' \, A_z(x^0, z') \right\} \ , \tag{6.60}$$

the gauge fields are rewritten as

$$\begin{aligned} A_0(x^0, z) &= \mathcal{A}_0(z) + \xi_+(x^0) \partial_0 \xi_+^{-1}(x^0) \omega_+(z) + \xi_-(x^0) \partial_0 \xi_-^{-1}(x^0) \omega_-(z) \ , \\ A_i(x^0, z) &= A_z(x^0, z) = 0 \ , \end{aligned}$$

where we have omitted the vector mesons $B_\mu^{(n)}$. The $\omega_\pm$ are obtained as zero mode solutions of (6.51) satisfying the boundary condition for $A_0(x^0, z)$:

$$\omega_\pm(z) \equiv \frac{1}{2} \pm \frac{1}{\int dZ(K^{-1}\Delta^{-3})} \int_0^Z dZ \frac{1}{K\Delta^3} \ . \tag{6.61}$$

By using the residual gauge symmetry $h(x^\mu)$ (6.18) and (6.19) we may express the gauge field as

$$A_0(x^0, z) = \mathcal{A}_0 + U^{-1}(x^0)\partial_0 U(x^0)\omega_+(z) \ . \tag{6.62}$$

The field strength is

$$F_{z\mu} = \dot{\mathcal{A}}_0 + U^{-1}\partial_0 U \widehat{\phi}_0^\omega(z) \ , \qquad F_{\mu\nu} = 0 \ , \tag{6.63}$$

where

$$\widehat{\phi}_0^\omega(z) \equiv \partial_z \omega_+(z) = \frac{1}{U_{\rm KK} \int dZ(K^{-1}\Delta^{-3})} \ \frac{1}{K\Delta^3} \ . \tag{6.64}$$

The action becomes

$$S_2 = \mathrm{tr} \int d^4x \left[\kappa M_{\rm KK}^2 \frac{1}{\int dZ K^{-1}\Delta^{-3}} \right] (U^{-1}\partial_0 U)^2 \ , \tag{6.65}$$

and we identify the time-like pion decay constant f_π^T as

$$f_\pi^{T\,2} = \frac{4\kappa M_{\rm KK}^2}{\int dZ K^{-1}\Delta^{-3}} \ , \tag{6.66}$$

by comparison with the Skyrme model.

Space-like field ($A_M = A_M(x^i, z)$)

Similarly, we consider the case $A_M = A_M(x^i, z)$. Using the same gauge transformation we can work with the gauge fields,

$$\begin{aligned} A_i(x^i, z) &= \xi_+(x^i)\partial_i \xi_+^{-1}(x^i)\psi_+^S(z) + \xi_-(x^i)\partial_i \xi_-^{-1}(x^i)\psi_-^S(z) \ , \\ A_0(x^i, z) &= \mathcal{A}_0(z) \ , \qquad A_z(x^i, z) = 0 \ , \end{aligned}$$

where $\psi_{\pm}^{S}$ are obtained as a zero mode solution of (6.42) satisfying the pertinent boundary condition of $A_i(x^i, z)$:

$$\psi_{\pm}^{S}(z) \equiv \frac{1}{2} \pm \frac{1}{\int dZ(K^{-1}\Delta^{-1})} \int_0^Z dZ \frac{1}{K\Delta} \tag{6.67}$$

Then the gauge field and the field strength in the gauge (6.18) are

$$\begin{aligned} A_0(x^0, z) &= \mathcal{A}_0 + U^{-1}(x^i)\partial_i U(x^i)\psi_{+}^{S}(z) \\ F_{z\mu} &= \dot{\mathcal{A}}_0 + U^{-1}\partial_i U\widehat{\phi}_0^{S}(z) \ , \end{aligned} \tag{6.68}$$

where we do not consider $F_{\mu\nu}$ since we are interested in the kinetic part and

$$\widehat{\phi}_0^{S}(z) \equiv \partial_z \psi_{+}^{S}(z) = \frac{1}{U_{\rm KK}\int dZ(K^{-1}\Delta^{-1})} \frac{1}{K\Delta} \ . \tag{6.69}$$

The action is

$$S_2 = \mathrm{tr} \int d^4x \left[\kappa M_{\rm KK}^2 \frac{1}{\int dZ K^{-1}\Delta^{-1}}\right] (U^{-1}\partial_i U)^2 \ , \tag{6.70}$$

and f_{π}^{S} is identified by

$$f_{\pi}^{S2} = \frac{4\kappa M_{\rm KK}^2}{\int dZ K^{-1}\Delta^{-1}} \ . \tag{6.71}$$

6.2.4 Vector Mesons Interactions

In this section we study the interactions of the fields $B_0^{(1)}$, $B_i^{(1)}$ and $\varphi^{(0)}$ corresponding to the lowest medium modes Ω_1, Ψ_1, and Φ_1. For simplicity, we use the following notation,

$$v_0 \equiv B_0^{(1)} \ , \quad v_i \equiv B_i^{(1)} \ , \quad \Pi \equiv \varphi^{(0)} \ . \tag{6.72}$$

The details of the computation are relegated to Appendix A [3].

[3] Both in Appendix A and this section, the vector meson field is considered as anti Hermitian. Although in Appendix A, we are working with the vacuum modes instead of the medium modes, the conversion can be done by inspection using the formula tabulated in Table (6.3,6.4)

Time-like Fields $A_M = A_M(x^0, z)$

$$S_2 = \mathrm{tr} \int d^4x \Big\{ -\partial_0\Pi\partial^0\Pi + \partial_0 v_i \partial^0 v^i + m_1^2 v_i v^i + M_{\mathrm{KK}}^2 \lambda_1^{\Omega} v_0 v^0 \Big\}$$
$$-2g^T_{v\Pi^2}\, v_0[\Pi, \partial^0\Pi] + g^T_{v^3}\, 2\partial_0 v_i [v^0, v^i] + \cdots \Big\} \,, \qquad (6.73)$$

where the couplings can be read from (6.3,6.4) in Appendix A by substituting the vacuum mode functions by the medium mode functions

$$g^T_{v\Pi^2} = \frac{1}{\sqrt{\kappa}} \frac{\int dZ \frac{\Omega_1}{K\Delta^3}}{\int dZ \frac{1}{K\Delta^3}} \,, \qquad (6.74)$$
$$g^T_{v^3} = \frac{1}{\sqrt{\kappa}} \int dZ\, K^{-1/3} \Omega_1 (\Psi_1^T)^2 \Delta \,. \qquad (6.75)$$

Space-like Fields $A_M = A_M(x^i, z)$

$$S_2 = \mathrm{tr} \int d^4x \Big\{ -\partial_i\Pi\partial^i\Pi + \partial_i v_0 \partial^i v^0 + \frac{1}{2} f_{ij} f^{ij} + \mathcal{M}_1^{\shortparallel\, 2} v_0 v^0 + \mathcal{M}_1^{\perp\, 2} v_i v^i$$
$$-2g^S_{v\Pi^2}\, v_i[\Pi, \partial^i\Pi] + g^S_{v^3}\, 2\partial_i v_0 [v^i, v^0] + \widetilde{g}^S_{v^3}\, f_{ij}[v^i, v^j] + \cdots \Big\} \,,$$

where the couplings can be read from (6.3,6.4) in Appendix A, again by substituting the vacuum mode functions by the medium mode functions

$$g^S_{v\Pi^2} = \frac{1}{\sqrt{\kappa}} \frac{\int dZ \frac{\Psi_1^S}{K\Delta}}{\int dZ \frac{1}{K\Delta}} \,,$$
$$g^S_{v^3} = \frac{1}{\sqrt{\kappa}} \int dZ\, K^{-1/3} (\Omega_1)^2 \Psi_1^S \Delta^{-1} \,,$$
$$\widetilde{g}^S_{v^3} = \frac{1}{\sqrt{\kappa}} \int dZ\, K^{-1/3} (\Psi_1^S)^3 \Delta^{-1} \,. \qquad (6.76)$$

Zero Density Limit

To check the current mode decomposition used in this section, we take the zero baryon density limit. In this case, Lorentz symmetry is enforced and the

action reads

$$S_2 = \mathrm{tr}\int d^4x\Big\{ -\partial_\mu\Pi\partial^\nu\Pi + \frac{1}{2}f_{\mu\nu}f^{\mu\nu} + m_1^2 v_\mu v^\nu\Big\}$$
$$-2g_{v\Pi^2}\, v_\mu[\Pi,\partial^\mu\Pi] + g_{v^3}\, f_{\mu\nu}[v^\mu,v^\nu] + \cdots\Big\}\ , \quad (6.77)$$

which is the same as Eqn.(5.40) in [28] except the $v\Pi\Pi$ coupling. The difference comes from the gauge choice. In [28] $A_z = 0$ gauge is used and we chose $A_M(z\to\infty)\to 0$. Since the difference is merely a gauge choice, physics will not be changed. However we will repeat the analysis of couplings at zero density with (6.77), since the action in our gauge is more convenient for reading off physical quantities. Also it is readily extendable to finite baryon density.

First we examine the KSRF relation by defining a_{KSRF} as

$$a_{\mathrm{KSRF}} \equiv \frac{4\, g_{v\Pi^2}^2\, f_\pi^2}{m_1^2} \sim \begin{cases} 2.03 & \text{Experiment} \\ 1.3 & \text{Sakai Sugimoto model} \end{cases}\ , \quad (6.78)$$

which is the same value reported in [28, 29], as expected. The universality of the vector meson coupling can be checked by a_{U} defined as

$$a_{\mathrm{U}} \equiv \frac{g_{v\Pi^2}}{g_{v^3}} \sim \begin{cases} 1 & \text{The universality of the vector meson coupling} \\ 0.93 & \text{Sakai Sugimoto model} \end{cases} \quad (6.79)$$

which is also the same value as in [28]. Notice that both relations include $g_{v\Pi^2}$ and can be read from (6.77). In the $A_z = 0$ gauge we should convert $g_{v\Pi^2}$ to $a_{v\Pi^2}$ by [28]

$$a_{v\Pi^2} = \frac{2g_{v\Pi^2}}{m_1^2}\ . \quad (6.80)$$

When we consider the field redefinition in (6.77)

$$v_\mu \to v_\mu + \frac{a_{v^3}}{2}[\Pi,\partial_\mu\Pi]\ , \quad (6.81)$$

the algebraic relation (6.80) appears immediate. However when we look at the

integral expression of $g_{v\Pi^2}$ and $a_{v\Pi^2}$ the equivalence is obscured.

$$
\begin{aligned}
& a_{v\Pi^2} = \frac{2g_{v\Pi^2}}{m_1^2} \\
\Leftrightarrow\ & \frac{\pi^2}{8}\int dZ K^{-1/3}\Psi_1(1-4\widehat{\psi}_0^2)\int dZ K(\partial_Z\Psi_1)^2 = \int dZ K^{-1}\Psi_1 \ .
\end{aligned}
$$

Next and following [28], we compare (6.77) with the action from the hidden local symmetry approach

$$
\begin{aligned}
S_H \equiv \mathrm{tr}\int d^4x\Big\{ & -\partial_\mu\Pi\partial^\nu\Pi + \frac{1}{2}f_{\mu\nu}f^{\mu\nu} + ag^2f_\pi^2 v_\mu v^\nu\Big\} \\
& -ag\, v_\mu[\Pi,\partial^\mu\Pi] + g\, f_{\mu\nu}[v^\mu,v^\nu] + \cdots\Big\} \ . \qquad (6.82)
\end{aligned}
$$

The hidden local symmetry parameter (LHS) can be written in terms of the D-brane effective action parameter (RHS):

$$
\begin{aligned}
& g = g_{v^3} \ , && (6.83)\\
& a = \frac{2g_{v\Pi^2}}{g} = \frac{2g_{v\Pi^2}}{g_{v^3}} \ , && (6.84)\\
& f_\pi^2 = \frac{m_1^2}{ag^2} = \frac{m_1^2}{2g_{v^3}g_{v\Pi^2}} \ , && (6.85)
\end{aligned}
$$

where we used the first two relations to get the last. We may define the parameter a_{H} which quantify the difference between hidden local symmetry approach and our model: [4]

$$
a_{\mathrm{H}} \equiv \frac{2g_{v^3}g_{v\Pi^2}f_\pi^2}{m_1^2} \ \sim\ \begin{cases} 1 & \text{Hidden local symmetry} \\ 0.72 & \text{Sakai Sugimoto model} \end{cases} \ , \qquad (6.86)
$$

which is the same value reported in [28], as expected. a_{H} may be interpreted as follows. Since f_π is an input parameter the Hidden local symmetry has two adjustable parameters, so a is not uniquely determined. It can be fixed by (6.84) or (6.85). When these two procedures yield the same value, $a_{\mathrm{U}} = 1$.

[4] For a=2 the hidden local symmetry approach implies KSRF relation and the universality of the vector meson coupling. Here, we do not require this value since we want to compare our model with the hidden local symmetry itself.

6.2.5 Numerical results

All the numerical work reported here has been carried out for the lowest modes $v_\mu \equiv B_\mu^{(1)}$ and $\Pi \equiv \varphi^{(0)}$ with the parameters discussed in section 3.

Mass and Screening Mass

From the previous section the meson masses (6.59) (time-like) and the screening masses (6.47) (space-like) are defined as

$$\begin{aligned} m_n &\equiv \sqrt{\lambda_n^T} M_{\rm KK} \ , \\ \mathcal{M}_n^{\shortparallel} &\equiv \sqrt{\lambda_n^\Omega} M_{\rm KK} \ , \qquad \mathcal{M}_n^{\perp} \equiv \sqrt{\lambda_n^S} M_{\rm KK} \ , \end{aligned} \tag{6.87}$$

where λ_n^T, λ_n^Ω, and λ_n^S are determined as the eigenvalues of the following equations ((6.50),(6.51),(6.42)), respectively:

$$-K^{1/3}\Delta^{-1}\partial_Z\left(K\Delta\ \partial_Z\Psi_n^T\right) = \lambda_n^T\Psi_n^T \ , \tag{6.88}$$

$$-K^{1/3}\Delta^{-1}\partial_Z\left(K\Delta^3\ \partial_Z\Omega_n\right) = \lambda_n^\Omega\Omega_n \ , \tag{6.89}$$

$$-K^{1/3}\Delta\ \partial_Z\left(K\Delta\ \partial_Z\Psi_n^S\right) = \lambda_n^S\Psi_n^S \ . \tag{6.90}$$

Their dependense on the baryon density normalized to the nuclear matter density is shown in (8.1) for the lowest eigenmode. The time-like and transverse screening mass are seen to decrease midly with density. The longitudinal screening mass increases moderatly with baryon density. The mild dependence on the density for the SS model indicates that the vector mesons are weakly affected by the baryon density in this version of the SS model. As the inserted baryons are point like, at large N_c their interaction is chiefly repulsive through ω's as induced by D8-$\overline{\rm D8}$. The ω interactions with vectors and axials is mostly anomalous (through the WZ term) and therefore small as we ignored the WZ term.

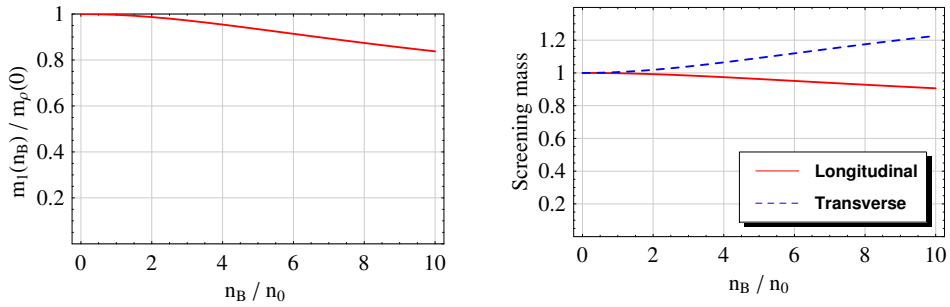

(a) (b)

Figure 6.1: (a) Mass (b) Screening mass (Longitudinal mode: $\mathcal{M}_1^{\shortparallel}(n_B)/m_\rho(0)$, Transverse mode: $\mathcal{M}_1^{\perp}(n_B)/m_\rho(0)$)

Pion decay constant

The pion decay constant is identified from ((6.66),(6.71)) respectively,

$$f_\pi^{T2} = \frac{4\kappa M_{\rm KK}^2}{\int dZ K^{-1}\Delta^{-3}} \ ,$$
$$f_\pi^{S2} = \frac{4\kappa M_{\rm KK}^2}{\int dZ K^{-1}\Delta^{-1}} \ . \tag{6.91}$$

The explicit dependence on the baryon density is shown in Fig.(6.2). Both

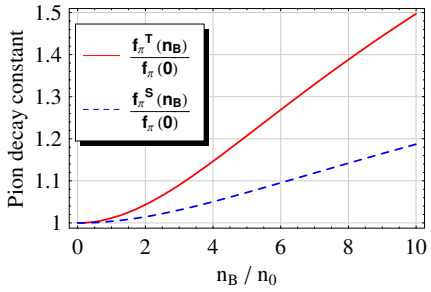

Figure 6.2: Pion decay constant

the time-like and space-like pion decay constant are found to *increase* with the baryon density. The increase is quadratic at small densities. Since the S-wave pion scattering length with baryons is $1/N_c$ this explains the absence of a linear term. Moreover, for point-like external baryon sources the pion-Axial-Vector

coupling in matter at the origin of the pion decay constant involves two baryon sources and is repulsive.

Vector Couplings and KSRF Relation

The vector couplings are identified in (6.75) and (6.76). Their overall dependence on the baryon density is again mild as explained above.

vΠΠ couplings:

$$g^T_{v\Pi^2} = \frac{1}{\sqrt{\kappa}} \frac{\int dZ \, \frac{\Omega_1}{K\Delta^3}}{\int dZ \, \frac{1}{K\Delta^3}} \, ,$$
$$g^S_{v\Pi^2} = \frac{1}{\sqrt{\kappa}} \frac{\int dZ \, \frac{\Psi_1^S}{K\Delta}}{\int dZ \, \frac{1}{K\Delta}} \, ,$$

vvv couplings:

$$g^T_{v^3} = \frac{1}{\sqrt{\kappa}} \int dZ \, K^{-1/3} \Omega_1 (\Psi_1^T)^2 \Delta$$
$$g^S_{v^3} = \frac{1}{\sqrt{\kappa}} \int dZ \, K^{-1/3} (\Omega_1)^2 \Psi_1^S \Delta^{-1} \, ,$$
$$\widetilde{g}^S_{v^3} = \frac{1}{\sqrt{\kappa}} \int dZ \, K^{-1/3} (\Psi_1^S)^3 \Delta^{-1} \, .$$

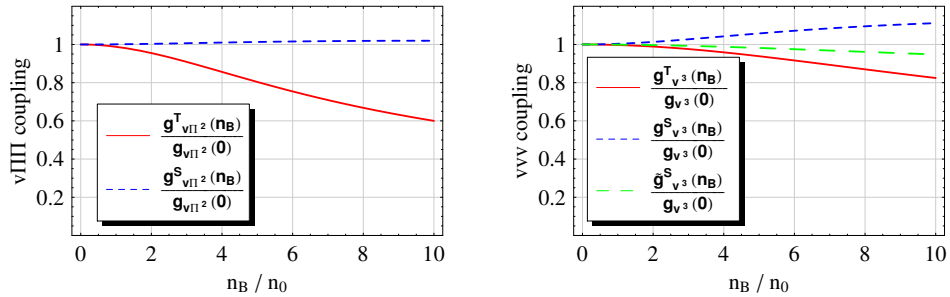

(a) (b)

Figure 6.3: (a) $v\Pi\Pi$ coupling (b) vvv coupling

KSRF relations

In the matter rest frame Lorentz symmetry is no longer manifest. As a result, we expect a *variety* of KSFR relations depending on wether time-like or space-like parameters are used. Indeed, for instance the a-parameter at the origin of the KSFR relations can now take 4 different forms depending on the time-like/space-like arrangement. Specifically

$$a^{T1}_{\rm KSRF} \equiv \frac{4\,(g^T_{v\Pi^2})^2\,(f^T_\pi)^2}{m_1^2}\ , \qquad a^{T2}_{\rm KSRF} \equiv \frac{4\,(g^T_{v\Pi^2})^2\,(f^T_\pi)^2}{(\mathcal{M}_1^{\shortparallel})^2}$$
$$a^{S1}_{\rm KSRF} \equiv \frac{4\,(g^S_{v\Pi^2})^2\,(f^S_\pi)^2}{(\mathcal{M}_1^{\perp})^2}\ , \qquad a^{S2}_{\rm KSRF} \equiv \frac{4\,(g^S_{v\Pi^2})^2\,(f^S_\pi)^2}{(\mathcal{M}_1^{\shortparallel})^2}$$

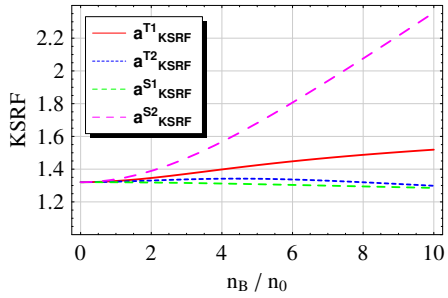

Figure 6.4: Generalized a-parameter

6.3 Conclusion

Using linear response theory, we have probed this dense baryonic system using pions, vectors and axials. The point like nature of the baryons with a size of order $1/\sqrt{\lambda}$ and the large N_c nature as noted above, causes rather mild changes in the masses and couplings as a function of baryon density. In contrast, the pion decay constants are found to change appreciably. The quadratic increases at small baryon densities is mediated by omega's. The scalar S-wave pion-baryon scattering length is noted to vanish at large N_c, causing f_π to increase instead of decreasing at finite density. This behaviour is unphysical.

6.4 Appendix

6.4.1 The Effective Action Using the Vacuum Modes

Let us only consider the lightest vacuum meson modes corresponding to the pion and ρ meson fields. This vacuum mode decomposition was studied in [**?**] at zero baryon density. Here we just add $\mathcal{A}_0$ as obtained in section 3.1 to the gauge field A_M. Since the mode decomposition is complete, this approach should be complementary to the one discussed in the text. It is the same as the one we used in [**?**]. As we will show, the results are overall similar to the ones discussed in the main text regarding the density dependence.

In the gauge $A_z = 0$ and $\xi \equiv e^{\frac{i\Pi(x^\mu)}{f_\pi}}$ (6.23), A_μ reads[5]

$$\begin{aligned} A_\mu(x^\mu, z) &= -i\mathcal{A}_0(z) + v_\mu(x^\mu)\,\psi_1(z)\ . \\ &+ \left(\frac{2i}{f_\pi}\partial_\mu\Pi + [\partial_\mu\Pi^3]\right)\widehat{\psi}_0(z) + \frac{1}{2f_\pi^2}[\Pi, \partial_\mu\Pi] + \mathcal{O}(\Pi^4)\ , \end{aligned} \tag{6.92}$$

where $\mathcal{A}_0$ is the background field, $v_\mu \equiv B_\mu^{(1)}$. We have set $B_\mu^{(n)} = 0$ for $n \geq 2$. The corresponding field strengths are

$$\begin{aligned} F_{\mu\nu} &= (\partial_\mu v_\nu - \partial_\nu v_\mu)\psi_1 + [v_\mu, v_\nu]\psi_i^2 \\ &+ \frac{2i}{f_\pi}([\partial_\mu\Pi, v_\nu] + [v_\nu, \partial_\nu\Pi])\psi_1\widehat{\psi}_0 + \frac{1}{f_\pi^2}[\partial_\mu\Pi, \partial_\nu\Pi](1 - 4\widehat{\psi}_0^2) + \mathcal{O}((\Pi, v_\mu)^3) \\ F_{z\mu} &= -i\dot{\mathcal{A}}_0 + \left(\frac{2i}{f_\pi}\partial_\mu\Pi + [[\partial_\mu\Pi^3]]\right)\widehat{\phi}_0 + v_\mu\dot{\psi}_1 + \mathcal{O}(\Pi^4) \end{aligned}$$

where $\dot{\mathcal{A}}_0 = \frac{d\mathcal{A}_0}{dz}$, $\dot{\psi}_1 = \frac{d\psi_1}{dz}$, and

$$\widehat{\phi}_0 = \partial_z\widehat{\psi}_0 = \frac{1}{\pi U_{\rm KK}}\frac{1}{K} \sim \phi_0 \text{ in (6.7)} \tag{6.93}$$

Notice that $\mathcal{A}_0$ does not contribute to $F_{\mu\nu}$ and affect only $F_{z\mu}$.

[5] In this section the gauge field A_μ is treated as anti-Hermitian. $\mathcal{A}_0$ and Π is Hermitian so i was introduced, while v_μ is anti-Hermitian. Note that we are working in a different gauge from Section 6.2.

In order to compute the DBI action (6.9),

$$S^{DBI}_{\text{D8-}\overline{\text{D8}}} = -\widetilde{T}\int d^4x dz\, U^2$$
$$\text{tr}\,\sqrt{1-(2\pi\alpha')^2\frac{R^3}{2U^3}F_{\mu\nu}F^{\mu\nu}-(2\pi\alpha')^2\frac{9}{4}\frac{U}{U_{\text{KK}}}F_{\mu z}F^{\mu z}+[F^3]+[F^4]+[F^5]}\ ,$$

we need to know $F_{\mu\nu}F^{\mu\nu}, F_{\mu z}F^{\mu z}, [F^3], [F^4]$, and $[F^5]$, which have many complicated contributions. Again, we use the observations noted in the text to simplify. Thus

$$[F^4] = (2\pi\alpha')^4\frac{9}{8}\frac{U}{U_{\text{KK}}}\left(\frac{R}{U}\right)^3 F_{0z}F^{0z}F_{ij}F^{ij}+\mathcal{O}((v_\mu,\varphi)^4)\ . \tag{6.94}$$

Table (6.2) lists all relevant terms. We have introduced $f_{\mu\nu}$ defined as

$$f_{\mu\nu}\equiv\partial_\mu v_\nu-\partial_\nu v_\mu\ , \tag{6.95}$$

with $\mu\nu=0,1,2,3$ and $i,j=1,2,3$. Table (6.2) should be understood in the integral and trace operation. We have omitted some terms vanishing in the operation and rearranged some terms by using the cyclicity of the trace.

In terms of the entries in the RHS of the table, the action reads

$$S^{DBI}_{\text{D8-}\overline{\text{D8}}} = -\widetilde{T}\int d^4x dz\, U^2\,\text{tr}\,\sqrt{P_0+P_1}\ , \tag{6.96}$$

with

$$P_0 \equiv 1-(2\pi\alpha')^2\frac{9}{4}\frac{U}{U_{\text{KK}}}\,\beta_0 = 1-bK^{\frac{1}{3}}(\partial_Z\mathcal{A}_0)^2\ , \tag{6.97}$$

$$\begin{aligned}P_1 &\equiv (2\pi\alpha')^2\frac{R^3}{2U^3}(\alpha_2+\alpha_3)+(2\pi\alpha')^2\frac{9}{4}\frac{U}{U_{\text{KK}}}(\beta_1+\beta_2)\\ &+ (2\pi\alpha')^4\frac{9}{8}\frac{R^3}{U_{KK}U^2}(\gamma_2+\gamma_3)\ .\end{aligned} \tag{6.98}$$

Again, P_0 does not include meson fields and has carries the baryon density.

$F_{\mu\nu}F^{\mu\nu}$	$\to$	$f_{\mu\nu}f^{\mu\nu}\psi_1^2$	$\equiv$	α_2
		$2f_{\mu\nu}[v^\mu, v^\nu]\psi_1^3 + \frac{2}{f_\pi^2}f_{\mu\nu}[\partial^\mu\Pi, \partial^\nu\Pi]\psi_1(1-4\widehat{\psi_0^2})$	$\equiv$	α_3
$F_{\mu z}F^{\mu z}$	$\to$	$(\dot{\mathcal{A}}_0)^2$	$\equiv$	β_0
		$-\frac{4}{f_\pi}(\partial_0\Pi)\widehat{\phi}_0\dot{\mathcal{A}}_0 + 2iv_0\dot{\psi}_1\dot{\mathcal{A}}_0$	$\equiv$	β_1
		$-\frac{4}{f_\pi^2}(\partial_\mu\Pi\partial^\mu\Pi)\widehat{\phi}_0^2 + v_\mu v^\mu\dot{\psi}_1^2 + \frac{2i}{f_\pi}\{\partial_\mu\Pi, v^\mu\}\widehat{\phi}_0\dot{\psi}_1$	$\equiv$	β_2
$[F^4]$	$\to$	$f_{ij}f^{ij}(\dot{\mathcal{A}}_0)^2\psi_1^2$	$\equiv$	γ_2
		$\Big[2f_{ij}[v^i, v^j](\dot{\mathcal{A}}_0)^2\psi_1^3 - 2iv_0f_{ij}f^{ij}\dot{\mathcal{A}}_0\dot{\psi}_1\psi_1^2$ $+\frac{2}{f_\pi^2}f_{ij}[\partial^i\Pi, \partial^j\Pi](\dot{\mathcal{A}}_0)^2\psi_1(1-4\widehat{\psi_0^2})\Big]$	$\equiv$	γ_3

Table 6.2: The relevant terms in evaluating DBI action up to third order in the fields (Π, v). All entries are understood in the integral and trace operation.

Expanding the action by fluctuating the fields we have

$$\begin{aligned} S^{DBI}_{\text{D8-}\overline{\text{D8}}} &= -\widetilde{T}\int d^4xdz\, U^2\,\text{tr}\,\left[\sqrt{P_0} + \frac{1}{2}\frac{P_1}{\sqrt{P_0}} - \frac{1}{8}\frac{P_1^2}{\sqrt{P_0}^3} + \frac{1}{16}\frac{P_1^3}{\sqrt{P_0}^5}\right] + \cdots \\ &= S_1 + S_2 + \mathcal{O}((\Pi, v_\mu)^4)\ , \end{aligned} \tag{6.99}$$

with

$$S_1 \equiv -\widetilde{T}\int d^4xdz\, U^2\text{tr}\ \Delta^{-1}\ , \tag{6.100}$$

$$S_2 \equiv -\widetilde{T}\int d^4xdz\, U^2\text{tr}\ \left[\frac{1}{2}\Delta P_1 - \frac{1}{8}\Delta^3 P_1^2 + \frac{1}{16}\Delta^5 P_1^3\right]\ , \tag{6.101}$$

where we defined a modification factor $\Delta(Q)$ as

$$\Delta(Q) \equiv \frac{1}{\sqrt{P_0}} = \frac{1}{\sqrt{1 - bK^{\frac{1}{3}}(\partial_Z\mathcal{A}_0)^2}} = \sqrt{1 + \frac{n_B^2}{4a^2b}K^{-5/3}}\ .$$

Notice that $-S_1$ is the grand potential discussed in section 3.1, and S_2 will be

reduced to the action of mesons. To accomplish it we plug (6.98) into (6.101) and evaluate all z integrals and identify them as coefficients of each term in the remaining 4-D action.

Let us first check which terms we have and how they are affected by finite baryon density schematically. It can be read off from Table (6.2). At zero density we set $\mathcal{A}_0 = 0$ and $\Delta = 1$. Then $\alpha_2, \alpha_3, \beta_2$ survive. α_2, β_2 correspond to the free action of Π and ρ, and α_3 is the couplings of vvv, $v\Pi\Pi$ interaction. At finite density all terms are enhanced by Δ, Δ^2,or Δ^3. Furthermore there are nontrivial modification. The free action part will be affected by γ_2 and β_1^2. (β_1 itself does not contribute because the first term has odd parity in z and the second term is traceless.) The couplings are modified by γ_3. There are new interaction terms such as $v_0(\partial_\mu v_\nu - \partial_\nu v_\mu)^2$, $v_0 v_\mu v^\mu$, $v_0 \partial_\mu \Pi \partial^\mu \Pi$, $\partial_0 \Pi \{\partial_\mu \Pi, v^\mu\}$, which all vanish at zero density.

Considering all these modification we get the final form of the meson action

$$\begin{aligned} S_2 = \int d^4x \Bigg[& - a^T_{\Pi^2} \mathrm{tr}\, \left(\partial_0 \Pi \partial^0 \Pi\right) - a^S_{\Pi^2} \mathrm{tr}\, \left(\partial_i \Pi \partial^i \Pi\right) \\ & + a^T_{v^2} \mathrm{tr}\, f_{0i} f^{0i} + \frac{1}{2} a^S_{v^2} \mathrm{tr}\, f_{ij} f^{ij} \\ & + m_v^{2\,T} \mathrm{tr}\, v_0 v^0 + m_v^{2\,S} \mathrm{tr}\, v_i v^i \\ & + a^T_{v^3} \mathrm{tr}\, \Big(2 f_{0i} [v^0, v^i]\Big) + a^S_{v^3} \mathrm{tr}\, \Big(f_{ij} [v^i, v^j]\Big) \\ & + a^T_{v\Pi^2} \mathrm{tr}\, \Big(2 f_{0i} [\partial^0 \Pi, \partial^i \Pi]\Big) + a^S_{v\Pi^2} \mathrm{tr}\, \Big(f_{ij} [\partial^i \Pi, \partial^j \Pi]\Big) + \cdots \Bigg] \,, \end{aligned} \tag{6.102}$$

where the coefficients of every term are defined in Table (6.3). At zero density all coefficients agree with those in [28]. There are three types of modification due to the baryon density: Δ, Δ^{-1}, and Δ^3. Δ simply comes from $\frac{1}{2}\Delta P_1$ in (6.101). Since Δ is common to all coefficients, Δ^3 and Δ^{-1} can be understood as $\Delta \cdot \Delta^2$ and $\Delta \cdot \Delta^{-2}$. An enhancing factor Δ^2 is due to additional contribution from β_1^2 and a suppressing factor Δ^{-1} is from γ_2, γ_3, which explains the calculational similarities in all the results.

Finally we want to mention without details, the character of the action in the gauge $A_M(z \to \infty) \to 0$ instead of $A_z = 0$. The action is the same as

Coefficients	Definition	$Q=0(\Delta=1)$
$a^T_{\Pi^2}$	$\frac{1}{\pi}\int dZ K^{-1}\Delta^3$	1
$a^S_{\Pi^2}$	$\frac{1}{\pi}\int dZ K^{-1}\Delta$	1
$a^T_{v^2}$	$\int dZ\, K^{-\frac{1}{3}}\Psi_1^2\,\Delta$	1
$a^S_{v^2}$	$\int dZ\, K^{-\frac{1}{3}}\Psi_1^2\,\Delta^{-1}$	1
m_v^{2T}	$M_{\rm KK}^2\int dZ\, K(\partial_Z\Psi_1)^2\,\Delta^3$	m_ρ^2
m_v^{2S}	$M_{\rm KK}^2\int dZ\, K(\partial_Z\Psi_1)^2\,\Delta$	m_ρ^2
$a^T_{v^3}$	$\frac{1}{\sqrt{\kappa}}\int dZ\, K^{-\frac{1}{3}}\Psi_1^3\,\Delta$	$\frac{1}{\sqrt{\kappa}}\cdot 0.446$
$a^S_{v^3}$	$\frac{1}{\sqrt{\kappa}}\int dZ\, K^{-\frac{1}{3}}\Psi_1^3\,\Delta^{-1}$	$\frac{1}{\sqrt{\kappa}}\cdot 0.446$
$a^T_{v\Pi^2}$	$\frac{1}{\sqrt{\kappa}}\frac{\pi}{4M_{\rm KK}^2}\int dZ\, K^{-1/3}\Psi_1(1-4\widehat{\psi}_0^2)\Delta$	$\frac{1}{\sqrt{\kappa}}\frac{\pi}{4M_{\rm KK}^2}\cdot 1.584$
$a^S_{v\Pi^2}$	$\frac{1}{\sqrt{\kappa}}\frac{\pi}{4M_{\rm KK}^2}\int dZ\, K^{-1/3}\Psi_1(1-4\widehat{\psi}_0^2)\Delta^{-1}$	$\frac{1}{\sqrt{\kappa}}\frac{\pi}{4M_{\rm KK}^2}\cdot 1.584$

Table 6.3: The definitions of the coefficients in the action (6.102). At finite density, there are enhancing factors Δ, Δ^3 and a suppressing factor Δ^{-1}.

in (6.102) except for the interaction term $v\Pi\Pi$

$$-2g^T_{v\Pi^2}\, v_0[\Pi,\partial^0\Pi]-2g^S_{v\Pi^2}\, v_i[\Pi,\partial^i\Pi]\ , \tag{6.103}$$

where $g^T_{v\Pi^2}$ and $g^S_{v\Pi^2}$ are defined in Table(6.4).

6.4.2 Numerical results

In this section we compute the coefficients in Table (6.3,6.4) numerically. Their physical meanings can be read off from the action (6.102). We use the same numerical inputs as detailed in section 3.

Coefficients	Definition	$Q=0(\Delta=1)$
$g^T_{v\Pi^2}$	$\sqrt{\kappa}M^2_{\rm KK}U^2_{\rm KK}\int dZ\, K\Delta^3\Psi_1\phi_0^2$	$\frac{1}{\sqrt{\kappa}\pi}\cdot 0.63$
$g^S_{v\Pi^2}$	$\sqrt{\kappa}M^2_{\rm KK}U^2_{\rm KK}\int dZ\, K\Delta\Psi_1\phi_0^2$	$\frac{1}{\sqrt{\kappa}\pi}\cdot 0.63$

Table 6.4: The definitions of the coefficients in the action (6.102). At finite density, there are enhancing factors Δ, Δ^3 and a suppressing factor Δ^{-1}.

Pion Decay Constant

The pion decay constant can be defined by the procedure of Section 6.2.3 with the vacuum mode function.

$$f_\pi^T \equiv f_\pi\sqrt{a^T_{\pi^2}}\ , \qquad f_\pi^S \equiv f_\pi\sqrt{a^S_{\pi^2}} \tag{6.104}$$

Velocity

The pion velocity and the lowest mode velocity are

$$v_\pi \equiv \sqrt{\frac{a^S_{\pi^2}}{a^T_{\pi^2}}} = \frac{f^S_\pi}{f^T_\pi}\ , \quad v_v \equiv \sqrt{\frac{a^S_{v^2}}{a^T_{v^2}}} \tag{6.105}$$

Mass

$$M_1 \equiv \sqrt{\frac{m^{2S}_v}{a^T_{v^2}}} \tag{6.106}$$

Screening mass

$$M^{\shortparallel}_{scr} \equiv \sqrt{\frac{m^{2T}_v}{a^T_{v^2}}}\ , \qquad M^{\perp}_{scr} \equiv \sqrt{\frac{m^{2S}_v}{a^S_{v^2}}}\ . \tag{6.107}$$

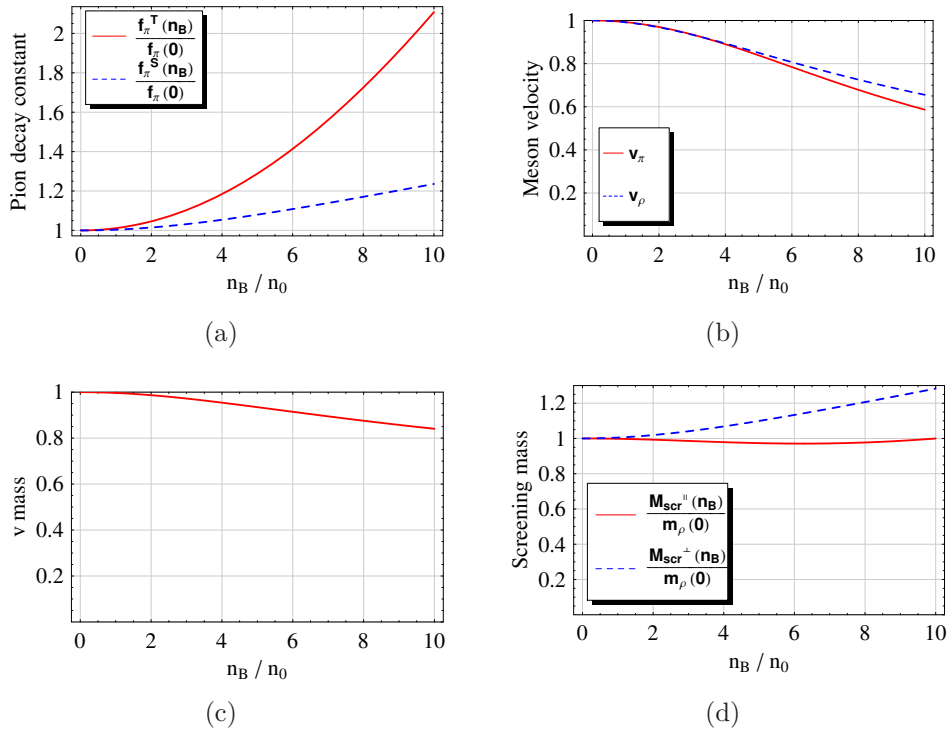

Figure 6.5: (a) Pion decay constant vs $\frac{n_B}{n_0}$ $\left[\frac{f_\pi^T}{f_\pi} = \sqrt{a_{\pi^2}^T},\ \frac{f_\pi^S}{f_\pi} = \sqrt{a_{\pi^2}^S}\ \right]$, (b) Velocity of Π and ρ (v) vs $\frac{n_B}{n_0}$ $\left[\ v_\pi \equiv \sqrt{\frac{a_{\pi^2}^S}{a_{\pi^2}^T}}\right.$ and $\left. v_v \equiv \sqrt{\frac{a_{v^2}^S}{a_{v^2}^T}}\ \right]$, (c) v mass vs $\frac{n_B}{n_0}$ $\left[\frac{M_1}{m_\rho} \equiv \sqrt{\frac{m_v^{2S}}{a_{v^2}^T m_\rho^2}}\ \right]$, (d) Screening masses vs $\frac{n_B}{n_0}$ $\left[\frac{M_{scr}^{\parallel}}{m_\rho} \equiv \sqrt{\frac{m_v^{2T}}{a_{v^2}^T m_\rho^2}}\right.$, $\left.\frac{M_{scr}^{\perp}}{m_\rho} \equiv \sqrt{\frac{m_v^{2S}}{a_{v^2}^S m_\rho^2}}\right]$

Chapter 7

Baryon Form Factor

7.1 Introduction

Holographic QCD has provided an insightful look to a number of issues in baryonic physics at strong coupling $\lambda = g^2 N_c$ and large number of colors N_c. In particular, in [12, 33] baryons are constructed from a five-dimensional Shrodinger-like equation whereby the 5th dimension generates mass-like anomalous dimensions through pertinent boundary conditions. A number of baryonic properties have followed ranging from baryonic spectra to form factors [12, 34].

At large N_c baryons are chiral solitons in QCD. A particularly interesting framework for discussing this scenario is SS model [28–30]. In SS model (herethrough hQCD) D4 static instantons in bulk source the chiral solitons or Skyrmions on the boundary. The instantons have a size of order $1/\sqrt{\lambda}$ and a mass of order $N_c\lambda$ in units of M_{KK}, the Kaluza-Klein scale [28]. The static Skyrmion is just the instanton holonomy in the Z-direction, with a larger size of order λ^0 [17].

In this chapter we would like to elaborate further on the precedent observation by explicitly constructing the pertinent electromagnetic current for a holographic soliton following from the exact D4 instanton in bulk in a semi-classical expansion with $\hbar = 1/\lambda N_c$. The vector mesons are quantized using non-rigid constraints to preserve causality. The electromagnetic current is boundary valued as expected from the solitonic nature of the baryon as well as the holographic principle. To order $\hbar^0$ the current is entirely vector meson dominated in overall agreement with the effective analysis in [34]. Our semi-

classical analysis provides a book-keeping framework for analyzing the baryons in holographic QCD. It also clarifies a recent analysis [31].

We note that the instanton dynamics in bulk follows from the reduced DBI action. For instantons of size $1/\sqrt{\lambda}$, their field strengths are large and of order λ. In a way the use of the reduced DBI action is not justified. However, since the analysis to follow relies on semiclassics, we believe that our final results are generic enough to hold for the exact instanton solution as well.

In section 2 we briefly go over the soliton-instanton configuration of the Yang-Mills-Chern-Simons effective theory of the Sakai-Sugimoto model in 5 dimensions, including some generic symmetries of the instanton configuration. In section 3 we detail our semiclassical analysis to order $\hbar^0$. In section 4 we derive the baryon current also to order $\hbar^0$, and show that it is vector meson dominated. In section 5 we derive the electromagnetic form factor and show that the minimum and magnetic vector couplings are tied by the solitonic nature of the baryon to order $\hbar^0$. In section 6 the electromagetic charge and radius are worked out. While the instanton in bulk carries a size of order $1/\sqrt{\lambda}$, its holographic image the baryon carries a size of order λ^0 thanks to the trailing vector mesons. The baryon magnetic moments and the axial form factor are given in section 7 and 8 respectively. Our conclusions are in section 9. Some useful details can be found in the Appendices.

7.2 5D YM-CS Model

7.2.1 Action and equations of motion

In this section we review the action and its soliton solution obtained in [30]. We start with the Yang-Mills-Chern-Simons(YM-CS) theory in a 5D curved background, which has been derived as an effective theory of Sakai-Sugimoto(SS) model [28, 29]. The 5D Yang-Mills action is the leading terms in the $1/\lambda$ expansion of the DBI action of the D8 branes after integrating out the S^4. The 5D Chern-Simons action is obtained from the Chern-Simons action of the D8 branes by integrating F_4 RR flux over the S^4, which is nothing but N_C. The

action reads [28, 29]

$$S = S_{YM} + S_{CS} \ , \tag{7.1}$$

$$S_{YM} = -\kappa \int d^4x dZ \ \mathrm{tr} \left[\frac{1}{2} K^{-1/3} \mathcal{F}_{\mu\nu}^2 + M_{\mathrm{KK}}^2 K \mathcal{F}_{\mu Z}^2 \right] \ , \tag{7.2}$$

$$S_{CS} = \frac{N_c}{24\pi^2} \int_{M^4 \times R} \omega_5^{U(N_f)}(\mathcal{A}) \ , \tag{7.3}$$

where $\mu, \nu = 0, 1, 2, 3$ are 4D indices and the fifth(internal) coordinate Z is dimensionless. There are three things which are inherited by the holographic dual gravity theory: M_{KK}, κ, and K. M_{KK} is the Kaluza-Klein scale and we will set $M_{\mathrm{KK}} = 1$ as our unit. κ and K are defined as

$$\kappa = \lambda N_c \frac{1}{216\pi^3} \equiv \lambda N_c a \ , \qquad K = 1 + Z^2 \ . \tag{7.4}$$

$\mathcal{A}$ is the 5D $U(N_f)$ 1-form gauge field and $\mathcal{F}_{\mu\nu}$ and $\mathcal{F}_{\mu Z}$ are the components of the 2-form field strength $\mathcal{F} = \mathrm{d}\mathcal{A} - i\mathcal{A} \wedge \mathcal{A}$. $\omega_5^{U(N_f)}(\mathcal{A})$ is the Chern-Simons 5-form for the $U(N_f)$ gauge field:

$$\omega_5^{U(N_f)}(\mathcal{A}) = \mathrm{tr} \left(\mathcal{A}\mathcal{F}^2 + \frac{i}{2}\mathcal{A}^3\mathcal{F} - \frac{1}{10}\mathcal{A}^5 \right) \ , \tag{7.5}$$

Since $\mathcal{A}$ is $U(N_f)$ valued, it may be decomposed into an $SU(N_f)$ part(A) and a $U(1)$ part($\widehat{A}$),

$$\mathcal{A} = A + \frac{1}{\sqrt{2N_f}} \widehat{A} \ , \qquad \mathcal{F} = F + \frac{1}{\sqrt{2N_f}} \widehat{F} \ , \tag{7.6}$$

where $A \equiv A^a T^a, F \equiv F^a T^a$ and the $SU(N_f)$ generators T^a are normalized as

$$\mathrm{tr}\,(T^a T^b) = \frac{1}{2}\delta^{ab} \ . \tag{7.7}$$

For $N_f = 2$ the action (8.46) and (8.47) are reduced to

$$\begin{aligned} S_{YM} \ &= \ -\kappa \int d^4x dZ \ \mathrm{tr} \left[\frac{1}{2} K^{-1/3} F_{\mu\nu}^2 + K F_{\mu Z}^2 \right] \\ &\quad -\frac{\kappa}{2} \int d^4x dZ \ \left[\frac{1}{2} K^{-1/3} \widehat{F}_{\mu\nu}^2 + K \widehat{F}_{\mu Z}^2 \right] \ , \end{aligned} \tag{7.8}$$

$$
\begin{aligned}
S_{CS} &= \frac{N_c}{24\pi^2}\int\left[\frac{3}{2}\widehat{A}\mathrm{tr}\,F^2+\frac{1}{4}\widehat{A}\widehat{F}^2+\frac{1}{2}\,\mathrm{d}\left\{\widehat{A}\;\mathrm{tr}\;\left(2FA+\frac{i}{2}A^3\right)\right\}\right] \qquad (7.9)\\
&= \frac{N_c}{24\pi^2}\epsilon_{MNPQ}\int d^4xdZ\left[\frac{3}{8}\widehat{A}_0\mathrm{tr}\,(F_{MN}F_{PQ})-\frac{3}{2}\widehat{A}_M\mathrm{tr}\,(\partial_0A_NF_{PQ})\right.\\
&\quad +\frac{3}{4}\widehat{F}_MN\mathrm{tr}\,(A_0F_{PQ})+\frac{1}{16}\widehat{A}_0\widehat{F}_{MN}\widehat{F}_{PQ}-\frac{1}{4}\widehat{A}_M\widehat{F}_{0N}\widehat{F}_{PQ}\\
&\quad \left.+\frac{3}{2}\partial_N(\widehat{A}_M\mathrm{tr}\,A_0F_{PQ})\right]+\frac{N_c}{48\pi^2}\int\mathrm{d}\left\{\widehat{A}\;\mathrm{tr}\;\left(2FA+\frac{i}{2}A^3\right)\right\}\;, \qquad (7.10)
\end{aligned}
$$

where the $SU(2)$ and $U(1)$ parts are completely desentangled in the Yang-Mills action. The $\omega_5^{SU(2)}(A)$ vanishes in the CS action. The action (7.8) and (7.9) yield the 10 coupled equations of motion, of which the D4 instanton is a solution with topological charge 1. The coupled equations are specifically given by

$$
\begin{aligned}
\delta A_0 \to\ & \kappa\left\{D^\mu\left(K^{-1/3}F_{\mu0}\right)+D^Z\left(KF_{Z0}\right)\right\}\\
&-\frac{N_c}{64\pi^2}\epsilon_{MNPQ}(\widehat{F}_{MN}F_{PQ})=0\;, \qquad (7.11)\\
\delta A_i \to\ & \kappa\left\{D^\mu\left(K^{-1/3}F_{\mu i}\right)+D^Z\left(KF_{Zi}\right)\right\}\\
&-\frac{N_c}{64\pi^2}\epsilon_{iNPQ}(\widehat{F}_{N0}F_{PQ}+\widehat{F}_{PQ}F_{N0})=0\;, \qquad (7.12)\\
\delta A_Z \to\ & \kappa\left\{D^\mu\left(KF_{\mu Z}\right)\right\}-\frac{N_c}{64\pi^2}\epsilon_{ZNPQ}(\widehat{F}_{N0}F_{PQ}+\widehat{F}_{PQ}F_{N0})=0\;, \qquad (7.13)\\
\delta \widehat{A}_0 \to\ & \kappa\left\{\partial^\mu\left(K^{-1/3}\widehat{F}_{\mu0}\right)+\partial^Z\left(K\widehat{F}_{Z0}\right)\right\}\\
&-\frac{N_c}{64\pi^2}\epsilon_{MNPQ}\left(\mathrm{tr}\,(F_{MN}F_{PQ})+\frac{1}{2}\widehat{F}_{MN}\widehat{F}_{PQ}\right)=0\;, \qquad (7.14)\\
\delta \widehat{A}_i \to\ & \kappa\left\{\partial^\mu\left(K^{-1/3}\widehat{F}_{\mu i}\right)+\partial^Z\left(K\widehat{F}_{Zi}\right)\right\}\\
&-\frac{N_c}{16\pi^2}\epsilon_{iNPQ}\left(\mathrm{tr}\,(F_{N0}F_{PQ})+\frac{1}{2}\widehat{F}_{N0}\widehat{F}_{PQ}\right)=0\;, \qquad (7.15)\\
\delta \widehat{A}_Z \to\ & \kappa\left\{\partial^\mu\left(K\widehat{F}_{\mu Z}\right)\right\}\\
&-\frac{N_c}{16\pi^2}\epsilon_{ZNPQ}\left(\mathrm{tr}\,(F_{N0}F_{PQ})+\frac{1}{2}\widehat{F}_{N0}\widehat{F}_{PQ}\right)=0\;. \qquad (7.16)
\end{aligned}
$$

We note that δA_0 and $\delta\widehat{A}_0$ are constraint type equations or Gauss laws.

7.2.2 The Instanton Solution

The exact static $O(4)$ solution in x^M space in the large λ limit is not known. Some generic properties of this solution can be derived for large λ whatever the curvature. Indeed, since $\kappa \sim \lambda$, the instanton solution with unit topological charge that solves (7.11-7.16) follows from the YM part only in leading order. It has zero size at infinite λ. At finite λ the instanton size is of order $1/\sqrt{\lambda}$. The reason is that while the CS contribution of order λ^0 is repulsive and wants the instanton to inflate, the warping in the Z-direction of order λ^0 is attractive and wants the instanton to deflate in the Z-direction [30, 33].

For some insights to the warped instanton configuration at large λ we follow [30] and rescale the coordinates and the $U(2)$ gauge fields $\mathcal{A}$ as

$$\begin{aligned} &x^M = \lambda^{-1/2}\widetilde{x}^M \ , \quad x^0 = \widetilde{x}^0 \ , \quad \mathcal{A}_M = \lambda^{1/2}\widetilde{\mathcal{A}}_M \ , \quad \mathcal{A}_0 = \widetilde{\mathcal{A}}_0 \ , \\ &\mathcal{F}_{MN} = \lambda\widetilde{\mathcal{F}}_{MN} \ , \quad \mathcal{F}_{0M} = \lambda^{1/2}\widetilde{\mathcal{F}}_{0M} \ , \end{aligned} \tag{7.17}$$

where $M, N = 1, 2, 3, Z$ and $x^Z \equiv Z$. The variables with tilde are of order of λ^0. The equations of motions of order λ are

$$\widetilde{D}^N \widetilde{F}_{MN} = 0 \ , \tag{7.18}$$

$$\widetilde{\partial}^N \widehat{\widetilde{F}}_{MN} = 0 \ , \tag{7.19}$$

which yield $\widehat{\widetilde{\mathbb{A}}}_M = 0$ [1] for the $U(1)$ part and the BPST instanton solution for the $SU(2)$ part:

$$\widetilde{\mathbb{A}}_M = \eta_{iMN}\frac{\sigma_i}{2}\frac{2\widetilde{x}_N}{\widetilde{\xi}^2 + \widetilde{\rho}^2} \ , \qquad \widetilde{\mathbb{F}}_{MN} = \eta_{iMN}\frac{\sigma_i}{2}\frac{-4\widetilde{\rho}^2}{(\widetilde{\xi}^2 + \widetilde{\rho}^2)^2} \ . \tag{7.20}$$

The instanton is located at the origin so $\widetilde{\xi} \equiv \sqrt{\vec{\widetilde{x}}^2 + \widetilde{Z}^2}$. η_{iMN} is t'Hooft symbol defined as $\eta_{ijk} \equiv \epsilon_{ijk}$, and $\eta_{iMZ} = \delta_{iM}$. At this order $\widetilde{A}_0$ and $\widehat{\widetilde{A}}_0$ are not determined and there is no restriction on the size of the BPST instanton.

[1] For clarity we summarize our convention here. Greek indices $\{\mu, \nu\} = 0, 1, 2, 3, 4$, capital latin indices $\{M, N, P, Q\} = 1, 2, 3, 4$, and small latin indices $\{i, j, k\} = 1, 2, 3$. The fifth coordinate Z has index 4. i.e. $4 \equiv Z$. The gauge field and field strength with hat are $U(1)$ valued and without hat they are $SU(2)$ valued. All variables with tilde are of order of λ^0 and without tilde they behave as (8.50). We denote the classical field by the boldface. (e.g $\mathbb{A}$). A and F are understood as form without component indices.

The equations of motion to order λ^0 are

$$\widetilde{D}_M^2 \widetilde{A}_0 = 0 \ , \tag{7.21}$$

$$\widetilde{\partial}_M^2 \widehat{\widetilde{A}}_0 - \frac{1}{64\pi^2 a} \epsilon_{MNPQ} \mathrm{tr}\,(\widetilde{F}_{MN}\widetilde{F}_{PQ}) = 0 \ , \tag{7.22}$$

$$\frac{2}{3}\widetilde{Z}^2 \widetilde{D}_j \widetilde{F}_{ij} + 2\widetilde{Z}^2 \widetilde{D}_Z \widetilde{F}_{iZ} + 2\widetilde{D}_0 \widetilde{F}_{0i} - \frac{1}{8\pi^2 a}\epsilon_{ijkZ} \widehat{\widetilde{A}}_0 (\widetilde{D}_j \widetilde{F}_{kZ}) = 0 \ , \tag{7.23}$$

$$-2\widetilde{Z}^2 \widetilde{D}_i \widetilde{F}_{iZ} + 2\widetilde{D}_0 \widetilde{F}_{0Z} - \frac{1}{8\pi^2 a}\epsilon_{ijkZ} \widehat{\widetilde{A}}_0 (\widetilde{D}_k \widetilde{F}_{ij}) = 0 \ , \tag{7.24}$$

Gauss law (7.21) and (7.22) fix $\widetilde{\mathbb{A}}_0$ and $\widehat{\widetilde{\mathbb{A}}}_0$ as

$$\widetilde{\mathbb{A}}_0 = 0 \ , \qquad \widehat{\widetilde{\mathbb{A}}}_0 = -\frac{1}{8\pi^2 a} \frac{2\widetilde{\rho}^2 + \widetilde{\xi}^2}{(\widetilde{\rho}^2 + \widetilde{\xi}^2)^2} \ . \tag{7.25}$$

To this order, the leading BPST solution together with (7.25) solve (7.23) and (7.24) for fixed size $\tilde{\rho}$ of order λ^0. Equivalently, this size follows from the the minimum of the energy to order $1/\lambda$ [30]. For completeness, we note in this section that in terms of the unrescaled variables the instanton gauge fields are

$$\mathbb{A}_0 = 0 \ , \qquad \mathbb{A}_M = \eta_{iMN} \frac{\sigma_i}{2} \frac{2x_N}{\xi^2 + \rho^2} \ , \tag{7.26}$$

$$\widehat{\mathbb{A}}_0 = -\frac{1}{8\pi^2 a\lambda} \frac{2\rho^2 + \xi^2}{(\rho^2 + \xi^2)^2} \ , \qquad \widehat{\mathbb{A}}_M = 0 \ , \tag{7.27}$$

and the nonvanishing field strengths are

$$\mathbb{F}_{MN} = \eta_{iMN} \frac{\sigma_i}{2} \frac{-4\rho^2}{(\xi^2 + \rho^2)^2} \ , \qquad \widehat{\mathbb{F}}_{M0} = \frac{x^M (3\rho^2 + \xi^2)}{4\pi^2 a\lambda (\rho^2 + \xi^2)^3} \ , \tag{7.28}$$

with the size $\rho = \tilde{\rho}/\sqrt{\lambda}$,

$$\rho^2 = \frac{1}{8\pi^2 a\lambda} \sqrt{\frac{6}{5}} \ . \tag{7.29}$$

We note that near the origin $\xi \sim 0$, the field strengths are large with $\mathbb{F} \sim 1/\rho^2 \sim \lambda$ and $\widehat{\mathbb{F}} \sim 1/(\lambda\rho^4) \sim \lambda$. In a way the reduced DBI action (8.47) is not justified for such field strengths since higher powers of the field strength contribute. For our semiclassical analysis below this does not really matter, since an exact solution of the instanton problem with the full DBI action

will not affect the generic nature of most results below as we noted in the introduction.

For large Z and finite λ, the warped instanton configuration is not known. While we do not need it for the semiclassical analysis we will detail below, some generic properties can be inferred. Indeed, the small-Z BPST configuration above has maximal spherical symmetry. That is that an isospin rotation is equivalent to (minus) a space rotation, a feature that is immediately checked through

$$(\mathbb{R}\mathbb{A})_Z = \mathbb{A}_Z(\mathbb{R}\vec{x}) \ , \qquad (\mathbb{R}^{ab}\mathbb{A}^b)_i = \mathbb{R}^T_{ij}\mathbb{A}^a_j(\mathbb{R}\vec{x}) \ , \tag{7.30}$$

with $\mathbb{R}$ a rigid $SO(3)$ rotation. When semiclassically quantized, the instanton-baryon configuration yields a tower of states with isospin matching minus the spin. This is expected, since the holographic instanton is a Skyrmion on the boundary with hedgehog symmetry. These symmetries can be used to construct variationally the warped instanton configuration, a point we will present elsewhere.

7.3 Non-rigid SemiClassical Expansion

In this section we assume that the instanton configuration $\mathbb{A}$ solves exactly the equations of motion for all Z and all λ and proceed to quantize it semiclassically using $\hbar = 1/\kappa \sim 1/\lambda N_c$. For the book-keeping to work we count ρ^2 of order $\hbar^0$. Since the holographic pion decay constant $f_\pi^2 \sim \kappa$, this is effectively the analogue of the semiclassical $1/N_c$ expansion of the boundary Skyrmion, albeit at strong λ coupling.

We now note that $\mathbb{A}$ exhibits exact flavor, translational and rotational zero modes as well as soft or quasi-zero modes in the size ρ and conformal direction Z. We will use collective coordinates to quantize them in general. While for the electromagnetic analysis below we focus on the isorotations (minus the spatial rotations) only, we will discuss in this section the semiclassical anlysis in general.

Generically, we have in the body fixed frame

$$A_M(t,x,Z) = \mathbb{R}(t)\,(\mathbb{A}_M(x-X_0(t),Z-Z_0(t)) + C_M(t,x-X_0(t),Z-Z_0(t)))\ , \tag{7.31}$$

with $\rho = \rho(t)$. The classical part transforms inhomogeneously under flavor gauge transformation, while the quantum part transforms homogeneously. The fluctuations C are quantum and of order $\sqrt{\hbar}$ (see below). The isoration $\mathbb{R}$ is an $SO(3)$ matrix which is the adjoint representation of the $SU(2)$ flavor group. Its generators are real $(G^B)^{ab} = \epsilon^{aBb}$. To order $\hbar^0$ the constrained field $\widehat{\mathbb{A}}_0$ remains unchanged, while the constrained field $\mathbb{A}_0 = 0$ shifts by a time-dependent zero mode as detailed in Appendix A. The collective coordinates $\mathbb{R}, X_0, Z_0, \rho$ and the fluctuations C in (7.31) form a redundant set. Indeed, the true zero modes

$$\delta^B_R \mathbb{A}_M = G^B \mathbb{A}_M\ , \qquad \delta^i \mathbb{A}_M = \nabla^i \mathbb{A}_M\ , \tag{7.32}$$

and the quasi-zero or soft modes are

$$\delta_Z \mathbb{A} = \partial_Z \mathbb{A}\ , \qquad \delta_\rho \mathbb{A}_M = \partial_\rho \mathbb{A}_M\ , \tag{7.33}$$

modulo gauge transformations. All the analysis to follow will be carried to order $\hbar^0$. To avoid double counting, we need to orthogonalize (gauge fix) the vector fluctuations C from (7.32-7.33) though pertinent constraints. In the *rigid quantization*, the exact zero modes are removed from the spectrum of C. For example, the isorotations are removed by the constraint

$$\int d\xi\, C\, G^B \mathbb{A}_M\ , \tag{7.34}$$

and similarly for the translations. For an application to chiral baryons of this method we refer to [112]. This constraint violates causality as the fluctuation orthogonalizes instantaneously to an infinitesimal isorotation throughout the instanton body. A causal semiclassical quantization scheme has been discussed in [113]. Here, it means that for instance (7.34) should only be enforced at the

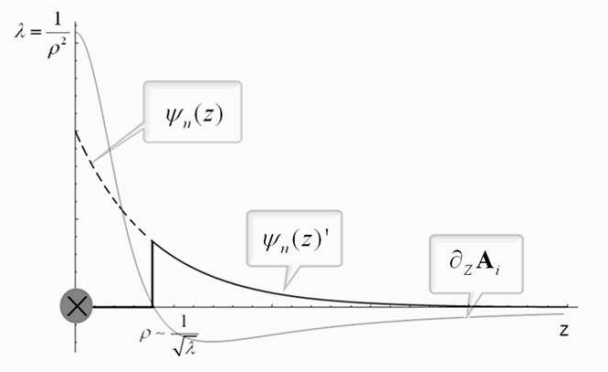

Figure 7.1: The Z-mode in the non-rigid gauge vs $\partial_Z \mathbb{A}_i$.

location of the instanton, i.e.

$$\int_{x=Z=0} d\hat{\xi} C\, G^B \mathbb{A}_M \ . \tag{7.35}$$

For Z and ρ the non-rigid constraints are more natural to implement since these modes are only soft near the origin at large λ. The vector fluctuations at the origin linearize through the modes

$$d^2\psi_n/dZ^2 = \lambda_n \psi_n \ , \tag{7.36}$$

with $\psi_n(Z) \sim e^{-\sqrt{\lambda_n} Z}$. In the spin-isospin 1 channel they are easily confused with $\partial_Z \mathbb{A}_i$ near the origin as we show in Fig.(7.1). Using the non-rigid constraint, the double counting is removed by removing the origin from the vector mode functions

$$\psi_n'(Z) = \theta(|Z| - Z_c)\psi_n(Z) \ , \tag{7.37}$$

with $Z_C \sim \rho \sim 1/\sqrt{\lambda}$ which becomes the origin for large λ. In the non-rigid semiclassical framework, the baryon at small $\xi < |Z_C|$ is described by an instanton located at the origin of R^4 and rattling in the vicinity of Z_C. At large $\xi > |Z_C|$, the rattling instanton sources the vector meson fields described by a semi-classical expansion with non-rigid Dirac constraints. Changes in Z_c (the core boundary) are reabsorbed by a residual gauge transformation on the core instanton. This is a holographic realization of the Cheshire cat principle [114]

where Z_c plays the role of the Cheshire cat smile.

For simplicity, and throughout the semiclassical expansion we will ignore the translational zero modes. Also for simplicity, the expansion will not rely on the Dirac constraint of the isorotations since to order $\hbar^0$ their contribution does not arise in the electromagnetic current. A similar observation was made in the Skyrme model where pion-baryon couplings are found to be leading and time-like [113, 115]. At order $\hbar$ and higher the Dirac constraints matter. The constraint on the Z-mode is implemented by Z_C throughout.

To order $\hbar^0$ the semiclassical expansion will be carried out covariantly in the action formalism, whereby Gauss law is unfolded for both $\widehat{\mathbb{A}}_0$ and $\mathbb{A}_0$ as detailed in Appendix A. To this order there is no difference between the canonical Hamiltonian formalism, with the advantage of manifest covariance for the derived flavor currents.

Having said this, we now use the gauge field decomposition presented in [29] for the non-rigid semiclassical expansion and refer to this work for further references. Specifically,

$$A_\mu = \mathbb{A}_\mu + C_\mu \ , \qquad C_\mu \equiv v_\mu^n \psi_{2n-1} + a_\mu^n \psi_{2n} + \mathcal{V}_\mu + \mathscr{A}_\mu \psi_0 \ , \tag{7.38}$$

$$A_Z = \mathbb{A}_Z + C_Z \ , \qquad C_Z \equiv -i\Pi\phi_0 \ , \tag{7.39}$$

$$\widehat{A}_\mu = \widehat{\mathbb{A}}_\mu + \widehat{C}_\mu \ , \qquad \widehat{C}_\mu \equiv \widehat{v}_\mu^n \psi_{2n-1} + \widehat{a}_\mu^n \psi_{2n} + \widehat{\mathcal{V}}_\mu + \widehat{\mathscr{A}}_\mu \psi_0 \ , \tag{7.40}$$

$$\widehat{A}_Z = \widehat{\mathbb{A}}_Z + \widehat{C}_Z \ , \qquad \widehat{C}_Z \equiv -i\widehat{\Pi}\phi_0 \ , \tag{7.41}$$

where $\{\mathbb{A}, \widehat{\mathbb{A}}\}$ refer to the instanton configuration and $\{C, \widehat{C}\}$ to the vector meson fluctuations. The $\mathbb{R}$ rotation is subsumed. $\{v^n, \widehat{v}^n\}$, $\{a^n, \widehat{a}^n\}$, and $\{\Pi, \widehat{\Pi}\}$ are the vector mesons, the axial vector mesons and the pions respectively. $\{\mathcal{V}, \widehat{\mathcal{V}}\}$ is the vector source and $\{\mathscr{A}, \widehat{\mathscr{A}}\}$ is the axial vector source. Theses meson and source fields are all functions of x^μ. They are attached to the mode functions $\{\psi, \phi\}$ in bulk which are functions of Z as expounded in [29]:

$$-K^{1/3}\partial_Z(K\partial_Z\psi_n) = m_{v^n}^2 \psi_n \ , \qquad \kappa \int dZ K^{-1/3} \psi_n \psi_m = \delta_{nm} \ , \tag{7.42}$$

$$\alpha_{v^n} \equiv \kappa \int dZ K^{-1/3} \psi_{2n-1} \ , \qquad \alpha_{a^n} \equiv \kappa \int dZ K^{-1/3} \psi_{2n} \psi_0 \ , \tag{7.43}$$

$$\psi_0 \equiv \frac{2}{\pi} \arctan Z \ , \qquad \phi_0 \equiv \frac{1}{\sqrt{\pi\kappa} K} \ . \tag{7.44}$$

With the gauge field (7.38)-(7.41) the $SU(2)$ YM action reads

$$
\begin{aligned}
S_{YM} &= -\frac{\kappa}{2}\int d^4x dZ \Big[\partial^Z\left(2K\widehat{\mathbb{F}}_{Z\mu}\widehat{C}^\mu\right) \\
&\quad +\frac{1}{2}K^{-1/3}\left(\partial_\mu\widehat{C}_\nu-\partial_\nu\widehat{C}_\mu\right)^2+K\left(\partial_Z\widehat{C}_\mu-\partial_\mu\widehat{C}_Z\right)^2\Big] \ , \qquad (7.45)\\
&\quad -\kappa\int d^4x dZ \mathrm{tr}\ \Big[\partial^Z\left(2K\mathbb{F}_{Z\nu}C^\nu\right) \\
&\quad +\frac{1}{2}K^{-1/3}\left\{2\mathbb{F}_{\mu\nu}[C^\mu,C^\nu]+\left(\mathbb{D}_\mu C_\nu-\mathbb{D}_\nu C_\mu-i[C_\mu,C_\nu]\right)^2\right\} \\
&\quad +K\left\{2\mathbb{F}_{Z\mu}[C^Z,C^\mu]+\left(\mathbb{D}_Z C_\mu-\mathbb{D}_\mu C_Z-i[C_Z,C_\mu]\right)^2\right\}\Big] \ , (7.46)
\end{aligned}
$$

where $\mathbb{D}_\alpha$ is the covariant derivative with the slowly rotating instanton in flavor space: $\mathbb{D}_\alpha * = \partial_\alpha - i[\mathbb{A}_\alpha, *]$. We dropped the leading and pure instanton part for convenience. Some details regarding the expansion including the CS part are briefly given in Appendix.

All the linear terms to $\{C, \widehat{C}\}$ except the *boundary terms* in the YM and CS action vanish due to the equations of motion. There is no coupling in bulk between the vector mesons and the instanton configuration except through boundary terms and/or time derivatives. This is the hallmark of solitons. While it apparently looks different from the effective and holographic description presented in [33, 34] as couplings are involved in bulk, we will show below that the results are indeed similar for the electromagnetic form factors to order $\hbar^0$. Below, we will explain why the similarity.

We note that without the instanton $\{\mathbb{A}, \widehat{\mathbb{A}}\}$, the action reduces to the one in [29], where the vector meson dominance (VMD) of the pion form factor follows from the field redefinitions

$$
v^n \to v^n_{\rm new} = v^n + \alpha_{v^n}\mathcal{V} + \frac{b_{v^n\pi\pi}}{2f_\pi^2}[\Pi, \mathrm{d}\Pi] \ , \qquad (7.47)
$$

$$
b_{v^n\pi\pi} \equiv \kappa\int dZ K^{-1/3}(1-\psi_0^2) \ , \qquad (7.48)
$$

with f_π the pion decay constant. This redefinition yields a direct vector-photon coupling $v^n - \mathcal{V}$

$$
m^2_{v^n}\left(v^n_{\rm new} - \alpha_{v^n}\mathcal{V}\right)^2 \ , \qquad (7.49)
$$

while removing all pion-photon couplings $\Pi - \mathcal{V}$ through various sum rules. Holographic QCD obeys the strictures of VMD in the meson sector. This point will carry semiclassically to the baryon sector as we detail below.

Substituting the 5D fields for the 4D fields with mode functions we have to order $\hbar^0$

$$
\begin{aligned}
&S_{\rm eff} = \\
&-\sum_{n=1}^{\infty}\int d^4x \Big[\Big[\kappa K\widehat{\mathbb{F}}^{Z\mu}\Big((\widehat{v}_\mu^n - \alpha_{v^n}\widehat{\mathcal{V}}_\mu)\psi_{2n-1} \\
&\qquad\qquad +(\widehat{a}_\mu^n - \alpha_{a^n}\widehat{\mathscr{A}}_\mu)\psi_{2n} + \widehat{\mathcal{V}}_\mu + \widehat{\mathscr{A}}_\mu\psi_0\Big)\Big]_{Z=B} \\
&\qquad\qquad +\frac{1}{4}\Big(\partial_\mu\widehat{v}_\nu^n - \partial_\nu\widehat{v}_\mu^n\Big)^2 + \frac{1}{2}m_{v^n}^2(\widehat{v}_\mu^n - \alpha_{v^n}\widehat{\mathcal{V}}_\mu)^2 \\
&\qquad\qquad +\frac{1}{4}\Big(\partial_\mu\widehat{a}_\nu^n - \partial_\nu\widehat{a}_\mu^n\Big)^2 + \frac{1}{2}m_{a^n}^2\Big(\widehat{a}_\mu^n - \alpha_{a^n}\widehat{\mathscr{A}}_\mu\Big)^2\Big] \quad ,(7.50) \\
&-\sum_{n=1}^{\infty}2\mathrm{tr}\int d^4x \Big[\Big[\kappa K\mathbb{F}^{Z\nu}\Big((v_\mu^n - \alpha_{v^n}\mathcal{V}_\mu)\psi_{2n-1} \\
&\qquad\qquad +(a_\mu^n - \alpha_{a^n}\mathscr{A}_\mu)\psi_{2n} + \mathcal{V}_\mu + \mathscr{A}_\mu\psi_0\Big)\Big]_{Z=B} \\
&\qquad\qquad +\frac{1}{4}\Big(\partial_\mu v_\nu^n - \partial_\nu v_\mu^n\Big)^2 + \frac{1}{2}m_{v^n}^2\Big(v_\mu^n - \alpha_{v^n}\mathcal{V}_\mu\Big)^2 \\
&\qquad\qquad +\frac{1}{4}\Big(\partial_\mu a_\nu^n - \partial_\nu a_\mu^n\Big)^2 + \frac{1}{2}m_{a^n}^2\Big(a_\mu^n - \alpha_{a^n}\mathscr{A}_\mu\Big)^2\Big] \quad , \quad (7.51)
\end{aligned}
$$

where all meson fields are the redefined fields, $v_{\rm new}^n$ and $a_{\rm new}^n$, but we drop the subscript for simplicity. $[\cdots]_{Z=B}$ will be evaluated at the boundary $Z = B$, which is collectively denoted by $\{\pm\infty, \pm Z_c\}$. We retained only the terms relevant to the baryon form factor. For the complete expansion of the meson fluctuation part we refer to [29].

Figure 7.2: Left: Direct coupling, Right: Vector meson mediated coupling(VMD)

7.4 Baryon current

Now, consider the effective action for the $U(1)_V$ source to order $\hbar^0$

$$S_{\rm eff}[\widehat{\mathcal{V}}_\mu] = \sum_{n=1}^{\infty} \int d^4x \left[-\frac{1}{4}\Big(\partial_\mu \widehat{v}^n_\nu - \partial_\nu \widehat{v}^n_\mu\Big)^2 - \frac{1}{2} m^2_{v^n} (\widehat{v}^n_\mu)^2 \right.$$
$$-\kappa K \widehat{\mathbb{F}}^{Z\mu} \widehat{\mathcal{V}}_\mu (1 - \alpha_{v^n} \psi_{2n-1})\Big|_{Z=B}$$
$$\left. + a_{v^n} m^2_{v^n} \widehat{v}^n_\mu \widehat{\mathcal{V}}^\mu - \kappa K \widehat{\mathbb{F}}^{Z\mu} \widehat{v}^n_\mu \psi_{2n-1}\Big|_{Z=B} \right] , \quad (7.52)$$

The first line is the free action of the massive vector meson which gives the meson propagator

$$\Delta^{mn}_{\mu\nu}(x) = \int \frac{d^4p}{(2\pi)^4} e^{-ipx} \left[\frac{-g_{\mu\nu} - p_\mu p_\nu / m^2_{v^n}}{p^2 + m^2_{v^n}} \delta^{mn} \right] , \quad (7.53)$$

in our convention. The rest are the coupling terms between the source and the instanton: the second line is the direct coupling (Fig.7.2(a)) and the last line corresponds to the coupling mediated by the $U(1)$ (omega, omega', ...) vector meson couplings (Fig.7.2(b)),

$$\kappa K \widehat{\mathbb{F}}^{Z\mu} \widehat{v}^n_\mu \psi_{2n-1} , \quad (7.54)$$

which is large and of order $1/\sqrt{\hbar}$ since $\psi_{2n-1} \sim \sqrt{\hbar}$. When ρ is set to $1/\sqrt{\lambda}$ after the book-keeping noted above, the coupling scales like $\lambda\sqrt{N_c}$, or $\sqrt{N_c}$ in the large N_c limit taken first [2].

[2]The reader may object that such strong couplings may upset the semiclassical expansion through perturbative corrections. This is not the case when the Dirac constraints are imposed properly as noted in [113] for the Skyrme model.

The direct coupling drops by the sum rule

$$\sum_{n=1}^{\infty} \alpha_{v^n} \psi_{2n-1} = 1 \ , \tag{7.55}$$

following from closure in curved space

$$\delta(Z - Z') = \sum_{n=1}^{\infty} \ \kappa \psi_{2n-1}(Z) \psi_{2n-1}(Z') K^{-1/3}(Z') \ . \tag{7.56}$$

in complete analogy with VMD for the pion [29].

The baryon current is entirely vector dominated to order $\hbar^0$ and reads

$$J^{\mu}_{B}(x) = -\sum_{n,m} \ m^2_{v^n} \alpha_{v^n} \psi_{2m-1} \int d^4y \ \kappa K \widehat{\mathbb{F}}_{Z\nu}(y, Z) \Delta^{\nu\mu}_{mn}(y - x) \Big|_{Z=B} \ . \tag{7.57}$$

This point is in agreement with the effective holographic approach described in [34]. The static baryon charge distribution is

$$J^{0}_{B}(\vec{x}) = -\sum_{n} \ \int d\vec{y} \ \ \frac{2}{N_c} \kappa K \widehat{\mathbb{F}}_{Z0}(\vec{y}, Z) \ \Delta_n(\vec{y} - \vec{x}) \ a_{v^n} m^2_{v^n} \psi_{2n-1} \ \Big|_{Z=B} \ , \tag{7.58}$$

with

$$\Delta_n(\vec{y} - \vec{x}) \equiv \int \frac{d\vec{p}}{(2\pi)^3} \frac{e^{-i\vec{p}\cdot(\vec{y}-\vec{x})}}{\vec{p}^2 + m^2_{v^n}} \ , \tag{7.59}$$

and the extra factor $2/N_c$ comes from the relation between $\widehat{\mathcal{V}}_{\mu}$ and the baryon number source $\widehat{B}_0(\vec{x})$: by $\widehat{\mathcal{V}}_{\mu} = \delta_{\mu 0} \frac{\sqrt{2N_f}}{N_c} \widehat{B}_0(\vec{x})$.

7.5 Electromagnetic Current and Form Factor

In addition to the baryon current discussed above, we now need the flavor or isospin current to construct the electromagnetic current. For that, consider the 4 dimensional effective action for the SU(2)-valued flavor source again to

order $\hbar^0$

$$S_{\rm eff}[\mathcal{V}^a_\mu] = \sum_{b=1}^{3}\sum_{n=1}^{\infty}\int d^4x\left[-\frac{1}{4}\Big(\partial_\mu v^{b,n}_\nu - \partial_\nu v^{b,n}_\mu\Big)^2 - \frac{1}{2}m^2_{v^n}(v^{b,n}_\mu)^2 + \alpha_{v^n}m^2_{v^n}v^{a,n}_\mu\mathcal{V}^{a,\mu} - \kappa K\mathbb{F}^{b,Z\mu}v^{b,n}_\mu\psi_{2n-1}\Big|_{Z=B}\right] , \quad (7.60)$$

where the direct coupling vanishes due to the sum rule (7.96) and only the VMD part contributes through the $SU(2)$ (rho, rho', ...) meson couplings

$$\kappa K\mathbb{F}^{b,Z\mu}v^{b,n}_\mu\psi_{2n-1} , \quad (7.61)$$

which is large and of order $1/\sqrt{\hbar}$. Again, this coupling is of order $\sqrt{N_c}\lambda^{3/2}$ after the book-keeping. This contribution is similar to (7.52) apart from the $SU(2)$ labels.

The isospin current is,

$$J^\mu_{I,a}(x) = -\sum_{n,m}m^2_{v^n}\alpha_{v^n}\psi_{2n-1}\int d^4y\ \ \kappa K\mathbb{F}^a_{Z\nu}(y,Z)\Delta^{\nu\mu}_{mn}(y-x)\Big|_{Z=B} , \quad (7.62)$$

From (7.57) and (7.99) the electromagnetic current is given by

$$\begin{aligned} J^\mu_{\rm EM}(x) &= J^\mu_{I,3}(x) + \frac{1}{2}J^\mu_B(x) \\ &= -\sum_{n,m}m^2_{v^n}\alpha_{v^n}\psi_{2m-1}\int d^4y\ \ \mathcal{Q}_\nu(y,Z)\Delta^{\nu\mu}_{mn}(y-x)\Big|_{Z=B} , \end{aligned} \quad (7.63)$$

with

$$\mathcal{Q}_\mu(x,Z) \equiv \kappa K\mathbb{F}^3{}_{Z\mu}(x,Z) + \frac{1}{N_c}\kappa K\widehat{\mathbb{F}}_{Z\mu}(x,Z) . \quad (7.64)$$

The electromagnetic charge density is

$$\begin{aligned} J^0_{\rm EM}(x) &= -\sum_n\int d^4y\ \mathcal{Q}_0(y,Z)\int\frac{d^4p}{(2\pi)^4}e^{-ip\cdot(y-x)}\frac{m^2_{v^n}}{p^2+m^2_{v^n}}\alpha_{v^n}\psi_{2n-1}\Big|_{Z=B} \\ &\quad +\sum_n\int d^4y\ \mathcal{Q}_\mu(y,Z)\int\frac{d^4p}{(2\pi)^4}e^{-ip\cdot(y-x)}\frac{p^\mu p^0}{p^2+m^2_{v^n}}\alpha_{v^n}\psi_{2n-1}\Big|_{Z=B} , \end{aligned} \quad (7.65)$$

and the static electromagnetic form factor follows readily in the form

$$\begin{aligned} J^0_{\rm EM}(\vec{q}) &= \int d\vec{x} e^{i\vec{q}\cdot\vec{x}} J^0_{\rm EM}(x) \\ &= -\sum_n \int dZ \partial_Z \left[\left(\int d\vec{x} e^{i\vec{q}\cdot\vec{x}} \mathcal{Q}_0(x,Z) \right) \psi_{2n-1} \right] \frac{\alpha_{v^n} m^2_{v^n}}{\vec{q}^{\,2} + m^2_{v^n}} \ , \end{aligned} \tag{7.66}$$

after setting $p^0 = 0$ in (7.65) so that $\mathcal{Q}_i$ is irrelevant. Recall that the instanton configuration we are using is adiabatically rotating in flavor space. In the charge $\mathcal{Q}$, these rotations generate a velocity dependence to leading order in $\hbar$ which is proportional to the angular momentum upon semiclassical quantization. With this in mind, there is effectively no time-dependence left in the density $\mathcal{Q}_\mu(x,Z)$ to leading order in $\hbar$.

We now note that the electromagnetic form factor (7.66) can be rewritten as

$$J^0_{\rm EM}(\vec{q}) = \sum_n \left(g^n_{V,min} + g^n_{V,mag} \right) \frac{\alpha_{v^n} m^2_{v^n}}{\vec{q}^{\,2} + m^2_{v^n}} \ , \tag{7.67}$$

with

$$\begin{aligned} g^n_{V,min} &= \int dZ \partial_Z \left[\left(\int d\vec{x} e^{i\vec{q}\cdot\vec{x}} \mathcal{Q}_0(x,Z) \right) \right] \psi_{2n-1} \ , \\ g^n_{V,mag} &= \int dZ \left(\int d\vec{x} e^{i\vec{q}\cdot\vec{x}} \mathcal{Q}_0(x,Z) \right) \partial_Z \psi_{2n-1} \ , \end{aligned}$$

which are the analogue of the minimal and magnetic coupling used in the effective baryon description of [34]. The solitonic character of the solution implies that the two contributions are *tied* and sum up to a purely surface term in the Z-direction a point that is not enforced in the effective approach [34]. Also our results are organized in $\hbar$ starting from the original D4 instanton.

7.6 Electromagnetic Charge and Charge Radius

The nucleon electromagnetic form factor is written as a boundary term

$$\begin{aligned} J^0_{\rm EM}(\vec{q}) &= \int d\vec{x} e^{i\vec{q}\cdot\vec{x}} J^0_{\rm EM}(\vec{x}) \\ &= \int d\vec{x} e^{i\vec{q}\cdot\vec{x}} \sum_n \frac{\alpha_{v^n} m_{v^n}^2}{\vec{q}^{\,2} + m_{v^n}^2} \, \psi_{2n-1}(Z_C) 2\mathcal{Q}_0(\vec{x}, Z_C) \ , \end{aligned} \tag{7.68}$$

where the boundary term at $Z = \infty$ vanishes since $\psi_{2n-1} \sim 1/Z$ for large Z. In the limit $q \to 0$ we pick the electromagnetic charge

$$\int d\vec{x} \, e^{i\vec{q}\cdot\vec{x}} \, 2\mathcal{Q}_0(\vec{x}, Z_C) \ , \tag{7.69}$$

due to the sum rule (7.96). Since Z_c will be set to zero ultimatly at large λ, the limits $\lim_{q\to 0} \lim_{Z\to 0}$ will be understood sequentially. To proceed, we need to work out the surface densities $\mathcal{Q}_0$ i.e. the $U(1)$ and $SU(2)$ parts $K\widehat{\mathbb{F}}_{Z0}(\vec{x}, Z_c)$ and $K\mathbb{F}_{Z0}(\vec{x}, Z_c)$ respectively. By the equations of motion (7.14) and (7.11), they read

$$\begin{aligned} \frac{4}{N_c}\kappa K\widehat{\mathbb{F}}_{Z0}(Z_c) &= \int_{-Z_C}^{Z_C} dZ \frac{1}{32\pi^2} \epsilon_{MNPQ} \left(\mathrm{tr}\,(\mathbb{F}_{MN}\mathbb{F}_{PQ}) + \frac{1}{2}\widehat{\mathbb{F}}_{MN}\widehat{\mathbb{F}}_{PQ} \right) \\ &\quad + \frac{2}{N_c} \int_{-Z_C}^{Z_C} dZ \kappa K^{-1/3} \partial^i \widehat{\mathbb{F}}_{0i} \ , \\ 2\kappa K\mathbb{F}^a{}_{Z0}(Z_c) &= \int_{-Z_C}^{Z_C} dZ \ 2i\kappa \ \mathrm{tr}\left\{ K^{-1/3} \left([\mathbb{F}_{0i}, \mathbb{A}_i] + K[\mathbb{F}_{0Z}, \mathbb{A}_Z] \right) t^a \right\} \\ &\quad + \int_{-Z_C}^{Z_C} dZ \kappa K^{-1/3} \partial^i \mathbb{F}^a_{0i} + \int_{-Z_C}^{Z_C} dZ \frac{N_c}{64\pi^2} \epsilon_{MNPQ} (\widehat{\mathbb{F}}_{MN}\mathbb{F}^a_{PQ}) \ . \end{aligned} \tag{7.70}$$

The $U(1)$ number density readily integrates to 1 since

$$\begin{aligned} B &= \int d\vec{x} J^0_B(\vec{x}) = \int d\vec{x} \frac{4}{N_c} \kappa K \widehat{\mathbb{F}}_{Z0}(Z_c) \\ &= \int d\vec{x} \int_{-Z_C}^{Z_C} dZ \frac{1}{32\pi^2} \epsilon_{MNPQ} \mathrm{tr}\,(\mathbb{F}_{MN}\mathbb{F}_{PQ}) = 1 \ , \end{aligned} \tag{7.71}$$

as the spatial flux vanishes on R^3_X and the $U(1)$ winding number arezero for a

sufficiently localized SU(2) instanton in $R^3_X \times R_Z$. We note that the integrand is manifestly gauge invariant. To contrast, the isovector charge is

$$\begin{aligned} I^A &= \int d\vec{x} 2\kappa K \mathbb{F}^A{}_{Z0}(Z_c) \\ &= \int d\vec{x} \int_{-Z_C}^{Z_C} dZ \; 2i\kappa \; \mathrm{tr} \left\{ K^{-1/3} \left([\mathbb{F}_{0i}, \mathbb{A}_i] + K[\mathbb{F}_{0Z}, \mathbb{A}_Z] \right) t^A \right\} \; , \end{aligned} \tag{7.72}$$

again after dropping the surface term in R^3_X and the Chern-Simons contribution for a sufficiently localized instanton in $|Z_C|$. Although the integrand in (7.72) is not manifestly gauge invariant, it is only sensitive to a rigid gauge transformation at Z_C which is reabsorbed by gauge rotating the cloud as is explicit from the mode decomposition.

As noted earlier, the D4 instanton has maximal spherical symmetry so that its isospin I^A is just minus its angular momentum J^A,

$$\begin{aligned} J^A &= \int d\vec{x} dZ J^{0A} = \int d\vec{x} dZ \epsilon_{Ajk} x^j T^{0k} \\ &= \int d\vec{x} dZ \epsilon_{Ajk} x^j \left[-\kappa K^{-1/3} \mathbb{F}^{l0,a} \mathbb{F}^{lk,a} - \kappa K \mathbb{F}^{Z0,a} \mathbb{F}^{Zk,a} \right] \; . \end{aligned} \tag{7.73}$$

Both I^A and J^A are driven by the adiabatic rotation $\mathbb{R}$. For the D4 instanton part, it is

$$\mathbb{A}^a_R = \mathbb{R}^{ab}(t) \mathbb{A}^b \; , \qquad \dot{\mathbb{A}}^a_R = \left(\dot{\mathbb{R}}(t) \mathbb{R}^{-1}(t) \right)^{ab} \mathbb{A}^b_R \; , \tag{7.74}$$

with $\omega^A G^A \equiv -\dot{\mathbb{R}}\mathbb{R}^{-1}$ [3]. The ω's are quantum and of order $\hbar$. Recalling the result for $\mathbb{A}^R_0$ for the constrained field and the zero mode ($\mathbb{Z}^R$) from Appendix, we obtain to leading order

$$\begin{aligned} J^A = -I^A &= \int d\vec{x} dZ \epsilon_{Ajk} x^j \left[-\kappa K^{-1/3} \mathbb{F}^{l0,a} \mathbb{F}^{lk,a} - \kappa K \mathbb{F}^{Z0,a} \mathbb{F}^{Zk,a} \right] \\ &= \int d\vec{x} \int_{-Z_c}^{Z_c} dZ \epsilon_{Ajk} x^j \left[-\kappa (\mathbb{D}^M \mathbb{Z}^R)^a \mathbb{F}^{Mk,a} \right] \\ &\to -\frac{1}{2} M_0 \rho^2 \, \omega^A \equiv -\mathbb{I} \, \omega^A \; . \end{aligned} \tag{7.75}$$

[3] We recall that both the BPST instanton and the fluctuations are rotating in the body fixed frame. As noted earlier, the R-labeling of the fields is subsumed.

The last relation follows from the BPST instanton (7.28). As expected, the core instanton has a moment of inertia $\mathbb{I} = M_0\rho^2/2$ where $M_0 = 8\pi^2\kappa$ is the D4 instanton mass in units of M_{KK} and to leading order in $1/\lambda$. $\mathbb{I}$ is of order N_c. Maximum spherical symmetry results in a symmetric inertia tensor.

Finally, the nucleon charge is then

$$\int d\vec{x} J^0_{\rm EM}(x) = \int d\vec{x} 2\mathcal{Q}_0(x, Z_c) = I_3 + \frac{B}{2} \ . \tag{7.76}$$

While our analysis is to order $\hbar^0$ this normalization should hold to all orders in $\hbar$. The vector meson cloud encodes the exact charges in holography thanks to the exact sum rule (7.96).

The electromagnetic charge radius $\langle r^2\rangle_{EM}$ can be read from the q^2 terms of the form factor

$$\langle r^2\rangle_{EM} = \int d\vec{x}\ r^2\, 2\mathcal{Q}_0(\vec{x}, Z_c) + 6\sum_{n=1}^{\infty} \frac{\alpha_{v^n}\psi_{2n-1}(Z_c)}{m_n^2} \int d\vec{x}\ 2\mathcal{Q}_0(\vec{x}, Z_c) \ , \tag{7.77}$$

with $r \equiv \sqrt{(\vec{x})^2}$. The first contribution is from the core, while the second contribution is from the cloud. For a sufficiently localized instanton in bulk the first contribution is of order $1/\lambda$,

$$\begin{aligned} \langle r^2\rangle'_{I=0} &= \int d\vec{x}\ r^2\, 2\mathcal{Q}_0(\vec{x}, Z_c) \\ &= \frac{3}{2}\rho^2 \frac{Z_c}{\sqrt{Z_c^2+\rho^2}} \to \frac{3}{2}\rho^2 \, . \end{aligned} \tag{7.78}$$

The meson cloud contribution is of order λ^0. It can be exactly asessed by noting that

$$\begin{aligned} \sum_{n=1}^{\infty} \frac{\alpha_{v^n}\psi_{2n-1}(Z_c)}{m_n^2} &= \int dZ \sum_{n=1}^{\infty} \frac{\psi_{2n-1}(Z_c)\psi_{2n-1}(Z)K^{-1/3}(Z)}{m_n^2} \\ &= \int dZ \langle Z_c|\Box_{\mathbf{C}}^{-1}|Z\rangle \ , \end{aligned} \tag{7.79}$$

where $\Box_{\mathbf{C}}^{-1} \equiv -\partial_Z^{-1}K^{-1}\partial_Z^{-1}K^{-1/3}$ is the inverse of (7.42). This is just the

vector meson propagator in curved space [4]. It follows that

$$\sum_{n=1}^{\infty} \frac{\alpha_{v^n} \psi_{2n-1}(Z_c)}{m_n^2} = -\int dZ \int dZ' \langle Z_c | \partial_Z^{-1} | Z' \rangle K^{-1}(Z') \langle Z' | \partial_Z^{-1} | Z \rangle K^{-1/3}(Z) \ , \quad (7.80)$$

where $\langle Z' | \partial_Z^{-1} | Z \rangle = \frac{1}{2} \mathrm{sgn}(Z' - Z)$ and $K = 1 + Z^2$. It is zero for $Z_c = \infty$ and 2.377 for $Z_c = \tilde{Z}_c / \sqrt{\lambda}$ in the double limit $\lambda \to \infty$ followed by $\tilde{Z} \to \infty$. See Appendix for details.

Thus the charge radius for the nucleon is

$$\sqrt{\langle r^2 \rangle_{EM}} \approx 14.26 \left(\frac{1}{2} + I_3 \right) M_{\rm KK}^{-2} \approx 0.784 \left(\frac{1}{2} + I_3 \right) \mathrm{fm}, \quad (7.81)$$

where we used $M_{\rm KK} = 950$MeV [28]. The experimental values are [116]

$$\sqrt{\langle r^2 \rangle_{EM}^{\rm proton}} = 0.875 \text{ fm} \ , \qquad \langle r^2 \rangle_{EM}^{\rm neutron} = -0.1161 \text{ fm}^2 \ . \quad (7.82)$$

7.7 Baryon Magnetic moment

The magnetic moments follow from the moments of the electromagnetic current,

$$\begin{aligned} \mu^i &= \frac{1}{2} \epsilon_{ijk} \int d\vec{x} x^j J^k_{\rm EM}(x) \\ &= \epsilon_{ijk} \int d\vec{y} \sum_n m_{v^n}^2 \alpha_{v^n} \psi_{2n-1}(Z_c) \mathcal{Q}_m(\vec{y}, Z_c) \int d\vec{x} x^j \Delta_n^{mk}(\vec{y} - \vec{x}) \\ &= \epsilon_{ijk} \int d\vec{y} \sum_n m_{v^n}^2 \alpha_{v^n} \psi_{2n-1}(Z_c) \mathcal{Q}_m(\vec{y}, Z_c) y^j \frac{-g^{mk}}{m_{v^n}^2} \\ &= -\epsilon_{ijk} \int d\vec{y} y^j \mathcal{Q}^k(\vec{y}, Z_c) \ , \end{aligned} \quad (7.83)$$

with

$$\mathcal{Q}_k(\vec{x}, Z_c) \equiv \kappa K(Z_c) \mathbb{F}^3{}_{Zk}(\vec{x}, Z_c) + \frac{1}{N_c} \kappa K(Z_c) \widehat{\mathbb{F}}_{Zk}(\vec{x}, Z_c) \ . \quad (7.84)$$

[4] The vector-meson coupling to the instanton in the propagator is subleading in $1/\lambda$ and thus dropped.

While the electromagnetic current is meson mediated at the core boundary, its contribution to the magnetic moment to order $\hbar^0$ is core-like owing to the exact sum-rule (7.97) in warped space. By resumming over the tower of infinite vector mesons, the magnetic moment shrunk to the core at strong coupling with g^2 large and N_c large. This remarkable feature is absent in the Skyrme model and its variants since they all truncate the number of mesons.

First consider the iso-scalar contribution to the magnetic moment in (7.84). As we are assessing $\mathcal{Q}_k(x, Z_c)$ at the core boundary, the small Z instanton configuration is sufficient. From (7.15) it follows that

$$\begin{aligned}\frac{1}{N_c}\kappa\widehat{\mathbb{F}}^R_{Zk}(\vec{x}, Z_c) &= \int_{-Z_c}^{Z_c} dZ \left[\frac{1}{32\pi^2}\epsilon_{kNPQ}\Big(\mathrm{tr}\,(\mathbb{F}^R_{N0}\mathbb{F}^R_{PQ})\right] \\ &= \int_{-Z_c}^{Z_c} dZ \left[\frac{1}{32\pi^2}\epsilon_{kNPQ}\Big(\mathrm{tr}\,(\mathbb{D}_n\mathbb{Z}^R\mathbb{F}_{PQ})\right], \end{aligned} \tag{7.85}$$

where we have dropped the U(1) CS contribution as it is subleading as well as surface contributions on R^3_X since we will integrate over R^3_X at the end. The upper R-labels refer to the rigid SO(3) rotation $\mathbb{R}$ and $\mathbb{Z}^R$ is the zero mode from the Gauss constraint. In the second line the R-label drops because of tracing. Thus

$$\begin{aligned}\mu^A_{I=0} &= -\epsilon_{Ajk}\int d\vec{y}y^j\frac{2}{N_c}\kappa K(Z_c)\widehat{\mathbb{F}}^R_{Zk}(\vec{x}, Z_c) \\ &= -\frac{\rho^2\omega^A}{4}\frac{Z_c}{\sqrt{Z_c^2+\rho^2}} \to -\frac{\rho^2\omega^A}{4} \\ &= \frac{\langle r^2\rangle'_{I=0}}{6}\frac{J^A}{\mathbb{I}}\,, \end{aligned} \tag{7.86}$$

where we used the BPST solution (7.28) since $Z_c \sim \rho \sim 0$. The contribution is of order $\hbar$ but subleading in $1/\lambda$. The last relation uses that $I^A = -J^A$. This relation for the isoscalar magnetic moment is similar to the one derived in the Skyrme model with the notable difference that only the isoscalar core radius and core moment of inertia are involved.

Now, consider the iso-vector contribution to the magnetic moment. Using

(7.12), we have

$$\begin{aligned}\kappa\mathbb{F}^{R,3}_{Zk}(\vec{x},Z_c) &= \int_{-Z_c}^{Z_c} dZ i\kappa \mathrm{tr}\,\{[\mathbb{A}^{R,M},\mathbb{F}^{R}_{Mk}]t^3\}\\ &\to -\int_{-Z_c}^{Z_c} dZ\frac{\kappa}{4}\mathbb{A}^a_M\mathbb{F}^b_{Mk}\epsilon_{abc}\mathbb{R}_{3c}\ . \end{aligned} \tag{7.87}$$

Much like the iso-scalar, we have only retained the leading contribution to the magnetic moment. As noted earlier, the residual gauge variance of the integrand through Z_C is removed by gauge rotation of the cloud. In terms of the regular BPST solution (7.26) and (7.28) we get

$$\mathbb{A}^a_M\mathbb{F}^b_{Mk}\epsilon_{abc} = \frac{-8\rho^2}{(\xi^2+\rho^2)^3}(x_a\epsilon_{akc}-x_b\epsilon_{kbc})\ , \tag{7.88}$$

so that

$$\begin{aligned}\mu^i_{I=1} &= -\epsilon_{ijk}\int d\vec{y}y^j\kappa K(Z_c)\mathbb{F}^{R,3}{}_{Zk}(x,Z_c)\\ &= -\frac{32\pi}{3}\kappa\rho^2\mathbb{R}_{3i}\int_0^\infty dr\int_{-Z_c}^{Z_c}dZ\frac{r^4}{(\xi^2+\rho^2)^3}\\ &= -4\pi^2\kappa\rho^2\mathbb{R}_{3i}\log_c\\ &= -\frac{\mathbb{I}}{2}\mathbb{R}^{3i}\log_c\,, \end{aligned} \tag{7.89}$$

with a logarithmic cutoff sensitivity to the core size,

$$\log_c \equiv \log\left(\frac{Z_c+\sqrt{Z_c^2+\rho^2}}{-Z_c+\sqrt{Z_c^2+\rho^2}}\right)\ . \tag{7.90}$$

The isovector magnetic contribution is of order $\hbar^0$ and similar in structure to the Skyrmion, with the exception that $\mathbb{I}$ is solely driven by the core. The cutoff sensitivity $\log_c$ is absent if we were to use the BPST instanton in the singular gauge. The Cheshire Cat smile survives in the isovector magnetic contribution in the regular gauge (albeit weakly through a logarithm).

Combining the isoscalar and isovector contributions to the magnetic moment yields (singular gauge)

$$\mu^i = \frac{\langle r^2\rangle'_{I=0}}{6}\frac{J^i}{\mathbb{I}} - \frac{\mathbb{I}}{2}\mathbb{R}^{3i}\ , \tag{7.91}$$

which results in the Skyrme-like independent relation [117],

$$\frac{\mu_p - \mu_n}{\mu_p + \mu_n} = \frac{3}{4}\frac{M_\Delta + M_N}{M_\Delta - M_N} \ , \tag{7.92}$$

expected from a soliton. Here $M_{N,\Delta}$ are the nucleon and delta masses split by the inertia $\mathbb{I}$.

7.8 Axial Form Factor

The effective action for the SU(2)-valued axial vectors to order $\hbar^0$ is

$$\begin{aligned} S_{\rm eff}[\mathscr{A}^a_\mu] = \sum_{b=1}^{3}\sum_{n=1}^{\infty}\int d^4x \Bigg[& -\frac{1}{4}\Big(\partial_\mu a^{b,n}_\nu - \partial_\nu a^{b,n}_\mu\Big)^2 - \frac{1}{2}m^2_{a^n}(a^{b,n}_\mu)^2 \\ & -\kappa K \mathbb{F}^{b,z\mu}\mathscr{A}^b_\mu(\psi_0 - \alpha_{a^n}\psi_{2n})\Big|_{z=B} \\ & + a_{a^n} m^2_{a^n} a^{b,n}_\mu \mathscr{A}^{b,\mu} - \kappa K \mathbb{F}^{b,z\mu} a^{b,n}_\mu \psi_{2n}\Big|_{z=B}\Bigg] \ , \end{aligned} \tag{7.93}$$

The first line is the free action of the massive axial vector meson which gives the meson propagator

$$\Delta^{mn,ab}_{\mu\nu}(x) = \int \frac{d^4p}{(2\pi)^4} e^{-ipx}\left[\frac{-g_{\mu\nu} - p_\mu p_\nu/m^2_{a^n}}{p^2 + m^2_{a^n}}\delta^{mn}\delta^{ab}\right] \ , \tag{7.94}$$

in Lorentz gauge. The rest are the coupling terms between the source and the instanton: the second line is the direct coupling and the last line corresponds to the coupling mediated by the $SU(2)$ (a, a', ...) vector meson couplings,

$$\kappa K \mathbb{F}^{b,z\mu} a^{b,n}_\mu \psi_{2n} \ , \tag{7.95}$$

which is large and of order $1/\sqrt{\hbar}$ since $\psi_{2n} \sim \sqrt{\hbar}$. When ρ is set to $1/\sqrt{\lambda}$ after the book-keeping noted above, the coupling scales like $\lambda\sqrt{N_c}$, or $\sqrt{N_c}$ in the large N_c limit taken first

The direct coupling drops by the sum rule

$$\sum_{n=1}^{\infty}\alpha_{a^n}\psi_{2n} = \psi_0 \ = \frac{2}{\pi}\arctan z, \tag{7.96}$$

following from closure in curved space

$$\delta(z-z') = \sum_{n=1}^{\infty} \kappa\psi_n(z)\psi_n(z')K^{-1/3}(z') \ . \tag{7.97}$$

in complete analogy with VMD for the pion [28] and the electromagnetic baryon form factor. It follows form (7.96) that

$$\sum_{n=1}^{\infty} \alpha_{a^n}\psi_{2n}(z_c) = \frac{1}{2}\int_{-z_c}^{z_c} dz\partial_z\psi_0(z) = \frac{\kappa}{\pi}\int_{-z_c}^{z_c} dz\phi_0(z) \ . \tag{7.98}$$

The axial vector contributions at the core sum up to the axial zero mode.

The iso-axial current is,

$$J^{\mu}_{A,b}(x) = -\sum_{n,m} m^2_{a^n} a_{a^n}\psi_{2n}\int d^4y \ \ \mathcal{Q}^b_{\nu}(y,z)\Delta^{\nu\mu}_{mn}(y-x)\Big|_{z=B} \ , \tag{7.99}$$

with

$$\mathcal{Q}^b_{\nu}(y,z) \equiv \kappa K\mathbb{F}^b{}_{z\nu}(y,z) \ . \tag{7.100}$$

The static axial-iso-vector form factor follows readily in the form

$$\begin{aligned} J^{bi}_A(\vec{q}) &= \int d\vec{x}e^{i\vec{q}\cdot\vec{x}}J^{bi}_A(x) \\ &= (\delta^{ij}-\hat{q}^i\hat{q}^j)\int d\vec{x}e^{i\vec{q}\cdot\vec{x}}\sum_n \frac{\alpha_{a^n}m^2_{a^n}}{\vec{q}^{\ 2}+m^2_{a^n}}\psi_{2n}(z)\,\mathcal{Q}^b_j(\vec{x},z)\Big|_{z=B} \ , \end{aligned} \tag{7.101}$$

and is explicitly transverse for massless pions. The zero momentum limit of the transverse momentum projector is ambiguous owing to the divergence of the spatial integrand for $\vec{q}=\vec{0}$. We use the rotationally symmetric limit with the convention $(\delta^{ij}-\hat{q}^i\hat{q}^j)\to 2\delta^{ij}/3$. Thus

$$J^{bi}_A(0) = \frac{2}{3}\int d\vec{x}\,\kappa K\mathbb{F}^b{}_{zi}(\vec{x},z)\psi_0(z)\Big|_{z=B} \ , \tag{7.102}$$

by the sum rule (7.98). Since the rotated instanton yields

$$\int d\vec{x}\,\mathbb{F}^{R,a}_{zi} = R^{ai}\frac{4\pi^2\rho^2}{\sqrt{z_c^2+\rho^2}} \ , \tag{7.103}$$

the spatial component of the axial-vector reads

$$J_A^{Rbi}(0) = \frac{32\kappa\pi\rho^2}{3}(1+z_c^2)\frac{\arctan(z_c)}{\sqrt{\rho^2+z_c^2}}\,R^{bi}\ , \tag{7.104}$$

In the nucleon state

$$\begin{aligned}\langle s't'|J_A^{Rbi}(0)|st\rangle &= \frac{32\kappa\pi\rho^2(1+z_c^2)}{9\sqrt{\rho^2+z_c^2}}\arctan(z_c)(\sigma^b)^{ss'}(\tau^i)^{tt'} \\ &\equiv \frac{1}{3}g_A(\sigma^b)^{ss'}(\tau^i)^{tt'}\ ,\end{aligned} \tag{7.105}$$

where we used $\langle s't'|R^{bi}|st\rangle = -\frac{1}{3}(\sigma^b)^{ss'}(\tau^i)^{tt'}$. Thus

$$g_A = \frac{32\kappa\pi\rho^2(1+z_c^2)}{3\sqrt{\rho^2+z_c^2}}\arctan(z_c) \approx \frac{32}{3}\kappa\pi\rho^2\ , \tag{7.106}$$

where the limit $\rho \to 0$ is followed by $z_c \to 0$. It is 2 times $\widehat{g}_A = \frac{16}{3}\kappa\pi\rho^2$ as quoted in [32]. This discrepancy maybe traced back to a factor of 2 discrepancy in the normalization of the axial-vector current in [32].

7.9 Conclusions

We have shown how the non-rigid quantization of the D4 instanton in holographic QCD yields baryon electromagnetic form factors that obey the strictures of VMD in agreement with the effective approach discussed in [33, 34]. The holographic baryon at the boundary is composed by a core instanton in the holographic direction at $Z = 0$ of size $1/\sqrt{\lambda}$ that is trailed by a cloud of bulk vector mesons and pions of size λ^0 all the way to $Z = \infty$. The core and the cloud interface at Z_C which plays the role of the Cheshire Cat smile (gauge movable). At strong coupling, the baryon size is of order λ^0 thanks to vector meson dominance. The meson-baryon couplings are large and of order $1/\sqrt{\hbar}$ (or lower) and surface-like only owing to the solitonic nature of the instanton.

The electromagnetic form factors, radii and magnetic moments of the ensuing baryons compare favorably with the results obtained in the Skyrme model, as well as data for a conservative value of $M_{KK} = 950$ MeV. For instance the electromagnetic charge radii are 0.784 fm (proton) and zero (neutron). They

are derived in the triple limit of zero pion mass (chiral limit) and strong coupling λ (large g^2 and large N_c). The magnetic moments are completly driven by the core D4 instanton through a remarkable sum rule of the vector meson cloud. They obey a model independent relation of the type encountered in the Skyrme model, a hall-mark of large N_c and strongly coupled models.

The non-rigid quantization scheme presented here offers a systematic framework for discussing quantum baryons in the context of the semi-classical approximation. It is causal with retardation effects occuring in higher order in $\hbar$. These semiclassical corrections are only part of a slew of other quantum corrections in holography which are in contrast hard to quantify. Also, the small instanton size calls for the use of the full DBI action to characterize the instanton field more faithfully in the holographic core. We note that beyond the $\hbar^0$ contribution discussed here, the issue of Dirac constraints needs to be addressed. This is best addressed in the canonical Hamiltonian formalism whereby Gauss laws are explicitly removed by their constaint equations. The drawback are lack of manifest covariance and operator orderings.

The extension of our analysis to the axial-vector channels is straightforward with minimal changes in our formulae as can be readily seen by inspection. Indeed, the axial vector source differs from the vector one we used by the extra mode function $\psi_0(Z)$ which is odd in Z. Also the pion field Π now contributes. In the axial-vector channel the pion-baryon coupling is expected to be formally of order $\sqrt{\hbar}$ but *time-like* thus effectively of order $1/\sqrt{N_c}$ and not $\sqrt{N_c}$. The Goldberger-Treiman relation in this case follows from the non-rigid quantization of the instanton much like its counterpart for the Skyrmion [113]. Some of these issues and others will be discussed next.

7.10 Appendix

7.10.1 Gauss Law

For the flavor rotated instanton, the rotated form of Gauss law (7.11) reads

$$\mathbb{D}_M^R \mathbb{F}_{M0}^R = \mathcal{O}\left(1/\lambda\right) \ , \tag{7.107}$$

to leading order as the curvature effects are subleading in $1/\lambda$. All upper R-labels refer to the rigid SO(3) rotation $\mathbb{R}$ with $\mathbb{D}^R_M = \partial_M + \mathbb{A}^{R,A} G^A$. While this is subsumed throughout in the main text, here it is recalled explicitly for the clarity of the argument. The formal solution reads

$$\mathbb{A}^R_0 = \frac{1}{(\mathbb{D}^{R'})^2}\, \mathbb{D}^R_N \dot{\mathbb{A}}^R_N + \mathbb{Z}^R \ , \tag{7.108}$$

where the primed inverted operator excludes the zero mode. Following [30], the rotated zero mode solution reads

$$\mathbb{Z}^{R,A} = C\, \mathbb{R}\overline{\mathbb{R}}(g)\omega^A\, f(\xi) \ , \tag{7.109}$$

up to an arbitrary constant C. Here $f(\xi) = \xi^2/(\xi^2+\rho^2)$ and

$$\overline{\mathbb{R}}^{AB}(g) = \mathrm{tr}\, \left(t^A g^{-1} t^B g\right) \ , \qquad\qquad g = \frac{z - i\vec{x}\cdot\vec{\sigma}}{\xi} \ . \tag{7.110}$$

We note that for an unrotated BPST instanton with $\omega^A = 0$, the formal solution (7.108) yields $\mathbb{A}_0 = 0$ as it should. The normalization is $C = 1$ which is fixed by the asymptotic of the $\mathbb{A}^R_0$ field: $\mathbb{A}^R_0(x, Z=\infty) = U^{R\dagger}\partial_0 U^R$. $U = e^{i\tau_a \hat{r}^a(\theta,\phi,\psi)}$ is the identity map and (θ,ϕ,ψ) are the canonical angles on S^3.

In terms of (7.108) the rotated electric field is

$$\mathbb{F}^R_{M0} = \mathbb{D}^R_M \mathbb{A}^R_0 - \dot{\mathbb{A}}^R_M = \mathbb{D}^R_M \mathbb{Z}^R \ . \tag{7.111}$$

The kinetic energy for the rotated instanton is

$$H = \kappa \int d\vec{x}\, dZ\, \mathrm{tr}\, (\mathbb{F}^R_{M0})^2 = \kappa \int d\vec{x}\, dZ\, \mathrm{tr}\, \left(\mathbb{D}_M \mathbb{Z}^R\right)^2 = \frac{1}{2} M_0 \rho^2 \omega^2 \ . \tag{7.112}$$

The upper R-label drops out by tracing. Here $M_0 = 8\pi^2\kappa$ is the instanton mass in units of M_{KK} to leading order in $1/\lambda$.

7.10.2 Action

With the gauge field (7.38)-(7.41) the $SU(2)$ YM action reads

$$
\begin{aligned}
S_{YM}^{SU(2)} = -\kappa \int d^4xdZ \mathrm{tr} \Big[& \frac{1}{2} K^{-1/3} \mathbb{F}_{\mu\nu}^2 + K \mathbb{F}_{Z\mu}^2 \\
& + \partial^\mu \left(2K^{-1/3} \mathbb{F}_{\mu\nu} C^\nu \right) + \partial^Z \left(2K \mathbb{F}_{Z\nu} C^\nu \right) + \partial^\mu \left(2K \mathbb{F}_{\mu Z} C^Z \right) \\
& - \left\{ \mathbb{D}^\mu \left(2K^{-1/3} \mathbb{F}_{\mu\nu} \right) + \mathbb{D}^Z \left(2K \mathbb{F}_{\mathbb{Z}\nu} \right) \right\} C^\nu - \mathbb{D}^\mu \left(2K \mathbb{F}_{\mu\mathbb{Z}} \right) C^Z \\
& + \frac{1}{2} K^{-1/3} \left\{ 2\mathbb{F}_{\mu\nu} [C^\mu, C^\nu] + \left(\mathbb{D}_\mu C_\nu - \mathbb{D}_\nu C_\mu - i[C_\mu, C_\nu] \right)^2 \right\} \\
& + K \left\{ 2\mathbb{F}_{Z\mu} [C^Z, C^\mu] + \left(\mathbb{D}_Z C_\mu - \mathbb{D}_\mu C_Z - i[C_Z, C_\mu] \right)^2 \right\} \Big] \quad ,(7.113)
\end{aligned}
$$

where $\mathbb{D}_\alpha$ is the covariant derivative with the soliton configuration: $\mathbb{D}_\alpha * = \partial_\alpha - i[\mathbb{A}_\alpha, *]$. Similary U(1) YM action is

$$
\begin{aligned}
S_{YM}^{U(1)} = -\frac{\kappa}{2} \int d^4xdZ \Big[& \frac{1}{2} K^{-1/3} \widehat{\mathbb{F}}_{\mu\nu}^2 + K \widehat{\mathbb{F}}_{Z\mu}^2 \\
& + \partial^\mu \left(2K^{-1/3} \widehat{\mathbb{F}}_{\mu\nu} \widehat{C}^\nu \right) + \partial^Z \left(2K \widehat{\mathbb{F}}_{Z\nu} \widehat{C}^\nu \right) + \partial^\mu \left(2K \widehat{\mathbb{F}}_{\mu Z} \widehat{C}^Z \right) \\
& - \left\{ \partial^\mu \left(2K^{-1/3} \widehat{\mathbb{F}}_{\mu\nu} \right) + \partial^Z \left(2K \widehat{\mathbb{F}}_{Z\nu} \right) \right\} \widehat{C}^\nu - \partial^\mu \left(2K \widehat{\mathbb{F}}_{\mu Z} \right) \widehat{C}^Z \\
& + \frac{1}{2} K^{-1/3} \left(\partial_\mu \widehat{C}_\nu - \partial_\nu \widehat{C}_\mu \right)^2 + K \left(\partial_Z \widehat{C}_\mu - \partial_\mu \widehat{C}_Z \right)^2 \Big] \quad , \quad (7.114)
\end{aligned}
$$

and the CS term is

$$
\begin{aligned}
S_{CS} \quad = \quad & \frac{N_c}{24\pi^2} \epsilon_{MNPQ} \int d^4xdZ \\
& \Big[\frac{3}{8} \left(\widehat{\mathbb{A}}_0 + \widehat{C}_0 \right) \mathrm{tr} \left\{ \mathbb{F}_{MN} \mathbb{F}_{PQ} + 4\mathbb{F}_{MN} \mathbb{D}_P C_Q + 4\mathbb{F}_{MN} C_P C_Q) \right. \\
& \qquad \left. + 4(\mathbb{D}_M C_N + C_M C_N)(\mathbb{D}_P C_Q + C_P C_Q) \right\} \\
& - \frac{3}{2} \left(\widehat{\mathbb{A}}_M + \widehat{C}_M \right) \mathrm{tr} \left\{ \partial_0 (\mathbb{A}_N + C_M)(\mathbb{F}_{PQ} + 2\mathbb{D}_P C_Q + 2C_P C_Q) \right\} \\
& + \frac{3}{4} \left(\widehat{\mathbb{F}}_{MN} + 2\partial_M \widehat{C}_N \right) \mathrm{tr} \left\{ (\mathbb{A}_0 + C_0)(\mathbb{F}_{PQ} + 2\mathbb{D}_P C_Q + 2C_P C_Q) \right\} \\
& + \frac{1}{16} \left(\widehat{\mathbb{A}}_0 + \widehat{C}_0 \right) \left\{ \widehat{\mathbb{F}}_{MN} \widehat{\mathbb{F}}_{PQ} + 4\widehat{\mathbb{F}}_{MN} \partial_P \widehat{C}_Q + 4(\partial_M \widehat{C}_N)(\partial_P \widehat{C}_Q) \right\}
\end{aligned}
$$

$$
\begin{aligned}
&-\frac{1}{4}\Big(\widehat{A}_M+\widehat{C}_M\Big)\Big\{\widehat{\mathbb{F}}_{0N}\widehat{\mathbb{F}}_{PQ}+2\widehat{F}_{0N}\partial_P\widehat{C}_Q+\widehat{F}_{PQ}(\partial_0\widehat{C}_N-\partial_N\widehat{C}_0)\\
&\qquad\qquad +2(\partial_0\widehat{C}_N-\partial_N\widehat{C}_0)\partial_P\widehat{C}_Q\Big\}\\
&+\frac{3}{2}\partial_N\left[\Big(\widehat{\mathbb{A}}_M+\widehat{C}_M\Big)\mathrm{tr}\left\{(\mathbb{A}_0+C_0)(\mathbb{F}_{PQ}+2\mathbb{D}_PC_Q+2C_PC_Q)\right\}\right]\\
&+\frac{N_c}{48\pi^2}\int \mathrm{d}\left[\Big(\widehat{\mathbb{A}}+\widehat{C}\Big)\ \mathrm{tr}\left\{2\mathrm{d}(\mathbb{A}+C)(\mathbb{A}+C)-\frac{3i}{2}(\mathbb{A}+C)^3\right\}\right]\ .
\end{aligned}
\tag{7.115}
$$

7.10.3 Integral

In this appendix we work out the integral in (7.80):

$$
G(Z_c)\equiv-\int dZ\int dZ'\langle Z_c|\partial_Z^{-1}|Z'\rangle K^{-1}(Z')\langle Z'|\partial_Z^{-1}|Z\rangle K^{-1/3}(Z)\ . \tag{7.116}
$$

We start with the Green function

$$
\langle Z'|\partial_Z^{-1}|Z\rangle=\frac{1}{2}\mathrm{sgn}(Z'-Z)\ . \tag{7.117}
$$

Since there are two sgn functions in (7.116) we divide the integral region into six pieces reflecting all possible sign difference:

$$
\begin{aligned}
G(Z_c) \ = \ & -\frac{1}{4}\left[\int_{-\infty}^{Z_c}dZ'\int_{-\infty}^{Z'}dZ-\int_{-\infty}^{Z_c}dZ'\int_{Z'}^{Z_c}dZ\right.\\
&-\int_{Z_c}^{\infty}dZ'\int_{Z_c}^{Z'}dZ+\int_{Z_c}^{\infty}dZ'\int_{Z'}^{\infty}dZ\\
&\left.-\int_{Z_c}^{\infty}dZ'\int_{-\infty}^{Z_c}dZ-\int_{-\infty}^{Z_c}dZ'\int_{Z_c}^{\infty}dZ\right](K^{-1}(Z')K^{-1/3}(Z))\ .
\end{aligned}
$$

In two extreme(symmetric) case the expression becomes simple. For $Z_c=\infty$

$$
-\frac{1}{4}\left[\int_{-\infty}^{\infty}dZ'\int_{-\infty}^{Z'}dZ-\int_{-\infty}^{\infty}dZ'\int_{Z'}^{\infty}dZ\right](K^{-1}(Z')K^{-1/3}(Z))=0\ ,
$$

and for $Z_c = 0$

$$
\begin{aligned}
&-\frac{1}{2}\left[\int_{-\infty}^{0} dZ' \int_{-\infty}^{Z'} dZ - \int_{-\infty}^{0} dZ' \int_{Z'}^{0} dZ \right. \\
&\qquad\qquad \left. - \int_{0}^{\infty} dZ' \int_{-\infty}^{0} dZ \right] (K^{-1}(Z')K^{-1/3}(Z)) \\
&= \int_{0}^{\infty} dZ' K^{-1}(Z') \int_{0}^{Z'} dZ K^{-1/3}(Z) \sim 2.377 \ .
\end{aligned}
$$

Chapter 8

Nuclear Force

8.1 Introduction

In the past the Skyrmion-Skyrmion interaction was mostly analyzed using the product ansatz [118, 119] or some variational techniques [120]. While the product ansatz reveals a pionic tail in the spin and tensor channels, it lacks the intermediate range attraction in the scalar channel expected from two-pion exchange. In fact the scalar potential to order N_c is found to be mostly repulsive, and therefore unsuited for binding nuclear matter at large N_c. The core part of the Skyrmion-Skyrmion interaction in the product of two Skyrmions is ansatz dependent. In [121] it was shown that the ansatz dependence could be eliminated in the two-pion range by adding the pion cloud to the core Skyrmions. In a double expansion using large N_c and the pion-range, a scalar attraction was shown to develop in the two-pion range in the scalar channel [121]. The expansion gets quickly involved while addressing shorter ranges or core interactions.

In this paper we analyze the two-baryon problem using the D4 two-instanton solution [123, 124] to order N_c/λ. The ensuing Skyrmion-Skyrmion[1] interac-

[1]In hQCD D4 static instantons in bulk source the chiral solitons or Skyrmions on the boundary. The instantons have a size of order $1/\sqrt{\lambda}$ and a mass of order $N_c\lambda$ in units of M_{KK}, the Kaluza-Klein scale [30]. The static Skyrmion is just the instanton holonomy in the z-direction

$$\mathbb{U}(\vec{x}) = Pe^{-i\int_{-\infty}^{\infty} dz \mathbb{A}_z(\vec{x},z)} \ , \tag{8.1}$$

where $\mathbb{A}_z$ is the 5-dimensional ADHM instanton. The static 3-dimensional Skyrmion is sourced by a static 4-dimensinal flavour instanton embedded in D8-$\overline{\text{D8}}$.

tion is essentially that of the two cores and the meson cloud composed of (massles) pions and vector mesons. At strong coupling, holography fixes the core interactions in a way that the Skyrme model does not. Although in QCD very short ranged interactions are controlled by asymptotic freedom, the core interactions at intermediate distances maybe still in the realm of strong coupling and therefore unamenable to QCD perturbation theory. In this sense, holography will be helpful. Also, in holographic QCD the mesonic cloud including pions and vectors is naturally added to the core Skyrmions in the framework of semiclassics. These issues will be quantitatively addressed in this paper.

In section 2, we review the ADHM construction for one and two-instanton following on recent work in [123, 124]. In section 3, we show how this construction translates to the one and two baryon configuration in holography. In section 4, we construct the bare or core Skyrmion-Skyrmion interaction for defensive and combed Skyrmions. We unwind the core Skyrmion-Skyrmion interaction at large separations in terms of a dominant Coulomb repulsion in regular gauge. Core issues related to the singular gauge are also discussed. In section 5, we project the core Skyrmion-Skyrmion contributions onto the core nucleon-nucleon contributions at large separation using semiclassics in the adiabatic approximation. In section 6, we include the effects of the mesonic cloud to order N_c/λ in the Born-Oppenheimer approximation. At large separations, the cloud contributions yield a tower of meson exchanges. In section 7, we summarize the general structure of the NN potential as a core plus cloud contribution in holographic QCD. Our conclusions are in section 8. In Appendix 9.1, we check our semiclassical cloud calculations in the regular gauge, using the strong coupling source theory in the singular gauge. In Appendix 9.2 we detail the $k = 1, 2$ instantons in the singular gauge and we revisit the core interaction in the singular gauge.

8.2 YM Instantons from ADHM

The starting point for baryons in holographic QCD are instantons in flat $R^3_X \times R_Z$. In this section we briefly review the ADHM construction [125] for SU(2) Yang-Mills instantons. Below SU(2) will be viewed as a flavor group associated

to D8-$\overline{\text{D8}}$ branes. For a thorough presentation of the ADHM construction we refer to [126] and references therein.

In the ADHM construction, all the instanton information is encoded in the matrix-data whose elements are quaternions q. The latters are represented as

$$q \equiv q_M \sigma^M \ , \qquad \sigma^M \equiv (i\tau^i, \mathbb{1}) \ , \tag{8.2}$$

with $M = 1, 2, 3, 4$, $\mathbb{1} \equiv 1_{2\times 2}$, and τ^i the standard Pauli matrices. q_M are four real numbers. The conjugate ($q^\dagger$) and the modulus ($\|q\|$) of the quaternion, are defined as

$$q^\dagger \equiv q_M (\sigma^M)^\dagger \ , \quad \|q\|^2 \equiv q^\dagger q = q q^\dagger = |\, q|\, \mathbb{1} = \sum_M q_M^2 \mathbb{1} \ , \tag{8.3}$$

$$\mathrm{Re}\, q \equiv \frac{q + q^\dagger}{2} = q_0 \sigma^0 \ , \quad \mathrm{Im}\, q \equiv \frac{q - q^\dagger}{2} = \sum_i q_i \sigma^i \ , \tag{8.4}$$

where $|\, q|$ is the determinant of a matrix q. For clarity, our label conventions are: $M, N, P, Q \in \{1, 2, 3, 4\}$, $\mu, \nu, \rho, \sigma, \in \{0, 1, 2, 3\}$, and $i, j, k, l \in \{1, 2, 3\}$ with $z \equiv x_4$. The flavor $SU(2)$ group indices are $a, b \in \{1, 2, 3\}$.

The basic block in the matrix-data is the $(1 + k) \times k$ matrix, Δ, for the charge k instanton

$$\Delta = \mathbb{A} + \mathbb{B} \otimes x \ , \tag{8.5}$$

where $\mathbb{A}$ and $\mathbb{B}$ are x-independent $(1 + k) \times k$ quaternionic matrices with information on the moduli parameters. We define $x = x_M \sigma^M$ and $\mathbb{B} \otimes x$ means that each element $\mathbb{B}$ is multiplied by x. $\mathbb{A}$ and $\mathbb{B}$ are not arbitrary. They follow from the ADHM constraint

$$\Delta^\dagger \Delta = f^{-1} \otimes \mathbb{1} \ , \tag{8.6}$$

where $\Delta^\dagger$ is the transpose of the quaternionic conjugate of Δ. f is a $k \times k$ invertible quaternionic matrix. $f^{-1} \otimes \mathbb{1}$ means each element f^{-1} is multiplied by $\mathbb{1}$. The null-space of $\Delta^\dagger$ is 2-dimensional since it has 2 fewer rows than columns. The basis vectors for this null-space can be assembled into an $(1 + k) \times 1$

quaternionic matrix U

$$\Delta^\dagger U = 0 \ , \tag{8.7}$$

where U is normalized as

$$U^\dagger U = \mathbb{1} \ . \tag{8.8}$$

The instanton gauge field A_μ is constructed as

$$A_M = iU^\dagger \partial_M U \ , \tag{8.9}$$

which yields the field strengths

$$F_{MN} = -2\eta_{aMN} U^\dagger \mathbb{B}(f \otimes \tau^a)\mathbb{B}^\dagger U \ . \tag{8.10}$$

Self-duality is explicit from 't Hooft's self-dual eta symbol

$$\eta_{aMN} = -\eta_{aNM} = \begin{cases} \epsilon_{aMN} & \text{for } M, N = 1, 2, 3 \\ \delta_{aM} & \text{for } N = 4 \end{cases} \ . \tag{8.11}$$

The action density, $\mathrm{tr}\, F_{MN}^2$, can be calculated directly from f, without recourse to the null-space U and F_{MN} [130]

$$\mathrm{tr}\, F_{MN}^2 = \Box^2 \log |f| \ , \tag{8.12}$$

where $\Box \equiv \partial_M^2$, $\Box^2 = \partial_N^2 \partial_M^2$, and $|f|$ is the determinant of f.

8.2.1 $k = 1$ instanton

The $k = 1$ instanton in the regular gauge is encoded in a quaternionic matrix Δ

$$\Delta \equiv \begin{pmatrix} \lambda \\ -x + X \end{pmatrix} \ , \qquad \Delta^\dagger \equiv \begin{pmatrix} \lambda^\dagger & (-x + X)^\dagger \end{pmatrix} \ , \tag{8.13}$$

which yields

$$f^{-1} = \rho^2 + (x_M - X_M)^2 \ , \tag{8.14}$$

after using (8.6). Here ρ ($=\sqrt{\lambda_M^2}$) is the size and $\{X_M\}$ is the position of the one instanton. The field strength is

$$F_{MN} = W\eta_{aMN}\frac{\tau^a}{2}\frac{-4\rho^2}{((x_M - X_M)^2 + \rho^2)^2}W^\dagger \ , \tag{8.15}$$

which follows from (8.10) with

$$U = \frac{\rho}{\sqrt{(x_M - X_M)^2} + \rho^2}\begin{pmatrix} -\frac{\lambda(x-X)^\dagger}{\rho^2} \\ \mathbb{1} \end{pmatrix} W^\dagger \ , \qquad B = \begin{pmatrix} 0 \\ -\mathbb{1} \end{pmatrix} \ , \tag{8.16}$$

where $\rho^2 \equiv \lambda^\dagger\lambda$ and $W \in SU(2)$. The action density follows from (8.15) or (8.12)

$$\mathrm{tr}\, F_{MN}^2 = \Box^2 \log f \ = \frac{96\rho^4}{((x_M - X_M)^2 + \rho^2)^4}, \tag{8.17}$$

which gives the instanton number $\frac{1}{16\pi^2}\int d^4x \mathrm{tr}\, F_{MN}^2 = 1$ by self duality. The $k = 1$ instanton in the singular gauge is detailed in Appendix A.

8.2.2 $k = 2$ instanton

A charge 2 ($k = 2$) instanton in the regular gauge is encoded in a quaternionic matrix Δ [**?**]

$$\Delta \equiv \begin{pmatrix} \lambda_1 & \lambda_2 \\ -\big[x - (X + D)\big] & u \\ u & -\big[x - (X - D)\big] \end{pmatrix} \ , \tag{8.18}$$

where the coordinates x_M are defined as $x = x_M\sigma^M$, and the moduli parameters are encoded in the free parameters $\lambda_1, \lambda_2, X, D$: $|\lambda_i| \equiv \rho_i\mathbb{1}$ are the size parameters, $\lambda_1^\dagger\lambda_2/(\rho_1\rho_2) \in SU(2)$ is the relative gauge orientation, and $X \pm D$ is the location of the constituents. u is not a free parameter and will be determined in terms of other moduli parameters by the ADHM constraint

(8.6).

Since we are interested in the relative separation we set $X = 0$, so that

$$\Delta = \begin{pmatrix} \lambda_1 & \lambda_2 \\ D-x & u \\ u & -D-x \end{pmatrix} , \qquad \Delta^\dagger \equiv \begin{pmatrix} \lambda_1^\dagger & (D-x)^\dagger & u^\dagger \\ \lambda_2^\dagger & u^\dagger & (-D-x)^\dagger \end{pmatrix} , \tag{8.19}$$

which yields

$$\begin{aligned} &\Delta^\dagger\Delta \\ &= \begin{pmatrix} \|\lambda_1\|^2 + \|x-D\|^2 + \|u\|^2 & \lambda_1^\dagger\lambda_2 + D^\dagger u - u^\dagger D - (x^\dagger u + u^\dagger x) \\ \left[\lambda_1^\dagger\lambda_2 + D^\dagger u - u^\dagger D - (x^\dagger u + u^\dagger x)\right]^\dagger & \|\lambda_2\|^2 + \|x+D\|^2 + \|u\|^2 \end{pmatrix} . \end{aligned} \tag{8.20}$$

The ADHM constraint (8.6) implies that each entry must be proportional to $\mathbb{1}$. The diagonal terms satisfy the constraint. The off-diagonal entries are also proportional to $\mathbb{1}$ provided that u is chosen to be

$$u = \frac{D\Lambda}{2\,|D|^2} + \gamma D , \qquad \Lambda \equiv \mathrm{Im}(\lambda_2^\dagger\lambda_1) = \frac{1}{2}(\lambda_2^\dagger\lambda_1 - \lambda_1^\dagger\lambda_2) , \tag{8.21}$$

with γ an arbitrary real constant. The coordinate u is the inverse of the coordinate D. It plays the role of the dual distance. Throughout we follow [**?**] and choose $\gamma = 0$ for a *physical identification of the moduli parameters*. By that we mean a $k = 2$ configuration which is the closest to the superposition of two instantons in the regular gauge at large separation. In Appendix A, we briefly discuss a minimal $k = 2$ configuration in the singular gauge.

Inserting u into (8.20) yields

$$f^{-1} = \begin{pmatrix} \rho_1^2 + (x_M - D_M)^2 + \frac{\rho_1^2\rho_2^2 - (\lambda_1\cdot\lambda_2)^2}{4D_M^2} & \lambda_1\cdot\lambda_2 + 2x\cdot u \\ \lambda_1\cdot\lambda_2 + 2x\cdot u & \rho_2^2 + (x_M + D_M)^2 + \frac{\rho_1^2\rho_2^2 - (\lambda_1\cdot\lambda_2)^2}{4D_M^2} \end{pmatrix} ,$$

where we introduced the notation $q \cdot p$ for two quaternions q and p

$$q \cdot p \equiv \sum_M q_M p_M . \tag{8.22}$$

$\rho_i = \sqrt{\lambda_i \cdot \lambda_i}$ are the size parameters, $\pm D_M$ the relative positions of the in-

stantons, and

$$2x\cdot u=\frac{1}{D\cdot D}\left[(\lambda_2\cdot D)(\lambda_1\cdot x)-(\lambda_1\cdot D)(\lambda_2\cdot x)-\epsilon^{MNPQ}(\lambda_2)_M(\lambda_1)_N D_P x_Q\right]\ .$$

We made use of the identity

$$\begin{aligned}&\sigma^P\bar\sigma^{MN}=\delta^{PM}\sigma^N-\delta^{PN}\sigma^M-\epsilon^{PMNQ}\sigma^Q\ ,\\&\bar\sigma^{MN}\equiv\frac{1}{2}(\bar\sigma^M\sigma^N-\bar\sigma^N\sigma^M)\ ,\quad \epsilon^{1234}=1\ .\end{aligned}\tag{8.23}$$

8.2.3 Explicit Parametrization

Without loss of generality, we may choose the moduli parameters to be

$$\lambda_1=\rho_1\,(0,0,0,1)\ ,\quad \lambda_2=\rho_2\left(\widehat{\theta}_a\sin|\,\theta|\,,\cos|\,\theta|\right)\ ,\quad D=\left(\frac{d}{2},0,0,0\right)\ ,\tag{8.24}$$

with $a=1,2,3$, $|\,\theta|\equiv\sqrt{(\theta_1)^2+(\theta_2)^2+(\theta_3)^2}$ and $\widehat{\theta}_a\equiv\frac{\theta_a}{|\,\theta|}$. The spatial x^1 axis is chosen as the separation axis of two instantons at large distance d. The flavor orientation angles (θ_a) are relative to the λ_1 orientation. We assign an $SU(2)$ matrix U to the relative angle orientations in flavor space

$$U\equiv\frac{\lambda_1^\dagger\lambda_2}{\rho_1\rho_2}=e^{i\theta_a\tau^a}\in SU(2)\ ,\tag{8.25}$$

which is associated with the orthogonal $SO(3)$ rotation matrix R as

$$\begin{aligned}R_{ab}&=\frac{1}{2}\mathrm{tr}\,\left(\tau_aU\tau_bU^\dagger\right)\\&=\delta_{ab}\cos 2|\,\theta|+2\widehat{\theta}_a\widehat{\theta}_b\sin^2|\,\theta|+\epsilon_{abc}\widehat{\theta}_c\sin 2|\,\theta|\ .\end{aligned}\tag{8.26}$$

For instance R_{ab} reads

$$\begin{pmatrix}\cos 2\theta_3 & \sin 2\theta_3 & 0\\ -\sin 2\theta_3 & \cos 2\theta_3 & 0\\ 0 & 0 & 1\end{pmatrix}\ ,\qquad \begin{pmatrix}1 & 0 & 0\\ 0 & \cos 2\theta_1 & \sin 2\theta_1\\ 0 & -\sin 2\theta_1 & \cos 2\theta_1\end{pmatrix}\ ,\tag{8.27}$$

for $\theta_1=\theta_2=0$ and $\theta_2=\theta_3=0$ respectively. Note the double covering in going from SU(2) to SO(3).

In this coordination for the moduli space,

$$\Lambda = \rho_1 \mathrm{Im}(\lambda_2^\dagger) = \rho_1\rho_2(-i\widehat{\theta}_a\tau^a \sin|\,\theta|) \ , \tag{8.28}$$

$$u = \frac{D\Lambda}{2\,|D|^2} = \frac{i\tau^1\Lambda}{d} = \frac{\rho_1\rho_2}{d}\sin|\,\theta|\,\widehat{\theta}_a\tau^1\tau^a \ , \tag{8.29}$$

$$u_M = \frac{\rho_1\rho_2}{d}\sin|\,\theta|\left(0, -\widehat{\theta}_3, \widehat{\theta}_2, \widehat{\theta}_1\right) \ , \tag{8.30}$$

$$x\cdot u = \frac{\rho_1\rho_2\sin|\,\theta|}{d}\left(\widehat{\theta}_1 x_4 + \widehat{\theta}_2 x_3 - \widehat{\theta}_3 x_2\right) \ , \tag{8.31}$$

and the inverse potential f^{-1} is written as

$$f^{-1} = \begin{pmatrix} g_- + A & B \\ B & g_+ + A \end{pmatrix} \ , \tag{8.32}$$

$$g_\pm \equiv x_\alpha^2 + \left(x_1 \pm \frac{d}{2}\right)^2 + \rho^2 \ , \quad x_\alpha^2 \equiv x_2^2 + x_3^2 + x_4^2 \ ,$$

$$A \equiv \frac{\rho^4 \sin^2|\,\theta|}{d^2} \ , \quad B \equiv \rho^2\left(\cos|\,\theta| + \frac{2}{d}\sin|\,\theta|\left[\widehat{\theta}_1 z + \widehat{\theta}_2 x_3 - \widehat{\theta}_3 x_2\right]\right) \ ,$$

with $\rho \equiv \rho_1 = \rho_2$. The action density can be assessed using (8.12). In terms of this notation, for the $k = 1$ instanton in the regular gauge (8.14), the logarithmic potential $\log|f|$ is

$$\log f_\pm = -\log g_\pm \ , \tag{8.33}$$

where the subscript $\pm$ refers to the position $\mp\frac{d}{2}$ of the instanton along the x_1 axis. For the $k = 2$ instanton (8.32), we have

$$\log|f_{-+}| \ \equiv \ -\log\left[(g_- + A)\,(g_+ + A) - B^2\right] \ . \tag{8.34}$$

8.2.4 Asymptotics

To understand in details the structure of the $k = 2$ instanton it is best to work out its asymptotic form for the case $d/\rho \gg 1$. For that we use (8.10) in the special case

$$F_{iz} = -2U^\dagger \mathbb{B}(f\otimes\tau^i)\mathbb{B}^\dagger U \ , \tag{8.35}$$

with

$$\mathbb{B} = \begin{pmatrix} 0 & 0 \\ -\mathbb{1} & 0 \\ 0 & -\mathbb{1} \end{pmatrix} . \tag{8.36}$$

Below, we will show that the field strength F_{iz} sources the pion-nucleon coupling in the axial gauge $A_z = 0$ for the quantum fluctuations. The asymptotics is useful for a physical identification of the coset parameters.

Near the singularity center with $x = D$, (8.19) approximates to

$$\Delta^\dagger \approx \begin{pmatrix} \lambda_1^\dagger & 0 & u^\dagger \\ \lambda_2^\dagger & u^\dagger & -2D^\dagger \end{pmatrix} , \tag{8.37}$$

whose null vector U is

$$U \approx \begin{pmatrix} -\frac{1}{\rho_1} u^\dagger \\ \frac{1}{|u|^2}\frac{1}{\rho_1} u \left(\lambda_2^\dagger u^\dagger + 2\rho_1 D^\dagger\right) \\ \mathbb{1} \end{pmatrix} D\Lambda^\dagger D^\dagger. \tag{8.38}$$

From (8.8) and (8.21) it follows that

$$U \approx \begin{pmatrix} 0 \\ \mathbb{1} - \left(\frac{\rho}{d}\right)^2 \frac{1}{2} \sin 2|\theta|\, \widehat{\theta}_a (i\tau^1\tau^a\tau^1) \\ \left(\frac{\rho}{d}\right)^2 \sin|\theta|\, \widehat{\theta}_a (i\tau^1\tau^a\tau^1) \end{pmatrix} + \begin{pmatrix} \mathcal{O}\left(\frac{\rho}{d}\right)^3 \\ \mathcal{O}\left(\frac{\rho}{d}\right)^4 \\ \mathcal{O}\left(\frac{\rho}{d}\right)^4 \end{pmatrix} . \tag{8.39}$$

We have used the explicit parametrization (8.24) and (8.28). We may expand f near the center $X = D$,

$$f|_{X\approx D} = \begin{pmatrix} \frac{1}{g_+} + \mathcal{O}\left(\frac{1}{d}\right)^4 & -\frac{\lambda_1\lambda_2 + 2x\cdot u}{g_- g_+} + \mathcal{O}\left(\frac{1}{d}\right)^4 \\ -\frac{\lambda_1\lambda_2 + 2x\cdot u}{g_- g_+} + \mathcal{O}\left(\frac{1}{d}\right)^4 & \frac{1}{g_-} + \mathcal{O}\left(\frac{1}{d}\right)^2 \end{pmatrix} . \tag{8.40}$$

For $X = D$, the leading contributions to f_{11}, f_{12}, and f_{21} are of order $1/d^2$ while that of f_{22} is of order d^0.

From (8.36) and (8.39) we have

$$U^\dagger B|_{X\approx D} = \left(-\mathbb{1} + \mathcal{O}\left(\frac{\rho}{d}\right)^2, \mathcal{O}\left(\frac{\rho}{d}\right)^2\right) \equiv \left(\mathfrak{b}_1^\dagger, \mathfrak{b}_2^\dagger\right) , \tag{8.41}$$

which yields (8.35)

$$\begin{aligned} F_{iz}|_{X\approx D} &= -2U^\dagger B(f\otimes\tau^i)B^\dagger U|_{X\approx D} \\ &= -2\left(f_{11}\mathfrak{b}_1^\dagger\tau^i\mathfrak{b}_1+f_{12}\mathfrak{b}_1^\dagger\tau^i\mathfrak{b}_2+f_{21}\mathfrak{b}_2^\dagger\tau^i\mathfrak{b}_1+f_{22}\mathfrak{b}_2^\dagger\tau^i\mathfrak{b}_2\right) \\ &= -2\frac{\tau^i}{g_+}+\mathcal{O}(d^{-4})\ . \end{aligned} \tag{8.42}$$

Thus

$$F^a_{iz}|_{X\approx D}\approx -2\delta^{ia}\frac{1}{g_+} \tag{8.43}$$

A rerun of the argument for the center $x=-D$ yields

$$F^a_{iz}|_{X\approx -D}\approx -2R^{ia}\frac{\tau^i}{g_-}\ , \tag{8.44}$$

since $U^\dagger\sim(0,0,\mathbb{1})$. For asymptotic distances $d/\rho\gg 1$ the $k=2$ configuration splits into two independent $k=1$ configurations with relative flavor orientation R^{ab}. This separation makes explicit the physical interpretation of the coset parameters: ρ the instanton size, d the instanton relative separation, u the inverse or dual separation and R their relative orientations asymptotically.

8.3 Baryons in hQCD

Baryons in hQCD are sourced by instantons in bulk. The induced action by pertinent brane embeddings and its instanton content was discussed in [**?**]. The 5D *effective* Yang-Mills action is the leading terms in the $1/\lambda$ expansion of the DBI action of the D8 branes after integrating out the S^4. The 5D Chern-Simons action is obtained from the Chern-Simons action of the D8 branes by integrating F_4 RR flux over the S^4, which is nothing but N_C. The action reads [28, 30]

$$S=S_{YM}+S_{CS}\ , \tag{8.45}$$

$$S_{YM}=-\kappa\int d^4xdz\ \mathrm{tr}\left[\frac{1}{2}K^{-1/3}\mathcal{F}^2_{\mu\nu}+M^2_{\mathrm{KK}}K\mathcal{F}^2_{\mu z}\right]\ , \tag{8.46}$$

$$S_{CS}=\frac{N_c}{24\pi^2}\int_{M^4\times R}\omega_5^{U(N_f)}(\mathcal{A})\ , \tag{8.47}$$

where $\mu, \nu = 0, 1, 2, 3$ are 4D indices and the fifth(internal) coordinate z is dimensionless. There are three things which are inherited by the holographic dual gravity theory: $M_{\rm KK}, \kappa$, and K. $M_{\rm KK}$ is the Kaluza-Klein scale and we will set $M_{\rm KK} = 1$ as our unit. κ and K are defined as

$$\kappa = \lambda N_c \frac{1}{216\pi^3} \equiv \lambda N_c a \ , \qquad K = 1 + z^2 \ . \tag{8.48}$$

$\mathcal{A}$ is the 5D $U(N_f)$ 1-form gauge field and $\mathcal{F}_{\mu\nu}$ and $\mathcal{F}_{\mu z}$ are the components of the 2-form field strength $\mathcal{F} = \mathrm{d}\mathcal{A} - i\mathcal{A} \wedge \mathcal{A}$. $\omega_5^{U(N_f)}(\mathcal{A})$ is the Chern-Simons 5-form for the $U(N_f)$ gauge field

$$\omega_5^{U(N_f)}(\mathcal{A}) = \mathrm{tr} \left(\mathcal{A}\mathcal{F}^2 + \frac{i}{2}\mathcal{A}^3\mathcal{F} - \frac{1}{10}\mathcal{A}^5 \right) \ , \tag{8.49}$$

The exact instanton solutions in warped x^M space are not known. Some generic properties of these solutions can be inferred from large λ whatever the curvature. Indeed, since $\kappa \sim \lambda$, the instanton solution with unit topological charge that solves the full equations of motion, follows from the YM part only in leading order. It has zero size at infinite λ. At finite λ the instanton size is of order $1/\sqrt{\lambda}$. The reason is that while the CS contribution of order λ^0 is repulsive and wants the instanton to inflate, the warping in the z-direction of order λ^0 is attractive and wants the instanton to deflate in the z-direction [30, 34].

These observations suggest to use the flat space instanton configurations to leading order in $N_c\lambda$, with $1/\lambda$ corrections sought in perturbation theory. The latter is best achieved by rescaling the coordinates and the instanton fields as

$$\begin{aligned} x^M &= \lambda^{-1/2}\widetilde{x}^M \ , \quad x^0 = \widetilde{x}^0 \ , \\ \mathcal{A}_M &= \lambda^{1/2}\widetilde{\mathcal{A}}_M \ , \quad \mathcal{A}_0 = \widetilde{\mathcal{A}}_0 \ , \\ \mathcal{F}_{MN} &= \lambda\widetilde{\mathcal{F}}_{MN} \ , \quad \mathcal{F}_{0M} = \lambda^{1/2}\widetilde{\mathcal{F}}_{0M} \ . \end{aligned} \tag{8.50}$$

The corresponding energy density associated to the action (8.47) reads [30]

$$E = 8\pi^2\kappa\left[\frac{1}{16\pi^2}\int d^3\widetilde{x}d\widetilde{z}\mathrm{tr}\,\widetilde{F}_{MN}^2\right] + \frac{\kappa}{\lambda}\int d^3\widetilde{x}d\widetilde{z}\left[-\frac{\widetilde{z}^2}{6}\mathrm{tr}\,\widetilde{F}_{ij}^2 + \widetilde{z}^2\mathrm{tr}\,\widetilde{F}_{iz}^2 - \frac{1}{2}(\widetilde{\partial}_M\widehat{\widetilde{A}}_0)^2 - \frac{1}{32\pi^2 a}\widehat{\widetilde{A}}_0\mathrm{tr}\,\widetilde{F}_{MN}^2\right] . \tag{8.51}$$

All quantities are dimensionless in units of $M_{\rm KK}$. The U(1) contribution $\widehat{\widetilde{A}}_0$ follows from the equation of motion [30]

$$\widetilde{\Box}\widehat{\widetilde{A}}_0 = \frac{1}{32\pi^2 a}\mathrm{tr}\,\widetilde{F}_{MN}^2 . \tag{8.52}$$

The $\widehat{\widetilde{A}}_0$ field can be obtained in closed form using (8.12),

$$\widehat{\widetilde{A}}_0 = \frac{1}{32\pi^2 a}\widetilde{\Box}\log|f| . \tag{8.53}$$

According to (8.50) *both* the size of the instanton ρ and the distance d between two instantons are rescaled, i.e. $\widetilde{\rho} = \sqrt{\lambda}\rho$ and $\widetilde{d} = \sqrt{\lambda}d$. While the size $\widetilde{\rho}$ is fixed to $\widetilde{\rho}_0$ (see below) by the energy minimization process, the distance is not. Therefore, when discussing the energy at the subleading order, the distance $\widetilde{d}$ is always short for $\sqrt{\lambda}d$. It will be recalled whenever appropriate. The first term in (8.51) is $8\pi^2\kappa\times$ instanton number, which is identified with the bare soliton mass. The second term ($\equiv \Delta E$) is subleading and corresponds to the correction to the mass or the interaction energy

$$\begin{aligned}\Delta E &= \frac{\kappa}{\lambda}\int d^3\widetilde{x}d\widetilde{z}\left[-\frac{\widetilde{z}^2}{6}\mathrm{tr}\,\widetilde{F}_{ij}^2 + \widetilde{z}^2\mathrm{tr}\,\widetilde{F}_{iz}^2 - \frac{1}{2}(\widetilde{\partial}_M\widehat{\widetilde{A}}_0)^2 - \frac{1}{32\pi^2 a}\widehat{\widetilde{A}}_0\mathrm{tr}\,\widetilde{F}_{MN}^2\right] \\ &= \frac{\kappa}{6\lambda}\int d^3\widetilde{x}d\widetilde{z}\left(\widetilde{z}^2 - \frac{3^7\pi^2}{2^4}\widetilde{\Box}\log|f|\right)\widetilde{\Box}^2\log|f| ,\end{aligned} \tag{8.54}$$

where we used the self-duality, $\mathrm{tr}\,\widetilde{F}_{ij}^2 = 2\mathrm{tr}\,\widetilde{F}_{iz}^2 = \frac{1}{2}\mathrm{tr}\,\widetilde{F}_{MN}^2$, and integrated $(\partial_M\widehat{\widetilde{A}}_0)^2$ by part so that it can be reduced to the form $\widehat{\widetilde{A}}_0\mathrm{tr}\,\widetilde{F}_{MN}^2$.

8.3.1 One baryon

The one baryon solution is the $k = 1$ instanton. This is best seen through the holonomy (8.1). Indeed from (8.14) it follows that

$$f^{-1} = \widetilde{\rho}^2 + \widetilde{x}_M^2 \ , \tag{8.55}$$

for $k = 1$, for which

$$U(\vec{x}) = e^{i\tau\cdot\vec{x}F(\vec{x})} \ , \tag{8.56}$$

with the Skyrmion profile $F(\vec{x}) = \frac{\pi|\vec{x}|}{\sqrt{\vec{x}^2+\rho^2}}$. We have set $\widetilde{X}_i = 0$ by translational symmetry. We have also set $\widetilde{X}_4 = 0$ as a finite $\widetilde{X}_4$ costs energy [30]. Thus

$$\widetilde{\Box}\log f = -4\frac{\widetilde{x}_M^2 + 2\widetilde{\rho}^2}{(\widetilde{x}_M^2 + \widetilde{\rho}^2)^2} \ , \tag{8.57}$$

$$\widetilde{\Box}^2\log f = \frac{96\widetilde{\rho}^4}{(\widetilde{x}_M^2 + \widetilde{\rho}^2)^4} \ . \tag{8.58}$$

The mass correction $\Delta M \equiv \Delta E$, reads

$$\Delta M(\rho) = \frac{\kappa}{6\lambda}\int d^3\widetilde{x}d\widetilde{z}\left(\widetilde{z}^2 + \frac{3^7\pi^2}{4}\frac{\widetilde{x}_M^2 + 2\widetilde{\rho}^2}{(\widetilde{x}_M^2 + \widetilde{\rho}^2)^2}\right)\frac{96\widetilde{\rho}^4}{(\widetilde{x}_M^2 + \widetilde{\rho}^2)^4} \tag{8.59}$$

$$= \frac{8\pi^2\kappa}{\lambda}\left(\frac{\widetilde{\rho}^2}{6} + \frac{1}{320\pi^4a^2}\frac{1}{\widetilde{\rho}^2}\right) \ . \tag{8.60}$$

It depends on the size $\widetilde{\rho}$ as plotted in Fig.(8.1). All integrals in ΔM are analytical, since $\widetilde{\Box}\log|f|$ and $\widetilde{\Box}^2\log|f|$ are simple. For $k = 2$ the expressions for ΔM are more involved and require numerical unwinding. As a prelude to these numerics, we have carried the integrals in (8.59) both analytically and numerically as illustrated in Fig.(8.1).

The one-instanton stabilizes for

$$\widetilde{\rho}_0 = \sqrt{\frac{1}{8\pi^2a}\sqrt{\frac{6}{5}}} \sim 9.64 \ , \tag{8.61}$$

with a mass correction

$$\Delta M(\widetilde{\rho}_0 \sim 9.64) \sim 0.365 \ . \tag{8.62}$$

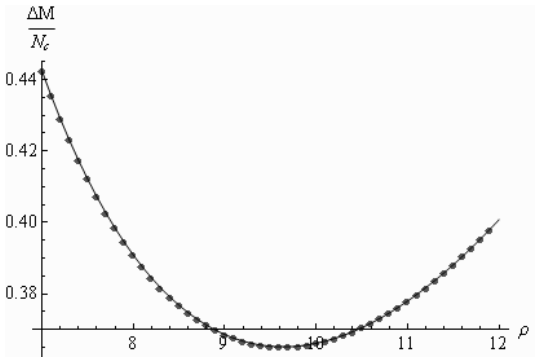

Figure 8.1: $\Delta M/N_c$: solid (exact) and dotted (numerical).

We recall that the physical instanton size $\rho_0 = \widetilde{\rho}_0/\sqrt{\lambda}$ following the unscaling as detailed above.

8.3.2 Two baryon

The two baryon solution corresponds to the $k = 2$ instanton. The corresponding potential f for the $k = 2$ instanton is given in (8.32) and yields

$$\begin{aligned}
\mathrm{tr}\, \widetilde{F}_{\mu\nu}^2 &= \widetilde{\Box}^2 \log|f| \\
&= -\widetilde{\Box}^2 \log\left[\left(g_-(\widetilde{x}_M) + \frac{\widetilde{\rho}_1^2\widetilde{\rho}_2^2 \sin^2|\theta|}{\widetilde{d}^2}\right)\left(g_+(\widetilde{x}_M) + \frac{\widetilde{\rho}_1^2\widetilde{\rho}_2^2 \sin^2|\theta|}{\widetilde{d}^2}\right)\right. \\
&\qquad \left. -\widetilde{\rho}_1^2\widetilde{\rho}_2^2\left(\cos|\theta| + \frac{2}{\widetilde{d}}\sin|\theta|\left[\widehat{\theta}_1\widetilde{x}_0 + \widehat{\theta}_2\widetilde{x}_3 - \widehat{\theta}_3\widetilde{x}_2\right]\right)^2\right] \quad . \quad (8.63)
\end{aligned}$$

Its leading contribution in (8.51) is

$$8\pi^2\kappa\left[\frac{1}{16\pi^2}\int d^3\widetilde{x}d\widetilde{z}\mathrm{tr}\,\widetilde{F}_{MN}^2\right] = 2\times 8\pi^2\kappa \ ,$$

as expected by self-duality. To order $N_c\lambda$ the energy of the 2-baryon system is just $2M_0$ or twice the bare soliton mass. There is complete degeneracy in the moduli parameters $\widetilde{d}$ and θ_a. This degeneracy is lifted at order $N_c\lambda^0$, which is the next contribution in (8.51). This will be detailed below.

Here we recall briefly some labeling for Skyrmion-Skyrmion interaction in the context of the product ansat, for which most NN-potential were obtained.

For 2-Skyrmions at large relative separation, the ansatz reads

$$\mathbb{U}_2(\vec{x}) = \mathbb{U}(\vec{x}+\vec{d}/2)U\mathbb{U}(\vec{x}-\vec{d}/2)U^\dagger \ , \tag{8.64}$$

with U, $SU(2)$ valued as defined in (8.25). For $U=1$ the 2-Skyrmions are said to be in the defensive configuration, while for $U=i\tau_x$, they are said to be in the combed configuration. The defensive configuration is maximally repulsive with $\mathbb{U}_2(\vec{x})=\mathbb{U}(\vec{x})^2$ for $\vec{d}=0$. The combed configuration is partially attractive.

For two parallel instantons $|\,\theta|=0$ and the instanton action density (8.63) reads

$$\mathrm{tr}\,\widetilde{F}^2_{\mu\nu} \;=\; -\widetilde{\Box}^2\log\left[g_-(\widetilde{x}_M)g_+(\widetilde{x}_M)-\widetilde{\rho}_1^2\widetilde{\rho}_2^2\right] \ . \tag{8.65}$$

The baryon number distribution in space follows from

$$B(x)=\frac{1}{16\pi^2}\int_{-\infty}^{+\infty}dz\,\mathrm{tr}\,F^2_{\mu\nu} \ , \tag{8.66}$$

which integrates to 2. Since the instanton in bulk is localized near $z\approx\rho\approx 1/\sqrt{\lambda}$, we may approximate the integral by the value of the integrand for $z\approx 0$, or $B(x)\approx \mathrm{tr}\,\widetilde{F}^2_{\mu\nu}(z\approx 0)/16\pi^2$. In Fig.(8.2) we show $\mathrm{tr}\,\widetilde{F}^2_{\mu\nu}$ for $\widetilde{z}=\widetilde{x}_3=0$ and $\widetilde{\rho}_1=\widetilde{\rho}_2=9.64$ for various separations $\widetilde{d}$ in the $(\widetilde{x}_1,\widetilde{x}_2)$ space for two paralell Skyrmions. The separation is in units of the size $\widetilde{\rho}_0=9.64$. For small separations a narrow Skyrmion develops on top of the broad Skyrmion. The configuration is maximally repulsive (defensive Skyrmions).

A paralell and antiparalell Skyrmion (combed Skyrmions) corresponds to the choice $\theta_1=\theta_2=0$ and $\theta_3=\frac{\pi}{2}$ or $|\,\theta|=\pi/2$. This is a π rotation along x_3 in the SO(3) notation (8.26). The resulting instanton action density (8.63) reads

$$\mathrm{tr}\,\widetilde{F}^2_{\mu\nu}=-\widetilde{\Box}^2\log\left[\left(g_-(\widetilde{x}_M)+\frac{\widetilde{\rho}_1^2\widetilde{\rho}_2^2}{\widetilde{d}^2}\right)\left(g_+(\widetilde{x}_M)+\frac{\widetilde{\rho}_1^2\widetilde{\rho}_2^2}{\widetilde{d}^2}\right)-4\frac{\widetilde{\rho}_1^2\widetilde{\rho}_2^2}{\widetilde{d}^2}\widetilde{x}_2^2\right] \ . \tag{8.67}$$

In Fig.(8.3) we show the baryon density in the plane (x_1,x_2) for various separations in units of the instanton size with $\widetilde{\rho}_1=\widetilde{\rho}_2=9.64$. For large separation two lumps form along the x^1 axis. For smaller separation the two lumps are

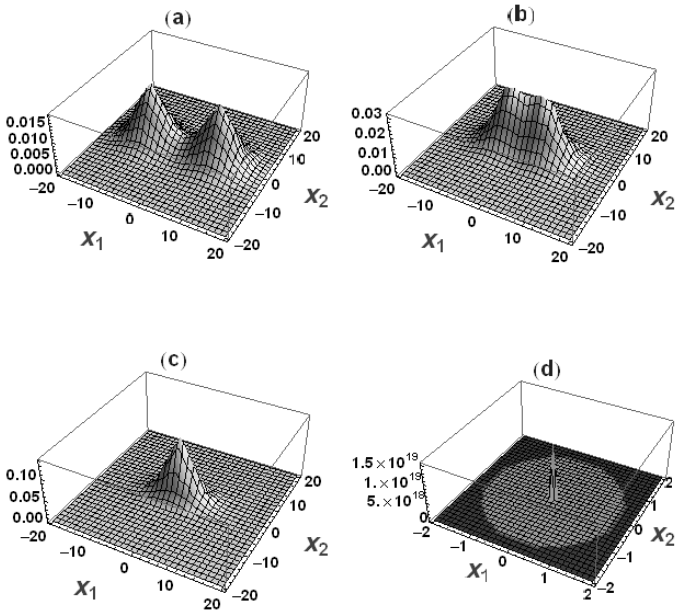

Figure 8.2: Defensive Skyrmions: (a) $\widetilde{d} = 2$, (b) $\widetilde{d} = \sqrt{2}$, (c) $\widetilde{d} = 1$, (d) $\widetilde{d} = 10^{-5}$

seen to form in the orthogonal or x_2 direction. In between a hollow baryon 2 configuration is seen which is the precursor of the donut seen in the baryon number 2 sector of the Skyrme model [131]. The concept of $\widetilde{d}$ as a separation at small separations is no longer physical given the separation taking place in the transverse direction. What is physical is the dual distance u in the transverse plane.

For two Skyrmions orthogonal to each other, the choice of angles is $\theta_1 = \theta_2 = 0, \theta_3 = \frac{\pi}{4}$. The corresponding action density is given by (8.63)

$$\begin{aligned} \mathrm{tr}\, \widetilde{F}^2_{\mu\nu} &= -\widetilde{\Box}^2 \log \left[\left(g_-(\widetilde{x}_M) + \frac{\widetilde{\rho}_1^2 \widetilde{\rho}_2^2 \sin^2\theta_3}{\widetilde{d}^2} \right) \left(g_+(\widetilde{x}_M) + \widetilde{\rho}_2^2 + \frac{\widetilde{\rho}_1^2 \widetilde{\rho}_2^2 \sin^2\theta_3}{\widetilde{d}^2} \right) \right. \\ &\qquad \left. - \widetilde{\rho}_1^2 \widetilde{\rho}_2^2 \left(\cos\theta_3 - \frac{2\widetilde{x}_2}{\widetilde{d}} \sin\theta_3 \right)^2 \right] , \end{aligned} \tag{8.68}$$

which is also seen to reduce to (8.65) and (8.67) for $\theta_3 = 0$ or π and $\theta_3 = \pi/2$ respectively. The $\theta_3 = \frac{\pi}{4}$ is our two orthogonal Skyrmions. This configuration is shown in Fig.(8.4). For small separations a narrow Skyrmion develops on top of a broad one, a situation reminiscent of the Defensive Skyrmion configuration

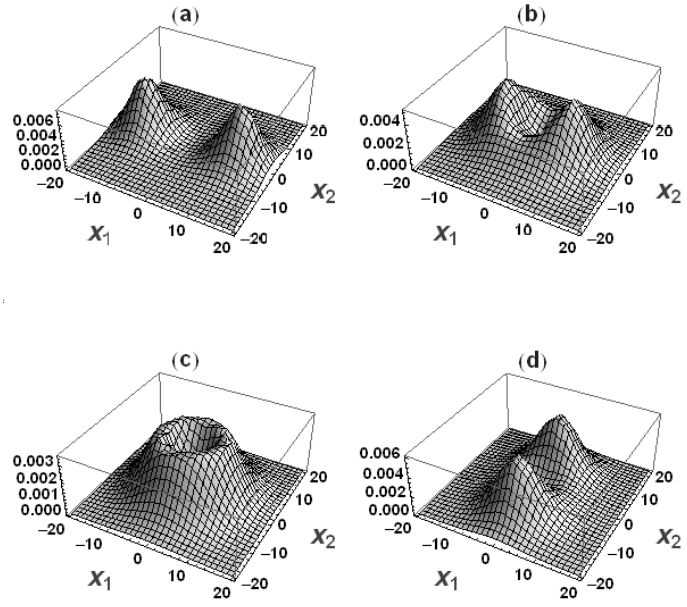

Figure 8.3: Combed Skyrmions: (a) $\widetilde{d} = 2.5$, (b) $\widetilde{d} = 1.7$, (c) $\widetilde{d} = \sqrt{2}$, (d) $\widetilde{d} = 1$

above. This situation can be seen in many other relative orientations and is somehow generic.

8.4 Skyrmion-Skyrmion Interaction

The Skyrmion-Skyrmion interaction in hQCD is of order N_c/λ and it follows from (8.54) which is the second term in (8.51). The baryon two minimum energy configuration should follow by minimizing this contribution in the 6-dimensional coset space ρ, d, θ. This will be reported elsewhere. Instead, we report on the interaction energy between two Skyrmions versus their separation for a size fixed in the baryon 1 sector and different relative orientations θ_a. In the adiabatic quantization scheme, θ_a are raised to collective coordinates. They are not fixed by minimization. This approach will be subsumed here. We note that the mass shift are of order $N_c\lambda^0$.

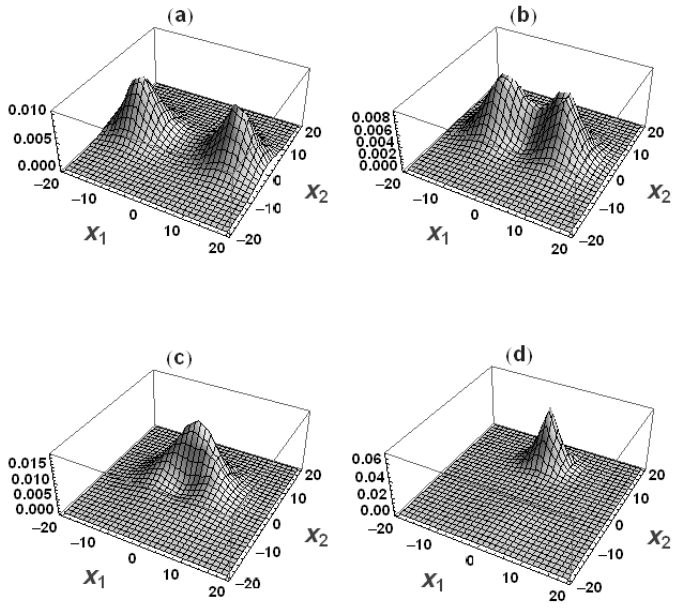

Figure 8.4: Orthogonal Skyrmions: (a) $\widetilde{d} = 2.5$, (b) $\widetilde{d} = 1.7$, (c) $\widetilde{d} = 1.2$, (d) $\widetilde{d} = 0.6$.

8.4.1 General

Consider the case where $\theta_1 = \theta_2 = 0$ and $\theta_3 \neq 0$, with fixed sizes $\widetilde{\rho}_1 = \widetilde{\rho}_2 = \widetilde{\rho}_0$. Here $\widetilde{\rho}_0$ is the value fixed by minimization in the 1 Skyrmion sector (8.61). In Fig. (8.5) we show the interaction energy $(\Delta E - 2\Delta M)/N_c$ versus the relative distance d in units of the instanton size, where

$$\Delta E = \frac{\kappa}{6\lambda}\int d^3\widetilde{x}d\widetilde{z}\left(\widetilde{z}^2 - \frac{3^7\pi^2}{2^4}\widetilde{\Box}\log|f|\right)\widetilde{\Box}^2\log|f| \ , \tag{8.69}$$

$$|f| = \left(g_-(\widetilde{x}_M) + \frac{\widetilde{\rho}_1^2\widetilde{\rho}_2^2\sin^2\theta_3}{\widetilde{d}^2}\right)\left(g_+(\widetilde{x}_M) + \frac{\widetilde{\rho}_1^2\widetilde{\rho}_2^2\sin^2\theta_3}{\widetilde{d}^2}\right) - \widetilde{\rho}_1^2\widetilde{\rho}_2^2\left(\cos\theta_3 - \frac{2\widetilde{x}_2}{\widetilde{d}}\sin\theta_3\right)^2 \ . \tag{8.70}$$

The interaction energy is repulsive for all values of θ_3. The repulsion decreases for θ_3 in the range $0 \to \pi/2$, that is from the defensive to combed configuration. The combed or $\theta_3 = \pi/2$ is still repulsive even for small relative distances, as the two Skyrmions separate in the transverse direction. In Fig. (8.6) we show separatly the interaction energy for the defensive configuration (left)

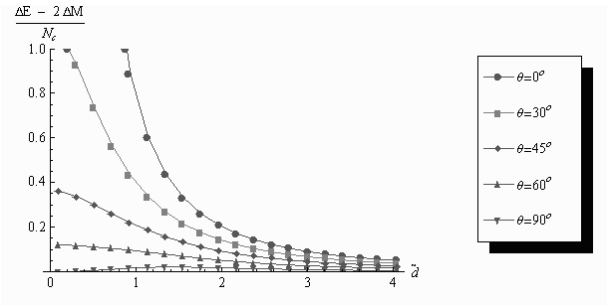

Figure 8.5: Skyrmion-Skyrmion interaction in regular gauge.

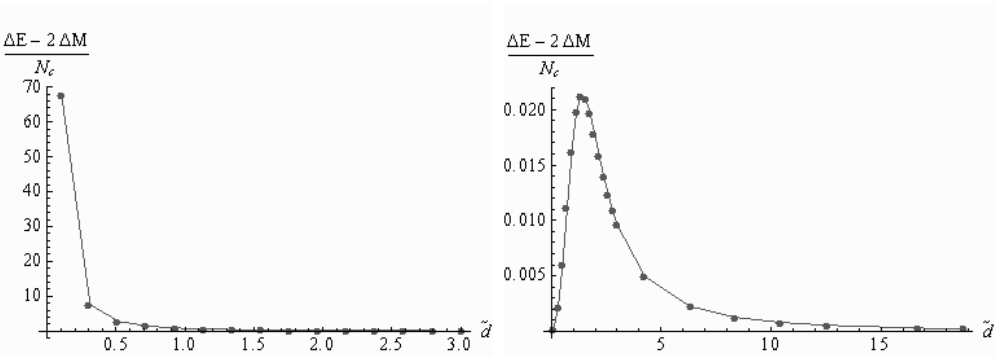

Figure 8.6: Skyrmion-Skyrmion interaction: Defensive (left) and Combed (right)

and combed configuration (right). The repulsion is seen to drop by 3 orders of magnitude.

The core interaction is modified in the singular gauge as we detail in Appendix A and B. In Fig. (8.7) we show the analogue of Fig. (8.5) in the singular gauge. The switch from repulsion to attraction follows from the switch from repulsive Coulomb (regular gauge) to attractive dipole (singular gauge) interactions. The plot is versus $\tilde{d}$ which is the rescaled distance in units of the rescaled size $\tilde{\rho}$. In the unscaled distance d, the dipole attraction is of order N_c/λ^4 and subleading.

8.4.2 Interaction at Large Separation

To understand the nature of the Skyrmion-Skyrmion interaction to order N_c/λ as given by the classical instantons in bulk, we now detail it for large separa-

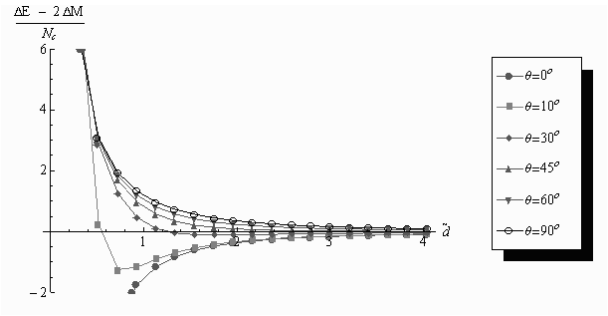

Figure 8.7: Skyrmion-Skyrmion interaction in singular gauge

tions between the instanton cores, i.e. $d \gg \rho$ but still smaller than the pion range (which is infinite for massless pions). We recall that the interaction follows from the subleading contribution in (8.51), which can be split

$$\Delta E[f] = N_c b\,(C[f] + c\,D[f]) \ , \tag{8.71}$$

$$C[f] \equiv \int d^3\widetilde{x} d\widetilde{z}\,\widetilde{z}^2\,\widetilde{\Box}^2 \log|f| \ , \tag{8.72}$$

$$D[f] \equiv -\int d^3\widetilde{x} d\widetilde{z}\,(\,\widetilde{\Box}^2 \log|f|\,)\,\frac{1}{\widetilde{\Box}}\,(\,\widetilde{\Box}^2 \log|f|\,) \ , \tag{8.73}$$

with $b = \frac{1}{6\cdot 216\pi^3}$ and $c \equiv \frac{3^7\pi^2}{2^4}$.

For large separations between the cores or $d \gg \rho$, we have from (8.34)

$$\begin{aligned} \log|f_{-+}| &= -\log\left[(g_-g_+)\left(1 + A\frac{g_- + g_+}{g_-g_+} + \frac{A^2 - B^2}{g_-g_+}\right)\right] \\ &\approx -\log g_- - \log g_+ - A\frac{g_- + g_+}{g_-g_+} + \frac{B^2}{g_-g_+} \ , \end{aligned} \tag{8.74}$$

after dropping the A^2 contribution as it is subleading in ρ/d. We note that after fixing the size of the single instanton to $\widetilde{\rho}_0$ and *unscaling* the distance $\widetilde{d}$ as we indicated above, the expansion $\widetilde{\rho}/\widetilde{d}$ is an expansion in $\widetilde{\rho}_0/(\sqrt{\lambda}d)$.

The Skyrmion-Skyrmion core interaction follows from

$$V = \Delta E[f_{-+}] - \Delta E[f_-] - \Delta E[f_+] \ , \tag{8.75}$$

after subtraction of the classical self-energies which are of order $N_c\lambda^0$. The

$C[f]$ contribution to the interaction reads

$$V_C = \sin^2|\,\theta|\,V_{C\alpha} + \sin^2|\,\theta|\,\widehat{\theta}_1^2 V_{C\beta} + \sin^2|\,\theta|\,(\widehat{\theta}_2^2+\widehat{\theta}_3^2)V_{C\gamma} + \cos^2|\,\theta|\,V_{C\delta}\ , \quad (8.76)$$

with

$$V_{C\alpha} \equiv N_c b\frac{\widetilde{\rho}^4}{\widetilde{d}^2}\int d^3\widetilde{x}d\widetilde{z}\,\widetilde{z}^2\,\widetilde{\Box}^2\left(\frac{g_-+g_+}{g_-g_+}\right)\ , \quad (8.77)$$

$$V_{C\beta} \equiv N_c b\frac{\widetilde{\rho}^4}{\widetilde{d}^2}\int d^3\widetilde{x}d\widetilde{z}\,\widetilde{z}^2\,\widetilde{\Box}^2\left(\frac{4\widetilde{z}^2}{g_-g_+}\right)\ , \quad (8.78)$$

$$V_{C\gamma} \equiv N_c b\frac{\widetilde{\rho}^4}{\widetilde{d}^2}\int d^3\widetilde{x}d\widetilde{z}\,\widetilde{z}^2\,\widetilde{\Box}^2\left(\frac{4\widetilde{x}_2^2}{g_-g_+}\right)\ , \quad (8.79)$$

$$V_{C\delta} \equiv N_c b\frac{\widetilde{\rho}^4}{\widetilde{d}^2}\int d^3\widetilde{x}d\widetilde{z}\,\widetilde{z}^2\,\widetilde{\Box}^2\left(\frac{1}{g_-g_+}\right)\ , \quad (8.80)$$

where the cross term in B^2 drops by parity and we have rescaled the variable $\widetilde{x}_M/\widetilde{d}\to\widetilde{x}_M$. Thus $g_\pm\to\widetilde{x}_\alpha^2+\left(\widetilde{x}_1\pm\frac{1}{2}\right)^2+\widetilde{\rho}^2/\widetilde{d}^2$. All integrals are understood in dimensional regularization that preserves both gauge and $O(4)$ symmetry. The results are

$$V_{C\alpha} = -V_{C\beta} = -V_{C\gamma} = N_c b\frac{\widetilde{\rho}^4}{\widetilde{d}^2}16\pi^2\ , \qquad V_{C\delta}=0\ . \quad (8.81)$$

The $D[f]$ contribution to the interaction reads

$$V_D \approx -2bcN_c\int(\,\widetilde{\Box}^2\log g_-\,)\,\frac{1}{\widetilde{\Box}}\,(\,\widetilde{\Box}^2\log g_+\,)\ . \quad (8.82)$$

The Coulomb propagator $1/\widetilde{\Box}=-1/(4\pi^2|\widetilde{x}_+-\widetilde{x}_-|^2)$ in 4-dimensions. At large separations $|\widetilde{x}_+-\widetilde{x}_-|\approx\widetilde{d}$ and (8.82) simplifies to

$$V_D \approx 128\pi^2\,bcN_c\frac{1}{d^2}\left|\frac{1}{16\pi^2}\int d^3\widetilde{x}d\widetilde{z}\,\widetilde{\Box}^2\log g\right|^2 = \frac{27\pi N_c}{2}\frac{1}{\widetilde{d}^2}\ , \quad (8.83)$$

where the $||$ integrates to the baryon charge 1. V_D captures the Coulomb repulsion between two unit baryons in 4 dimensions in the regular gauge. This is not the case in the singular as we show in Appendix B.

We note that after unscaling $\widetilde{d}=\sqrt{\lambda}d$, $V_D\approx N_c/\lambda$. In regular gauge, this monopole core repulsion is the Coulomb repulsion between *4-dimensional*

Coulomb charges. We show in Appendix C that this is the natural extension of the *3-dimensional* omega repulsion at shorter distances in holography. The repulsion dominates the many-body problem at finite chemical potential as discussed recently in [15, 17]. Indeed, for baryonic matter at large baryonic density n_B, the energy is dominated by the Coulomb repulsion (8.83). The corresponding effective interaction is

$$V_{\text{eff}} = \frac{1}{2}\int \vec{dx}\vec{dy}\left(\phi^+\phi\right)(\vec{x})V_D(\vec{x}-\vec{y})\left(\phi^+\phi\right)(\vec{y}) \ , \tag{8.84}$$

leading to an energy per volume of order $N_c\, n_B^{5/3}/\lambda$ as in [17].

8.5 Nucleon-Nucleon Interaction: Core

At large separation, the nucleon-nucleon core interaction can be readily extracted from the Skyrmion-Skyrmion core interaction (8.76) as it is linear in the $SO(3)$ rotation R. Indeed, using the standard decomposition [121]

$$R^{ab} = \frac{1}{3}(R_T^{ab} + \delta^{ab}R_S) \ , \tag{8.85}$$

with

$$R_S = \text{tr}\, R \ , \quad R_T^{ab} = 3R^{ab} - \delta^{ab}\text{tr}\, R \ , \tag{8.86}$$

the spin R_S and tensor R_T contributions respectively, we may decompose the core potential as

$$V = V_1 + V_S R_S + V_T^{ab}R_T^{ab} \ . \tag{8.87}$$

The scalar V_1, spin V_S and tensor V_T contributions can be unfolded by a pertinent choice of orientations of the core Skyrmion-Skyrmion interaction. In general,

$$V = V_1 + V_S\left(4\cos^2|\,\theta| - 1\right) + V_T^{ab}\left[\left(6\hat{\theta}^a\hat{\theta}^b - 2\delta^{ab}\right)\sin^2|\,\theta| + 3\epsilon^{abc}\widehat{\theta}^c\sin 2|\,\theta|\right] \ ,$$

after using the SO(3) parametrization (8.26)

$$R^{ab} = \delta^{ab}\cos 2|\,\theta| + 2\widehat{\theta}^a\widehat{\theta}^b \sin^2|\,\theta| + \epsilon^{abc}\widehat{\theta}^c \sin 2|\,\theta| \ . \tag{8.88}$$

The axial symmetry $V(\theta_1,\theta_2,\theta_3) = V(\theta_1,\theta_3,\theta_2)$ implies that the tensor components of the core satisfy $V_T^{22} = V_T^{33}, V_T^{12} = V_T^{31}$, and $V_T^{13} = V_T^{21}$. Thus, V is reduced to

$$\begin{aligned} V(\theta_1,\theta_2,\theta_3) = V_1 + V_S\left(4\cos^2|\,\theta| - 1\right) + (V_T^{11} - V_T^{22})(6\hat{\theta}_1^2 - 2)\sin^2|\,\theta| \\ +(V_T^{12} + V_T^{13})(6\hat{\theta}_1(\hat{\theta}_2 + \hat{\theta}_3))\sin^2|\,\theta|) + (V_T^{12} - V_T^{13})(3(\hat{\theta}_2 + \hat{\theta}_3)\sin 2|\,\theta|) \\ +(V_T^{23} + V_T^{32})(6\hat{\theta}_2\hat{\theta}_3\sin^2|\,\theta|) + (V_T^{23} - V_T^{32})(3\hat{\theta}_1\sin 2|\,\theta|) \ . \end{aligned} \tag{8.89}$$

In particular,

$$V(0,0,0) = V_1 + 3V_S \ , \quad V(0,0,\pi/2) = V_1 - V_S - 2(V_T^{11} - V_T^{22}) \ , \tag{8.90}$$

$$V(\pi/2,0,0) = V_1 - V_S + 4(V_T^{11} - V_T^{22}) \ , \tag{8.91}$$

so that

$$V_1 = \frac{1}{4}\left[V(0,0,0) + V(0,0,\pi/2) + V(0,\pi/2,0) + V(\pi/2,0,0)\right] \ , \tag{8.92}$$

$$V_S = \frac{1}{4}\left[V(0,0,0) - \frac{1}{3}\left(V(0,0,\pi/2) + V(0,\pi/2,0) + V(\pi/2,0,0)\right)\right] \ , \tag{8.93}$$

$$V_T^{11} - V_T^{22} = \frac{1}{6}\left[V(\pi/2,0,0) - V(0,0,\pi/2)\right] \ . \tag{8.94}$$

Using (8.77)-(8.80) we deduce the scalar, spin and tensor core contributions in the form

$$\begin{aligned} V_1 &= \frac{1}{4}\left(3V_{C\alpha} + V_{C\beta} + 2V_{C\gamma} + V_{C\delta}\right) + V_D = V_D \ , \\ V_S &= \frac{1}{4}\left(-V_{C\alpha} - \frac{1}{3}V_{C\beta} - \frac{2}{3}V_{C\gamma} + V_{C\delta}\right) = 0 \ , \\ V_T^{11} - V_T^{22} &= \frac{1}{6}(V_{C\beta} - V_{C\gamma}) = 0 \ . \end{aligned}$$

The off-diagonal tensor V_T core contribution vanishes. This is clear from (8.76).

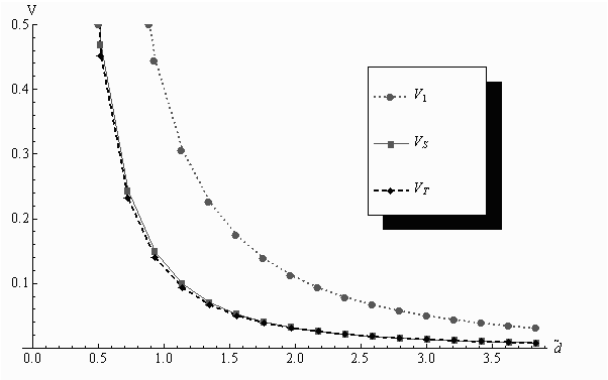

Figure 8.8: V_1, V_S, V_T in regular gauge

Indeed (8.76) can be decomposed as

$$\begin{aligned} V &= \sin^2|\theta|\, V_{C\alpha} + \sin^2|\theta|\, \widehat{\theta}_1^2 V_{C\beta} + \sin^2|\theta|\, (\widehat{\theta}_2^2 + \widehat{\theta}_3^2) V_{C\gamma} + \cos^2|\theta|\, V_{C\delta} + V_D \\ &= \sin^2|\theta|\, (V_{C\alpha} + V_{C\gamma}) + \sin^2|\theta|\, \widehat{\theta}_1^2 (V_{C\beta} - V_{C\gamma}) + \cos^2|\theta|\, V_{C\delta} + V_D \\ &= \frac{1}{4}(3V_{C\alpha} + V_{C\beta} + 2V_{C\gamma} + V_{C\delta}) + V_D \\ &\quad + \frac{1}{4}\left(-V_{C\alpha} - \frac{1}{3}V_{C\beta} - \frac{2}{3}V_{C\gamma} + V_{C\delta}\right)\left(4\cos^2|\theta| - 1\right) \\ &\quad + \frac{1}{6}(V_{C\beta} - V_{C\gamma})(6\hat{\theta}_1^2 - 2)\sin^2|\theta| \ , \end{aligned} \tag{8.95}$$

in agreement with (8.95). In summary

$$V_1 = V_D \ , \tag{8.96}$$

and all others vanish. For general distances, we plot V_1, V_S and V_T with (8.92)-(8.94) in Fig.(8.8) in the regular gauge. The relative separation $\tilde{d}$ is in units of the core size $\tilde{\rho} = 9.64$.

In the singular gauge, the V_C core contribution to the nucleon-nucleon interaction remains unchanged while the V_D contribution changes. As a result, the spin and tensor channels remain the same for both regular and singular gauges. The central or scalar channel $V_1 = V_D$ changes from repulsive $N_c/\lambda\widetilde{d}^2$ (regular) to attractive $-N_c/\lambda^4\widetilde{d}^8$ (singular) asymptotically. The flip is from monopole to dipole as we detail in Appendix B. The short distance repulsion in the regular gauge is the 4-dimensional extension of the 3-dimensional omega

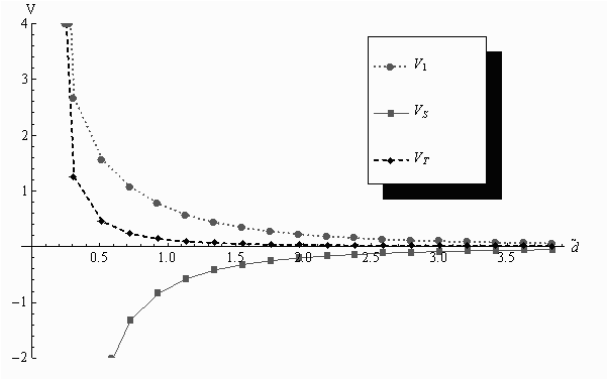

Figure 8.9: V_1, V_S, V_T in singular gauge

repulsion. In Fig.(8.9) we show V_1, V_S and V_T with (8.92)-(8.94) and (8.164) in the singular gauge.

8.6 Nucleon-Nucleon Interaction: Cloud

To assess the nucleon-nucleon interaction beyond the core contribution we need to do a semiclassical expansion around the $k = 2$ configuration, thereby including the effects of pions and vector mesons as quantum fluctuations around the core. We refer to these contributions as the cloud. The semiclassical expansion around the $k = 2$ configuration parallells entirely the same expansion around the $k = 1$ instanton as detailed in [19]. The expansion will be carried out in the axial gauge $A_z = 0$ for the fluctuations. This gauge has the merit of exposing explicitly the pion-nucleon coupling. All cloud calculations will be carried with the background $k = 2$ instanton in the regular gauge. Some of the results in the singular gauge are reported in Appendix.

8.6.1 Pion

In the axial gauge $A_z = 0$ for the fluctuations, the pion coupling to the flavor instanton is explicit in bulk. Indeed, following the general expansion in [19] we have for the pion-instanton linear coupling

$$S = -\kappa \int d^4x dz \partial_z \left(K F^a_{z\mu} C^{\mu,a} \right) \ , \tag{8.97}$$

with the explicit pion field

$$C^{\mu,a} \equiv \frac{1}{f_\pi}\partial^\mu \Pi^a \psi_0 \ , \quad \psi_0 = \frac{2}{\pi}\arctan z \ , \tag{8.98}$$

and $f_\pi = 4\kappa/\pi$. As noted in [19] all linear meson couplings to the flavor instanton are boundary-like owing to the soliton character of the $k = 2$ instanton. Since $KF_{zi}\psi_0$ is odd in z, for a static instanton,

$$S = \kappa \int d^4x F^a_{zi}\, K\psi_0\Big|_B \frac{\partial_i \Pi^a}{f_\pi} \ . \tag{8.99}$$

Here $B = \pm z_c$ refers to boundary of the core when using the non-rigid quantization scheme. To avoid double counting, for $z < z_c$ the mesons are excluded in the holographic direction. z_c plays the role of the bag radius. It will be reduced to $z_c \to 0$ at the end of all calculations, making the non-rigid quantization constraint point-like.

The linear pion-2-instanton vertex (8.99) contributes to the energy through second order perturbation. Specifically,

$$\begin{aligned} V_\Pi &= \frac{4\kappa^2 K(z_c)^2\psi_0(z_c)^2}{2f_\pi^2}\int d\vec{x}d\vec{y}F^a_{iz}(\vec{x},z_c)\langle\partial_i\Pi(\vec{x})^a\partial_j\Pi(\vec{y})^b\rangle F^b_{jz}(\vec{y},z_c) \\ &= \frac{\kappa^2 K(z_c)^2\psi_0(z_c)^2}{2\pi f_\pi^2}\int d\vec{x}d\vec{y}F^a_{iz}(\vec{x},z_c)\partial_i\partial_j\frac{1}{|\vec{x}-\vec{y}|}F^a_{jz}(\vec{y},z_c) \ , \end{aligned} \tag{8.100}$$

for massless pions. At large separations, the field strength F^a_{iz} splits into two single instantons of relative distance d and flavor orientation R. At large relative separation d, (8.100) simplifies to

$$V_\Pi \approx \frac{9}{16\pi f_\pi^2} J_A^{ai}(0) D_{ij} J_A^{Raj}(0) \ , \tag{8.101}$$

with $D_{ij} = (3\hat{d}_i\hat{d}_j - \delta_{ij})/d^3$. The spatial component of the axial vector current J_A is unrotated while J_A^R is rotated. From Appendix D, its zero momentum limit reads

$$J_A^{ai}(0) \equiv J_A^{ai}(\vec{q}=0) = -\frac{4}{3}\kappa K(z_c)\psi_0(z_c)\int d\vec{x}\, F^a_{iz}(\vec{x},z_c) \ . \tag{8.102}$$

The projected potential V_Π yields

$$\langle s_1t_1s_2t_2|V_\Pi|s_1t_1s_2t_2\rangle = \frac{9}{16\pi f_\pi^2}\langle s_1t_1|J_A^{ai}(0)|s_1t_1\rangle D_{ij}\langle s_2t_2|J_A^{RAj}(0)|s_2t_2\rangle$$
$$\equiv \frac{1}{16\pi}\left(\frac{g_A}{f_\pi}\right)^2\frac{1}{d^3}\left(3(\vec\sigma_1\cdot\widehat{d})(\vec\sigma_2\cdot\widehat{d})-\vec\sigma_1\cdot\vec\sigma_2\right)(\vec\tau_1\cdot\vec\tau_2)\ , \qquad (8.103)$$

where $g_A = 32\kappa\pi\rho^2/3$ is the axial-vector charge of the nucleon as detailed in Appendix D. $g_A \approx N_c\lambda^0$ in hQCD.

In the $A_z = 0$ gauge, the linear pion-2-instanton vertex (8.97) yields a tensor contribution to the nucleon-nucleon potential

$$V_{T,\Pi} = \frac{1}{16\pi}\left(\frac{g_A}{f_\pi}\right)^2\frac{1}{d^3}\ . \qquad (8.104)$$

This is in agreement with the pseudo-vector one-pion exchange potential

$$V_{T,\Pi} = \frac{(g_{\pi NN}/2M)^2}{4\pi}\frac{1}{d^3}\ , \qquad (8.105)$$

if we identify

$$\frac{g_{\pi NN}}{M_N} = \frac{g_A}{f_\pi}\ . \qquad (8.106)$$

This is just the Goldberger-Treiman relation which is also satistified by the holographic construction in the $A_z = 0$ gauge and for massless pions.

In reaching (8.103) and the relation (8.106) there is a subtlety. Indeed in (8.101) the pion propagator D_{ij} is supposed to be longitudinal and the axial vector source J_A^{ij} transverse, so that the contraction vanishes. The subtlety arises from the ambiguity in the axial vector source at zero momentum and for massless pions as discussed in Appendix D. The contraction is ambiguous through 0/0. The ambiguity is lifted by the order of limits detailed in Appendix D, which effectively amounts to a longitudinal component of the axial vector source at zero momentum. This result is independently confirmed by using the strong coupling source theory discussed in Appendix C.

Finally, the pion coupling (8.99) in the axial gauge is pseudoscalar and strong and of order $\sqrt{N_c/\lambda}$. The reader may object that this conclusion maybe at odd with naive $1/N_c$ power counting whereby the pseudovector coupling is

of order $\sqrt{N_c}/N_c \approx 1/\sqrt{N_c}$ with the extra $1/N_c$ suppression brought about by the γ_5 in the nucleon axial vector source [121]. In strongly coupled models such as hQCD the nucleon source is of order N_c^0 not $1/N_c$, and yet chiral symmetry is fully enforced in the nucleon sector. hQCD is a chiral and dynamical version of the static Chew model of the Δ for strong coupling [132]. Also, the reader may object that the one-pion iteration which is producing a potential of order N_c/λ, may cause an even stronger correction by double iteration of order $(N_c/\lambda)^2$ and so on. This does not happen though, since the direct and crossed diagram to order $(N_c/\lambda)^2$ cancel at strong coupling. The same cancellation is at the origin of unitarization in $\pi\, N \to \pi\, N$ scattering (Bhabha-Heithler mechanism).

8.6.2 Axials

The linear vertex (8.97) also couples vector and axial vector mesons to the 2-instanton solution at the core in bulk. For instance, the axial-vector meson contribution follows from (8.97) by inserting

$$C^{\mu,a} \equiv a_\mu^{a,n}\psi_{2n} \ , \tag{8.107}$$

so that

$$S = 2\kappa \int d^4x \left(K\mathbb{F}^{b,z\mu}a_\mu^{b,n}\psi_{2n}\right)\Big|_{z=z_c} . \tag{8.108}$$

The sum over n is subsumed. We have used the fact that $KF_{zi}\psi_{2n}$ is odd in z (axial exchange) and that the surface contribution at $z=\infty$ is zero since $F^b{}_{z\nu} \sim \delta(z)$ is localized in bulk to leading order in $1/\lambda$.

In second order perturbation, (8.108) contributes a static potential

$$V_A = 2\kappa^2 K(z_c)^2\psi_{2n}(z_c)\psi_{2m}(z_c)\int d\vec{x}d\vec{y}F_{iz}^a(\vec{x},z_c)\Delta_{ij}^{mn,ab}F_{jz}^b(\vec{y},z_c) \ . \tag{8.109}$$

At large separations, the field strength F_{iz}^a splits into two single instantons of relative distance d and flavor orientation $R = R_1^T R_2$. At large relative

separation d, (8.109) simplifies to [2]

$$\begin{aligned} V_A &\approx \frac{9}{16\pi}\sum_n J_A^{ai}(0)\left(\frac{\psi_{2n}}{\psi_0}\right)^2\left(-\delta_{ij}+\frac{\partial_i\partial_j}{m_{2n}^2}\right)\frac{e^{-m_{2n}d}}{d}J_A^{Raj}(0) \\ &= \frac{9}{16\pi}\sum_n J_A^{ai}(0)\left(\frac{\psi_{2n}}{\psi_0}\right)^2\left[\left(1+\frac{2}{m_{2n}d}+\frac{3}{m_{2n}^2d^2}\right)\widehat{d}_i\widehat{d}_j\right. \\ &\qquad \left.-\delta_{ij}\left(1+\frac{1}{m_{2n}^2d^2}\right)\right]\frac{e^{-m_{2n}d}}{d}J_A^{Raj}(0)\ , \end{aligned} \tag{8.110}$$

where $J_A^{ai}(0)$ is defined in (8.102) and the spatial component of the axial vector current J_A is unrotated while J_A^R is rotated. The projected potential V_A yields

$$\begin{aligned} &\langle s_1t_1s_2t_2|V_A|s_1t_1s_2t_2\rangle \\ &\quad\approx \frac{g_A^2}{16\pi}\sum_n\left(\frac{\psi_{2n}}{\psi_0}\right)^2 e^{-m_{2n}d}\left(-\frac{1}{d}-\frac{1}{m_{2n}^2d^3}\right)(\vec{\sigma}_1\cdot\vec{\sigma}_2)\,(\vec{\tau}_1\cdot\vec{\tau}_2) \\ &\quad\quad+\frac{g_A^2}{16\pi}\sum_n\left(\frac{\psi_{2n}}{\psi_0}\right)^2 e^{-m_{2n}d}\left(\frac{1}{d}+\frac{2}{m_{2n}d^2}+\frac{3}{m_{2n}^2d^3}\right)(\vec{\sigma}_1\cdot\widehat{d})(\vec{\sigma}_2\cdot\widehat{d})\,(\vec{\tau}_1\cdot\vec{\tau}_2) \\ &\quad\approx \frac{g_A^2}{16\pi}\sum_n\left(\frac{\psi_{2n}}{\psi_0}\right)^2\frac{e^{-m_{2n}d}}{d}\Big[(\vec{\sigma}_1\cdot\widehat{d})(\vec{\sigma}_2\cdot\widehat{d})-(\vec{\sigma}_1\cdot\vec{\sigma}_2)\Big](\vec{\tau}_1\cdot\vec{\tau}_2)\ , \end{aligned}$$

which contributes to the spin $V_{S,A}$ and tensor part $V_{T,A}$ of the NN interaction. Specifically,

$$\begin{aligned} &V_{S,A}\approx\sum_n G_{SA,2n}^2\frac{e^{-m_{2n}}d}{4\pi\,d}\ ,\quad V_{T,A}\approx\sum_n G_{TA,2n}^2\frac{e^{-m_{2n}}d}{4\pi\,d}\ , \\ &G_{SA,2n}\equiv-\frac{g_A\psi_{2n}}{\sqrt{6}\psi_0}\sim g_Am_{2n}/\sqrt{\kappa}\ ,\qquad G_{TA,2n}\equiv\frac{g_A\psi_{2n}}{\sqrt{12}\psi_0}\sim g_Am_{2n}/\sqrt{\kappa}\ , \end{aligned} \tag{8.111}$$

with $G_{SA,2n}\approx\sqrt{N_c/\lambda}$ and $G_{TA,2n}\approx\sqrt{N_c/\lambda}$ the spin and tensor couplings of the tower of axials to the nucleon.

8.6.3 Vectors

For the vector mesons the time component F_{0z} contribution is leading in N_c compared to the space component F_{iz}. This is the opposite of the axial vector

[2] For simplicity we often omit $|_{z=z_c}$ and $\psi_n\equiv\psi_n(z_c)$.

contribution. For the SU(2) part (rho, rho', ...), we have

$$V_V = \frac{1}{2\pi}\sum_n \kappa^2 K(z_c)^2 \psi_{2n-1}^2(z_c) \int d\vec{x} d\vec{y} F_{0z}^a(\vec{x}, z_c) \frac{e^{-m_{2n-1}|\vec{x}-\vec{y}|}}{|\vec{x}-\vec{y}|} F_{0z}^a(\vec{y}, z_c)$$
$$\approx \frac{1}{4\pi}\sum_n J^a \psi_{2n-1}^2 \frac{e^{-m_{2n-1}d}}{d} J^{Ra} \ , \tag{8.112}$$

where $J^a \equiv \int d\vec{x} 2\kappa K F_{z0}^a \Big|_{z=z_c}$ is the unrotated angular momentum in [**?**]. We note that $R = R_1^T R_2$ and that $R_2^{ab} J^b = -I_2^a$ where I_2^a is the unrotated isovector charge of the nucleon labelled 2. The same holds for label 1. Thus

$$\langle s_1 t_1 s_2 t_2 | V_V | s_1 t_1 s_2 t_2 \rangle \approx \sum_n \frac{1}{4} \psi_{2n-1}^2 \frac{e^{-m_{2n-1}d}}{4\pi\, d} (\vec{\tau}_1 \cdot \vec{\tau}_2) \ , \tag{8.113}$$

which is seen to contribute to the isospin part of the central potential

$$V_{1,V}^- \approx \sum_n G_{1V,2n-1}^2 \frac{e^{-m_{2n-1}d}}{4\pi\, d} \ , \tag{8.114}$$

with $G_{1V,2n-1} = \psi_{2n-1}/2 \approx 1/\sqrt{N_c\lambda}$. This contribution is subleading in the potential.

Similarly, the U(1) vector contribution part (omega, omega', ...) reads

$$V_{\widehat{V}} \approx \frac{N_c^2}{16\pi}\sum_n B \psi_{2n-1}^2 \frac{e^{-m_{2n-1}d}}{d} B = \frac{N_c^2}{4}\sum_n \psi_{2n-1}^2 \frac{e^{-m_{2n-1}d}}{4\pi d} \ , \tag{8.115}$$

where $B \equiv \int d\vec{x} \frac{4}{N_c} \kappa K \widehat{F}_{z0} \Big|_{z=z_c}$ is the baryon number introduced in [19]. This contribution to the central potential is leading

$$V_{1,\widehat{V}} \equiv V_{\widehat{V}} \approx \sum_n G_{\widehat{V},2n-1}^2 \frac{e^{-m_{2n-1}d}}{4\pi\, d} \ , \tag{8.116}$$

$$G_{\widehat{V},2n-1} \equiv \frac{N_c}{2} \psi_{2n-1} \ , \tag{8.117}$$

with $G_{\widehat{V},2n-1} \approx \sqrt{N_c/\lambda}$.

For completeness, we quote the spatial contributions from the vectors, both of which are subleading in the potential. The $SU(2)$ vector meson contribution

is

$$V_V^- \;=\; 2\kappa^2 K(z_c)^2 \psi_{2n-1}(z_c)\psi_{2m-1}(z_c) \int d\vec{x} d\vec{y} F^a_{iz}(\vec{x},z_c)\Delta^{mn,ab}_{ij} F^b_{jz}(\vec{y},z_c) \quad (8.118)$$

At large separations, the field strength F^a_{iz} splits into two single instantons of relative distance d and flavor orientation $R = R_1^T R_2$. At large relative separation d, (8.109) simplifies to

$$\begin{aligned} V_V^- &\approx \frac{9}{16\pi}\sum_n J_V^{ai}(0)\left(\psi_{2n-1}\right)^2 \left(-\delta_{ij} + \frac{\partial_i\partial_j}{m_{2n-1}^2}\right)\frac{e^{-m_{2n-1}d}}{d} J_A^{Raj}(0) \\ &= \frac{9}{16\pi}\sum_n J_V^{ai}(0)\left(\psi_{2n-1}\right)^2 \left[\left(1+\frac{2}{m_{2n-1}d}+\frac{3}{m_{2n-1}^2 d^2}\right)\widehat{d}_i\widehat{d}_j \right. \\ &\qquad \left. -\delta_{ij}\left(1+\frac{1}{m_{2n-1}^2 d^2}\right)\right]\frac{e^{-m_{2n-1}d}}{d} J_V^{Raj}(0)\ , \end{aligned} \quad (8.119)$$

where $J_V^{ai}(0) \equiv -(4/3)\kappa K \int d\vec{x} F^a_{iz}$ and the spatial component of the vector current J_V is unrotated while J_V^R is rotated. The projected potential V_V' yields

$$\begin{aligned} &\langle s_1 t_1 s_2 t_2 | V_V^- | s_1 t_1 s_2 t_2\rangle \\ &\quad\approx \frac{g_V^2}{16\pi}\sum_n \left(\psi_{2n-1}\right)^2 e^{-m_{2n-1}d}\left(-\frac{1}{d}-\frac{1}{m_{2n-1}^2 d^3}\right)(\vec{\sigma}_1\cdot\vec{\sigma}_2)(\vec{\tau}_1\cdot\vec{\tau}_2) \\ &\qquad + \frac{g_V^2}{16\pi}\sum_n \left(\psi_{2n-1}\right)^2 e^{-m_{2n-1}d}\left(\frac{1}{d}+\frac{2}{m_{2n-1}d^2}+\frac{3}{m_{2n-1}^2 d^3}\right) \\ &\qquad\qquad (\vec{\sigma}_1\cdot\widehat{d})(\vec{\sigma}_2\cdot\widehat{d})(\vec{\tau}_1\cdot\vec{\tau}_2) \\ &\quad\approx \frac{g_V^2}{16\pi}\sum_n \left(\psi_{2n-1}\right)^2 \frac{e^{-m_{2n-1}d}}{d}\left[(\vec{\sigma}_1\cdot\widehat{d})(\vec{\sigma}_2\cdot\widehat{d}) - (\vec{\sigma}_1\cdot\vec{\sigma}_2)\right](\vec{\tau}_1\cdot\vec{\tau}_2)\ , \end{aligned} \quad (8.120)$$

with $J_V^{ai}(0) = g_V \mathbb{R}^{ai}$. To leading order $g_V = \mathcal{O}(1/N_c)$,

$$J_V^{ai}(0) \;=\; \frac{2}{3}\int d\vec{x}\kappa K F^a_{zi}(\vec{x},z)\mathbb{1}\Big|_{z=B} = \frac{2}{3}\int d\vec{x}\kappa K\ \mathbb{R}^{ai}\frac{4\rho^2}{(\xi^2+\rho^2)^2}\mathbb{1}\Big|_{z=B} = 0\ ,$$

since $K F^a_{zi}(\vec{x},z)\mathbb{1}$ is even in z. (8.120) contributes to both the spin $V^-_{S,V}$ and

tensor part $V^-_{T,V}$ of the NN interaction,

$$V^-_{S,V} \approx \frac{1}{4\pi}\sum_n G^2_{SV,2n-1}\frac{e^{-m_{2n-1}d}}{d}\ , \quad V^-_{T,V} \approx \frac{1}{4\pi}\sum_n G^2_{TV,2n-1}\frac{e^{-m_{2n-1}d}}{d}\ ,$$
$$G_{SV,2n} \equiv -\frac{g_V\psi_{2n-1}}{\sqrt{6}}\ , \qquad G_{TV,2n} \equiv \frac{g_V\psi_{2n-1}}{\sqrt{12}}\ . \tag{8.121}$$

The holographic description of the nucleon-nucleon potential is consistent with the meson-exchange potentials in nuclear physics. Holography allows a systematic organization of the NN potential in the context of semiclassics, with the NN interaction of order N_c/λ in leading order.

8.7 Holographic NN potentials

In general, the NN potential in holography is composed of the core and the cloud contributions to order N_c/λ. For non-asymptotic distances, both the core and cloud contributions have a non-linear dependence on the rotation matrix $R(U)$, making the projection on the NN channel involved. Formally, the potential (core plus cloud) can be expanded using the irreducible representations of SU(2). Specifically

$$V(d,U) = \sum_{j=0}^{\infty}\sum_{m=-j}^{+j} V_{jm}(d)\, D^j_{mm}(U)\ , \tag{8.122}$$

where $D^j_{m,m'}(U)$ are U-valued Wigner functions. For $k=2$ the azimuthal symmetry restrics $m'=m$ with $V_{jm}=V_{j,-m}$. In particular

$$V_{jm}(d) = \frac{2\pi^2}{(2j+1)}\int dU\, V(d,U)\, D^{j\ *}_{m,m}(U)\ . \tag{8.123}$$

The projection on the NN channel follows by sandwiching (8.122) between the normalized NN states $D^{1/2}(1)\otimes D^{1/2}(2)$. While straightforward, this procedure is involved owing to the complicated nature of the $k=2$ instanton both in the core and in the cloud on $R(U)$. In general

$$V(d,U) = V_{\rm core}(d,U) + V_{\rm cloud}(d,U)\ . \tag{8.124}$$

$V_{\rm core}(d,U)$ is defined as

$$V_{\rm core}(d,U) \equiv \Delta E[f_{-+}] - \Delta E[f_-] - \Delta E[f_+] \ ,$$
$$\Delta E[f] = \frac{\kappa}{6\lambda}\int d^3\widetilde{x}d\widetilde{z}\left(\widetilde{z}^2 - \frac{3^7\pi^2}{2^4}\widetilde{\Box}\log|f|\right)\widetilde{\Box}^2\log|f| \ , \quad (8.125)$$

where

$$\log|f_{-+}| \equiv -\log\left[(g_- + A)(g_+ + A) - B^2\right] \ , \quad (8.126)$$
$$\log|f_\pm| = -\log g_\pm \ , \quad (8.127)$$
$$g_\pm = \sum_{\alpha=2,3,4}\widetilde{x}_\alpha^2 + \left(\widetilde{x}_1 \pm \frac{\widetilde{d}}{2}\right)^2 + \widetilde{\rho}^2 \ , \qquad A = \frac{\widetilde{\rho}^4\sin^2|\theta|}{\widetilde{d}^2} \ , \quad (8.128)$$
$$B = \widetilde{\rho}^2\left(\cos|\theta| + \frac{2}{\widetilde{d}}\sin|\theta|\left[\widehat{\theta}_1\widetilde{z} + \widehat{\theta}_2\widetilde{x}_3 - \widehat{\theta}_3\widetilde{x}_2\right]\right) \ . \quad (8.129)$$

$V_{\rm cloud}(d,U)$ is defined as

$$V_{\rm cloud}(d,U) \equiv 2\kappa^2K^2\sum_n\psi_n^2\int d\vec{x}d\vec{y}$$
$$\Big[F_{iz}^a(x_M;-+)\Delta_n^{ij}(\vec{x}-\vec{y})\,F_{iz}^a(y_M;-+) + \widehat{F}_{0z}(x_M;-+)\Delta_n^{00}(\vec{x}-\vec{y})\widehat{F}_{0z}(y_M;-+)$$
$$-2F_{iz}^a(x_M;-)\Delta_n^{ij}(\vec{x}-\vec{y})\,F_{jz}^a(y_M;-) - 2\widehat{F}_{0z}(x_M;-)\Delta_n^{00}(\vec{x}-\vec{y})\widehat{F}_{0z}(y_M;-)\Big]\Big|_{z=z_c} \ ,$$

where $F_{iz}^a(x_M;-)$ and $F_{iz}^a(x_M;-+)$ are the field strengths of the $k=1$ and the $k=2$ $SU(2)$ instanton respectively,

$$F_{iz}^a(x_M;-) = -2\delta_{ai}\tau^a\frac{\rho^2}{(\xi_-^2+\rho^2)^2} \ , \quad (8.130)$$
$$F_{iz}^a(x_M;-+) = -2\delta_{ai}U^\dagger\mathbb{B}\,(f_{-+}\otimes\tau^a)\,\mathbb{B}^\dagger U \ , \quad (8.131)$$
$$\mathbb{B}^\dagger = \begin{pmatrix}0 & -\mathbb{1} & 0\\ 0 & 0 & -\mathbb{1}\end{pmatrix} \ , \qquad f_{-+}^{-1} = \begin{pmatrix}g_- + A & B\\ B & g_+ + A\end{pmatrix} \ ,$$
$$g_\pm \equiv x_\alpha^2 + \left(x_1 \pm \frac{d}{2}\right)^2 + \rho^2 \ , \quad x_\alpha^2 \equiv x_2^2 + x_3^2 + x_4^2 \ ,$$
$$A \equiv \frac{\rho^4\sin^2|\theta|}{d^2} \ , \quad B \equiv \rho^2\left(\cos|\theta| + \frac{2}{d}\sin|\theta|\left[\widehat{\theta}_1 z + \widehat{\theta}_2 x_3 - \widehat{\theta}_3 x_2\right]\right) \ ,$$
$$\begin{pmatrix}\lambda_1^\dagger & \frac{d}{2}\tau^1 - x^\dagger & \frac{\rho^2}{d}\sin|\theta|\,\widehat{\theta}_a\tau^a\tau^1\\ \lambda_2^\dagger & \frac{\rho^2}{d}\sin|\theta|\,\widehat{\theta}_a\tau^a\tau^1 & -\frac{d}{2}\tau^1 - x^\dagger\end{pmatrix}U = 0 \ , \qquad U^\dagger U = \mathbb{1} \ .$$

The U(1) fields $\widehat{F}_{z0}(x_M;-+)=\partial_z\widehat{A}_0(x_M;-+)$ and $\widehat{F}_{z0}(x_M;-)=\partial_z\widehat{A}_0(x_M;-)$ follow from

$$\widehat{A}_0(x_M;-+)=\frac{1}{32\pi^2 a}\Box\log|f_{-+}|\ ,\quad \widehat{A}_0(x_M;-)=\frac{1}{32\pi^2 a}\Box\log|f_{-}|\ . \tag{8.132}$$

The propagators are defined as

$$\Delta_n^{ij}(\vec{x}-\vec{y})=(-\delta_{ij}+\widehat{\partial}_i\widehat{\partial}_j)\frac{e^{-m_n|\vec{x}-\vec{y}|}}{4\pi\,|\vec{x}-\vec{y}|}\ ,\quad \Delta_n^{00}(\vec{x}-\vec{y})=\frac{e^{-m_n|\vec{x}-\vec{y}|}}{4\pi\,|\vec{x}-\vec{y}|}\ . \tag{8.133}$$

If we were to saturate (8.122) by $j=0,1$ which is exact asymptotically as we have shown both for the core and cloud, then the projection procedure is much simpler. In particular, the NN potential simplifies to

$$V_{NN}=V_1^+ +\vec{\tau}_1\cdot\vec{\tau}_2\,V_1^- +\vec{\sigma}_1\cdot\vec{\sigma}_2\left(V_S^+ +\vec{\tau}_1\cdot\vec{\tau}_2\,V_S^-\right) \tag{8.134}$$

$$+\left(3(\vec{\sigma}_1\cdot\widehat{d})(\vec{\sigma}_2\cdot\widehat{d})-\vec{\sigma}_1\cdot\vec{\sigma}_2\right)\left(V_T^+ +\vec{\tau}_1\cdot\vec{\tau}_2\,V_T^-\right)\ , \tag{8.135}$$

with the core contributions

$$V^+_{1,\rm core}=\frac{1}{4}\left[V(0,0,0)+2V(0,0,\pi/2)+V(\pi/2,0,0)\right]\ , \tag{8.136}$$

$$V^-_{S,\rm core}=\frac{1}{4}\left[V(0,0,0)-\frac{2}{3}V(0,0,\pi/2)-\frac{1}{3}V(\pi/2,0,0)\right]\ , \tag{8.137}$$

$$V^-_{T,\rm core}=V_T^{11}-V_T^{22}=\frac{1}{6}\left[V(\pi/2,0,0)-V(0,0,\pi/2)\right]\ , \tag{8.138}$$

as detailed above. The cloud contributions V_1, V_S and V_T remain the same. At large distances d the core contribution is dominant and repulsive in the regular gauge (8.83)

$$V^+_{1,\rm core}\approx\frac{27\pi N_c}{2\lambda}\frac{1}{d^2}\ , \tag{8.139}$$

and subdominant and attractive in the singular gauge (8.166)

$$V^+_{1,\rm core}\approx-\frac{81\pi N_c}{\lambda^4}\frac{\rho^6}{d^8}\ . \tag{8.140}$$

The dominant cloud contributions are

$$
\begin{aligned}
V^{+}_{1,\widehat{V}} &\approx \sum_n G^2_{1\widehat{V},2n-1}\frac{e^{-m_{2n-1}d}}{4\pi\, d}\ , & G_{1\widehat{V},2n-1} &\equiv \frac{N_c}{2}\psi_{2n-1} \ \sim\ \sqrt{\frac{N_c}{\lambda}}\ ,\\
V^{-}_{S,A} &\approx \sum_n G^2_{SA,2n}\frac{e^{-m_{2n}d}}{4\pi d}\ , & G_{SA,2n} &\equiv -\frac{g_A\psi_{2n}}{\sqrt{6}\psi_0} \ \sim\ \sqrt{\frac{N_c}{\lambda}}\ ,\\
V^{-}_{S,V} &\approx \sum_n G^2_{SV,2n-1}\frac{e^{-m_{2n-1}d}}{4\pi d}\ , & G_{SV,2n} &\equiv -\frac{g_V\psi_{2n-1}}{\sqrt{6}} \ \sim\ \frac{1}{\sqrt{\lambda N_c}}\\
V^{-}_{T,A} &\approx \sum_n G^2_{TA,2n}\frac{e^{-m_{2n}d}}{4\pi d}\ , & G_{TA,2n} &\equiv \frac{g_A\psi_{2n}}{\sqrt{12}\psi_0} \ \sim\ \sqrt{\frac{N_c}{\lambda}}\ ,\\
V^{-}_{T,V} &\approx \sum_n G^2_{TV,2n-1}\frac{e^{-m_{2n-1}d}}{4\pi d}\ , & G_{TV,2n} &\equiv \frac{g_V\psi_{2n-1}}{\sqrt{12}} \ \sim\ \frac{1}{\sqrt{\lambda N_c}}\ ,\\
V^{-}_{T,\Pi} &\approx \frac{1}{16\pi}\left(\frac{g_A}{f_\pi}\right)^2\frac{1}{d^3} \ \sim\ \frac{N_c}{\lambda}\ .
\end{aligned}
$$

from (8.104), (8.111), (8.116), and (8.121). To order N_c/λ we note that $V_1^- = V_S^+ = V_T^+ = 0$.

The relative vector-to-pion contribution to the tensor potential, can be assessed asymptotically. For a realistic estimate, we make the pion massive. Thus

$$
\frac{V^-_{T,A}}{V^-_{T,\Pi}} \ \approx\ \frac{\frac{1}{4\pi}G^2_{TA,2}e^{-m_2 d}}{\frac{1}{48\pi}\left(\frac{g_A m_\pi}{f_\pi}\right)^2 e^{-m_\pi d}} \ \approx\ \left(\frac{f_\pi\psi_2}{m_\pi\psi_0}\right)^2 e^{(m_\pi-m_1)d} \ \approx\ 60.8\ e^{(m_\pi-m_1)d}
$$

with $\psi_2/\psi_0 \sim 11.4$, $f_\pi \sim 93$MeV and $m_\pi \sim 136$MeV.

8.8 Conclusions

We have extended the holographic description of the nucleon suggested in [30] to the two nucleon problem. In particular, we have shown how the exact $k = 2$ ADHM instanton configuration applies to the NN problem. The NN potential is divided into a short distance core contribution and a large distance cloud contribution that is meson mediated. This is a first principle description of meson exchange potentials sucessfully used for the nucleon-nucleon problem in pre-QCD [133].

The core contribution in the regular gauge is of order N_c/λ. It is Coulomb like in the central channel. Remarkably, the repulsion is 4-dimensional Coulomb, a hallmark of holography. This repulsion dominates the high baryon density problem in holography as discussed recently in [15, 17]. The dominant Coulomb repulsion is changed to subdominant dipole attraction for instantons in the singular gauge.

We have shown in the context of semiclassics, that the meson-instanton interactions in bulk is strong and of order $\sqrt{N_c/\lambda}$. In the Born-Oppenheimer approximation they contribute to the potentials to order N_c/λ. These cloud contributions dominate at large distances. The central potential is dominated by a tower of omega exchanges, the tensor potential by a tower of pion exchanges, while the spin and tensor potentials are dominated by a tower of axial-vector exchanges. The isovector exchanges are subdominant at large N_c and strong coupling. Holography, fixes the potentials at intermediate and short distances without recourse to *adhoc* form factors [133] or truncation as in the Skyrme model [**?**].

The present work provides a quantitative starting point for an analysis of the NN interaction in strong coupling and large N_c. For a realistic comparison with boson exchange models, we need to introduce a pion mass. It also offers a systematic framework for discussing the deuteron problem, NN form factors and NN-meson and NN-photon emissions in the context of holography. We plan to address some of these issues next.

8.9 Appendix

8.9.1 Strong Source Theory

In this Appendix, we check our cloud calculation in the singular gauge using the strong coupling source theory used for small cores in [132, 134] and more recently in holography in [32]. This method provides an independent check on our semiclassics in the $k = 2$ sector.

The energy in the leading order of λ is

$$E = \kappa \ \mathrm{tr} \int d^3xdz \left(\frac{1}{2}K^{-1/3}F_{ij}^2 + KF_{iz}^2\right) + \frac{\kappa}{2} \int d^3xdz \left(\frac{1}{2}K^{-1/3}\widehat{F}_{ij}^2 + K\widehat{F}_{iz}^2\right) .$$

where, in the region $1 \ll \xi$,

$$
\begin{aligned}
\widehat{A}_0 &\approx -\frac{1}{2a\lambda}(G_- + G_+) \ , \\
A^a_i &\approx -2\pi^2\rho^2 \left(\left(\epsilon^{iaj}\partial_{+j} - \delta^{ia}\partial_{+Z} \right) G_+ + R^{ab} \left(\epsilon^{ibj}\partial_{-j} - \delta^{ib}\partial_{-Z} \right) G_- \right) \ , \\
A^a_z &\approx -2\pi^2\rho^2 \left(\partial_{+a} H_+ + R^{ab}\partial_{-b} H_- \right) \ ,
\end{aligned}
$$

with

$$
\begin{aligned}
G_\pm &\approx \kappa \sum_{n=1}^{\infty} \psi_n(z)\psi_n(\pm Z) Y_n \left(\left| \vec{x} - \vec{X}_\pm \right| \right) \ , \\
H_\pm &\approx \kappa \sum_{n=0}^{\infty} \phi_n(z)\phi_n(\pm Z) Y_n \left(\left| \vec{x} - \vec{X}_\pm \right| \right) \ , \\
\phi_0(z) &\equiv \frac{1}{\sqrt{\kappa\pi}K(z)} \ , \quad \phi_n(z) = \frac{1}{\sqrt{\lambda_n}}\partial_z \psi_n(z) \quad (n = 1, 2, 3, \cdots) \ , \\
Y_n \left(\left| \vec{x} - \vec{X}_\pm \right| \right) &\equiv -\frac{e^{-\sqrt{\lambda_n}\left| \vec{x} - \vec{X}_\pm \right|}}{4\pi \left| \vec{x} - \vec{X}_\pm \right|} \ , \quad \partial_{\pm a} \equiv \frac{\partial}{\partial X^a_\pm} \ , \quad \partial_{\pm Z} \equiv \frac{\partial}{\partial Z_\pm} \ .
\end{aligned}
$$

Pion

The pion contribution stems from

$$
E_\Pi = \frac{\kappa}{2} \int d^3x dz K \left(\partial_i A^a_z \right) \left(\partial_i A^a_z \right) \ , \tag{8.141}
$$

where

$$
A^a_z \approx -2\pi^2\rho^2 \left(\partial_{+a} H_+ + R^{ab}\partial_{-b} H_- \right) \ , \tag{8.142}
$$

with $\phi_0(z)$ only. After subtracting the self-energy the pion interaction energy (V_Π) is

$$
\begin{aligned}
V_\Pi &= \kappa \left(2\pi^2\rho^2 \right)^2 R^{ab} \int d^3x dz K \left(\partial_i \partial_{+a} H_+ \right) \left(\partial_i \partial_{-b} H_- \right) \\
&\approx \frac{1}{2\,3^2\pi} \frac{N_c \lambda \rho^4}{d^3} R^{ab} \left(\widehat{d}_a \widehat{d}_b - \frac{\delta_{ab}}{3} \right) \ ,
\end{aligned} \tag{8.143}
$$

after using $2\partial_a = -\partial_{\pm a}$ and dropping the surface terms. $\vec{X}_+ = -\vec{X}_- = \frac{\vec{d}}{2}$ and $Z_c \approx 0$. The matrix element of (8.143) in the 2-nucleon state is

$$\langle s_1 s_2 t_1 t_2 | V_\Pi | s_1 s_2 t_1 t_2 \rangle = \frac{1}{2\,3^5\pi} \frac{N_c \lambda \rho^4}{d^3} \left(3(\vec{\sigma}_1 \cdot \widehat{d})(\vec{\sigma}_2 \cdot \widehat{d}) - \vec{\sigma}_1 \cdot \vec{\sigma}_2 \right) (\vec{\tau}_1 \cdot \vec{\tau}_2)$$
$$\equiv \frac{1}{4M^2} \frac{g^2_{\pi NN}}{4\pi} \frac{1}{d^3} \left(3(\vec{\sigma}_1 \cdot \widehat{d})(\vec{\sigma}_2 \cdot \widehat{d}) - \vec{\sigma}_1 \cdot \vec{\sigma}_2 \right) (\vec{\tau}_1 \cdot \vec{\tau}_2) \ , \qquad (8.144)$$

after using $\langle s_1 s_2 t_1 t_2 | R^{ab} | s_1 s_2 t_1 t_2 \rangle = \frac{1}{9} \sigma_1^a \sigma_2^b \vec{\tau}_1 \cdot \vec{\tau}_2$. The last equality follows from the canonical πN pseudovector coupling. Thus

$$\left(\frac{g_{\pi NN}}{M} \right)^2 = \frac{8 N_c \lambda \rho^4}{3^5} = \left(\frac{\widehat{g}_A}{f_\pi} \right)^2 \ , \qquad (8.145)$$

where $\widehat{g}_A = \frac{64}{3} \kappa \pi \rho^2$ obtained in [32], and $f_\pi^2 = 4\kappa/\pi$. This is just the Goldberger-Treiman relation following from the NN interaction using the strongly coupled source approximation [32]. As noted in Appendix D, our normalization of the axial-vector current appears to be twice the normalization of the same current used in [32].

Omega

The ω contribution stems from

$$E_{\widehat{V}} = \frac{\kappa}{2} \int d^3x dz K \left(\partial_z \widehat{A}_0 \right) \left(\partial_z \widehat{A}_0 \right) \ , \qquad (8.146)$$

where

$$\widehat{A}_0 \approx -\frac{1}{2a\lambda} (G_- + G_+) \ . \qquad (8.147)$$

After subtracting the self-energy the ω interaction energy ($V_{\widehat{V}}$) is

$$V_{\widehat{V}} = \frac{\kappa^2 \psi_n(Z_+) \psi_n(Z_-) m^2_{2n-1}}{(2a\lambda 4\pi)^2} \int d\vec{x} \, \frac{e^{-m_{2n-1}\left(|\vec{x}-\vec{X}_-|+|\vec{x}-\vec{X}_+|\right)}}{|\vec{x}-\vec{X}_-||\vec{x}-\vec{X}_+|} \qquad (8.148)$$
$$\approx \frac{N_c^2}{(8\pi)^2} \psi_n^2 m^2_{2n-1} \int dr (4\pi r^2) \, \frac{e^{-m_{2n-1}(r+d)}}{rd} \qquad (8.149)$$
$$\approx \frac{N_c}{4} \sum_n \psi^2_{2n-1} \frac{e^{-m_{2n-1} d}}{4\pi d} \ , \qquad (8.150)$$

where we used

$$\kappa \int dz K(z) \partial_z \psi_n(z) \partial_z \psi_m(z) = m_{2n-1}^2 \delta_{nm} \ . \tag{8.151}$$

The result is in agreement with (8.115). At large separations, the strongly coupled source theory and the semiclassical quantization yields the same results. This outcome is irrespective of the use of the singular gauge (strong coupling) or regular gauge (semiclassics). This a consequence of gauge invariance.

At short distances, gauge invariance is upset by the delta-function singularities present in the singular gauge. Indeed, for $\rho \ll \xi \ll 1$ the omega contribution stems from

$$E_{\widehat{V}} = \frac{\kappa}{2} \int d^3x dz K \left(\partial_z \widehat{A}_0\right) \left(\partial_z \widehat{A}_0\right) \ , \tag{8.152}$$

with now $K \approx 1$ and

$$\widehat{A}_0 \approx -\frac{1}{2a\lambda} (G_-^{\rm flat} + G_+^{\rm flat}) \ , \tag{8.153}$$

$$G_\pm^{\rm flat} = -\frac{1}{4\pi^2} \frac{1}{\xi_\pm^2} \ , \tag{8.154}$$

from [32]. After subtracting the self-energy the ω interaction energy ($V'_{\widehat{V}}$) is

$$\begin{aligned} V'_{\widehat{V}} &= \frac{\kappa}{(2a\lambda 4\pi)^2} \int d\vec{x} dz \frac{4z^2}{\left((x_1 - d/2)^2 + x_\alpha^2\right)^2 \left((x_1 + d/2)^2 + x_\alpha^2\right)^2} \\ &= \frac{27 N_c}{2\pi\lambda d^2} \int d\vec{x} dz \frac{z^2}{\left((x_1 - 1/2)^2 + x_\alpha^2\right)^2 \left((x_1 + 1/2)^2 + x_\alpha^2\right)^2} \\ &\approx \frac{27\pi N_c}{4\lambda d^2} \ . \end{aligned} \tag{8.155}$$

We have rescaled the variable $x_M \to x_M/d$ in the second line and carried numerically the integration through

$$\int d\vec{x} dz \frac{z^2}{\left((x_1 - 1/2)^2 + x_\alpha^2\right)^2 \left((x_1 + 1/2)^2 + x_\alpha^2\right)^2} \approx 4.9348 \approx \frac{\pi^2}{2} \ . \tag{8.156}$$

The omega repulsion at short distance is about $V_{\widehat{V}}/2$ in (8.83). The discrepancy may be due to the singularities introduced in the singular gauge and/or

the approximation in the matching region $\rho \ll \xi \ll 1$. It is worth noting that the standard omega repulsion at large ditances (8.150) transmutes to a 4-dimensional Coulomb repulsion in holography.

8.9.2 Singular gauge

Instantons in Singular gauge

The $k = 1$ instanton in the singular gauge follows from (8.9) through a gauge transformation $g^{-1} = \widehat{\xi} = \xi/|\xi|$ which is singular at $\xi = x - X = 0$. This is achieved through the shift $U \to Ug$, which amounts in general to the new inverse potential $1/f = 1 + \rho^2/\xi_M^2$. The corresponding action density is

$$\mathrm{tr}\, F_{MN}^2 = \Box^2 \log f \ = \frac{96\rho^4}{((x_M - X_M)^2 + \rho^2)^4} - 16\pi^2\delta(x_M - X_M) \ . \quad (8.157)$$

The instanton in the singular gauge is threaded by an antiinstanton of zero size at its center. Its topological charge is strictly speaking zero. It is almost 1 if the center $x = X$ is excluded. This point is usually subsumed. Singular instantons have more localized gauge fields than regular instantons.

The ADHM solution for $k = 2$ in singular gauge is not known. Following the $k = 1$ argument, we may seek it from the regular gauge by applying a doubly singular gauge transformation

$$g^{-1} \equiv g_+^{-1}\, g_-^{-1} = \widehat{\xi}_+\, \widehat{\xi}_- \ , \quad (8.158)$$

which is singular at the centers $\xi_\pm = x \pm D = 0$ in quaternion notations. This amounts to shifting $U \to Ug$ in the ADHM construction. We guess that (8.158) yields the new inverse potential

$$f^{-1} \to \frac{f^{-1}}{(|x - D||x + D|)} \ , \quad (8.159)$$

in the singular gauge. As a result, the instanton topological charge is

$$\mathrm{tr}\, F_{MN}^2 = \Box^2 \log f \to \Box^2 \log f - 16\pi^2 \left(\delta(\xi_{+M}) + \delta(\xi_{-M})\right) \ . \quad (8.160)$$

The $k = 2$ ADHM density is now threaded by two singular anti-instantons at

$\xi_\pm = 0$. Singular instantons have more localized gauge fields A_M than regular instantons. While this point is of relevance for gauge variant quantitities, it is irrelevant for gauge invariant quantities with the exception of the topological charge. This point is important for the central nucleon-nucleon potential as we now explain.

Core in Singular gauge

In the singular gauge we substitute $|f|$ as (8.159), which results in

$$\Box \log|f| \to \Box \log|f| + \frac{4}{\widetilde{\xi}_+^2} + \frac{4}{\widetilde{\xi}_-^2} \ , \tag{8.161}$$

$$\Box^2 \log|f| \to \Box^2 \log|f| - 16\pi^2 \left(\delta(\widetilde{\xi}_{+M}) + \delta(\widetilde{\xi}_{-M})\right) \ . \tag{8.162}$$

This gives extra contributions in addition to the result in regular gauge after the subtraction of the self-energy

$$\begin{aligned}
\Delta E &\to \Delta E + \Delta E_s \ , \\
\Delta E_s &\equiv \left(\frac{\kappa}{6\lambda}\right)\left(\frac{3^7\pi^2}{2^4}\right)\int d^3\widetilde{x}d\widetilde{z} \\
&\quad \Big[32\pi^2\big\{\widetilde{\Box}\log|f_\pm|\left(\delta\widetilde{\xi}_{+M}) + \delta(\widetilde{\xi}_{-M})\right) \\
&\quad -\widetilde{\Box}\log|f_+|\,\delta(\widetilde{\xi}_{+M}) - \widetilde{\Box}\log|f_-|\,\delta(\widetilde{\xi}_{-M})\big\} \\
&\quad +16\pi^2\left(\delta(\widetilde{\xi}_{-M})\frac{4}{\widetilde{\xi}_+^2} + \delta(\widetilde{\xi}_{+M})\frac{4}{\widetilde{\xi}_-^2}\right)\Big] \ ,
\end{aligned} \tag{8.163}$$

which comes from the second term in (8.69) while the first term in (8.69) remains the same. $f\pm, f_+$, and f_- are short for the expressions in the regular gauge in (8.33)-(8.34). Thus

$$\Delta E_s = \frac{N_c 27\pi}{8}\left[\int d^3\widetilde{x}d\widetilde{z}\Big[\widetilde{\Box}\log|f|\left(\delta(\widetilde{\xi}_{+M}) + \delta(\widetilde{\xi}_{-M})\right)\Big] + \frac{16}{\widetilde{\rho}^2} + \frac{4}{\widetilde{d}^2}\right]$$

$$
\begin{aligned}
&= \frac{N_c 27\pi}{2}\left\{\frac{4}{\widetilde{\rho}^2}+\frac{1}{\widetilde{d}^2}\right. \\
&- 2\widetilde{d}^2\Big[\widetilde{d}^6(2\widetilde{d}^4+5\widetilde{d}^2\widetilde{\rho}^2+4\widetilde{\rho}^4)+\widetilde{d}^4\widetilde{\rho}^2\cos^2|\theta|\,(-2\widetilde{d}^4-4\widetilde{d}^2\widetilde{\rho}^2-3\widetilde{\rho}^4\cos(2|\theta|)) \\
&\quad +2\widetilde{d}^4\widetilde{\rho}^2(\widetilde{d}^4+4\widetilde{d}^2\widetilde{\rho}^2+5\widetilde{\rho}^4)\sin^2|\theta|+\widetilde{d}^2\widetilde{\rho}^6(3\widetilde{d}^2+8\widetilde{\rho}^2)\sin^4|\theta|+2\widetilde{\rho}^{10}\sin^6|\theta|\Big] \\
&\left.\div\,\widetilde{\rho}^2\Big[\widetilde{d}^4(\widetilde{d}^2+\widetilde{\rho}^2)-\widetilde{d}^4\widetilde{\rho}^2\cos^2|\theta|+\widetilde{d}^2\widetilde{\rho}^2(\widetilde{d}^2+2\widetilde{\rho}^2)\sin^2|\theta|+\widetilde{\rho}^6\sin^4|\theta|\Big]^2\right\} \qquad (8.164) \\
&= -\left(\frac{N_c 27\pi}{2\lambda}\right)\frac{1+4\cos(2|\theta|)}{d^2}+\mathcal{O}(d^{-4}) \qquad (d\gg 1)\ .
\end{aligned}
$$

For large d, the monopole contribution in (8.164) is cancelled by the monopole contribution (8.83) in the regular gauge. This cancellation leads to a dipole attraction in the singular gauge.

The net dipole attraction in the singular gauge is best seen by noting that (8.82) now reads

$$
V_D \approx -2bcN_c\int\left(\widetilde{\Box}^2\log\left(1+\widetilde{\rho}^2/\widetilde{\xi}_+^2\right)\right)\frac{1}{\widetilde{\Box}}\left(\widetilde{\Box}^2\log\left(1+\widetilde{\rho}^2/\widetilde{\xi}_-^2\right)\right)\ , \qquad (8.165)
$$

where $\widetilde{x}_\pm$ refers to the shifted instanton positions. For large separations $\widetilde{d}/\widetilde{\rho}\gg 1$, the leading contribution to V_D is

$$
V_D \approx -768\pi^2\,bc\,N_c\frac{\widetilde{\rho}^6}{\widetilde{d}^8} = -81\pi N_c\frac{\widetilde{\rho}^6}{\widetilde{d}^8}\ , \qquad (8.166)
$$

by repeated use of the 4-dimensional formulae

$$
\Box\,\frac{1}{\xi^{2n}} = -4\pi^2\,\delta_{n1}\,\delta^4(\xi)+2n(2(n+1)-4)\frac{1}{\xi^{2(n+1)}}\ . \qquad (8.167)
$$

This contribution is of order N_c/λ^4 following the unscaling of $\widetilde{d}=\sqrt{\lambda}d$. (8.166) is dipole-like and attractive. As expected, the threading antiinstanton in the singular gauge cancels the leading N_c/λ repulsive monopole contribution in 4-dimensional Coulomb's law, resulting in the attractive dipole-like contribution (van der Waals).

Chapter 9

Conclusion

The final chapter summarize what we have learned in the course of this thesis about holographic QCD.

In chapter2 we defined SS model and collected the relevant formulas to appear in the subsequent chapters. SS model is composed of two actions: Dirac-Born-Infeld(DBI) action and Chern-Sioms(CS) action. The relevant degree of freedom are $U(N_c)$ gauge field living in the background of the curved metric field and Ramond-Ramond field. By choosing a suitable gauge field we can study many aspects of hadronic physics. We also presented D3/D7 model for comparison with SS model. D3/D7 model is discussed and compared with SS model in Ch4 and Ch5.

In chapter 3 we studied thermodynamics of dense matter. Hot and dense hadronic matter in QCD is difficult to track from first principles in current lattice simulations owing to the sign problem.

In the homogeneous phase we provide a holographic method to study hadronic matter at finite density (or chemical potential) in the context of the SS model [15]. In the canonical ensemble the baryon number density is introduced through compact D4 branes wrapping S^4 at the tip of D8-$\overline{\text{D8}}$ branes. Each baryon acts as a chiral point-like source distributed uniformly over $\mathbb{R}^3$, and leads a non-vanishing $U(1)_V$ potential on the brane. We derive the baryon density (or chemical potential) effect on the energy density.[1] For fixed baryon charge density n_B we analyze the energy density and pressure using the canon-

[1]In the grand canonical ensemble we can introduce the baryon chemical potential through the external $U(1)_V$ field in the DBI action of the D8 branes [14].

ical formalism. The baryonic matter with point like sources is always in the spontaneously broken phase of chiral symmetry, whatever the density. The point-like nature of the sources and large N_c cause the matter to be repulsive as all baryon interactions are omega mediated.

We investigate inhomogeneous cold dense matter in the context of SS model in the Wigner-Seitz approximation. In bulk, baryons are treated as instantons on $S^3 \times R^1$ in each Wigner-Seitz cell. In holographic QCD, Skyrmions are instanton holonomies along the conformal direction. The high density phase is identified with a crystal of holographic Skyrmions with restored chiral symmetry at about $4M_{\rm KK}^3/\pi^5$. As the average density goes up, it approaches to uniform distribution while the chiral condensate approaches to p-wave over a cell. The chiral symmetry is effectively restored in long wavelength limit since the chiral order parameter is averaged to be zero over a cell. The energy density in dense medium varies as $n_B^{5/3}$, which is the expected power for non-relativistic fermion. This shows that the Pauli exclusion effect in boundary is encoded in the Coulomb repulsion in the bulk.

In chapter 4 we investigated the response of dense hQCD to a static and baryonic electric field E using the SS model [18]. At zero temperature Strong fields with $E > (\sqrt{\lambda}M_{KK})^2$ free quark pairs, causing the confined vacuum and matter state to decay. At high temperature and density we derived the conductivity by using Ohm's law and this macroscopic result has been confirmed by the microscopic approach using real-time AdS/CFT in the small electric field limit.

In chapter 5 The response function of a homogeneous and dense hadronic system to a time-dependent (baryon) vector potential is discussed for holographic dense QCD (D4/D8 embedding) both in the confined and deconfined phases. Confined holographic QCD is an uncompressible and static baryonic insulator at large N_c and large λ, with a gapped vector spectrum and a massless pion. Deconfined holographic QCD is a diffusive conductor with restored chiral symmetry and a gapped transverse baryonic current. Similarly, dense D3/D7 is diffusive for any non-zero temperature at large N_c and large λ. At zero temperature dense D3/D7 exhibits a baryonic longitudinal visco-elastic mode with a first sound speed $1/\sqrt{3}$ and a small width due to a shear viscosity to baryon ratio $\eta/n_B = \hbar/4$. This mode is turned diffusive by arbitrarily small

temperatures, a hallmark of holography.

In chapter 6 we studied the effects of the fixed baryon charge density n_B on the pion and vector meson masses and couplings in the homogeneous matter studied in the chapter 3.

In chapter 7 the baryon form factor was computed. In the SS model, baryons are chiral solitons sourced by D4 instantons in bulk of size $1/\sqrt{\lambda}$ with $\lambda = g^2 N_c$. We quantize the D4 instanton semiclassically using $\hbar = 1/(N_c\lambda)$ and non-rigid constraints on the vector mesons. The holographic baryon is a small chiral bag in the holographic direction with a Cheshire cat smile. The vector-baryon interactions occur at the core boundary of the instanton in $D4$. They are strong and of order $1/\sqrt{\hbar}$. To order $\hbar^0$ the electromagnetic current is entirely encoded on the core boundary and vector-meson dominated. To this order, the electromagnetic charge radius is of order λ^0. The meson contribution to the baryon magnetic moments sums identically to the core contribution. The proton and neutron magnetic moment are tied by a model independent relation similar to the one observed in the Skyrme model.

In chapter 8 nuclear force was obtained. In the holographic model of QCD, baryons are chiral solitons sourced by D4 flavor instantons in bulk of size $1/\sqrt{\lambda}$ with $\lambda = g^2 N_c$. Using the ADHM construction we explicit the exact two-instanton solution in bulk. We use it to construct the core NN potential to order N_c/λ. The core sources meson fields to order $\sqrt{N_c/\lambda}$ which are shown to contribute to the NN interaction to order N_c/λ. In holographic QCD, the NN interaction splits into a small core and a large cloud contribution in line with meson exchange models. The core part of the interaction is repulsive in the central, spin and tensor channels for instantons in the regular gauge. The cloud part of the interaction is dominated by omega exchange in the central channel, by pion exchange in the tensor channel and by axial-vector exchange in the spin and tensor channels. Isovector meson exchanges are subdominant in all channels.

Outlook

For the last decade gauge/gravity duality has been applied to various strongly coupled gauge theories and helped in understanding strongly coupled QCD such as sQGP and low energy hadron physics. However there are many open

problems in applying the holographic approach.

There is no exact dual model of QCD yet, so we often resort to the universality argument. Furthermore, because of asymptotic freedom, QCD cannot be entirely described by the supergravity limit. Eventually it is important to go beyond the supergravity approximation for a more complete description of QCD. Within the supergravity approximation, we should understand its applicability more precisely: what properties of QCD can be studied, in what regime of QCD, and with what accuracy.

In spite of its many successes, the SS model has an apparent shortcoming that there is no parameter related to the bare quark mass or chiral condensation. There have been a few provoking proposals [136–140] but this issue has not been resolved yet.

With the advent of the Large Hadron Collider (LHC) we will soon explore a higher temperature regime than studied at the RHIC. This is particularly interesting because a gravity description worked well at the RHIC. Any new surprise from LHC will inspire gravity dual theory. It is often called gravity/hydrodynamics (or fluid dynamics) duality. More interestingly it is also closely related to the application of gauge theory to black hole physics [141, 142].

Last but not least, the recent active application of the gauge/gravity duality to condensed matter system is very intriguing [12]. It is now being applied to superfluidity, superconductivity, the Hall effect, and phase transitions.

I believe the gauge/gravity duality will be the key paradigm shift for understanding both gauge theory and gravity. It is clearly a very useful tool and worth more study.

Bibliography

[1] J. M. Maldacena, *The large N limit of superconformal field theories and supergravity*, *Adv. Theor. Math. Phys.* **2**, *231 (1998)*, *Int. J. Theor. Phys.* **38**, *1113 (1999)* [arXiv:hep-th/9711200];

[2] O. Aharony, S. S. Gubser, J. M. Maldacena, H. Ooguri and Y. Oz, *Large N field theories, string theory and gravity*, Phys. Rept. **323**, 183 (2000) [arXiv:hep-th/9905111].

[3] S. S. Gubser and A. Karch, "From gauge-string duality to strong interactions: a Pedestrian's Guide," arXiv:0901.0935 [hep-th].

[4] J. Erdmenger, N. Evans, I. Kirsch and E. Threlfall, "Mesons in Gauge/Gravity Duals - A Review," Eur. Phys. J. A **35**, 81 (2008) [arXiv:0711.4467 [hep-th]].

[5] K. Peeters and M. Zamaklar, "The string/gauge theory correspondence in QCD," Eur. Phys. J. ST **152**, 113 (2007) [arXiv:0708.1502 [hep-ph]].

[6] D. T. Son and A. O. Starinets, "Viscosity, Black Holes, and Quantum Field Theory," Ann. Rev. Nucl. Part. Sci. **57**, 95 (2007) [arXiv:0704.0240 [hep-th]].

[7] D. Mateos, "String Theory and Quantum Chromodynamics," Class. Quant. Grav. **24**, S713 (2007) [arXiv:0709.1523 [hep-th]].

[8] R. C. Myers and S. E. Vazquez, "Quark Soup al dente: Applied Superstring Theory," Class. Quant. Grav. **25**, 114008 (2008) [arXiv:0804.2423 [hep-th]].

[9] M. Natsuume, "String theory and quark-gluon plasma," arXiv:hep-ph/0701201.

[10] S. S. Gubser, S. S. Pufu, F. D. Rocha and A. Yarom, "Energy loss in a strongly coupled thermal medium and the gauge-string duality," arXiv:0902.4041 [hep-th].

[11] S. J. Brodsky and G. F. de Teramond, "Light-Front Holography and Novel Effects in QCD," arXiv:0812.3192 [hep-ph].

[12] S. A. Hartnoll, "Lectures on holographic methods for condensed matter physics," arXiv:0903.3246 [hep-th].

[13] D. T. Son, "Toward an AdS/cold atoms correspondence: a geometric realization of the Schroedinger symmetry," Phys. Rev. D **78**, 046003 (2008) [arXiv:0804.3972 [hep-th]].

[14] K. Y. Kim, S. J. Sin and I. Zahed, "Dense hadronic matter in holographic QCD," arXiv:hep-th/0608046.

[15] K. Y. Kim, S. J. Sin and I. Zahed, "The Chiral Model of Sakai-Sugimoto at Finite Baryon Density," JHEP **0801**, 002 (2008) [arXiv:0708.1469 [hep-th]].

[16] K. Y. Kim, S. J. Sin and I. Zahed, "Diffusion in an Expanding Plasma using AdS/CFT," JHEP **0804**, 047 (2008) [arXiv:0707.0601 [hep-th]].

[17] K. Y. Kim, S. J. Sin and I. Zahed, "Dense Holographic QCD in the Wigner-Seitz Approximation," JHEP **0809**, 001 (2008) [arXiv:0712.1582 [hep-th]].

[18] K. Y. Kim, S. J. Sin and I. Zahed, "Dense and Hot Holographic QCD: Finite Baryonic E Field," JHEP **0807**, 096 (2008) [arXiv:0803.0318 [hep-th]].

[19] K. Y. Kim and I. Zahed, "Electromagnetic Baryon Form Factors from Holographic QCD," JHEP **0809**, 007 (2008) [arXiv:0807.0033 [hep-th]].

[20] K. Y. Kim and I. Zahed, "Baryonic Response of Dense Holographic QCD," JHEP **0812**, 075 (2008) [arXiv:0811.0184 [hep-th]].

[21] K. Y. Kim and I. Zahed, "Nucleon-Nucleon Potential from Holography," JHEP **0903**, 131 (2009) [arXiv:0901.0012 [hep-th]].

[22] S. Nakamura, "Comments on Chemical Potentials in AdS/CFT," Prog. Theor. Phys. **119**, 839 (2008) [arXiv:0711.1601 [hep-th]].

[23] D. T. Son and A. O. Starinets, "Minkowski-space correlators in AdS/CFT correspondence: Recipe and applications," JHEP **0209**, 042 (2002) [arXiv:hep-th/0205051].

[24] G. Policastro, D. T. Son and A. O. Starinets, "From AdS/CFT correspondence to hydrodynamics," JHEP **0209**, 043 (2002) [arXiv:hep-th/0205052].

[25] G. Policastro, D. T. Son and A. O. Starinets, "From AdS/CFT correspondence to hydrodynamics. II: Sound waves," JHEP **0212**, 054 (2002) [arXiv:hep-th/0210220].

[26] C. P. Herzog and D. T. Son, "Schwinger-Keldysh propagators from AdS/CFT correspondence," JHEP **0303**, 046 (2003) [arXiv:hep-th/0212072].

[27] M. Kruczenski, D. Mateos, R. C. Myers and D. J. Winters, "Meson spectroscopy in AdS/CFT with flavour," JHEP **0307**, 049 (2003) [arXiv:hep-th/0304032].

[28] T. Sakai and S. Sugimoto, "Low energy hadron physics in holographic QCD," Prog. Theor. Phys. **113**, 843 (2005) [arXiv:hep-th/0412141].

[29] T. Sakai and S. Sugimoto, "More on a holographic dual of QCD," Prog. Theor. Phys. **114**, 1083 (2006) [arXiv:hep-th/0507073].

[30] H. Hata, T. Sakai, S. Sugimoto and S. Yamato, "Baryons from instantons in holographic QCD," arXiv:hep-th/0701280.

[31] H. Hata, M. Murata and S. Yamato, "Chiral currents and static properties of nucleons in holographic QCD," arXiv:0803.0180 [hep-th].

[32] K. Hashimoto, T. Sakai and S. Sugimoto, "Holographic Baryons : Static Properties and Form Factors from Gauge/String Duality," arXiv:0806.3122 [hep-th].

[33] D. K. Hong, M. Rho, H. U. Yee and P. Yi, "Chiral dynamics of baryons from string theory," arXiv:hep-th/0701276.

[34] D. K. Hong, M. Rho, H. U. Yee and P. Yi, "Dynamics of Baryons from String Theory and Vector Dominance," arXiv:0705.2632 [hep-th].

[35] D. K. Hong, M. Rho, H. U. Yee and P. Yi, "Nucleon Form Factors and Hidden Symmetry in Holographic QCD," arXiv:0710.4615 [hep-ph].

[36] J. Park and P. Yi, "A Holographic QCD and Excited Baryons from String Theory," arXiv:0804.2926 [hep-th].

[37] M. Rho, "Baryons and Vector Dominance in Holographic Dual QCD," arXiv:0805.3342 [hep-ph].

[38] D. Gazit and H. U. Yee, "Weak-Interacting Holographic QCD," Phys. Lett. B **670**, 154 (2008) [arXiv:0807.0607 [hep-th]].

[39] K. Nawa, H. Suganuma and T. Kojo, "Baryons in Holographic QCD," Phys. Rev. D **75**, 086003 (2007) [arXiv:hep-th/0612187].

[40] K. Nawa, H. Suganuma and T. Kojo, "Brane-induced Skyrmions: Baryons in holographic QCD," Prog. Theor. Phys. Suppl. **168**, 231 (2007) [arXiv:hep-th/0701007].

[41] K. Nawa, H. Suganuma and T. Kojo, "Baryons with holography," arXiv:0806.3040 [hep-th].

[42] S. Seki and J. Sonnenschein, "Comments on Baryons in Holographic QCD," arXiv:0810.1633 [hep-th].

[43] K. Hashimoto, "Holographic Nuclei," arXiv:0809.3141 [hep-th].

[44] K. Hashimoto, T. Sakai and S. Sugimoto, "Nuclear Force from String Theory," arXiv:0901.4449 [hep-th].

[45] Y. Kim, S. Lee and P. Yi, "Holographic Deuteron and Nucleon-Nucleon Potential," arXiv:0902.4048 [hep-th].

[46] P. Yi, "Holographic Baryons," arXiv:0902.4515 [hep-th].

[47] O. Aharony, J. Sonnenschein and S. Yankielowicz, "A holographic model of deconfinement and chiral symmetry restoration," Annals Phys. **322**, 1420 (2007) [arXiv:hep-th/0604161].

[48] A. Parnachev and D. A. Sahakyan, "Chiral phase transition from string theory," Phys. Rev. Lett. **97**, 111601 (2006) [arXiv:hep-th/0604173].

[49] K. Peeters, J. Sonnenschein and M. Zamaklar, "Holographic melting and related properties of mesons in a quark gluon plasma," Phys. Rev. D **74**, 106008 (2006) [arXiv:hep-th/0606195].

[50] N. Horigome and Y. Tanii, "Holographic chiral phase transition with chemical potential," JHEP **0701**, 072 (2007) [arXiv:hep-th/0608198].

[51] O. Bergman, G. Lifschytz and M. Lippert, "Holographic Nuclear Physics," arXiv:0708.0326 [hep-th].

[52] M. Rozali, H. H. Shieh, M. Van Raamsdonk and J. Wu, "Cold Nuclear Matter In Holographic QCD," arXiv:0708.1322 [hep-th].

[53] J. L. Davis, M. Gutperle, P. Kraus and I. Sachs, "Stringy NJL and Gross-Neveu models at finite density and temperature," arXiv:0708.0589 [hep-th].

[54] K. Nawa, H. Suganuma and T. Kojo, "Baryonic matter in holographic QCD," arXiv:0806.3041 [hep-th].

[55] H. Suganuma, K. Nawa and T. Kojo, "Baryons and Baryonic Matter in Holographic QCD from Superstring," arXiv:0809.0805 [hep-th].

[56] K. Nawa, H. Suganuma and T. Kojo, "Brane-induced Skyrmion on S^3: baryonic matter in holographic QCD," arXiv:0810.1005 [hep-th].

[57] A. Parnachev, "Holographic QCD with Isospin Chemical Potential," arXiv:0708.3170 [hep-th].

[58] J. Erdmenger, M. Kaminski and F. Rust, "Holographic vector mesons from spectral functions at finite baryon or isospin density," Phys. Rev. D **77**, 046005 (2008) [arXiv:0710.0334 [hep-th]].

[59] O. Aharony, K. Peeters, J. Sonnenschein and M. Zamaklar, "Rho meson condensation at finite isospin chemical potential in a holographic model for QCD," JHEP **0802**, 071 (2008) [arXiv:0709.3948 [hep-th]].

[60] K. Hashimoto, C. I. Tan and S. Terashima, "Glueball Decay in Holographic QCD," Phys. Rev. D **77**, 086001 (2008) [arXiv:0709.2208 [hep-th]].

[61] J. Babington, J. Erdmenger, N. J. Evans, Z. Guralnik and I. Kirsch, "Chiral symmetry breaking and pions in non-supersymmetric gauge / gravity duals," Phys. Rev. D **69**, 066007 (2004) [arXiv:hep-th/0306018].

[62] D. Mateos, R. C. Myers and R. M. Thomson, "Holographic phase transitions with fundamental matter," Phys. Rev. Lett. **97**, 091601 (2006) [arXiv:hep-th/0605046].

[63] T. Albash, V. G. Filev, C. V. Johnson and A. Kundu, "A topology-changing phase transition and the dynamics of flavour," Phys. Rev. D **77**, 066004 (2008) [arXiv:hep-th/0605088].

[64] S. Kobayashi, D. Mateos, S. Matsuura, R. C. Myers and R. M. Thomson, "Holographic phase transitions at finite baryon density," JHEP **0702**, 016 (2007) [arXiv:hep-th/0611099].

[65] D. Mateos, R. C. Myers and R. M. Thomson, "Thermodynamics of the brane," JHEP **0705**, 067 (2007) [arXiv:hep-th/0701132].

[66] R. C. Myers, A. O. Starinets and R. M. Thomson, "Holographic spectral functions and diffusion constants for fundamental matter," JHEP **0711**, 091 (2007) [arXiv:0706.0162 [hep-th]].

[67] K. Ghoroku, M. Ishihara and A. Nakamura, "D3/D7 holographic Gauge theory and Chemical potential," Phys. Rev. D **76**, 124006 (2007) [arXiv:0708.3706 [hep-th]].

[68] A. Karch and A. O'Bannon, "Holographic Thermodynamics at Finite Baryon Density: Some Exact Results," JHEP **0711**, 074 (2007) [arXiv:0709.0570 [hep-th]].

[69] D. Mateos, S. Matsuura, R. C. Myers and R. M. Thomson, "Holographic phase transitions at finite chemical potential," JHEP **0711**, 085 (2007) [arXiv:0709.1225 [hep-th]].

[70] I. Amado, C. Hoyos-Badajoz, K. Landsteiner and S. Montero, "Residues of Correlators in the Strongly Coupled N=4 Plasma," Phys. Rev. D **77**, 065004 (2008) [arXiv:0710.4458 [hep-th]].

[71] S. Matsuura, "On holographic phase transitions at finite chemical potential," JHEP **0711**, 098 (2007) [arXiv:0711.0407 [hep-th]].

[72] R. C. Myers and A. Sinha, "The fast life of holographic mesons," JHEP **0806**, 052 (2008) [arXiv:0804.2168 [hep-th]].

[73] S. Nakamura, Y. Seo, S. J. Sin and K. P. Yogendran, "A new phase at finite quark density from AdS/CFT," arXiv:hep-th/0611021.

[74] S. Nakamura, Y. Seo, S. J. Sin and K. P. Yogendran, " Baryon charge chemical potential in AdS/CFT," to appear

[75] M. Kruczenski, D. Mateos, R. C. Myers and D. J. Winters, "Towards a holographic dual of large-N(c) QCD," JHEP **0405**, 041 (2004) [arXiv:hep-th/0311270].

[76] S. K. Domokos and J. A. Harvey, "Baryon number-induced Chern-Simons couplings of vector and axial-vector mesons in holographic QCD," arXiv:0704.1604 [hep-ph].

[77] M.A. Nowak, M. Rho and I. Zahed, "Chiral Nuclear Dynamics", (1996) World Scientific.

[78] T. H. R. Skyrme, "A Nonlinear field theory," Proc. Roy. Soc. Lond. A **260**, 127 (1961).

[79] T. H. R. Skyrme, "A Unified Field Theory Of Mesons And Baryons," Nucl. Phys. **31** (1962) 556.

[80] I. Zahed and G. E. Brown, "The Skyrme Model," Phys. Rept. **142**, 1 (1986).

[81] I. R. Klebanov, "Nuclear Matter In The Skyrme Model," Nucl. Phys. B **262**, 133 (1985).

[82] L. McLerran and R. Pisarski, "Phases of cold, dense quarks at large N(c)," Nucl. Phys. A **796**, 83 (2007);

[83] N. S. Manton and P. J. Ruback, "Skyrmions in Flat Space and Curved Space," Phys. Lett. B **181**, 137 (1986).

[84] H. Forkel, A. Jackson, M. Rho, C. Weiss, A. Wirzba, Nucl. Phys. A **504**, 818 (1989).

[85] B. Y. Park, D. P. Min, M. Rho and V. Vento, "Atiyah-Manton approach to Skyrmion matter," Nucl. Phys. A **707**, 381 (2002) [arXiv:nucl-th/0201014].

[86] H. Forkel, "Yang-Mills instantons in closed Robertson-Walker spacetime," arXiv:hep-th/0407166.

[87] M. Kutschera, C. J. Pethick and D. G. Ravenhall, "Dense Matter In The Chiral Soliton Model," Phys. Rev. Lett. **53** (1984) 1041.

[88] H. A. Bethe and M. B. Johnson, "Dense Baryon Matter Calculations With Realistic Potentials," Nucl. Phys. A **230** (1974) 1.

[89] B. Friedman and V. R. Pandharipande, "Hot and cold, nuclear and neutron matter," Nucl. Phys. A **361** (1981) 502.

[90] A. Karch and A. O'Bannon, "Metallic AdS/CFT," JHEP **0709**, 024 (2007) [arXiv:0705.3870 [hep-th]].

[91] O. Bergman, G. Lifschytz and M. Lippert, "Response of Holographic QCD to Electric and Magnetic Fields," JHEP **0805**, 007 (2008) [arXiv:0802.3720 [hep-th]].

[92] O. Bergman, G. Lifschytz and M. Lippert, "Magnetic properties of dense holographic QCD," arXiv:0806.0366 [hep-th].

[93] E. G. Thompson and D. T. Son, "Magnetized baryonic matter in holographic QCD," Phys. Rev. D **78**, 066007 (2008) [arXiv:0806.0367 [hep-th]].

[94] C. V. Johnson and A. Kundu, "External Fields and Chiral Symmetry Breaking in the Sakai-Sugimoto Model," JHEP **0812**, 053 (2008) [arXiv:0803.0038 [hep-th]].

[95] A. Rebhan, A. Schmitt and S. A. Stricker, "Meson supercurrents and the Meissner effect in the Sakai-Sugimoto model," arXiv:0811.3533 [hep-th].

[96] J. Erdmenger, R. Meyer and J. P. Shock, "AdS/CFT with Flavour in Electric and Magnetic Kalb-Ramond Fields," JHEP **0712**, 091 (2007) [arXiv:0709.1551 [hep-th]].

[97] A. Karch, D. T. Son and A. O. Starinets, "Zero Sound from Holography," arXiv:0806.3796 [hep-th].

[98] A. Karch and A. O'Bannon, "Holographic Thermodynamics at Finite Baryon Density: Some Exact Results," JHEP **0711**, 074 (2007) [arXiv:0709.0570 [hep-th]].

[99] R. C. Myers and A. Sinha, "The fast life of holographic mesons," JHEP **0806**, 052 (2008) [arXiv:0804.2168 [hep-th]].

[100] L.D. Landau and E.M. Lifshitz, "Theory of elasticity,", Oxford, Butterworth-Heinemann(2002)

[101] M. Kulaxizi and A. Parnachev, "Comments on Fermi Liquid from Holography," arXiv:0808.3953 [hep-th].

[102] B. A. Gelman, E. V. Shuryak and I. Zahed, "Cold Strongly Coupled Atoms Make a Near-perfect Liquid," arXiv:nucl-th/0410067.

[103] C. P. Herzog, A. Karch, P. Kovtun, C. Kozcaz and L. G. Yaffe, "Energy loss of a heavy quark moving through N = 4 supersymmetric Yang-Mills plasma," JHEP **0607**, 013 (2006) [arXiv:hep-th/0605158].

[104] H. Liu, K. Rajagopal and U. A. Wiedemann, "Calculating the jet quenching parameter from AdS/CFT," Phys. Rev. Lett. **97**, 182301 (2006) [arXiv:hep-ph/0605178].

[105] J. Casalderrey-Solana and D. Teaney, "Heavy quark diffusion in strongly coupled N = 4 Yang Mills," Phys. Rev. D **74**, 085012 (2006) [arXiv:hep-ph/0605199].

[106] R. C. Myers, A. O. Starinets and R. M. Thomson, "Holographic spectral functions and diffusion constants for fundamental matter," JHEP **0711**, 091 (2007) [arXiv:0706.0162 [hep-th]].

[107] J. Mas, J. P. Shock, J. Tarrio and D. Zoakos, "Holographic Spectral Functions at Finite Baryon Density," JHEP **0809**, 009 (2008) [arXiv:0805.2601 [hep-th]].

[108] S. Caron-Huot, P. Kovtun, G. D. Moore, A. Starinets and L. G. Yaffe, "Photon and dilepton production in supersymmetric Yang-Mills plasma," JHEP **0612**, 015 (2006) [arXiv:hep-th/0607237].

[109] D. Mateos and L. Patino, "Bright branes for strongly coupled plasmas," JHEP **0711**, 025 (2007) [arXiv:0709.2168 [hep-th]].

[110] A. Nata Atmaja and K. Schalm, "Photon and Dilepton Production in Soft Wall AdS/QCD," arXiv:0802.1460 [hep-th].

[111] J. Mas, J. P. Shock, J. Tarrio and D. Zoakos, "Holographic Spectral Functions at Finite Baryon Density," JHEP **0809**, 009 (2008) [arXiv:0805.2601 [hep-th]].

[112] C. Adami and I. Zahed, "Soliton quantization in chiral models with vector mesons," Phys. Lett. B **215** (1988) 387.

[113] H. Verschelde and H. Verbeke, "Nonrigid quantization of the skyrmion," Nucl. Phys. A **495** (1989) 523.

[114] S. Nadkarni, H. B. Nielsen and I. Zahed, "Bosonization Relations As Bag Boundary Conditions," Nucl. Phys. B **253**, 308 (1985).

[115] H. J. Schnitzer, "The Soft Pion Skyrmion Lagrangian And Strong CP Violation," Phys. Lett. B **139**, 217 (1984).

[116] W. M. Yao *et al.* [Particle Data Group], "Review of particle physics," J. Phys. G **33** (2006) 1.

[117] I. Zahed and G. E. Brown, "The Skyrme Model," Phys. Rept. **142**, 1 (1986).

[118] A. Jackson, A. D. Jackson and V. Pasquier, "The Skyrmion-Skyrmion Interaction," Nucl. Phys. A **432** (1985) 567.

[119] R. Vinh Mau, M. Lacombe, B. Loiseau, W. N. Cottingham and P. Lisboa, "The Static Baryon Baryon Potential In The Skyrme Model," Phys. Lett. B **150**, 259 (1985).

[120] M. Oka, "The nuclear force in the Skyrme model," Phys. Rev. C **36**, 720 (1987).

[121] H. Yamagishi and I. Zahed, "Nucleon-nucleon Hamiltonian from Skyrmions," Phys. Rev. D **43**, 891 (1991);

[122] V. Thorsson and I. Zahed, "Central Nucleon-Nucleon Potential From Skyrmions," Phys. Rev. D **45**, 965 (1992).

[123] M. Garcia Perez, T. G. Kovacs and P. van Baal, "Comments on the instanton size distribution," Phys. Lett. B **472**, 295 (2000) [arXiv:hep-ph/9911485].

[124] M. Garcia Perez, T. G. Kovacs and P. van Baal, "Overlapping instantons," arXiv:hep-ph/0006155.

[125] M. F. Atiyah, N. J. Hitchin, V. G. Drinfeld and Yu. I. Manin, "Construction of instantons," Phys. Lett. A **65** (1978) 185.

[126] N. H. Christ, E. J. Weinberg and N. K. Stanton, "General self-dual Yang-Mills solutions," Phys. Rev. D **18**, 2013 (1978).

[127] A. Actor, "Classical Solutions Of SU(2) Yang-Mills Theories," Rev. Mod. Phys. **51**, 461 (1979).

[128] N. Dorey, V. V. Khoze and M. P. Mattis, "Multi-Instanton Calculus in N=2 Supersymmetric Gauge Theory," Phys. Rev. D **54**, 2921 (1996) [arXiv:hep-th/9603136].

[129] N. Dorey, T. J. Hollowood, V. V. Khoze and M. P. Mattis, "The calculus of many instantons," Phys. Rept. **371**, 231 (2002) [arXiv:hep-th/0206063].

[130] H. Osborn, "Calculation Of Multi - Instanton Determinants," Nucl. Phys. B **159**, 497 (1979).

[131] E. Braaten and L. Carson, "The deuteron as a toroidal Skyrmion", Phys. Rev. **D38**, 3525 (1988).

[132] G. F. Chew, "Renormalization of Meson Theory with a Fixed Extended Source," Phys. Rev. **94**, 1748 (1954).

[133] G. E. Brown and A. D. Jackson, "The Nucleon-Nucleon Interaction," North-Holland, Amsterdam, 1976. (References therein)

[134] J. A. Parmentola, "Static Bag Source Meson Field Theory: Strong Coupling Approximation," Phys. Rev. D **27**, 2686 (1983).

[135] J. A. Parmentola, "Some Implications Of A Small Bag Radius," Phys. Rev. D **29**, 2563 (1984).

[136] R. Casero, E. Kiritsis and A. Paredes, "Chiral symmetry breaking as open string tachyon condensation," Nucl. Phys. B **787**, 98 (2007) [arXiv:hep-th/0702155].

[137] N. Evans and E. Threlfall, "Quark Mass in the Sakai-Sugimoto Model of Chiral Symmetry Breaking," arXiv:0706.3285 [hep-th].

[138] O. Bergman, S. Seki and J. Sonnenschein, "Quark mass and condensate in HQCD," JHEP **0712**, 037 (2007) [arXiv:0708.2839 [hep-th]].

[139] A. Dhar and P. Nag, "Sakai-Sugimoto model, Tachyon Condensation and Chiral symmetry Breaking," JHEP **0801**, 055 (2008) [arXiv:0708.3233 [hep-th]].

[140] K. Hashimoto, T. Hirayama, F. L. Lin and H. U. Yee, "Quark Mass Deformation of Holographic Massless QCD," JHEP **0807**, 089 (2008) [arXiv:0803.4192 [hep-th]].

[141] S. Bhattacharyya, V. E. Hubeny, S. Minwalla and M. Rangamani, "Nonlinear Fluid Dynamics from Gravity," JHEP **0802**, 045 (2008) [arXiv:0712.2456 [hep-th]].

[142] S. Bhattacharyya, R. Loganayagam, S. Minwalla, S. Nampuri, S. P. Trivedi and S. R. Wadia, "Forced Fluid Dynamics from Gravity," JHEP **0902**, 018 (2009) [arXiv:0806.0006 [hep-th]].